HANDBOOK

SATELLITE TIME AND FREQUENCY TRANSFER AND DISSEMINATION

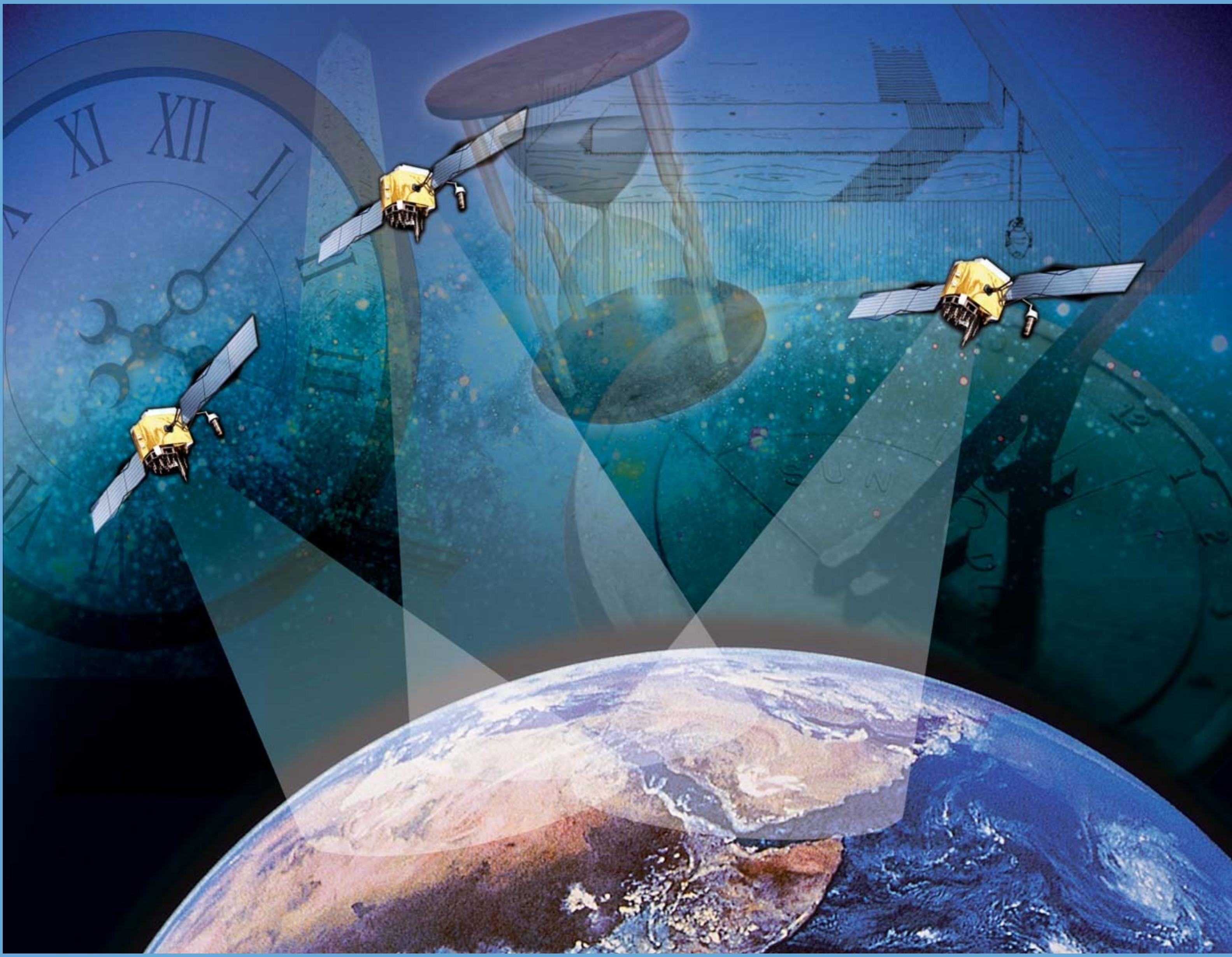

Edition 2010
Radiocommunication Bureau

HANDBOOK

SATELLITE TIME AND FREQUENCY TRANSFER AND DISSEMINATION

Edition 2010

Radiocommunication Bureau

THE RADIOCOMMUNICATION SECTOR OF ITU

The role of the Radiocommunication Sector is to ensure the rational, equitable, efficient and economical use of the radio-frequency spectrum by all radiocommunication services, including satellite services, and carry out studies without limit of frequency range on the basis of which Recommendations are adopted.

The regulatory and policy functions of the Radiocommunication Sector are performed by World and Regional Radiocommunication Conferences and Radiocommunication Assemblies supported by Study Groups.

Inquiries about radiocommunication matters
Please contact:

ITU
Radiocommunication Bureau
Place des Nations
CH -1211 Geneva 20
Switzerland

Telephone:	+41 22 730 5800
Fax:	+41 22 730 5785
E-mail:	brmail@itu.int
Web:	www.itu.int/itu-r

Placing orders for ITU publications
Please note that orders cannot be taken over the telephone. They should be sent by fax or e-mail.

ITU
Sales and Marketing Division
Place des Nations
CH -1211 Geneva 20
Switzerland

Fax:	**+41 22 730 5194**
E-mail:	**sales@itu.int**

The Electronic Bookshop of ITU: www.itu.int/publications

PREFACE

Technological development in general, and that of information-communication technologies and applications in particular, requires the increasingly precise timing and synchronization of different electronic devices.

The International Telecommunication Union carries out studies and establishes international standards on the relevant timing scales and their use by telecommunication and computer networks, electronic navigation systems, and so forth.

In 1974, the International Radio Consultative Committee (CCIR – *Comité Consultatif International des Radiocommunications*), in cooperation with the General Conference of Weights and Measures and the Bureau International de l'Heure, developed Coordinated Universal Time (UTC).

In 1978, CCIR approved the use of UTC "to designate the time in all international telecommunication activities and in all official documents of the International Telecommunication Union". CCIR also stated that UTC should be employed "as the ultimate reference for standard-frequency emissions".

The ITU World Administrative Radio Conference 1979 (WARC-79) included UTC in the international treaty status Radio Regulations, and since then UTC has been used as the main time-scale for telecommunication networks (wired and wireless) and for other time-related applications.

Modern satellite systems providing time and frequency signal dissemination through a clear, un-obstructed path with an easily modelled delay are the main source of precise time and frequency so essential to maritime and aviation services, navigation and positioning systems and for the proper functioning of telecommunication and computer networks.

This is the first ITU Handbook to provide detailed information on the applied methods, technologies, algorithms, data structure and practical use of frequency and timing signals provided by satellite systems.

Special attention is focused on the Global Navigation Satellite Systems (GNSSs) belonging to the radionavigation-satellite service. GNSS are providing time-frequency signals to any place on the Earth and currently represent the *de-facto* primary source of precise timing signals for governmental, commercial, transportation and scientific applications.

Dr. Valery TIMOFEEV
Director
Radiocommunication Bureau

TABLE OF CONTENTS

Page

FOREWORD

The Radiocommunication Study Group 7 for the Science Services (SG 7) was created through a structural reorganization in 1990 at the Düsseldorf CCIR Plenary Assembly. At that time, the Space Research and Radio Astronomy Study Group (SG 2) was consolidated with the Time and Frequency Standards SG 7 to form the new SG 7 on Science Services.

Many of the activities in the Science Services Study Group are associated with advancing the state of the art in the use of the radio spectrum to achieve scientific objectives. In this regard, the time and frequency standards community has long been associated with the International Telecommunication Union (ITU) with the express purpose of developing Recommendations for the use of the radio spectrum to facilitate the dissemination of precise time references and for standardizing the methods for this dissemination. An essential corollary is the specification of precise frequency standards and the techniques for their implementation.

The Radiocommunications Sector SG 7 (Science Services) comprises 4 Radiocommunication Working Parties (WPs) that addresses technical issues related to specific disciplines under the umbrella of science services. Working Party 7A, (Time Signals and Frequency Standards Emissions) is concerned with the generation and dissemination of Time and Frequency Signals by terrestrial and space radiocommunication services. In the past 15 to 20 years the precise time and frequency services provided by satellite systems, predominately navigation satellites, have become the primary means of dissemination and the capabilities of those services has increased dramatically. The resulting increase in capability and development of these satellite systems has made it difficult to keep pace with their development, their impact on the Time and Frequency Community and the Radio and Telecommunication communities in general.

This Handbook provides comprehensive technical and operational information on current satellite systems employed for dissemination of precise time and frequency signals.

As Chairman of SG 7, it is my great pleasure to present this Handbook to the above-mentioned communities of users, who will, I am sure, find it an important reference tool in their own work.

This Handbook is the result of several years of preparation and work to attempt to capture the development in satellite technologies and the growing capability they have produced. The Handbook could not have been completed without the contributions from many administrations participating in SG 7 and its WP 7A. Special thanks should be given to the Chairmen of WP 7A Mr. Ronald BEARD, for his leadership of this project. Our special gratitude is also due to Mr. A. VASSILIEV of the Radiocommunication Bureau who has played an important role in the preparation, editing and publication of the Handbook.

ACKNOWLEDGEMENTS

The work of the Rapporteurs for the various sections of the Handbook was outstanding and we would like to express appreciation to the contributors and the many others who have contributed their time and efforts on this Handbook.

Satellite Systems:

AXELRAD, P.

KLEPCZYNSKI, W. J.

BRUNET, M.

IMAE, M.

BARTENEV, V.

KLIMOV, V.

KOSSENKO, V.

KRASILSCHKOV, M.

REVNIVYKH, S.

REINHARDT, V.

VASSILIEV, A.

Timescales, Timekeeping and Reference Systems:

CORDARA, F.

McCARTHY, D.

NELSON, R.

ARIAS, E.

BAUCH, A.

Techniques:

LEWANDOWSKI, W. and AZOUBIB, J.

KLEPCZYNSKI, W. J.

KIRCHNER, D.

De JONG, G.

RAY, J.

SENIOR, K.

Propagation and Environmental Factors:

KLOBUCHAR, John A.

Our special thanks to the Chairman of WP 7A Mr. Ronald BEARD for his leadership of this project, his contribution and editing of this Handbook and to the Radiocommunication SG 7 Counsellor Mr. Alexandre VASSILIEV, Radiocommnication Bureau, for providing additional texts, editing and preparing it for publication.

Vincent MEENS
Chairman, Radiocommunication Study Group 7

INTRODUCTION

A little bit of history...

Long time ago people have marked time by the movement of the sun and other stars, by phases of the moon, by the changing of seasons, and by the passing of generations. Time intervals have been measured by sand-filled hour glasses, water clocks, and mechanical devices. The frequencies of musical instruments are tuned by comparison to tuning forks and pitch pipes.

History has recorded inventive examples of time, time interval and frequency measurement. An Egyptian device dating to c.1500 BC, similar in shape to a bent T-square, measured the passage of time from the shadow cast by its crossbar on a non-linear rule. The T was oriented eastward in the mornings. At noon, the device was turned around so that it could cast its shadow in the evening direction.

As early as 1000 B.C., the Chinese made frequency standards by counting the number of bean kernels that filled the pipe of a wind instrument. For pipes of the same diameter, the frequency (pitch) was specified by the number of kernels required to fill the pipe.

Time intervals were measured in 13th-century in Spain by burning candles on lever arms that lost weight as they burned, moving the arm to display the passage of time.

The Chinese burned incense clocks that marked time by changes in the scent given off by layers of incense impregnated with different oils. Cassini's tables of predicted eclipses of the moons of Jupiter were used to provide position-independent time measurements, accurate to a few minutes, for the mapping of France in 1679. Harrison's chronometer, perfected in 1759, allowed time to be kept aboard ship with accuracies in the 10-second range over periods of weeks [Dana and Penrod, 1990].

As early as 1450 astronomers had suggested longitude could be determined by the angle of the fixed stars to the moon, but the star tables were inadequate. In 1675 King Charles II had the Greenwich Observatory built, and the Greenwich meridian was established. It took 100 years to prepare the first Nautical Almanac. At this time in history, commerce to the new world was extremely important.

The critical importance of determining longitude was tragically brought to focus in 1707 when a fleet commanded by Admiral Sir Cloudsley Shovel ran into the Scilly Islands – loosing four ships and 2,000 men. The British Crown responded by offering £ 20,000 (about USD 2 million in today's money) for a chronometer good enough to determine longitude with an accuracy of 30 miles.

John Harrison, then 21, from Yorkshire took the challenge and spent his life building chronometers of wood and metal. He made one with gears of wood that did not vary more than a second a month during a 14 year period. A voyage using his No. 4 chronometer sailed from Plymouth to Madeira – giving a position accuracy of about 1 mile. The Astronomer Royal doubted the result. Another voyage was embarked on when John was 70 years old – this time to Barbados. After five months at sea, his No. 4 predicted the position of Barbados to within 10 miles. It took him another 10 years of painful pursuit to collect the reward money – which he never did receive in full.

Though significant progress occurred with navigation chronometers after Harrison's work, the next major step did not occur until the 1920s. This decade brought the discovery and development of the quartz-crystal oscillator. With this discovery, quartz clocks were developed which could detect the instabilities in earth-spin rate, UT1. These clocks moved all areas of chronometry a major step forward – for navigation and otherwise [Allan, 1995].

The development of radar and extremely high frequency radio communications in the 1930s and 1940s made possible the generation of the kind of electromagnetic waves (microwaves) needed to interact with atoms. Research aimed at developing an atomic clock focused first on microwave resonances in the ammonia molecule.

The first atomic clock based on ammonia was built in 1948 and presented in 1949. However, its performance (about 1×10^{-10}) wasn't much better than the existing standards, and attention shifted almost immediately to more promising atomic-beam devices based on cesium atomic resonance. The first practical cesium atomic frequency standard was built at the National Physical Laboratory in England in 1955. Atomic time has been kept ever since.

Descriptions of currently used precise frequency and time standards, sources and their characteristics, time scales, measurement methodologies, existing systems and operational experience are provided in the ITU-R Handbook – Selection and Use of Precise Frequency and Time Systems.

Importance of precise time and frequency and time synchronization

Precise frequency and time become the basis of many technological and life's processes. Precise timing is now used in:

– all communications systems;
– most navigation systems;
– telecommunication and computer systems and their networks;
– accounting and banking systems;
– aeronautical and maritime traffic control systems;
– much of scientific research;
– fault detection and efficiency monitoring of power grids;
– most military systems;
– space research and exploration;
– earth-quake detection and global plate tectonics;
– environmental sensing;
– ocean level and ocean current measurements; plane collision avoidance and precision landing;
– truck fleet tracking;
– auto route mapping.

More than two billion quartz resonators are made per year and the number of atomic clocks in use is about a hundred thousand.

The quality of the clocks, although an important issue, is not the only factor contributing to the accuracy of time measurement. Another important factor is the quality of the time links used to compare the clocks and clocks synchronization. One sample – telecommunication/computer networks. Most telecommunication and computer networks rely on clocks. When the clocks of telecommunication/computer equipment are not synchronised the following very negative consequences may arise, such as:

– operation failure due to violation of proper sequence of events initiated by the relevant software (protocols), backup data, etc.;
– data loss – incorrect time stamp may initiate incorrect data modification in data bases, some applications may perform an incorrect action or even crash;
– security holes – since server access logs are a compilation of information from different hosts, it is essential that the time stamps are correct. Bad time keeping may compromise the server's security because log files are inaccurate, and thus, administrators cannot trace hacker activities.

Satellite-based systems for precise time and frequency dissemination

Radio waves were used for time signal transfer and dissemination since the beginning of the 20th century. However, from the beginning it was known that radio time signals are delayed as they travel the path from the terrestrial transmitter to the terrestrial receiver, and that the accuracy of the received time signal can be no better than the knowledge of the path delay. Signals originating from a ground based transmitter have path delays that are difficult to estimate, since the delay continually changes due to changing ionospheric conditions. Some of these problems are reduced for line-of-sight signals with small coverage area.

On the contrary, the unobstructed path delay between a satellite-based transmitter and a ground-based receiver is more stable and can be more accurately determined than the delay between ground-based stations. This is an important advantage, because the accuracy of any distribution method is almost always limited by the uncertainty in whatever method is used to compensate for the time it takes the signal to travel from the source to the destination.

A time signal broadcast from the sky high above the Earth, where there was a clear, unobstructed path between the transmitter and receiver, is usually more accurate than any ground based signal. In addition, a signal broadcast from a satellite can be received over a wide area, so satellite-based systems can support time and frequency distribution over a large region much more easily than can be done by any terrestrial system. Moreover, the path delay between a satellite-based transmitter and a ground-based receiver can be more accurately modelled than the corresponding delay between the stations of a purely ground-based system.

This Handbook is intended to be an introduction to the field of satellite time and frequency transfer and dissemination. The first chapters present an overview of the satellite systems that are used for dissemination of time and frequency signals. With the pre-eminence of global navigation satellite systems such as the Global Positioning System (GPS), Global Navigation Satellite System (GLONASS) and Communications Satellites in their widespread influence in disseminating Time, chapters describing its generation and relationship to the international time scale are provided. Following the description of the satellite systems is an overview of the generation and maintenance of the international time scale, Coordinated Universal Time (UTC). This time scale is generated from the contribution of many national timing centres and laboratories. So a chapter is devoted to describing the makeup and operation of these national timing centres that support the generation and dissemination of the time scale. Time transfer and dissemination between these timing centres and individual users is accomplished by radio transmissions. The effects of relativistic and propagation effects on these transmissions are discussed before the final chapters describing the primary methods of time and frequency transfer in use.

References

ALLAN, D. W. [5-7 June 1995] The Impact of Precise Time in Our Lives, 50th Anniversary Annual Meeting, Institute of Navigation, Colorado Springs, Colorado, United States of America, (http://www.ALLANstime.com/Publications/DWA/PDF/95jungps.pdf).

DANA, P. and PENROD, B. [July-August, 1990] The Role of GPS in Precise Time and Frequency Dissemination, GPS World, (http://www.pdana.com/PHDWWW_files/gpsrole.pdf).

ITU-R [1997] Handbook on Selection and Use of Precise Frequency and Time Systems. Geneva Switzerland, (http://www.itu.int/publ/R-HDB-31/en).

CHAPTER 1

SATELLITES AND TIME AND FREQUENCY TRANSFER AND DISSEMINATION

Page

1.1 Introduction

Over the last few decades atomic clocks have moved from laboratory novelties to large scale usage. The improvement in quartz oscillator technology and in satellite timing systems has augmented the decades of improvement in atomic clocks. Navigation, communication and power systems have all benefited greatly from these improvements. Precise timing has moved from a novelty to a necessity. Hence, many applications depend on precise timing elements.

Glossary and definitions of time and frequency terms used in this Handbook are available in Recommendation ITU-R TF.686 – Glossary and definitions of time and frequency terms.

1.2 Space radiocommunication services and satellite systems employed for frequency and time transfer and dissemination

The Space Age began with the launch of the Russian satellite *Sputnik* 1 in October 1957, followed by the launch of the first American satellite, named *Explorer* 1, just four months later. The earliest satellites were used for solar and atmospheric studies, but the emphasis quickly turned to telecommunications. A passive-relay satellite, *Echo* 1, launched by the National Aeronautics and Space Administration (NASA) in August 1960, served as a "mirror" reflecting radio signals back to Earth [Whalen, 2002]. Early propagation studies conducted using *Echo* 1 in 1960 [Jakes Jr, 1961] are sometimes identified as the first satellite timing experiments. The first precise time experiment was probably performed via the active-relay satellite *Telstar* 1 in August 1962. This experiment allowed the United States Naval Observatory (USNO), and the United Kingdom's National Physical Laboratory (NPL) and Royal Greenwich Observatory (RGO) to perform a transatlantic clock comparison using a new technique called two-way satellite time transfer.

All satellite systems belonging to different space radiocommunication services (broadcasting-, fixed-, mobile-satellite, etc. services), in one or another way, have and use time and frequency transfer capability [Lowe *et al.*, 2007]. Time transfer is required for telemetry, tracking and command system, for ranging and time tagging purposes. However, frequency and time accuracy requirements for many communication satellites (especially commercial ones) are in general limited to that required for maintaining assigned radio-frequency band and for performing the above-mentioned functions. At the same time some communication satellite systems, e.g. utilizing time domain multiple access systems (TDMA), require precise time for communication purposes.

Earth exploration and meteorological satellite systems need precise timing facilities for measurement of different environmental parameters (for example, the sea level) and have been used for a long time in precise time dissemination [Lombardi and Hanson, 2005; EUMETSAT Satellite Jason-2, 2008].

Some systems, especially those belonging to radionavigation-satellite service [Radio Regulations, 2008], play a very important role in precise time and frequency dissemination. Time and frequency transfer plays a critical role in the functioning of these systems because their primary goal is to provide an effective position, velocity and time service over the world. These systems contain precise time/frequency sources on board satellites as well as effective ground-based segments monitoring operation of these satellites and maintaining the precision of on-board time/frequency sources.

The ITU Radio Regulations (RR) designated a special space radiocommunication service for dissemination of precise time and frequency signals over the world named the standard frequency and time signal-satellite service.

1.2.1 Standard frequency and time signal service

Recognizing the importance of precise time and frequency standards for many industries, scientific organizations and emergency telecommunications, the International Telecommunication Union included definitions [Radio Regulations, 2008] of the *standard frequency and time signal service* and the related radiocommunication stations in its international treaty RR. The definitions provided in the Edition 2008 of the RR are shown below:

“**1.53** *standard frequency and time signal service:* A *radiocommunication service* for scientific, technical and other purposes, providing the transmission of specified frequencies, time signals, or both, of stated high precision, intended for general reception.

1.54 *standard frequency and time signal-satellite service:* A *radiocommunication service* using *space stations* on earth *satellites* for the same purposes as those of the *standard frequency and time signal service*.

This service may also include *feeder links* necessary for its operation.

1.95 *standard frequency and time signal station:* A *station* in the *standard frequency and time signal service.*”

The World Radiocommunication Conferences (WRCs) allocate some portion of the radio-frequency spectrum for the standard frequency and time signal service. Table 1-1 contains an extract from the Table of Frequency Allocations of the RR describing frequency bands allocated to the standard frequency and time signal-satellite service.

TABLE 1-1

Frequency bands allocated to the standard frequency and time signal-satellite service (Radio Regulations, Edition of 2008)

Frequency band	Allocation	Status	Comment
400.05-400.15 MHz		primary	RR Nos. 5.261, 5.262 applied
4 202 ±2 MHz	space-to-Earth		Authorized by RR No. 5.440 subject to agreement obtained under No. 9.21
6 427 ±2 MHz	Earth-to-space		Authorized by RR No. 5.440 subject to agreement obtained under No. 9.21
13.4-13.75 GHz	Earth-to-space	secondary	
13.75-14 GHz	Earth-to-space	secondary	
20.2-21.2 GHz	space-to-Earth	secondary	
25.25-25.5 GHz	Earth-to-space	secondary	
30-31 GHz	space-to-Earth	secondary	
31-31.3 GHz	space-to-Earth	secondary	RR No. 5.149 applied

The Article 26 of the RR (see text, extracted from RR Edition of 2008 below) requests ITU Member States to support activities on providing effective operation of standard frequency and time signal systems (including satellite-based) and protection of these systems from harmful interference.

ARTICLE 26

Standard frequency and time signal service

26.1 § 1 1) To facilitate more efficient use of the radio frequency spectrum and to assist other technical and scientific activities, administrations providing or intending to provide a standard frequency and time signal service shall coordinate, in accordance with the provisions in this Article, the establishment and operation of such a service on a worldwide basis. Attention should be given to the extension of this service to those areas of the world not adequately served.

26.2 2) To this end, each administration shall take steps to coordinate, with the assistance of the Bureau, any new standard frequency or time signal transmission or any change in existing transmissions in the standard frequency bands. For this purpose, administrations shall exchange between themselves, and furnish to the Bureau, all relevant information. On this matter, the Bureau shall consult other international organizations having a direct and substantial interest in the subject.

26.3 3) In so far as is practicable, a new frequency assignment in the standard frequency bands should not be made or notified to the Bureau until appropriate coordination has been completed.

26.4 § 2 Administrations shall cooperate in reducing interference in the frequency bands to which the standard frequency and time signal service is allocated.

26.5 § 3 Administrations which provide this service shall cooperate through the Bureau in the collation and distribution of the results of the measurements of standard frequencies and time signals, as well as details concerning adjustments to the frequencies and time signals.

26.6 § 4 In selecting the technical characteristics of standard frequency and time signal transmissions, administrations shall be guided by the relevant ITU-R Recommendations.

It is worth noting that there is no satellite system exclusively dedicated to dissemination of standard frequency and time signals. As mentioned above, precise time and frequency equipment is usually combined with other applications on board of the same satellite.

Some countries have no assignments in the *standard frequency and time signal-satellite service*. Because they use as a precise timing and frequency source the satellite systems belonging to other space radiocommunication services which are able to transfer highly accurate time to any location on the Earth (for example GNSS).

1.2.2 Global navigation satellite systems

Currently (2010) global navigation satellite systems (GNSSs) belonging to *radionavigation-satellite service* (RNSS) [Radio Regulation, 2008] are, in practice, primary tools for precise frequency and time transfer on global basis.

There are two operational GNSS and three Satellite Based Augmentation Systems (SBAS):

– USA Global Positioning System (GPS) providing global coverage;

– Russian Global Navigation Satellite System (GLONASS) providing almost global coverage.

SBAS that provide increased local navigational coverage are:

– Wide Area Augmentation System (WAAS) provides additional GNSS signals using Inmarsat geostationary satellite for increased coverage in the United States of America.

– European Geostationary Navigation Overlay Service (EGNOS) provides additional GNSS signals using Inmarsat for increased coverage in Europe.

– Multi-Functional Satellite Augmentation System (MSAS) uses dedicated MSAS satellites to provide additional GNSS signals in Japan and surrounding Asian countries.

Detailed description of GPS, GLONASS and SBAS systems are provided in the following chapters.

Several other national and international systems are in design and development stages, such as COMPASS (China), Galileo (European Space Agency), the Indian Regional Navigational Satellite System (IRNSS) (India), and the QZSS (Japan).

Short descriptions of the above-mentioned systems and the basic technical characteristics of their space segments are also available in Recommendation ITU-R M.1787 – Description of systems and networks in the radionavigation-satellite service (space-to-Earth and space-to-space) and technical characteristics of transmitting space stations operating in the bands 1 164-1 215 MHz, 1 215-1 300 MHz and 1 559-1 610 MHz.

References

JAKES Jr, W.C. [1961] Participation of Bell Telephone Laboratories in Project Echo, Bell System Technical. Journal, 40, 975-1028.

LOMBARDI, M. A., HANSON D. W., [March-April 2005] The GOES Time Code Service, 1974-2004: A Retrospective. Journal of Research of the National Institute of Standards and Technology, Vol. 11, **2**, (http://nvl.nist.gov/pub/nistpubs/jres/110/2/j110-2lom.pdf).

Low Earth Orbiting (LEO) satellite Jason-2 Space segment, the European Organisation for the Exploitation of Meteorological Satellites (EUMETSAT), 2006, (http://www.eumetsat.int/Home/Main/What_We_Do/Satellites/Jason/SpaceSegment/?l=en).

LOWE, J., HEIDECKER, J., SWIDAN, M., HISHAM, A., SAMUEL, A. S. [2007] Standard time and frequency dissemination via egyptian digital satellite. 39th Annual Precise Time and Time Interval (PTTI) Meeting. Long Beach, California, USA, (http://tf.nist.gov/timefreq/general/pdf/2274.pdf).

WHALEN, D. J. [2002] The origins of Satellite Communications: 1945-1965. Smithsonian History of Aviation and Spaceflight Series, Smithsonian Books.

ITU-R texts

Radio Regulations, Edition of 2008, Volume 1, Article 1 – Terms and definitions, International Telecommunication Union, 2008, (http://www.itu.int/publ/R-REG-RR-2008/en).

Recommendation ITU-R TF.686-2 – Glossary and definitions of time and frequency terms, (http://web.itu.int/rec/R-REC-TF.686-2-200202-I/en).

Recommendation ITU-R M.1787 – Description of systems and networks in the radionavigation-satellite service (space-to-Earth and space-to-space) and technical characteristics of transmitting space stations operating in the bands 1 164-1 215 MHz, 1 215-1 300 MHz and 1 559-1 610 MHz, (http://www.itu.int/rec/R-REC-M.1787-0-200908-I/en).

CHAPTER 2

GLOBAL POSITIONING SYSTEM

Page

Time and frequency transfer play a critical role in the functioning of the Global Positioning System (GPS) and in turn are also greatly enhanced by its worldwide acceptance. This chapter highlights the role of clocks, time and frequency in the operation of GPS and the capabilities and limitations of GPS in providing a mechanism for their dissemination.

2.1 General description and principles of operation

GPS provides the infrastructure for worldwide determination of position, velocity, and time (PVT) plus a host of other applications that derive from these basic capabilities. The system comprises three so-called segments – the space segment, the control segment, and the user segment.

The most familiar is the space segment, a constellation nominally consisting of 24 satellites in semi-synchronous (11 h 58 min) orbits that continuously transmit spread spectrum ranging signals toward the earth. All satellites transmit at the same (around 1.5 GHz (L-Band)) frequencies modulated by several identifying pseudorandom noise codes.

The control segment monitors the health, status, and performance of the satellites, constructs a data message that is broadcast by the satellites, and takes action to report and remedy any satellite anomalies. The user segment includes both military and civilian receivers worldwide. GPS satellites carry rubidium or caesium standards (or both) providing a reference for generating the ranging signals transmitted by the satellites.

2.2 GPS basics

Many of the key features of GPS are summarized in Table 2-1. Each GPS satellite transmits two (or more) L-Band carrier signals modulated by two or more pseudo-random noise (PRN) codes, and a binary data stream. The PRN codes are essential for code division multiple access which allows all the satellites to use the same frequencies with minimal interference. The codes also enable high precision one-way ranging measurements to be made. To do this, the receiver generates a local replica of the satellite code it expects to see and searches for the correct alignment of the replica signal in both delay and Doppler. The data message, known as the "NAV-MSG" provides information on the satellite clock, precise position of the satellite, an almanac of the satellite constellation, health and status indications, and etc. There are a number of excellent references on GPS that cover the basic operation in far greater detail than we will do here. In particular the textbooks by Misra and Enge [Misra and Enge, 2001] and Kaplan [Kaplan and Hegarty, 2006] provide both detailed and accessible descriptions of all aspects of GPS. Parkinson, *et al.* [Parkinson, *et al.*, 1996] is a more comprehensive treatment with extensive discussions of applications as well as principles of operation. Here we provide only a brief overview to set the stage for the discussion of the role of timing in this important system.

TABLE 2-1

GPS system

Signal frequency	Spread spectrum codes	Code rates
L1 1575.42 MHz	Clear Acquisition – C/A	1.023 MHz
	Precision – P Code	10.23 MHz
	Y Code (military signal)	10.23 MHz
	NAV-MSG (satellite data)	50 bits/s
L2 1227.60 MHz	Precision – P Code	10.23 MHz
	Y Code (military signal)	10.23 MHz
	NAV-MSG (satellite data)	50 bits/s

GPS was designed in the early-1970's with the primary goal of providing an effective position, velocity, and time service for the U.S. Department of Defense (DoD) users and their allies. The requirements that defined the original system architecture were derived almost entirely from DoD missions. However, since that time, GPS has become a hallmark "dual-use" system. It is estimated that in 2002, GPS served approximately 300,000 DoD users and 4,000,000 civil and commercial users within the U.S. alone. The role of the civil user population has not gone unappreciated, and currently the system is controlled by a joint program office with representation from the DoD, NATO and the Department of Transportation that is responsible for civil applications.

The significance of the dual use of the system has been recognized within the U.S. government to the point that an executive steering group has been formed to coordinate and guide use of the system in its dual role. The Position Navigation and Time (PNT) Executive Committee is co-chaired by the Principal Deputies of Defense and Transportation with representatives of the other government agencies. A coordination office supports the Executive Committee to oversee the direction of the program affected.

2.2.1 PRN codes for CDMA and ranging

Pseudo-random noise (PRN) codes are used in GPS to enable both ranging measurements and multiple accesses at a common frequency. The two original GPS codes are the Precise Code (P) and the Coarse Acquisition (C/A) codes. The GPS C/A codes are selected from a family of Gold Codes, 1 023 bits in length that are generated within the satellite at a rate of 1.023 MHz.

Each GPS satellite transmits a unique C/A code so that the user receiver can readily distinguish it. The short duration (1 ms) of the C/A code facilitates rapid acquisition but also makes it vulnerable to interference. The duration of each C/A code bit is approximately 900 ns or 300 m. A user receiver code-tracking loop typically measures the alignment of the code to a precision of 1/100 to 1/1 000 of a bit.

The P-code is a much longer code, generated at 10.23 MHz. The entire code, at this rate, would take 37 weeks to complete. Each GPS satellite is assigned a 1-week segment of the P-code that begins transmitting at the week rollover, Saturday-Sunday midnight.

Under a process known as "A/S" or anti-spoofing, the P-code is normally not transmitted, but rather is replaced by an encrypted P-code with similar properties, known as the Y-code. The terminology P(Y) is generally used to represent this component of the signal. The P(Y) signal is far more resistant to interference than the C/A and with its shorter bit duration it has the potential for greater measurement precision.

The C/A and P(Y) codes were selected both for their cross-correlation and auto-correlation properties. Low cross-correlations among the codes within the family reduce the multiple access interference of all satellites transmitting simultaneously.

The autocorrelation properties of the PRN codes are similar to that of Gaussian white noise. For delays other than zero, the code does not match well with itself. This is important because it allows a receiver to unambiguously and precisely align its replica with the arriving GPS signal. Figure 2-1 illustrates the correlation properties of the GPS C/A codes.

Several new sets of codes are currently being defined and implemented for the next generation of GPS satellites. There are new civil codes added to the L2 frequency, known as L2C and a completely new frequency, 1 176.45 MHz, known as L5, and a new set of military codes known as M-codes.

The new code designs take advantage of improvements in coding, error correction, and digital signal processing that have taken place since the 1970's. It is expected that these new codes will begin coming on line initially with the next block of satellites to be launched known as the Block IIF satellites, eventually being transmitted by the full constellation with the implementation of next generation of GPS satellites known as GPS III.

FIGURE 2-1

GPS C/A code correlation properties

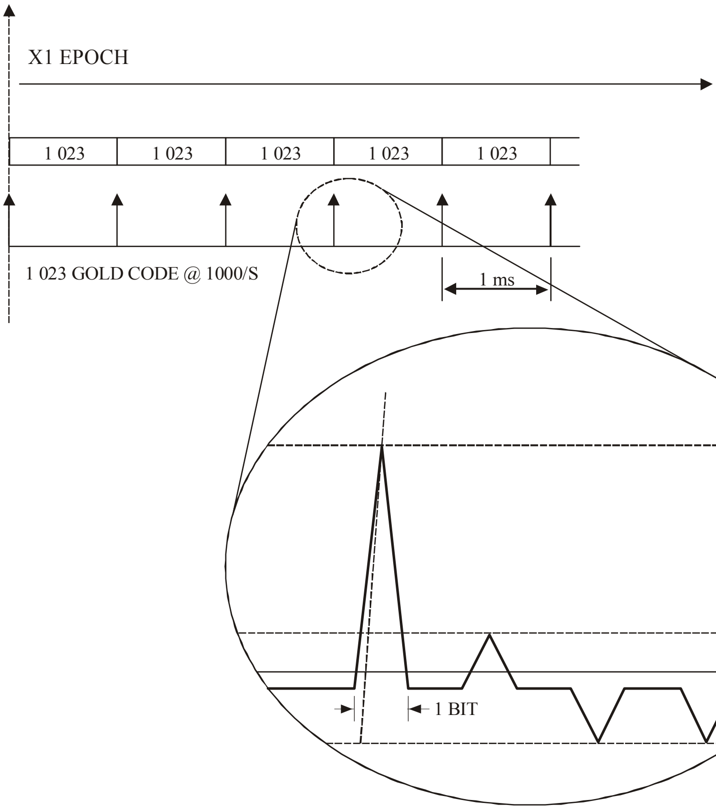

Sat_time_freq-02-01

2.2.2 GPS spectrum

Figure 2-2 illustrates the current and modernized GPS signal spectrum. All frequencies onboard the GPS satellites are derived from a 10.23 MHz reference atomic frequency standard, commonly known as atomic clocks. The two legacy carrier signals are the L1 at 1575.42 MHz and L2 at 1227.6 MHz.

As of 2002, the L2 signal carries only the P(Y) code at 10.23 MHz, whereas the L1 carries both the P(Y) and C/A in phase quadrature.

FIGURE 2-2

GPS signal spectrum

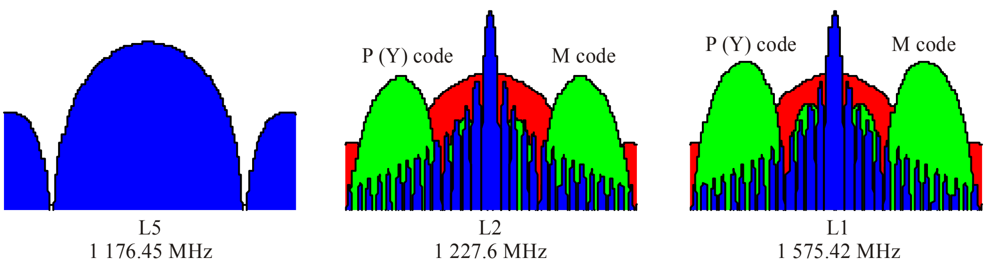

Sat_time_freq-02-02

The majority of low-cost receivers at this time track only the L1 C/A code signals. DoD receivers are largely capable of tracking P(Y) at both L1 and L2 frequencies. High performance commercial receivers, designed for scientific or other high precision functions also track both carrier signals using a variety of techniques to access the underlying RF signals, albeit with a significant reduction in signal-to-noise ratio [Misra and Enge, 2001].

The modernized GPS spectrum will add two narrowband distinct PRN civil signals to the L2 to make the L2C signal and an upgraded version of the navigation message known as CNAV. The M-code split spectrum will be added to both L1 and L2. The new L5C civilian signal is intended as a safety of life signal and is planned to be available with first GPS IIF launch (2010) [Kaplan and Hegarty, 2006]. Two PRN ranging codes are transmitted on L5: the in-phase code (denoted as the I5-code); and the quadrature-phase code (denoted as the Q5-code). Both codes are 10,230 bits long, transmitted at 10.23 MHz with a 1 ms repetition rate. The I5 stream is modulated with a 10-bit Neuman-Hofman code clocked at 1 kHz and the Q5-code is also modulated with a 20-bit Neuman-Hofman code clocked at 1 kHz.

In addition to the benefits conveyed by an additional frequency, the signal structure and codes are designed to:

– improve signal structure for enhanced performance;

– provide about 3 dB higher power;

– support a 10 x processing gain due to the wider bandwidth.

2.2.3 Navigation message

The Navigation message (NAV-MSG) includes all the data required by a receiver to construct a position, velocity, and time solution based on the observed pseudorange and/or Doppler [IS-GPS-200 rev D, 2006]. Figure 2-3 illustrates the elements of the NAV-MSG. It consists of a 1 500 bit frame composed of 5 sub-frames of 300 bits each. Transmitted at 50 bit/s each subframe takes 6 s to complete. However, subframes 4 and 5 combined are 1/25 of the entire satellite constellation almanac. This means that to transmit the entire almanac takes 12.5 min to complete.

FIGURE 2-3

Navigation message

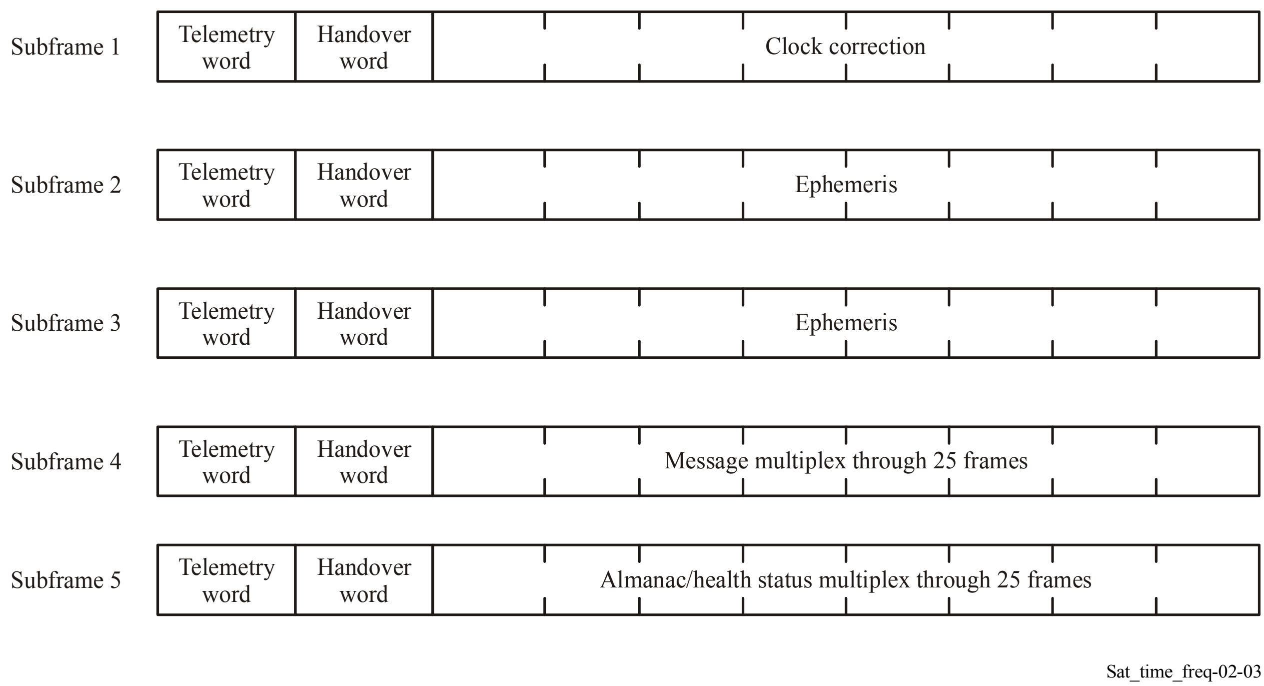

At the beginning of each sub-frame is the handover word or HOW. The HOW provides critical timing information required by Precise Positioning System (PPS) receivers to "handover" from C/A code to P(Y) code tracking. The HOW gives the absolute time of week of the beginning of the next sub-frame in units of 1.5 s. Thus a receiver that has decoded the HOW can unambiguously set its internal time based on this value.

The first two sub-frames contain information specific to the transmitting satellite. These data, collectively known as the ephemeris, include orbital parameters and clock error predictions. Sub-frame 1 includes 3 clock parameters that model the satellite clock deviation from GPS Time by a quadratic polynomial. The timing bias in seconds at the reference time (toc) is the af0 term; the frequency error in sec/sec at the reference time is the af1 term; and the frequency drift in sec/sec^2 is the af2 term.

An additional timing term included in the navigation message in subframe 4 is the UTC-GPS correction. UTC time can be computed from GPS and these parameters. This is also modelled by an offset and drift term. In the eventually of a leap second adjustment to UTC, an indication of the week of occurrence and when the leap second will be applied to the time output is contained in this subframe.

When the L2C and L5 become available they will both transmit an upgraded version of the NAV-MSG known as the CNAV message. Each of these signals will actually be a set of modulations onto the carrier frequency. A dataless acquisition aid called a pilot carrier in some cases broadcast alongside a data signal as an acquisition aid. This dataless signal is designed to be easier to acquire than the data encoded and, upon successful acquisition, can be used to acquire the data signal.

This technique improves acquisition of the GPS signal and boosts power levels at the correlator. The CNAV message will be on the data signal and will include the same information as the legacy message in an pseudo-packetized format of 12 s 300-bit message packets rather than the frame structure. It will use Forward Error Correction in a rate 1/2 convolution code. The resulting 100 symbols per second data stream is then added to the in-phase signal carrier to produce the data signal. The quadrature-phase carrier would then have no data and become the dataless pilot signal.

2.3 GPS segments

GPS is generally described as comprising three segments – satellites, control, and users. The burden of generating the signal is split between the satellites and the control segment.

2.3.1 Space segment

The nominal or operational GPS constellation comprises 24 satellites in semi-synchronous orbits. The satellites are deployed in 6 orbital planes at an inclination of 55°, with 4 satellites to a plane. The current constellation exceeds the nominal requirement for 24 functioning satellites and is shown in Fig. 2-4.

The satellites are three-axis stabilized to point the transmitting antenna array toward the earth and the solar panels toward the sun. Several "blocks" of satellites have been developed, beginning with the Block I prototype, up to the most recent deployment of the Block IIF satellites. Design of the next generation Block III satellites is currently ongoing.

The GPS signals are transmitted by an array of 12 helical antennas designed to produce a shaped pattern oriented toward the earth with almost constant received signal power at the surface of the earth. This was done to minimize inter-satellite interference and improve performance for the user. The GPS navigation payload includes 3 or 4 atomic clocks and electronics for generating spread spectrum signals derived from the clock. The use of atomic clocks was required to allow for improved orbit prediction and extended autonomous satellite operations in the event that the ground control segment was incapacitated. Thus, unlike a typical communication satellite which merely transponds signals generated by a ground station, the GPS satellites produce the reference signals onboard. Figure 2-4 shows the types of clocks onboard each satellite in the constellation as of 2008. At any time, only one of the clocks is used and the others are kept dormant until a failure or clock degradation occurs. The onboard clock serves as the frequency reference for producing the C/A and P(Y) codes and the L1 and L2 carrier signals.

FIGURE 2-4

GPS Satellites and clocks, as of December 2008

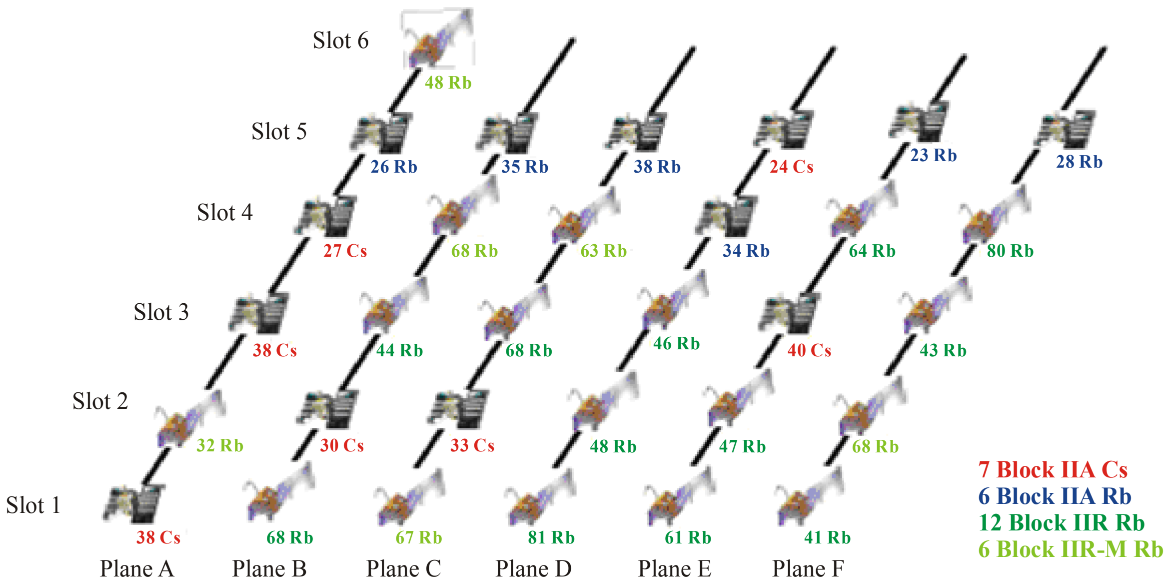

Sat_time_freq-02-04

2.3.2 Control segment

The control segment includes the Master Control Station (MCS) at Schriever Air Force Base outside of Colorado Springs, and DoD dedicated monitor stations in Hawaii, Ascension, Diego Garcia, and Kwajelein. The National Geophysical Intelligence Agency (NGA) also supports additional monitoring sites that provide GPS measurements to the GPS control segment to enhance ephemeris and clock accuracy. The monitor stations house PPS capable GPS receivers connected to high gain antennas that track GPS satellites across the sky. The monitor station receivers continuously record pseudorange, Doppler, and carrier phase measurements on both L1 and L2 at 1.5 s intervals.

The MCS is responsible for the analysis of the data collected by the monitor stations to determine the health and performance of the GPS satellite navigation payloads. The monitor station measurements are also processed by the MCS to determine the GPS satellite orbits and clock errors. The ephemeris and clock parameters in the navigation message are computed based on predictions of the orbits and clocks over the next 24 h. Navigation message uploads are performed typically once or twice per day.

2.3.3 User segment

User equipment for GPS is designed to passively acquire and track GPS signals. Figure 2-5 illustrates the key elements of a GPS receiver – the antenna, oscillator and frequency synthesizer, down-converter and analog-to-digital (A/D) converter, channel or signal processors, and navigation processor.

In a typical navigation receiver, the frequency reference is a quartz crystal oscillator; whereas in a time transfer receiver, an external reference oscillator may be supplied. The antennas are generally hemispherical with some installations employing so-called choke ring antennas to mitigate signal reflections from nearby surfaces [Misra and Enge, 2001]. Down-conversion and sampling produce IF samples of the noise-dominated GPS spectrum. By correlating the received samples with local replicas of the GPS codes, the receiver is able to acquire and make range measurements to each of the visible satellites.

FIGURE 2-5

GPS receiver generic block diagram

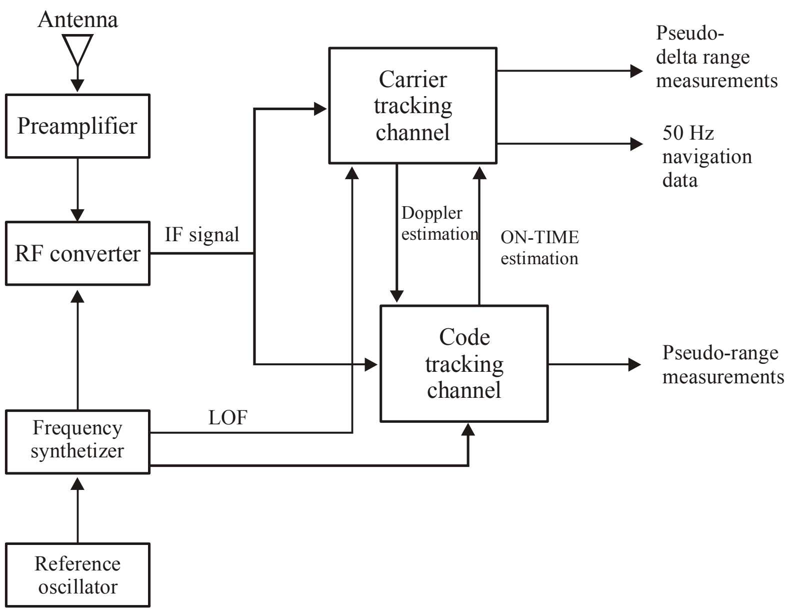

Sat_time_freq-02-05

2.4 Role of timing and synchronization in operations

This section describes the important role of precise timing in the normal operation of GPS for navigation and other applications.

2.4.1 Ranging measurements and performance factors

The measurement of one-way time delay and Doppler are the key measurements for GPS. Pseudorange is a measurement of the delay between the perceived arrival time of a signal at a receiver and the time of transmission of a signal from the GPS satellite.

In equation form:

$$PR = c(t_R - t_T) \tag{2-1}$$

The pseudorange is related to the position of the receiver as follows:

$$PR = R + b_R - b_T + I + T + MP + \varepsilon \tag{2-2}$$

Thus, errors in the assumed transmit time of the signal due to timing biases in the GPS satellite (b_T), the receive time of the signal due to timing biases in the receiver (b_R), ionospheric delays (I), tropospheric delays (T), multipath, and receiver errors (γ), all contribute to the pseudorange measurement error. Models to correct for the propagation delays are implemented in all GPS receivers. Receiver tracking errors (ε) tend to be high frequency and averaging over time can help to reduce their contribution. The error budget allotted to satellite clock prediction is given in Table 2-2 [Parkinson *et al.*, 1996].

The error contribution of the receiver clock, because it is not required to be an atomic oscillator, is essentially unbounded. Thus, this parameter must be estimated in the receiver navigation solution or eliminated through double differencing in a network solution.

TABLE 2-2

GPS system error budget

Error sources	Space (m)	Control (m)	User (m)	System (m)
Clock and Navigation subsystem stability	2.7	2.7	–	2.7
Satellite perturbation prediction	1.0	1.0	–	1.0
Other	0.5	0.5	–	0.5
Ephemeris and clock prediction	–	2.5	–	2.5
Ionospheric delay compensation	–	–	2.3	2.3
Tropospheric delay	–	–	2.0	2.0
Receiver noise and resolution	–	–	1.5	1.5
Multipath	–	–	1.2	1.2
Other	–	–	0.5	0.5
RSS	3.0	3.8	3.6	
System error (1 σ)				5.3

2.4.2 Satellite clock stability and prediction

The GPS satellite clock is the basis from which all transmitted signals are generated. As described in § 2.3.1, each satellite carries three or four redundant atomic clocks, only one of which is operated at any given time. The predictability of this clock determines the error contribution to positioning and absolute time transfer accuracy that can obtained by a stand-alone user, and the rate at which updates to the navigation message are required.

2.5 Assessment of GPS satellite clock performance

The Naval Center for Space Technology at the Naval Research Laboratory (NCST/NRL) monitors and reports on the performance of the GPS satellite clocks on a quarterly basis. An important aspect of the overall program support has been the evaluation of the on-orbit performance of the spacecraft atomic clocks to support development of new and improved space atomic clocks, evaluate system operational concepts, and measure system performance. The capability for accurate evaluation of GPS subsystem performance is enabled by a comprehensive, on-line database of NAVSTAR SV and MS observed pseudo-range data.

The database incorporates continuous data for the life of every NAVSTAR SV launched. Data from GPS operational control segment (OCS) and NGA monitor stations, as well as the precise post-processed NGA ephemerides are used to derive the clock signals from each operating atomic clock in the system.

This effort originated during NAVSTAR Block I joint NCST/NRL and GPS Joint Program Office (JPO) tracking of Navigation Technology Satellite Two and Block I demonstration satellites operating with the Interim Control Segment. It has extended into the operational Block II/IIA and IIR satellites and OCS operation.

In 2004 NRL began to produce clock estimates derived from carrier phase observations and precise ephemerides from the International GNSS Service (IGS). IGS consists of a federation of more than 200 national agencies, universities and research institutions in more than eighty countries.

Each participant brings contributes to a wide variety of GPS data acquisition and analysis products. These contributions result in the best models, analysis techniques, and data products available which in turn benefit each agency. IGS maintains more than 350 permanent continuously operating GPS tracking stations that use multi-channel, dual-frequency, code and carrier tracking receivers.

Common standards have been developed and accepted for data storage and exchange. The IGS Clock Products include estimates of GPS clocks and ground station clocks for both rapid and final products. IGS

Distributed Timescales (IGRT and IGST) are produced at NCST/NRL and provide a stable reference for analyzing GPS clock data that is independent of a single ground station clock.

The frequency stability of each operating SV and MS atomic clock is computed from data in the on-orbit database and evaluated from a continuous series of data. This analysis is independent of and complementary to other agencies analyses. Inter-comparison with other analyses is often coordinated informally as a test metric for independence. Nominal performance is reported in quarterly reports and detailed analysis is performed on observations indicating unusual or anomalistic behavior. The on-line archive of on-orbit data in the GPS database can be used to analyze past normal and anomalous clock performance. This on-line database enables frequency stability to be estimated from continuous data spans with averaging times ranging from 5 min to years referenced to a common standard.

Figure 2-6 illustrates the frequency stability of the satellite clocks in the GPS constellation.

FIGURE 2-6

Stability of GPS satellite atomic clocks

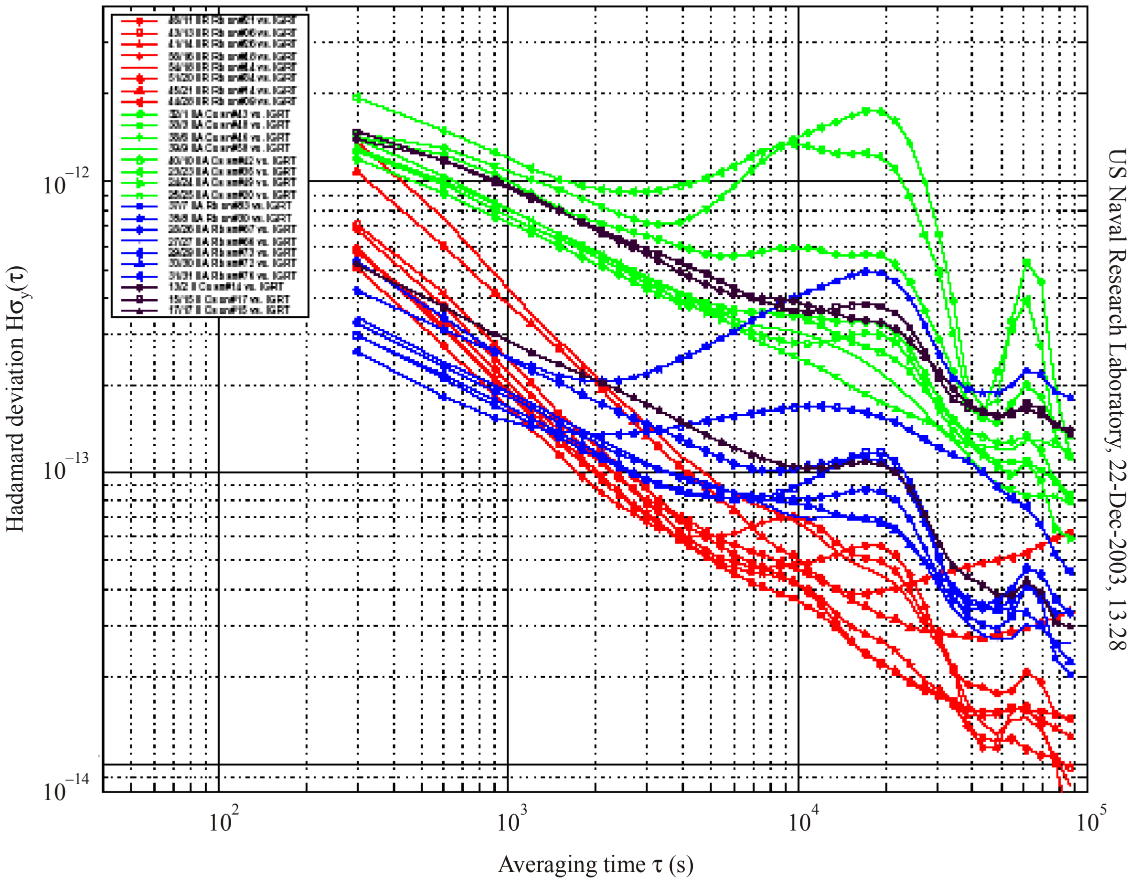

Sat_time_freq-02-06

2.5.1 Satellite path delays

In addition to the variability of the timing payload, path delays or differences within the GPS satellite also can contribute timing errors to the final user time transfer solution. In particular, differences in the path delay between L1 and L2 signal paths, differences in the phase and code delays, and antenna phase center variations must be considered.

The af0 and af1 clock corrections transmitted in the navigation message are computed for a dual frequency P(Y) code capable receiver. This is because the solution is based upon dual frequency observations from the

GPS control segment monitoring stations. The correction thus includes the effect of signal path differences on the ionosphere-free combination of P1 and P2. Single frequency users must apply a correction to the broadcast clock values, called the timing group delay (tgd). At one time a single tgd value was used for all satellites. However, individual group delay measurements were made for each satellite and are now included in the broadcast message.

Until recently, errors smaller than 1 carrier cycle (0.6 ns) were not considered significant for time transfer. However, with the advent of carrier phase-based time transfer solutions [Larson and Levine, 1999], phase center variations in the GPS antennas are now of increasing interest. Because of the right hand circularly polarized antenna, if the spacecraft were to make a complete revolution about the nadir direction, the carrier phase would wind-up by 1 full cycle (19.04 cm or 0.6 ns). Similarly, users receiving GPS transmissions in different parts of the earth will see different signal phase values. A correction for these offsets is now available for high precision applications [Larson *et al.*, 2000].

2.5.2 Relativity

Relativity plays a notable role in GPS timing and many articles and book chapters have been devoted to the subject. More detail on this important subject is contained in a later chapter. Here we mention only the key elements.

Because of its 20,000 km altitude above the geoid, a clock on-board a GPS satellite is affected by two relativistic effects that modify the frequency it generates. The combination of time dilation and gravitational frequency shift causes the GPS satellite clocks to run faster than an equivalent clock on the geoid by 38.59 μs/day.

To allow the satellites to more precisely produce the required signal frequencies as seen on the geoid, the spaceborne oscillators are offset to run 38.59 μs/day slower, so that the received signal frequencies are correct with respect to coordinate time on the geoid. In addition, a second relativistic frequency shift occurs because the satellite orbits are not perfectly circular. An approximate expression for the error resulting from this shift is given by:

$$\Delta t_r = \frac{2}{c^2}\sqrt{GM\,a}\; e \sin E = \frac{2\,\mathbf{r}\cdot\mathbf{v}}{c^2} \qquad (2\text{-}3)$$

where:

r and **v**: the position and velocity of the satellite and Δt_r is corrected in the GPS receiver processing using eccentricity information from the broadcast navigation message.

The magnitude of the timing error caused by the GPS orbit eccentricity is on the order of tens of nanoseconds and is the same for all receivers tracking the particular GPS satellite.

2.6 Receiver clock contributions

Within the GPS receiver, as in the GPS satellites, all timing is derived from a common oscillator. However, for most commercial and military receivers this reference is a quartz rather than rubidium or cesium standard. Receiver oscillator frequency errors and instabilities in the frequency synthesis section of the receiver manifest themselves in the measurement of Doppler and accumulated Doppler or carrier phase. Receiver clock bias errors or timing offsets and path delays in the receiver from the antenna to the A/D converter appear in the pseudo-range and carrier phase measurements, and in the time-tagging of the observations and position solutions. If measurements of all satellites are made simultaneously, the same frequency and bias errors are present in all measurements.

Several steps are typically implemented to establish time in the GPS receiver. This time base is referred to as receiver time or local time. Upon power up in a warm start mode, the receiver sets its time based upon values stored in non-volatile memory. Depending on the particular receiver, this is likely to be accurate to one second or worse. In cold-start it will have no knowledge of time and the starting time is initially set arbitrarily.

When the first satellite ephemeris message is decoded, the local time may be set to within 1-10 ms based upon the time of week (TOW) present in the navigation message. The accuracy of this initial time setting determines the remainder of the clock solution that must be corrected subsequently. The local time at the interrupt corresponding to the next measurement epoch is set equal to the TOW of transmission, plus the estimated time required for the signal to travel from the satellite at the time of transmission to the receiver location at the time of reception. A position estimate accurate to within 100 km is sufficient to set this to well within 1 ms. (For a receiver on the earth surface the transit time ranges from about 67 ms for a GPS satellite transmitter directly overhead to about 85 ms for a transmitter on the horizon.)

Once the local time has been established to within 1 ms, the clock bias is estimated as part of the applications processing. In some receivers, the bias is retained as what is known as a paper clock correction, that is, no physical adjustment is made to reduce the bias, but the value is monitored and reported. In some receivers, measurement timing is adjusted to compensate for the bias so that measurements are actually made on the GPS 1s epochs. This is particularly important for geodetic receivers where the measurements from multiple receivers are coordinated to achieve high precision kinematic or static relative positioning. Finally, some receivers do not adjust the actual time that the measurements are made, but do correct the reported time tags and measurements for the bias.

2.6.1 Navigation receiver clock

For most navigation applications, the actual value of the clock bias is not very significant. Synchronization of measurements with GPS time epochs is only necessary if coordination with other receiver measurements is to be performed, and even then it is only critical for applications requiring centimeter to millimeter precision. Correct time tagging of measurements and navigation solutions is important for fast moving platforms such as high speed aircraft and satellites. A subtle point on timing for near earth satellites is that a time tagging error of 1 ms produces along-track positioning errors on the order of 7 m. Meter-level positioning errors are also possible for similar time tagging errors on other platforms with high dynamics.

Pseudo-range biases and frequency errors resulting from the receiver clock bias are reliably solved for as part of the navigation position and velocity solution. Typically these values are not of interest in navigation applications. In relative navigation and survey applications a popular technique is the use of carrier phase double differencing [Misra and Enge, 2001]. This approach removes the clock bias parameter from the solution by differencing pairs of simultaneous observations from two receivers and two satellites. If measurement correlations are treated properly, double difference point solutions are equivalent to relative position solutions in which the clock is solved for.

2.6.2 Timing receiver clock

2.6.2.1 Relativity

In a receiver specifically designed for time transfer, the internal oscillator is typically bypassed or omitted in favor of an input from an external reference oscillator and One Pulse per Second (1 PPS) reference signal. The relativistic corrections are required to correct frequency and timing offsets of the GPS satellite clocks. Similar relativistic effects occur on the receiver clock for highly dynamic platforms. These shifts are common to all measurements, so they do not affect the navigation solution accuracy. For time transfer to a fast moving platform, the relativistic shifts of the reference oscillator should be compensated.

2.6.2.2 Paper clock corrections

As mentioned above, most GPS receivers do not modify their internal timing to correct for estimated clock errors. The errors are estimated and noted as “paper clock” corrections. In some cases the corrections are applied to times displayed and reported, and to the reported measurements.

2.6.2.3 Corrected output clocks – Frequency and 1 PPS

A timing receiver that is required to output a corrected frequency and 1 PPS signal, must internally apply the clock corrections to produce these synchronized outputs. This may be done by a closed loop adjustment of the internal oscillator or the frequency synthesis section of the receiver, or using a separate open loop circuit to generate the corrected signals. If performed in closed-loop, the control must be implemented in such a way as to not disrupt the signal tracking functions.

2.7 Determination and maintenance of timing

The basis for all GPS measurements is the so-called GPS Time (GPST). GPST is a continuous time base established at the GPS epoch, 00:00 January 6, 1980 UTC. GPST is related to the international time scale Universal Coordinated Time (UTC) by way of UTC (USNO) [ICD–GPS–202B Navstar, 2001]. However, unlike the UTC time scale, GPST does not apply leap second steps, and thus, continues to drift away from UTC with an offset which is currently 14 s. The control segment is responsible for maintaining GPST based on input from the USNO and monitoring the timing performance of each GPS satellite. The satellite transmissions are linked to GPST and by using measurements to the GPS satellites a receiver can connect its local time to GPST and subsequently to UTC (USNO).

2.7.1 Control segment operations

Since June 17, 1990, GPST time has been defined by a composite or ensemble of atomic frequency standards at the Master Control Station (MCS), the GPS Monitor Stations, and the satellite on-board clocks. Actual GPST time is not physically maintained by any one clock within the system. It is computed implicitly by a Kalman filter that operates as part of the MCS analysis and prediction function. Measurements from the individual frequency standards are weighted according to their stability during the estimation interval.

GPST thus consists of a weighted average of an ensemble of atomic clocks. Paper clock corrections for each frequency standard are also computed with the GPS satellite clock corrections forming the basis for the parameters transmitted in the broadcast message.

The MCS uses measurements from the monitoring stations to estimate the GPS satellite orbits and clocks, the monitor station clock errors, and other parameters. The MCS estimator divides the measurements and states to be estimated into several “partitions” each of which processes a subset of the GPS satellites and all the monitor stations. Partitioning originated due to computational limitations of the early MCS computers, but has been continued to ease the computational burden and to aid in the isolation of individual satellite problems [Hutsell, 1994]. Each partition includes states for up to six satellites and five GPS monitor stations. A separate “partition reconciliation” algorithm adjusts the MS states for consistency across the partitions.

A “grand average” across the partitions provides the MCS with the best estimates of the monitor station and satellite clock deviations from GPST.

The U.S. Naval Observatory (USNO) is responsible for maintaining a physical time reference for the U.S. Department of Defense. UTC(USNO) is the real-time realization of UTC for the DoD. USNO also maintains the USNO Alternate Master Clock (USNO/AMC) at the GPS MCS at Schriever AFB.

The USNO monitors GPS satellite Standard Positioning Service (SPS) and PPS transmissions using specialized timing receivers located in Washington, D.C. Measurements from individual satellites are collected at 6 s intervals over a 13 min track. The tracks for all satellites are used to form a 2-day linear fit for the estimate of the GPS-UTC (USNO) correction parameters a_0 and a_1. The r.m.s. of the 13 min solutions is on the order of 15-20 ns. The individual satellite observations and the linear estimates are provided to the MCS and are manually input to the MCS software in order to keep the GPS system a closed system with no external inputs.

2.7.2 GPS time steering

GPST is mandated by the interface control document to be maintained within ±1 μs of UTC (USNO) with the exception of the leap second offsets [ICD–GPS–202B Navstar, 2001]. Thus, GPST is steered into alignment with UTC (USNO) to meet this requirement. Steering is accomplished by analyzing the daily estimates of the GPS-UTC(USNO) bias, and determining if steering is required over the following day in order to keep the GPS-UTC(USNO) offset within specification.

The steering consists of setting a positive or negative fixed offset drift into GPST for one day. A fixed drift value of $\pm 2 \times 10^{-19}$ s/s^2 was used prior to 18 March 1994 and since then a value of $\pm 1 \times 10^{-19}$ s/s^2 has been used. Steering is implemented by modification of the broadcast satellite clock corrections and GPS-UTC corrections, and is transparent to the users [Hutsell, 1994]. If unnecessary steering were implemented, GPS users would see it as instability in GPST.

References

HUTSELL, S.T. [Sep 20-23, 1994] Recent MCS Improvements to GPS Timing. Proc. ION GPS-94, Salt Lake City, UT, p. 261-273.

KAPLAN, E.D. and HEGARTY, C.J., Editors [2006] Understanding GPS: Principles and applications. *2ed*., Artech Hose, Inc., 685 Canton Street, Norwood, MA 02062.

LARSON, K.M., *et al*. [March 2000] Assessment of GPS Carrier-Phase Stability for Time-Transfer Applications. IEEE Transactions on Ultrasonics, Ferroelectrics, and Frequency Control, Vol. 47, **2**, p. 484-494.

LARSON, K.M., and LEVINE, J. [July 1999] Carrier-Phase Time Transfer, IEEE Transactions on Ultrasonics, Ferroelectrics, and Frequency Control, Vol. 46, **4**, p. 1001-1012.

MISRA, P. and ENGE, P. [2001] Global Positioning System – Signals, Measurements, and Performance, Ganga-Jamuna Press.

Naval Observatory Time Transfer Interfaces ICD-GPS-202B [31 October, 2001] Navstar GPS Control Segment/U.S.

Navstar Global Positioning System Interface Specification IS-200 rev D [2006] Navstar GPS Space Segment/ Navigation User Interfaces, IRN-200D-001, ARINC Engineering Services, LLC, El Segundo, CA 90245.

PARKINSON, B.W., *et al*., Editors [1996] Global Positioning System: Theory and Applications, AIAA Press.

CHAPTER 3

SATELLITE BASED AUGMENTATION SYSTEM TO GPS

Page

3.1 Introduction

Historically, navigation systems have depended on time. This was clearly demonstrated by the sailing of Harrison's chronometer on HMS *Deptford* in 1761, to prove that the instrument allowed navigators for the first time to determine longitude accurately and reliably. Because of this relationship between navigation and time, the timekeeping community has always had a keen interest in the use of navigation systems for the *distribution* of time. Even today, the heart of the GPS rests on a highly evolved clock technology. Unlike navigators, who need four GPS satellites by which to determine their position, timekeepers who know their position need only one satellite to determine time. Observations of a single satellite could allow timekeepers to remotely synchronize clocks around the world.

3.2 Description of an SBAS

Satellite based augmentation systems (SBAS) are one of the most recent developments in the evolution of navigation systems. While they are similar to differential GPS systems in concept, SBAS give national civilian aviation administrations and air navigation a significantly higher level of performance than other differential GPS (DGPS) systems. Because of the augmentation methods utilized by SBAS, they provide not only improved accuracy, but also increased availability, integrity, and continuity of service. They do this by continually monitoring GPS transmissions from ground reference stations and by transmitting an augmenting message from geostationary communications satellites (GEOs). The signal from a GEO, while using the same frequency as the GPS L1, is different in format and bit rate.

The content of the message coming from the GEO gives to the user information that improves not only the accuracy of the user position determined from GPS signals but also gives to the user information concerning the reliability of that position. The signal from the GEO can also be used as another ranging source for navigation. But for this to happen, the signals must be synchronized to GPS Time.

Consequently, the signals from the GEO can also be used for time distribution and time transfer. Current studies on the use of SBAS for these timing functions indicate that they are already at the level of the GPS precise positioning system (PPS). We can reasonably expect improved levels of precision and accuracy as the systems mature.

3.3 WAAS description (United States of America)

Figure 3-1 schematically depicts the wide area augmentation system (WAAS) process. The basic unit is the WAAS reference station (WRS). Within the reference station, there is equipment that consists of redundant cesium beam frequency standards or other form of atomic clocks, several 12-channel, dual-frequency WAAS/GPS receivers, and specialized wide- and a narrow-band phase tracking GPS receivers. Each reference station continuously tracks as many GPS satellites and GEOs as it is able to see and acquire.

Each WRS performs the functions of data collection, reasonability checking, data processing, data recording, and data transferring. Each WRS consists of a triple redundant Wide-area reference station equipments (WREs) rack which collect independent sets of data including GPS satellite observables and GEO satellite observables and which transmit the data to each WAAS Master Station (WMS) in the system. Independence of the data sets is ensured by gathering the observable parameters through independent sets of hardware that are necessary to support the verification function performed by the WMS. The data is collected at a rate consistent with its expected level of variation; e.g., slowly changing weather conditions allow this data to be collected less frequently than data from the GPS satellites. Prior to transmitting data to the WMSs, each WRE verifies the reasonability of its collected data. Failed data is marked as having failed the reasonability test and is then forwarded to the WMSs. To ensure the availability of the data at each WMS, each WRS transmits data to each WMS through two independent backbone nodes of the terrestrial communications subsystem (TCS).

FIGURE 3-1

Simple, high-level overview of an SBAS System

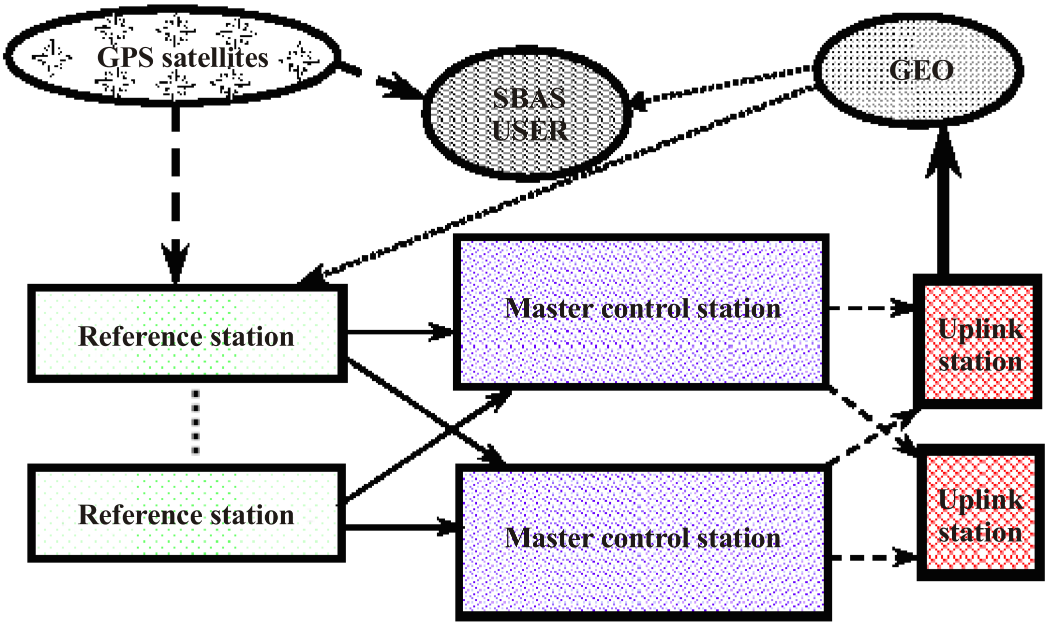

Sat_time_freq-03-01

Each WMS performs the functions of correction processing, satellite orbit determination, integrity determination, verification, validation, and WAAS message generation. Once per second, the WMS collects the data received from all WRSs and processes it to support the functions listed above. This processing is performed on all available WRS data and results in the transmission of a formatted 250-bit WAAS message once per second. These WAAS messages are sent to all Geostationary Uplink Subsystems (GUS).

The timing of WMS processing is scheduled to allow broadcast of the resulting WAAS message from the GEO satellite coincident with the following GPS 1-s Coarse/Acquisition (C/A) code epoch [Peck *et al.*, 1997]. The WAAS validates the Signal-in-Space (SIS) by checking the downlinked messages to ensure that they are identical to those transmitted to the GEO satellites and by comparing navigation position solutions from WAAS/GPS with the surveyed WRS locations. Each WMS includes an Operation and Maintenance (O & M) console from which control over the WAAS can be exercised via a computer human interface. To avoid conflicts, only one WMS within WAAS can be designated as the controlling WMS (active O & M console) at any one time.

Each geostationary communications system (GCS) performs the functions of broadcast and ranging. Each WAAS GCS consists of two signal generator subsystem (SGS), two RF Uplink (RFU) subsystems and one geostationary Earth orbiting (GEO) satellite. The combination of a SGS and a RFU is a GEO uplink station (GUS). The GCS broadcast function starts with the GCS receiving the 250-bit formatted WAAS messages once each second from each WMS in the System. To improve the availability of WAAS messages, each GUS is connected to two WAAS backbone nodes on the TCS. The GUS selects one WMS as its message source and encodes the received message using a 1/2 rate forward error correcting convolution code. The resulting 500-bit message is modulated on a GPS-type signal and uplinked to the GEO satellite. Each GEO satellite is served by two GUSs:

– one operating as the primary uplink; and
– the other operating as a hot standby.

The two GUSs serving a GEO satellite are operationally independent and located at geographically diverse ground earth stations (GES) separated by a minimum of 300 miles. A GES is a facility consisting of one or more GUSs, and provides shelter, power, and operations and maintenance services for the GUS. The GEO satellite "bent-pipe" transponder shifts the frequency of the signal and broadcasts it to the WAAS users. Transition between primary and backup GUS is initiated, when necessary, to maintain the availability of the WAAS signal-in-space.

The GCS ranging function is accomplished by transmitting a signal to the users on the GPS L1 frequency with the following information:

1. a precisely timed pseudo-random noise (PRN) code which is assigned to each GEO satellite
2. a precise ephemeris which is contained in the GEO Satellite Navigation Message sent periodically in the broadcast function.

This signal structure is achieved in a similar manner to that of GPS, except that the precise timing of the PRN code is carried out on the ground rather than on the GEO satellites. This function will allow the users to apply the GEO satellites as another GPS satellite, thereby increasing overall system availability.

3.4 MSAS description (Japan)

3.4.1 Overview

MSAS, multi-function transport satellite (MTSAT) satellite-based augmentation system, is configured as shown in Figure 3-2. GPS satellite data is received by ground monitoring stations (GMSs) installed at four locations in Japan; Sapporo, Tokyo, Fukuoka and Naha. The GPS satellite data and MTSAT geostationary satellite signal are also received by monitoring and ranging stations (MRSs) installed at other four locations; Kobe, Hitachiota, Hawaii and Australia. The received data is sent to master control stations (MCSs) installed at two locations in Japan; Kobe and Hitachiota.

FIGURE 3-2

MSAS configuration

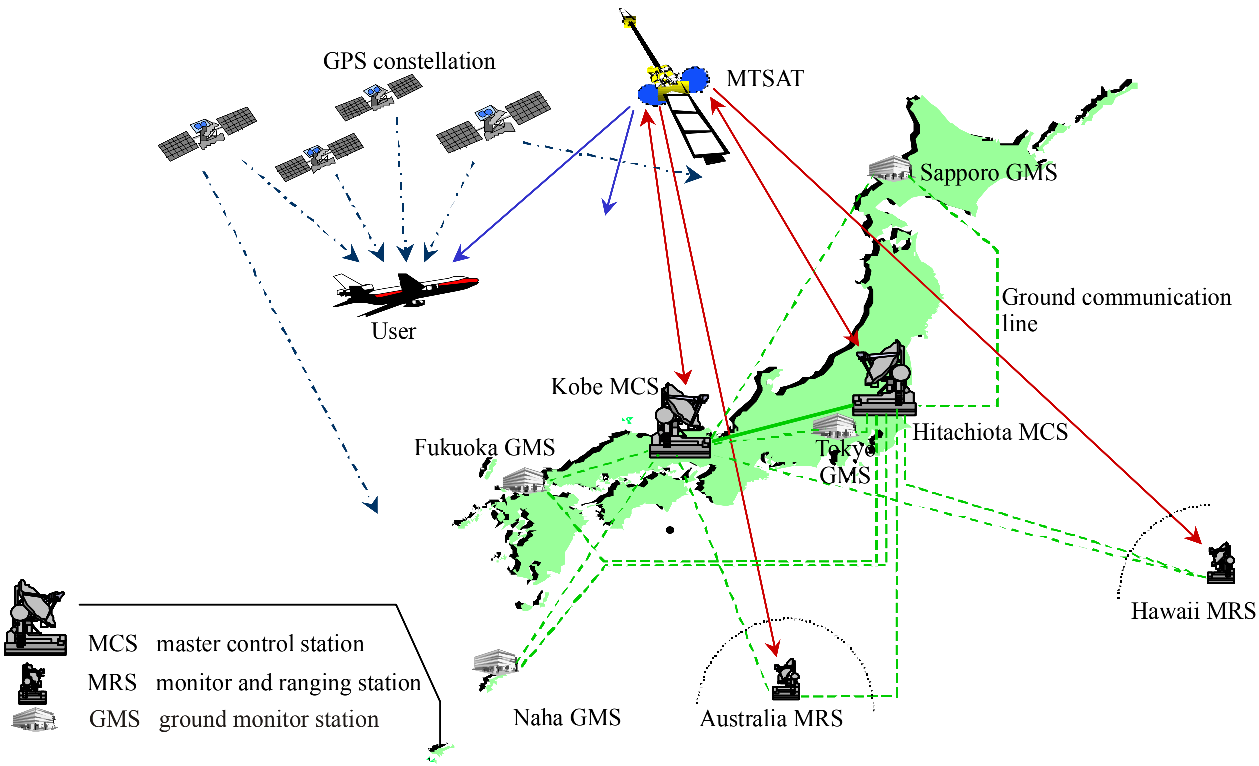

Sat_time_freq-03-02

In the MCS, the central processing facility (CPF) subsystem calculates corrections for satellites and Iono Grid Points (IGPs) which are predefined in MSAS, and monitors the integrity. MSAS network time (MNT), which is internal network time of MSAS, is maintained so that its deviation from GPS time is within a specified limit. The navigation earth station (NES) subsystem generates MSAS messages using the data from CPF, and modulates them to the Ku band. The MSAS messages are uplinked to MTSAT satellite from collocated ground earth station (GES) after the amplification by high power amplifier (HPA). In addition, communication between the ground facilities is handled by network communications subsystem (NCS).

The MSAS ground facilities have many features common to WAAS. On the other hand, MSAS features its own characteristics, i.e., Dual PRN function to operate with two types of PRNs for one geostationary satellite and uplink power control (UPC) to compensate the Ku band rainfall attenuation.

3.4.2 Dual pseudo-random noise function

MSAS normally operates with two MTSAT geostationary satellites (MTSAT-1R, MTSAT-2) as shown in Figure 3-3. Different pseudo-random noise (PRN) codes are uplinked to two MTSATs separately. Even when either of the MCSs is not available due to a failure in the ground facility or due to heavy rain, one of the PRNs continues to be distributed to a user because the user can receive more than two channels of signals from MTSAT geostationary satellites to prevent degradation of continuity and availability. If one of the MTSAT geostationary satellites fails, MSAS can switch itself to the Dual PRN operation.

FIGURE 3-3

Dual PRN operation

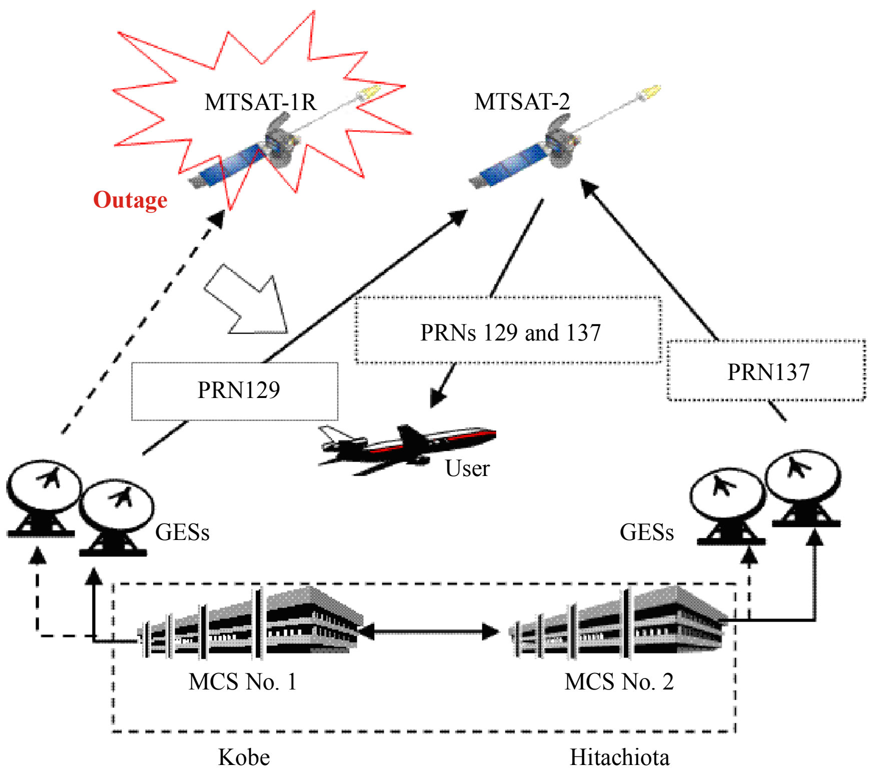

Sat_time_freq-03-03

In the Dual PRN operation, different PRNs are uplinked from two MCSs to one geostationary satellite. The interruption of uplink due to rainfall attenuation is small factors contributing to degradation of continuity in

MSAS. In the Dual PRN operation, even if the Ku-band attenuation due to heavy rain exceeds the compensation by the UPC in either MCS, the operation is continued by the PRN which is uplinked from other MCS, without requiring any switching between MCSs.

3.4.3 Uplink power control

During rainfall, MSAS controls the uplink power by the closed loop control to compensate the rainfall attenuation of the Ku band uplink signal in order to stabilize the link between MTSAT geostationary satellites and GESs. Uplink power control (UPC) uses L1-C/N_0 data of MTSAT geostationary satellites obtained by the UPC receiver that is installed in HPA. The closed loop control is performed by controlling the attenuator in the HPA based on the measured value of L1-C/N_0 and the predefined target value of C/N_0.

In addition, to ensure the control, C/N_0 in the Ku band is also used.

3.5 EGNOS description (Europe)

The EGNOS is composed of four segments: ground segment, space segment, user segment and support facilities similar to the segments described for the WAAS and MSAS.

1. The EGNOS Space segment is composed of transponders on board GEO satellites.
2. The EGNOS User segment consists of GNSS Standard receivers developed according to RTCA MOPS DO-229.
3. The EGNOS Support segment includes some facilities needed to support System Development, Operations and Qualification.

Finally, the EGNOS Ground segment as described § 3.5.1.

3.5.1 EGNOS ground segment overview

The EGNOS Ground segment consists of ranging and integrity monitoring stations (RIMS), which are connected to a set of redundant control and processing facilities called mission control center (MCC). The MCC determines the integrity, ephemeris and clock differential corrections for each monitored satellite, ionospheric delays, and generates GEO satellite ephemeris. This information is sent in a message to the navigation land earth station (NLES), to be up-linked along with the GEO Ranging Signal to GEO satellites. These GEO satellites downlink this data on the GPS Link 1 (L1) frequency with a modulation and coding scheme similar to the GPS one. All ground Segment components are interconnected by the EGNOS wide area communications network (EWAN).

3.5.2 EGNOS system overview related to time

The following sections will provide in response to the requirements, a description of each time functions and the expected performances, based on analysis and experiment.

Both GPS and GLONASS use time difference of arrival (TDOA) as the basis for the formation of receiver-to-satellite range measurements. Therefore, accuracies of the receiver and satellite clocks involved have a direct impact on the range measurement accuracy achieved. Both GPS and GLONASS satellites provide information in their broadcast navigation messages that enable system users to correct for satellite clock errors; i.e. the offset of individual satellite clocks from the nominal satellite system time-scale. These corrections are accurate to within a few ns.

However, in the case of GPS, they do not account for selective availability (SA) dither, and unless they are estimated and removed, they will degrade user-positioning performance. Furthermore, for high integrity applications it is desirable to produce independent estimates of the satellite clock errors, in order to monitor the broadcast corrections.

In order to determine highly accurate estimates of satellite clock errors and disseminate them to system users, the EGNOS system performs three basic clock functions located in the Central Processing Facility:

– RIMS clock synchronization and generation of the EGNOS Network Time (ENT).

– Steering of ENT to GPS time.

– Determination of the satellite clock offsets from ENT.

Estimation of the difference between ENT and UTC.

3.5.3 RIMS clock synchronization and generation of ENT

RIMS clock synchronization is performed using the *composite-clock* technique. In the composite-clock technique, ENT is defined as the implicit ensemble mean of all RIMS clocks and the synchronization process generates estimates of the offset and drift of each RIMS clock relative to it. These estimates can then be used to reference all RIMS's pseudo-range measurements to ENT. This synchronization process is necessary in order to allow simultaneously observed pseudo-range measurements from multiple RIMS to be combined in the function that estimates satellite clock errors.

A simpler, alternative synchronization technique is the *master-clock* technique, whereby one RIMS clock is nominated to provide the network time and all other RIMS clocks are synchronised to that clock. The composite-clock method has two significant advantages over this approach. Firstly, the master clock approach has a single point of failure; if the master clock is lost, ENT is lost. In contrast, the composite-clock ENT is maintained as long as there are two clocks in the ensemble. Secondly, the stability of ENT provided by the master-clock method is of course limited to the stability of the master clock itself. With the composite clock technique, the stability of ENT becomes the stability of the implicit ensemble mean of all of the RIMS clocks. Assuming an ensemble of n identical, independent, clocks, this gives a $\sqrt{n}$ improvement in stability. This last feature of the composite clock has the important side effect of increasing the ability of the system to detect and isolate clock failures.

The composite clock algorithm is executed by means of a Kalman filter. The filter measurement data comprises a linearly independent set of *common-view* observations with minimum a priori variance. A common-view observation for a pair of RIMS is formed by subtracting simultaneously observed pseudo-range measurements to a common satellite. Before subtraction, the pseudo-ranges are *pre-processed* to remove RIMS antenna-to-satellite antenna geometric ranges and reduce unwanted errors, such as multipath delays and thermal noise. The resulting common-view observations represent direct measurements of the RIMS's clock offsets plus residual errors.

The filter states comprise the offsets and drifts of each RIMS's clock relative to a hypothetical *ideal* time-scale. The consequence of this formulation is that the filter provides estimates the offsets and drifts relative to, the *implicit*, weighted average of all of the RIMS clocks. This implicit ensemble mean essentially defines the EGNOS time-scale, ENT. The relative weighing of clocks used within the filter is dependent upon several factors, but is largely determined by the process noise models associated with each of the clocks. These models characterise RIMS clock stability.

Since only clock difference measurements are available to the filter, the filter model has unobservable components that cause secular growth trends in the state error covariance matrices. Special measures must be employed to remove these trends. Otherwise they will eventually lead to numerical instability within the filter. It can be shown that, once the secular growth trends due to the unobservable components of the system model have been removed from the covariance matrix, the resulting covariance describes the errors in the filter state estimates relative to the implicit ensemble mean, *not* the ideal time-scale.

3.5.4 Steering of ENT to GPS time

In order to limit the dynamic range of the satellite clock corrections, thereby reducing the size of the WAD clock messages and improving the efficiency of the message dissemination process, it is necessary to steer ENT to the GPS time-scale. Steering of ENT to the GPS time-scale is performed using a second order, low-pass digital filter. The steering input signal is an instantaneous estimate of the ENT–GPS time-scale offset. This is computed from the estimated satellite clock offsets from ENT and the GPS broadcast satellite clock corrections, which are estimates of the satellite clock offsets from the GPS time-scale. The cut-off frequency of the filter is chosen to provide the best reduction of Selective Availability (SA), whilst avoiding significant lags due to the relative drift of ENT with respect to the GPS time-scale. The more stable ENT is, the lower the cut-off frequency can be set and the greater the reduction of SA.

The EGNOS system baseline will easily meet the ENT-GPS time-scale steering requirement of < 50 ns. The all caesium scenarios examined demonstrate that a steering accuracy of < 3 ns can be achieved. These results must be treated with caution, since they are based upon synthetic data sets with idealised models of SA and RIMS clocks. However, the results are consistent with other findings, such as those quoted in [Benedicto *et al.*, 1998].

Steering accuracy of < 3 ns will allow ENT realisations from different CPFs to be synchronised autonomously, without need for a dedicated ENT-A to ENT-B synchronization function. However, if such a function is required, experimentation with real and synthetic data has shown that synchronization of different ENTs can easily be achieved with an accuracy of better than 3 ns (2σ). This is the system requirement imposed to make CPF switchovers transparent to EGNOS users.

3.5.5 Satellite clock corrections

Satellite clock corrections and correction rates are computed using all available pseudo-range and Doppler measurements from the pre-processing function. The measurements are referenced to ENT using the RIMS synchronization parameters and then collected into groups by satellite. For each satellite, weighted least-squares estimates of its clock's offset and rate-of-change with respect to ENT are computed. The offsets are later separated by low-pass filtering, similar to that used for the ENT steering function, into the slow and fast components which comprise the satellite clock correction messages. The rate-of-change estimates are used to project the corrections forward in time by the expected system latency.

3.5.6 Broadcast ENT through geostationary Earth orbit (GEO) satellites

The satellite fast and slow clock corrections are disseminated to EGNOS users in via the GEO satellite in separate messages. The EGNOS user receiver decodes these messages and reconstitutes the combined satellite clock offsets from ENT for each of satellite it tracks and applies them to its pseudo-ranges, together with other WAD corrections provided by EGNOS. In this way, the ENT time-scale replaces the GPS-, or GLONASS-, time-scale in the receiver's navigation solution. Hence, not only does the receiver compute an improved estimate of position, because of the WAD corrections, it also computes an estimate of its internal receiver clock offset from ENT.

Once available on the ground, ENT has to be accurately transferred on board GEO satellites. Indeed, the GEO time is defined at the output of the GEO payload, precisely at the L1 antenna centre of phase. This function is ensured by the so-called Long-Loop, a servo-control mechanism, based on the almost symmetry between the up and down links from the NLES to the GEO satellite.

3.5.7 Estimation of the difference between ENT and UTC time-scales

UTC being a theoretical average of many clocks around the world, it is not possible to establish a direct link between ENT and UTC. Instead, it is necessary to use a physical clock participating to the elaboration of UTC.

Therefore, the time difference between ENT and UTC can be broken down into 2 terms:

$$\mathrm{ENT} - \mathrm{UTC} = [\ \mathrm{ENT} - \mathrm{UTC}(k)\ ] + [\ \mathrm{UTC}(k) - \mathrm{UTC}\ ] \tag{3-1}$$

where:

k standing for any European laboratory participating to the elaboration of UTC.

3.5.7.1 UTC(k) – UTC

The time differences (UTC – UTC(k)) are made available on a monthly basis by the BIPM through the Circular T, and are out of the scope of EGNOS.

Performance of the time difference (UTC – UTC(k)) is as follows:

– IUT and CCDS Recommendation is to keep (UTC – UTC(k)) within 100 ns (1σ).

– The estimated uncertainty for the time differences (UTC – UTC(k)) is currently at the level of 10 ns (1σ), provided in deferred time by *Circular T*.

– The estimated uncertainty of a prediction of the time difference (UTC – UTC(k)) depends on the period of prediction, and could be in the range of 20 ns (1σ).

3.5.7.2 ENT – UTC(k)

To synchronise ENT and UTC(OP), an EGNOS RIMS will be co-located with the SYRTE laboratory located in Paris Observatory, to be physically connected to its atomic clock (with interfaces at 10 MHz and 1pps levels). EGNOS RIMS synchronization module will estimate directly the time difference between ENT and RIMS(OP) with an uncertainty of less than 3 ns (2 σ). The time difference will be broadcast with Message Type 12 with the above uncertainty. See Appendix A for a brief description of the SBAS Message Content transmitted by an SBAS geostationary satellite.

3.5.8 SBAS and time

The main advantage of an SBAS for timekeeping is that it uses a geostationary satellite as a supplemental ranging satellite to GPS. Specifications for an SBAS are set such that the signals coming from the GEO will be on time to GPS Time to within 50 ns. Because the GEO stays at the same point in the sky a fixed, highly directional antenna such as, a feed horn or a dish, can be used to track the satellite by a timekeeping laboratory. Such an antenna gives increased signal to noise ratios and also helps to mitigate multi-path. Such an antenna should also help mitigate interference. In addition, one can track the GEO continuously during the evening when ionospheric activity is at a minimum, especially in the mid-latitude regions where scintillation is at a minimum.

There are many different types of timekeeping experiments to which an SBAS should be able to contribute. These include calibration experiments, multi-path mitigation experiments, comparisons between different timekeeping laboratories and comparisons between different SBAS.

Calibration, or measurement of the delays through a system, is a special concern for timekeeping. Estimating the delay through a timing system is crucial in accurately evaluating the difference between two clocks. Zero-baseline experiments [Brown, 1991] have played an important role in this process. An SBAS because of its continuous availability can provide a platform for long-term measurements in this area.

3.5.8.1 Time and the reference stations

The recording of the time of observations is an area of concern for an SBAS. All observations are made at the independent SBAS reference stations (SRS). In order to insure a uniform time basis at each SRS, a clock based on GPS Time is used as the reference.

Each SRS usually contains a number of independent threads referred to as reference station equipment (RSE). These threads are required for sufficient redundancy to provide data to the SBAS Master Station (SMS) in the event a single failure in the SRS occurs. In addition to other commercial off the shelf (COTS) components contained in the SRE, there is usually a Caesium Beam Frequency Standard (Atomic Clock).

The Frequency Standard needs to meet certain specifications to be useful in a SBAS architecture. The functional requirements include:

– accuracy;

– settability;

– stability;

– single side band phase noise;

– Warm-up time.

Accuracy shall be at least 2×10^{-12} with no aging for the life of the Caesium tube , so it can be tuned to a specified frequency. The frequency standard provides each reference station receiver a 10 MHz sinusoidal wave reference signal with a stability of at least 2×10^{-13} over 24 h in order to accurately compare GEO signals with GPS time. The SRS frequency standards require communication via some interface for interrogation and parameter adjustments.

The 10 MHz output from the Caesium Beam Frequency Standard is sometimes input to a GPS receiver which provides a 1 PPS output used as the epoch of observations. The receiver clock is set to GPS Time at start-up. Thus, SRS receivers are approximately synchronized to the several microsecond level. The output data stream of each SRS receiver, contains a parameter which has the offset of the receiver 1 PPS from GPS time. After that, the output 1 PPS is governed by the rate of the input caesium clock. In essence, the output from the SRS receiver is a free-running clock. This is necessary for the formation of an independent time scale.

3.5.8.2 Time and the Master Station

The SMS embodies processing equipment necessary to generate the corrections that are transmitted by the GEO and verify them. It also should perform operations and maintenance (O & M) functions, and have a GPS clock for synchronization with GPS.

The SMS performs several functions. Those involving time, directly or indirectly, include:

a) Determine GPS/GEO satellite orbits;

b) Monitor signal-in-space (SIS) performance;

c) Generate SNT;

d) Generate SNT/UTC offset message; and

e) Generate SBAS messages.

The data from the reference station equipment for each SRS is sent to the SMS corrections processor and the data from each single SRS are compared. The clocks are monitored relative to each other to determine if one clock is "bad", i.e., has a significant change in offset. This is the start of the formation of SBAS Network Time (SNT) that is described in § 3.5.8.3.

3.5.8.3 SBAS network time

In order for an SBAS signal to supplement the GPS navigation signals, the SBAS transmissions must be synchronized to them, i.e., GPS Time. This is done by establishing SBAS network time (SNT) as the reference time for the SBAS. SNT is steered to GPS Time. Measurements from all reference stations at all SRSs are sent to each master station where an algorithm computes an independent SNT time scale from the data received from the reference stations. All "good clocks" involved in the reference station measurements that a master station receives are used to form the SNT time scale. This time scale is then steered to the GPS with the same algorithm. The SNT algorithm sketchily described above is implemented in each master station.

The SBAS messages include fast and slow corrections that are transmitted by the GEO. Fast corrections shall be determined for each GPS satellite vehicle (SV). This is accomplished by using the long-term correction message that was broadcast from a GEO to remove the long-term clocks from the extrapolated fast correction. Note that the total of the long term and fast corrections must be added together.

It is estimated that the once per day steering may not be sufficient to keep SNT close to GPS Time. Therefore, the hardware steering will be supplemented by correction messages within the SBAS navigation messages. There will be slow correction messages (Message Type 9) and a fast correction message (Message Type 2-5) that are transmitted by the GEO. The slow correction will be updated at least every two minutes and take care of the major part of the correction. The fast corrections will be issued at a minimum of once per minute.

3.5.9 Time and the GEO

The manner in which time plays a role in the GEO will be illustrated by using the WAAS as an example. The caesium clock at the GUS will be slaved to SNT. Once per day, the SMS will issue commands to steer the

GUS clock in order to reduce any offset from GPS Time. The GUS clock controls the synchronization of the WAAS navigation message from the GEO.

The geostationary communications system (GCS) consists of the signal generation subsystem (SGS), the RFU and the geostationary satellite. The SGS provides a C/A pseudo-random noise (PRN) code plus a WAAS Message signal as a 70 MHz intermediate frequency (IF) to the RFU. The RFU converts the IF to the RF uplink frequency (6 455.42 MHz), amplifies it, and transmits the signal to the INMARSAT-3 GEO Satellite.

The C-band uplink is received by the GEO satellite and translated to the L1 and C-band downlinks, which are broadcast in right-hand circular polarization (RHCP) earth coverage beams to users and the RFU. The RFU receives the downlink L1 and C-band signals from the INMARSAT-3 GEO Satellite. The signals are amplified and the C-band is converted to L2. The RFU provides the L1 and L2 signals to the SGS.

The GUS Receiver accepts C/A PRN code signals at L1 and L2 frequencies from the RFU. The GUS Receiver measures code and carrier phase pseudo-range data for both input signals. This information is sent to the processors and signal generator, which have algorithms and hardware that develop time, frequency, and phase feedback correction signals. The processor also FEC encodes the WAAS message.

These correction signals adjust the time, frequency, and phase of the C/A PRN code signal to take out the uplink range, range rate, and ionospheric effects. The signal generator also combines the FEC-encoded WAAS message data with this uplink-corrected C/A PRN code, which is provided as an IF signal to the RFU. The frequency standard provides precise and stable frequency references for all the converters, signal generators, and receivers in the RFU and SGS.

The frequency offset of the 5 and 10 MHz output shall be settable over a range of $\pm 1 \times 10^{-9}$. The Settability requirement is only applicable for the frequency standard at the SGS because this must be able to compensate for any drift in the GEOs local translation oscillator.

The RF Uplink Subsystem transmits signals from the SGS containing integrity and correction data along with a GPS-like ranging signal to the GEO Satellite. The RF Uplink receives signals from GEOs at both C- and L-band frequencies. At the direction of the SGS, the RFU controls the uplink power levels to protect against uplink interference and variations in transmission losses. The RFU also provides frequency translation of the uplinked signal to C-band and translation of C-band downlink signal to L2 frequency.

The GEO satellite subsystem is a satellite in geostationary orbit in space, INMARSAT-3 AOR-E satellite at 15.5°W longitude. The INMARSAT-3 space segment will provide capacity for transmission of navigational signals in a 2.2 MHz bandwidth centered on 1 575.42 MHz.

3.5.9.1 SBAS and time distribution

An SBAS usually has the secondary mission of time distribution. The time standard reference for an SBAS is usually a Coordinated Universal Time (UTC) as maintained by some national or international institution. Time distribution will be accomplished by providing users with the time offset between the SBAS network time (SNT) and UTC in Message Type 12 (MT12). Various national timekeeping laboratories will determine this time offset. The laboratories will monitor the SBAS geostationary satellites within their view. They will compute the time difference between the epoch time of the start of a SBAS message and the 1 PPS of the laboratory that is the physical realization of UTC(lab). The data is then transferred to the SBAS Master Stations (SMS) through some kind of interface. The SMS collects the SNT/UTC offset and creates a MT12 that is then sent to the geostationary uplink station (GUS) that transmits it to the GEO satellite. The purpose of the MT12 is to provide time users with an accurate source of time referenced to UTC.

An SBAS promises to be the next generation of global transfer system. Many features of an SBAS point to this deduction. The geostationary satellites are always in view. This offers the ability for multiple sights to be permanently "phase-locked" together by locking themselves to the common satellite signal. The transmissions from a geostationary satellite allow for the use of a high-gain directional antenna that can provide cleaner signals and are less prone to interference and cycle-slips. The geostationary satellite signals are generated and controlled by a network of caesium-based GPS receivers that provide a reasonably stable reference. In addition, the SBAS message from the geostationary satellites also provides real-time estimates of the retardation of the GPS signals as they pass through the ionosphere through a model based on real-time observations of GPS satellites.

Navigation systems distribute their reference time scale and, sometimes, its relation to other time scales. For instance, GPS distributes what has been called "GPS Time" and its relation to Coordinated Universal Time maintained by the US Naval Observatory (UTC(USNO)). Using GPS, a user can set a local clock to UTC(USNO) and by continually monitoring GPS, the user can keep track of how well that clock is performing with respect to UTC(USNO). GPS Time differs from UTC by, currently, 15 s because of Leap Seconds.

WAAS network time (WNT), EGNOS network time (ENT) and MSAS network time (MNT) are each SBAS's estimation of GPS Time. The user should be able to determine the offset of his/her local time reference from WNT or ENT. In their final operational configuration, each SBAS will provide the user with an estimate of the difference between its SNT and UTC. WAAS and EGNOS will transmit corrections that will show the difference between WNT or ENT and UTC. The user can use this information to set a clock to UTC. However, this information may not always be available in these early stages of development.

3.5.9.2 CGGTTS format for distributing timing data

Through an ad hoc working group called the CGGTTS, the timing community has developed a format to facilitate the exchange of GPS timing data between users interested in high precision time transfer. These users are primarily the major timekeeping laboratories of the world. While not going into the exact details of the format, suffice it to say that there are two columns that contain data relevant to the timekeeping process. They are shown in Table 3-1. The first row is the heading of the columns and the second row indicates what data is contained in that column. "Lab MC" would refer to the Master Clock of the Laboratory making and reporting the measurements. SVN refers to the clock of a particular satellite whose SVN number is also given in the message format. GPS Time would refer to GPS system time.

TABLE 3-1

Data relevant to timekeeping

REFSV	**REFSYS**
Lab MC – SVN (for GPS satellite)	Lab MC – GPS Time

Because the message format and data coming from the WAAS satellites are different from that of GPS satellites, the standard format of the CGGTTS timing message had to be modified. It is the modified message, proposed by NovAtel, which is now being scrutinized by the CGGTTS. The proposed modification involves the augmentation of the already mentioned two columns contained in Table 3-2. A new third column of timing information is entitled GAT where the G stands for geostationary satellite, A stands for the WAAS (for EGNOS, this would be a B), and T stands for Time. This proposed format was made in order to maintain continuity with the prior adopted convention and still take into account the uniqueness of the WAAS navigation message and the manner in which the corrections are applied to the observed (measured) pseudo-range. Table 3-2 shows the interpretation that should be given to the data in the proposed revised CGGTTS format when it applies to an SBAS satellite.

In the proposed CGGTTS format, the column labelled REFSV contains the offset of the local clock from the geostationary satellite time of transmission of the signal. It is similar to that for a GPS satellite. Referring to Table 3-1, the first column in the second row of Table 3-2 is labelled Lab MC-Geo. However, "Geo" is still not SBAS Network Time (SNT). Application of the Slow Clock Corrections contained in Message Type 9, gets one closer to SNT. The second column is now called Lab MC-SBAS. "SBAS" is still not SNT, so it is called SBAS Time, something similar to GPS Time. After application of the Fast Corrections contained in Message Type 2 through 5, one finally derives the offset of the local clock from SNT.

TABLE 3-2

Data in the proposed revised CGGTTS format

REFSV	**REFSYS**	**GAT**
Lab MC – Geo	Lab MC – SBAS	Lab MC – SNT
Measured PSR + Iono + Tropo + Orbit	Slow clock Corrections	Fast clock and Orbit corrections
Geo orbit from MT9	Clock from MT9	MT2 (fast corrections)

The WAAS transmissions have been monitored at USNO using a NovAtel narrow band correlator system. Data is processed daily using a program that produces output data according to the proposed revised CGGTTS format.

The result of the processing yields the offset of the USNO Master Clock from WNT. This data will eventually be used for the preparation of a MT12 transmitted by the WAAS. MT12 will be transmitted by the SBAS geostationary satellites to allow users to obtain the difference of SNT from UTC (Lab). It should be pointed out that the USNO Master Clock that provides the time for the WAAS narrow band correlator used to make the measurements is a real-time estimate of UTC (USNO).

For this analysis, a forty-day span of data was chosen (Modified Julian Day (MJD) 52167 to MJD 52207). It is not a continuous data set. In order to facilitate the transfer of data from USNO to another computer over a telephone modem, several subsets of the data were transmitted during times of minimum usage.

Because the receiver used in this experiment has not been calibrated in the absolute sense, i.e., delays measured through all components of the system, values obtained for USNO MC – GPS Time, obtained with the WAAS receiver, were compared with values obtained with the USNO calibrated receivers. An average value of the differences over one day was formed. This average was used as an estimate for the systematic differences between the NovAtel receiver and the USNO receiver used to report GPS data to the GPS Master Control Station.

Figure 3-4 illustrates the data contained in the column labeled REFSV that is produced following the revised CGGTTS format. It shows the difference between the USNO MC and time from the WAAS geostationary satellite after application of corrections for the delays caused by the ionosphere, troposphere, and corrections to the orbit of the geostationary satellite contained in MT9 to the measured pseudo-ranges.

The clock corrections contained in MT9 were next applied to the data and the results are exhibited in Fig. 3-5. One can see a dramatic reduction in the offsets. However, there is still a reasonably large deviation starting around MJD 52198. This corresponds to a rather large ionospheric disturbance that occurred about October 13, 2001.

Application of the fast corrections contained in MT2-5 shows even further improvement as shown in Fig. 3-6.

While the values for UTC (USNO)–WNT are reduced to levels that are within the WAAS specification, they are still large for time distribution when compared with similar values obtained using GPS. Figure 3-7 shows daily averages made from the individual points that were contained in Fig. 3-6. There is a spread of about 40 ns in the values. This large spread is probably due to variations in the operating procedures being implemented during the early phases of WAAS implementation.

FIGURE 3-4

UTC (USNO) – GEO

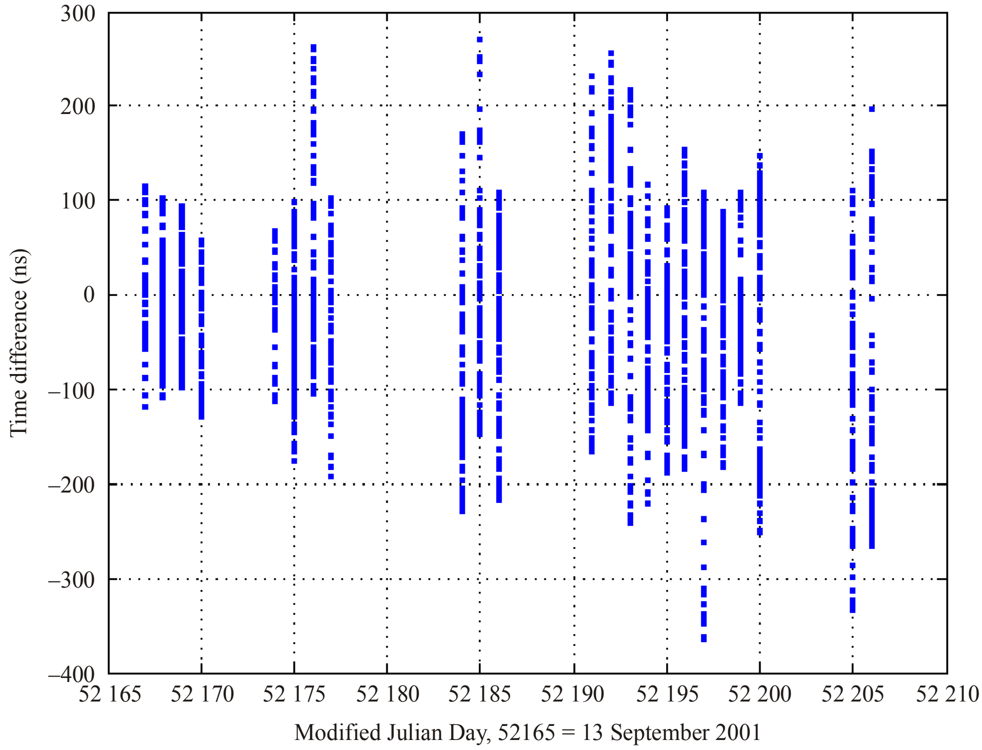

Sat_time_freq-03-04

FIGURE 3-5

UTC (USNO) – WAAS

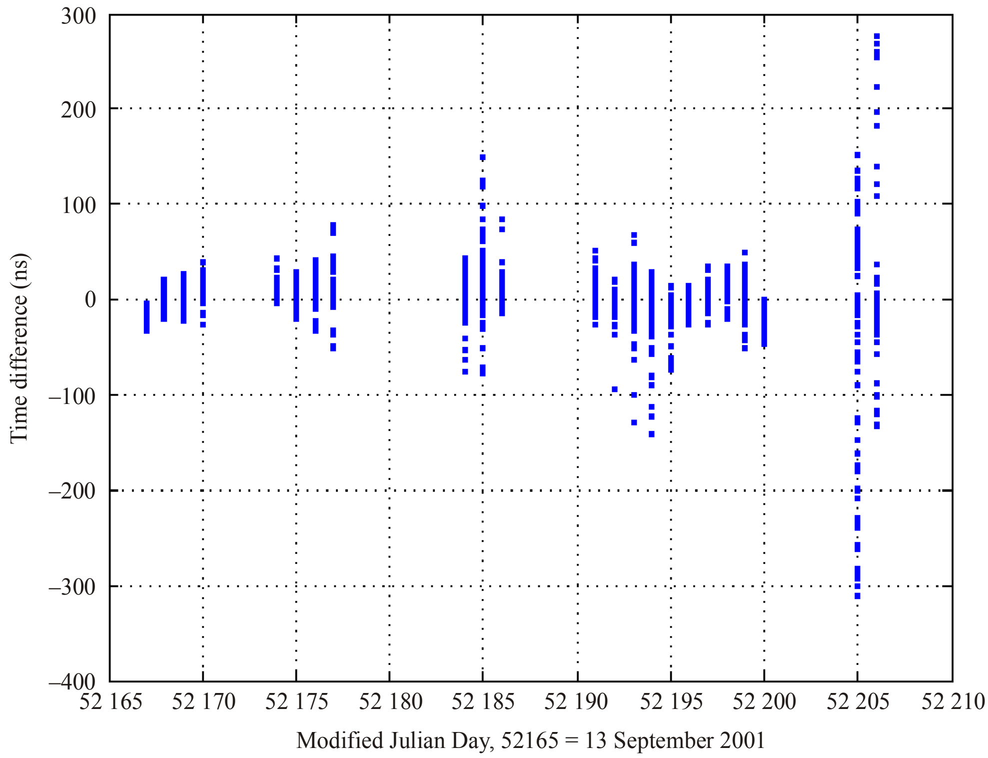

Sat_time_freq-03-05

FIGURE 3-6

UTC (USNO) – WNT

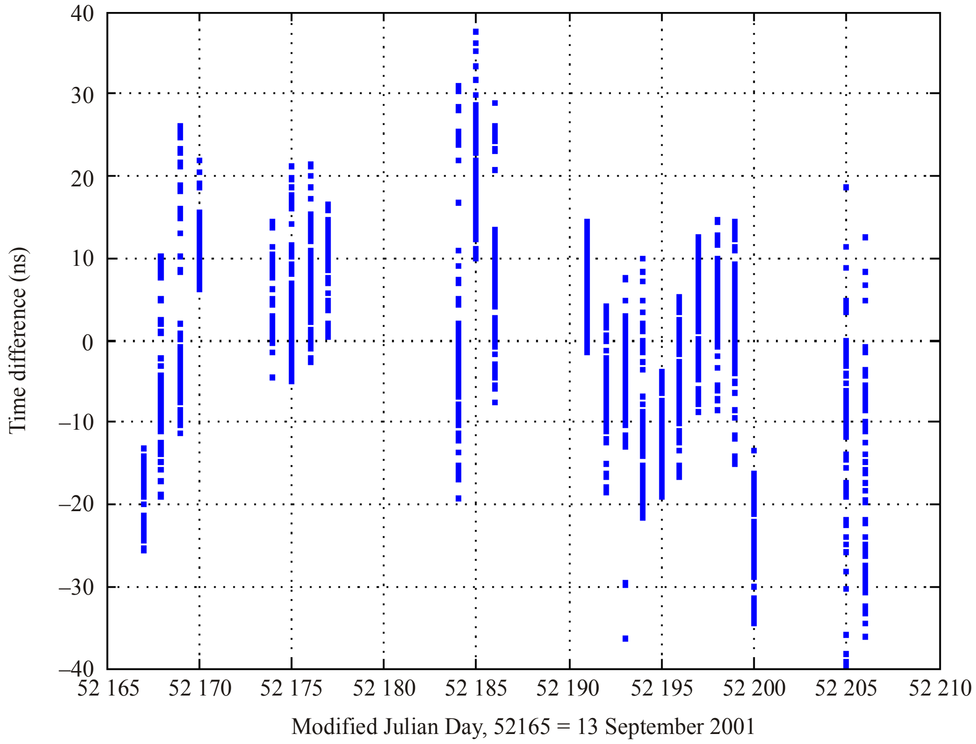

Sat_time_freq-03-06

FIGURE 3-7

Daily averages of UTC (USNO) – WNT

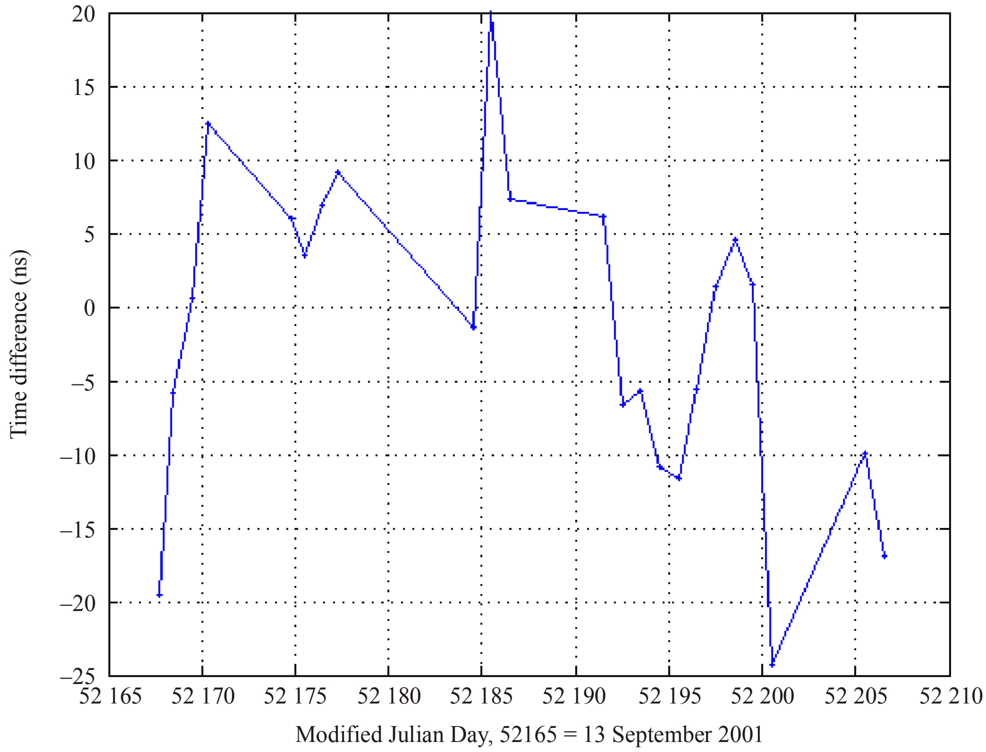

Sat_time_freq-03-07

Figure 3-8 shows two-day averages for the values of UTC (USNO) – GPS System Time. The spread in this case is about 20 ns.

FIGURE 3-8

Two-day averages of UTC (USNO)–GPS time

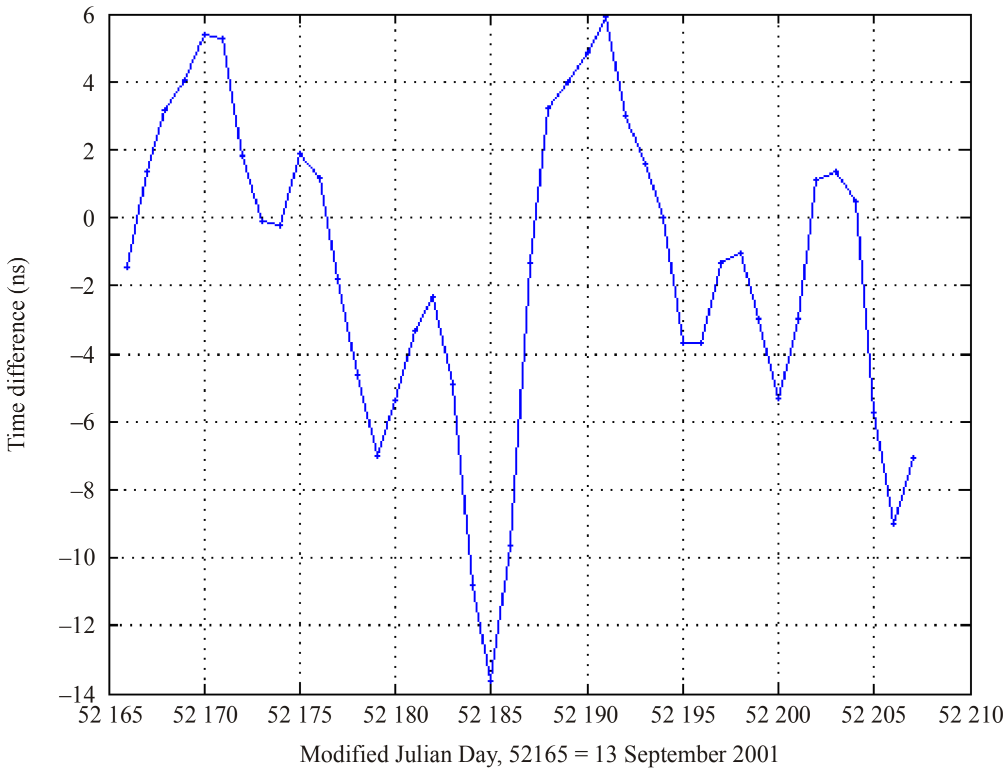

Sat_time_freq-03-08

3.5.9.3 SBAS and frequency distribution

The time transfer using GPS satellites has been widely used for many years for international comparisons between timing laboratories and for the computation of International Atomic Time (TAI). Thanks to a satellite in common view of 2 stations and to the acquisition by each station of the GPS observables, it is possible by a simple difference to determine the absolute time offset between the clocks that feed the GPS receivers. It requires the internal delays to be known in each station (antenna, cables, receiver, etc.). If you consider these delays as constant, you can perform a frequency transfer between the two stations, which gives access to the variations of the time offset between the two clocks and therefore to the stability of these clocks.

Geodetic GPS receivers are now able to handle several channels (so that several satellites can be observed in the same time) and two frequencies (so that the ionospheric delay can be removed). So, using all the code measurements, an extension of the classical technique is possible in order to have more precise results. Moreover, these receivers are able to record code and carrier phase observables. It is well known that the latter offers promising perspectives for accurate frequency transfer for integration times between several hours and several days.

Some GPS receivers can also track the GEO signals, that is, the GPS-like message coming from L-band navigation payload of geostationary satellites. These additional signals present an important advantage for time/frequency transfer. By definition, the GEO satellite is always in view, so it should offer the opportunity to be continuously phase locked to its signal. This permanent observability should also enable to simplify the processing of the signals. Moreover, the GEO signal is not subject to intentional degradation such as selective availability.

Nevertheless, the use of GEO satellites implies specific problems. First, they transmit on a single frequency, which prevents one from using the well-known iono-free combination. The ionosphere effect can be corrected by using the information broadcast by the SBAS or by computing the code/phase difference. In fact, the ionosphere distorts identically code and phase but with a different sign, thus the ionospheric correction can be easily computed as half of the code/phase difference.

Figure 3-9 shows the results obtained on a BIPM/CNES baseline (about 600 km) with parabolic antenna, both being pointed to INMARSAT AOR-E (EGNOS) :

First, we can compare the ionospheric correction computed on one station from code-carrier difference to the one broadcast by EGNOS.

FIGURE 3-9

Ionospheric corrections by code/phase difference and broadcast information

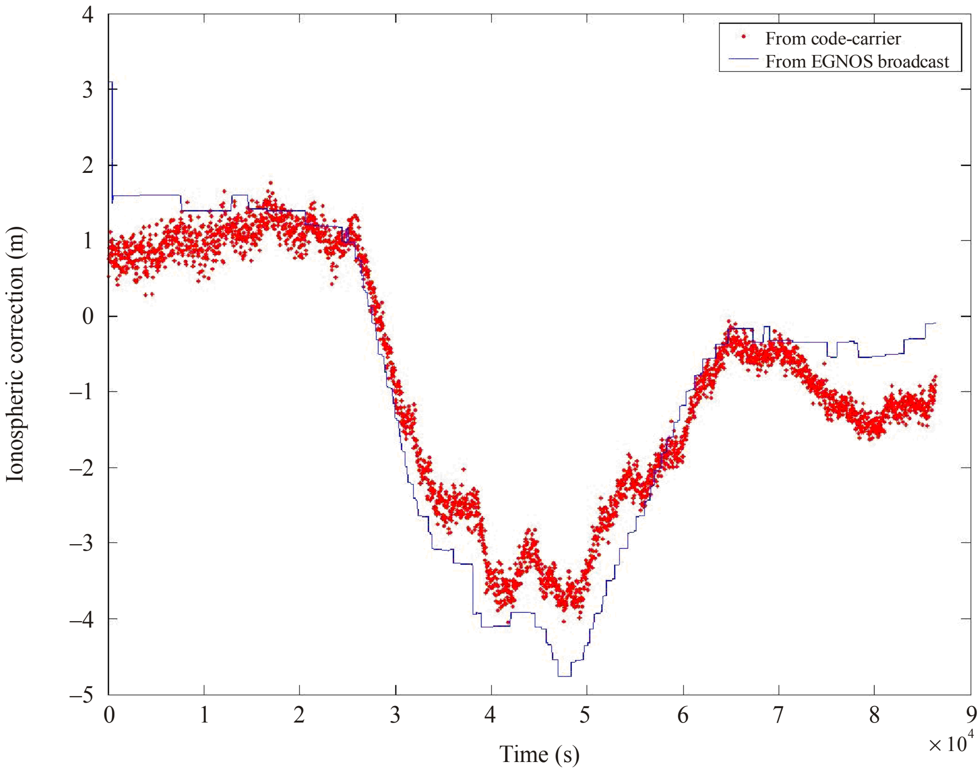

Sat_time_freq-03-09

The ionospheric correction computed from code-carrier difference is obviously noisier but is continuous, unlike the EGNOS broadcast that presents numerous steps.

Figure 3-10 compares the stability of the clock solution with ionospheric correction (the two methods) and without.

FIGURE 3-10

Allan deviation of the different clock solutions

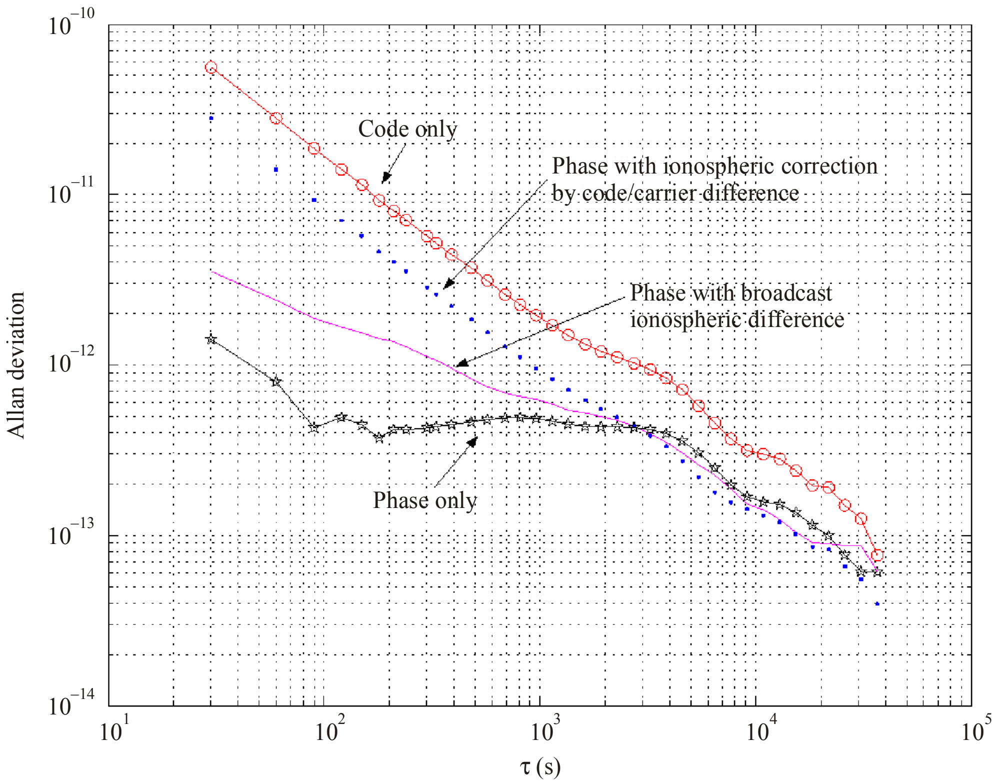

Sat_time_freq-03-10

The clock solution using uncorrected phase is obviously the best in the short-term, but the lack of ionospheric correction affects the mid-term stability. The clock solution using phase with ionospheric correction by code/carrier difference is very noisy in the short-term due to the noise of the code. After an integration time of about one hour, the uncorrected phase and the phase with both corrections are very close.

So, an important issue is the signal-to-noise ratio. The use of a big directional antenna improves it, which should be great advantage for the continuous phase lock (reduction of the number of cycle slips) and for the ionospheric correction by code/phase difference.

3.5.10 SBAS and time transfer

Users may want to set a remotely located clock to run at some prescribed time scale or simply want to know the difference between a local clock and a remote clock. This can be done through a technique known as Common View. In the Common View technique, two stations simultaneously observe the same satellite. Each of the users at both stations must record the difference between his/her local clock or local time reference at the same instant of time using the same satellite. This usually has been done using a GPS Time transfer receiver. However, with the capability being built into modern day receivers, it may be possible to do this with a more advanced receiver.

Using an SBAS for time transfer involves two users. For optimal results, they should observe the same satellite at the same time and use identical data reduction techniques when computing the offset of their local clocks from the SNT. This has the advantage that it significantly reduces the effects of any common error source.

3.5.11 Time transfer between 2 laboratories

Currently, the two SBAS are observable over a large region the globe. For time transfer, this provides some added bonus features. Figure 3-11 is a schematic that shows how two laboratories can use two SBAS for comparing their clocks. Each laboratory can observe the two SBASs. The results from one SBAS can then serve as a check on the other.

FIGURE 3-11

Schematic showing time transfer between two timekeeping laboratories using two SBASs in order to get the time difference between the two laboratories

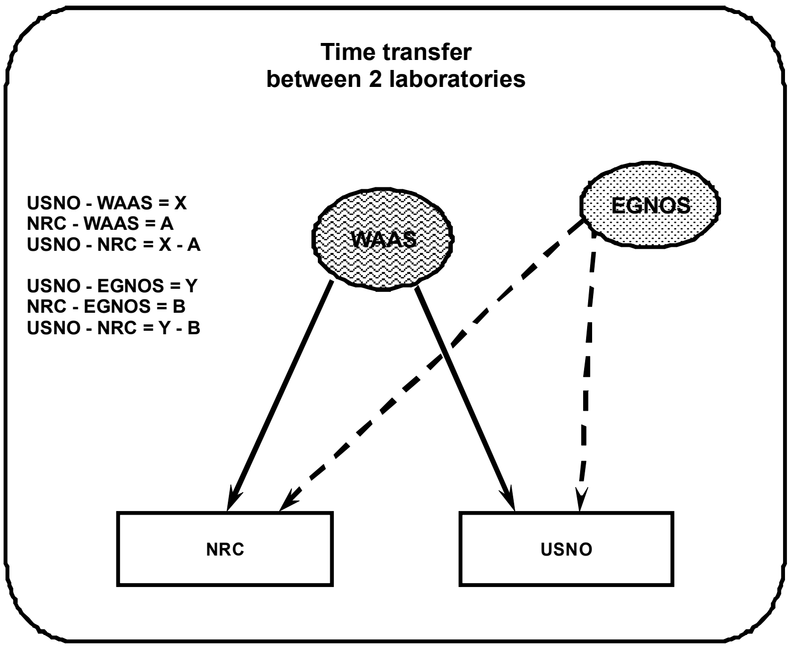

Sat_time_freq-03-11

In this example, observations are made at USNO in Washington, D.C and at NRC in Ottawa, Canada, using the WAAS GEO and the ESTB GEO as time transfer satellites. Figure 3-12 shows the difference between the USNO and NRC master clocks using the WAAS GEO and Fig. 3-13 shows the same using the ESTB GEO. Because the receivers used in this experiment have not been calibrated, an arbitrary zero point has been removed.

Therefore, this example can only be used to give an indication of the precision currently attainable with this technique. A linear regression through each of the data sets gives a standard error of 1.3 ns and 2.1 ns, respectively.

FIGURE 3-12

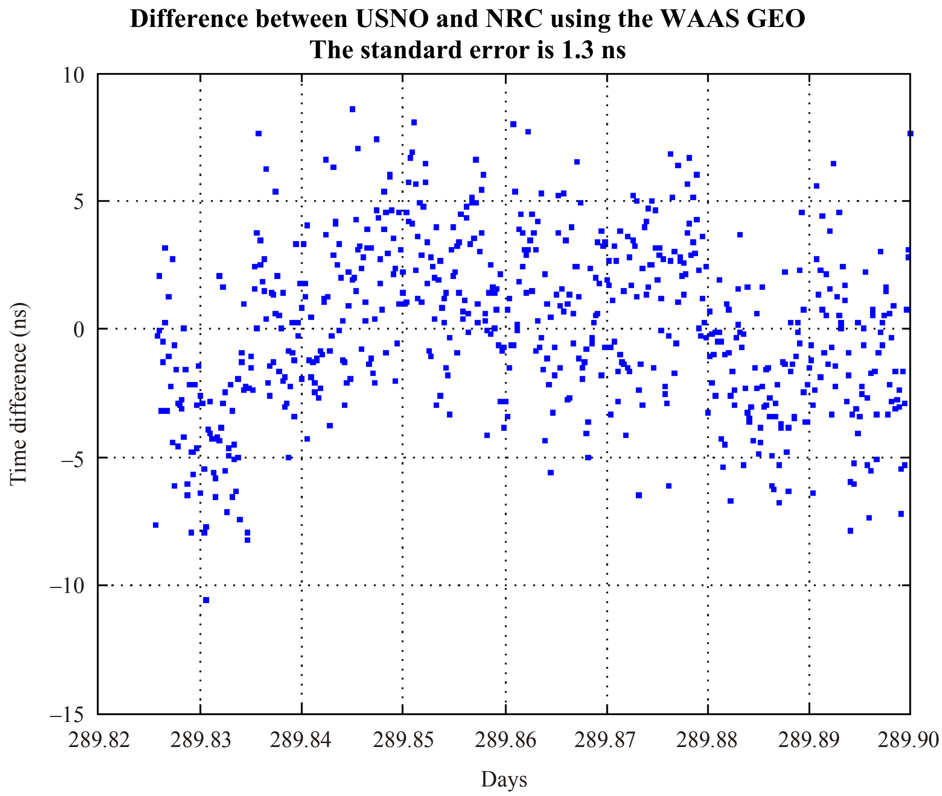

Sat_time_freq-03-12

FIGURE 3-13

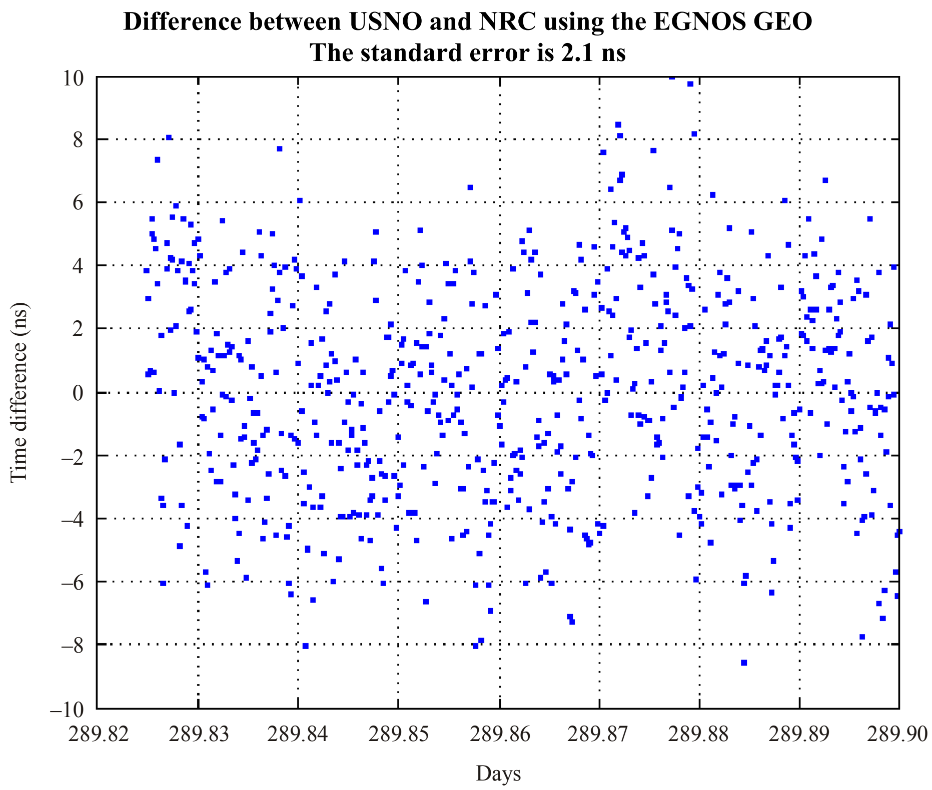

Sat_time_freq-03-13

3.5.12 Time transfer between 2 SBAS

Figure 3-14 is a schematic that shows how two laboratories can compare the time difference between two SBASs. Each laboratory provides a check on the other.

FIGURE 3-14

Schematic showing time transfer between two timekeeping laboratories using two SBASs in order to get the time difference between the two SBASs

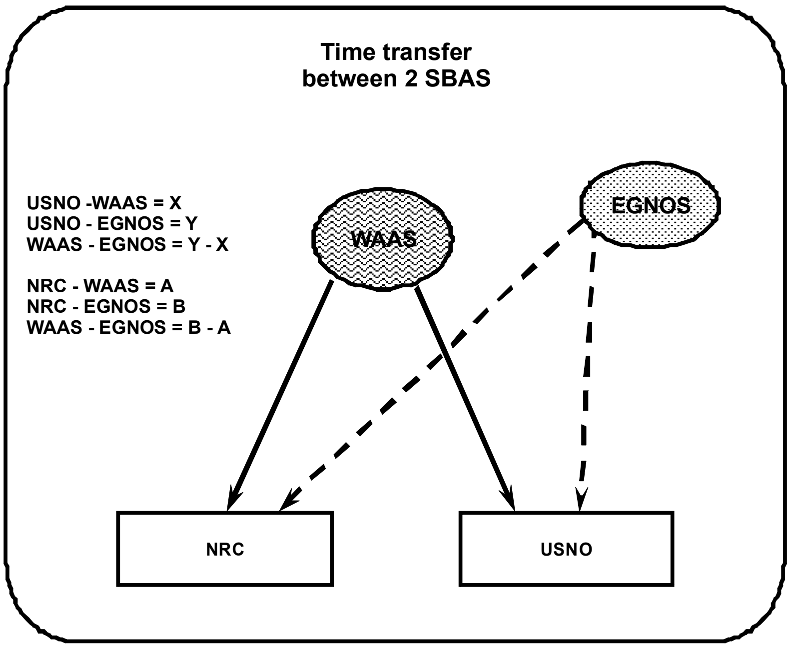

Sat_time_freq-03-14

Figure 3-15 shows the difference between WNT and ENT as obtained at USNO after a linear regression has been fit through the observations. Again, since no calibration of the receivers has been performed, this graph indicates the precision currently attainable with this technique. The standard error of a linear regression through this data is 1.2 ns.

Figure 3-16 shows the difference between WNT and ENT as obtained at NRC. The standard error of a linear regression through this data is almost identical to that obtained at USNO. It is 1.0 ns.

FIGURE 3-15

Difference between WAAS and EGNOS using USNO data
The standard error is 1.2 ns

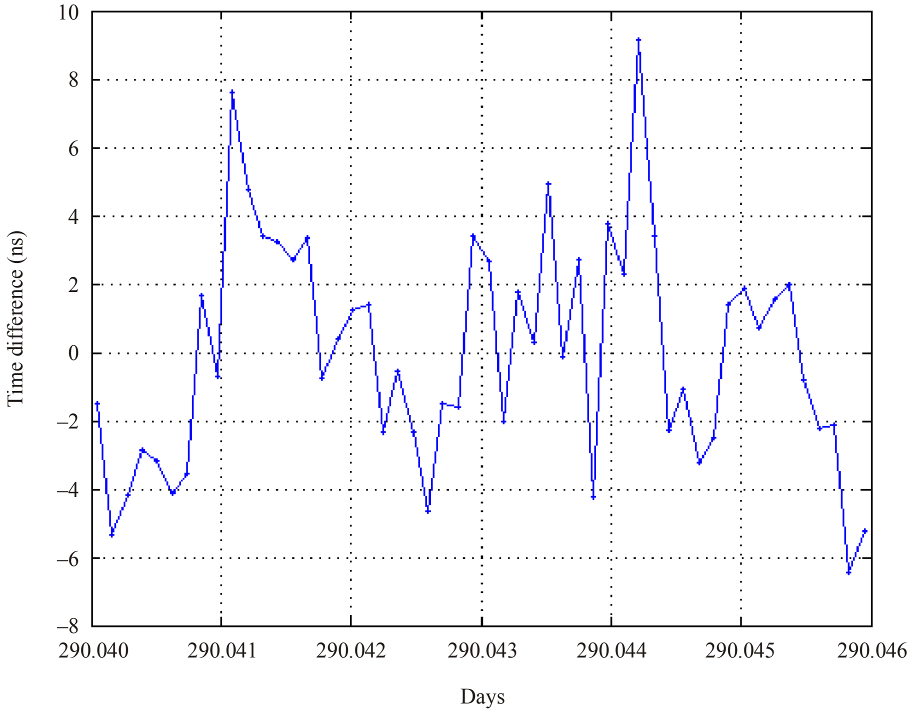

Sat_time_freq-03-15

FIGURE 3-16

Difference between WAAS and EGNOS using NRC data

The standard error is 1.0 ns

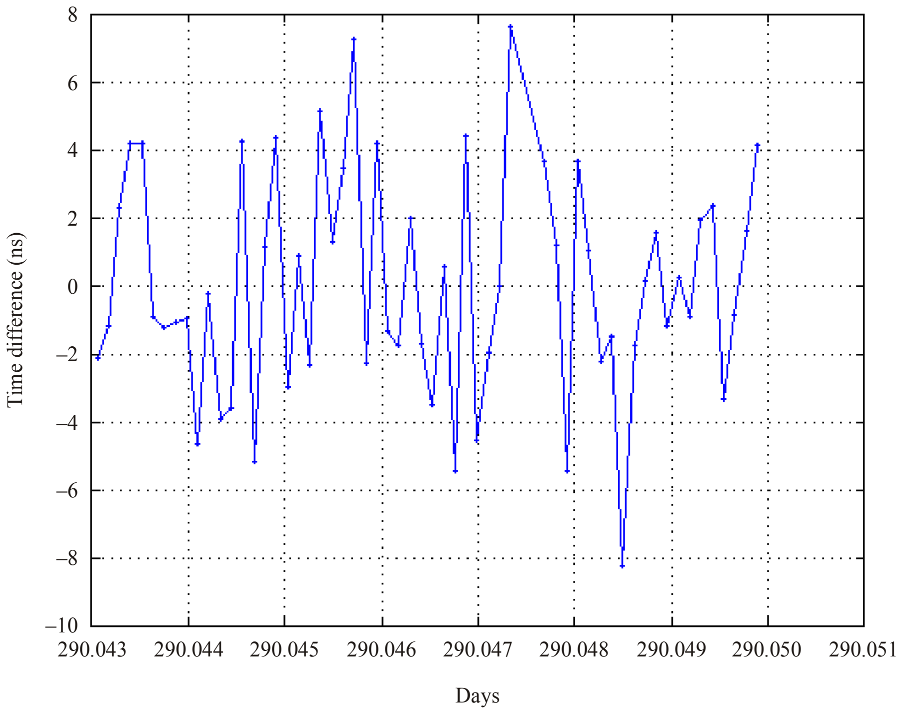

Sat_time_freq-03-16

3.5.12.1 SBAS and the timekeeping community

An SBAS can/will provide time globally for the recording of all events. It will also provide a very stable timing signal for the timekeeping community. It will not be affected by SA. The source remains at the same approximate point in the sky. Thus, a high gain antenna can be used to provide a very good signal to the stationary user. The offset of SNT from UTC is transmitted within the SBAS navigation message. The signal will be available continuously.

Such a signal provides some unusual capabilities for the timekeeping community. It should allow the *development of more economical timing systems* utilizing its signals. Cheaper crystals can now be used in systems which rely on atomic standards as their flywheel while they integrate GPS time to remove the effects of Selective Availability. Because of the absence of Selective Availability, it will be possible to *almost instantaneously detect any pathological behavior* in a system providing time. With GPS, one has to wait to see if the transients are due to Selective Availability or anomalous clock behavior. If one is within the footprint of two SBAS transmitting satellites, there is *an immediate redundancy check*. This can be used as an extremely robust check for many timed systems.

References

BENEDICTO, J. *et al.*, [1998] EGNOS: the European Satellite Based Augmentation to GPS and GLONASS. Proc. GNSS98.

BROWN, K.R. [1991] The theory of the GPS composite clock. Proc. ION GPS-91, p. 223-241 and GOUNI, Ph. *et al.* [1997] Time and Frequency aspects in EURIDIS, EFTF 1997.

BRUNET M. *et al.* [1998] The role of time and frequency in EGNOS. PTTI 1998.

FLAMENT, D. *et al.* [1998] EGNOS: the European Based Augmentation to GPS and GLONASS-mission and system architecture. Proc. GNSS98.

PECK, S. *et al*. [1997] WAAS network time performance and validation, Proc. ION GPS97, p. 1123-1131.

PIEPLU, J-M. *et al.* [1998] EGNOS algorithms performances status and experiment activities. Proc. GNSS98.

APPENDIX A

Brief description of SBAS message content

Type	Contents
0	Don't use this GEO for anything (for WAAS testing)
1	PRN mask assignments, set up to 51 of 210 bits
2 to 5	Fast corrections
6	Integrity information
7	Fast correction degradation factor
8	Reserved for future messages
9	GEO navigation message (X, Y, Z, time, etc.)
10	Degradation parameters
11	Reserved for future messages
12	SBAS network time / UTC offset parameters
13 to 16	Reserved for future messages
17	GEO satellite almanacs
18	Ionospheric grid point masks
19 to 23	Reserved for future messages
24	Mixed fast corrections/Long term satellite error corrections
25	Long term satellite error corrections
26	Ionospheric delay corrections
27	SBAS service message
28	Clock-ephemeris covariance matrix
29 to 61	Reserved for future messages
62	Internal test message
63	Null message

CHAPTER 4

GPS SYSTEM TIME

Page

4.1 Introduction

The GPS is a real-time predicted information operation. The five U.S. Air Force Monitor Stations maintain continuous real-time links to the MCS so that current tracking and status information can be combined with that from additional monitor stations established by the National Intelligence and Geophysical Agency (NGA) to provide additional coverage of the GPS satellite constellation. The increased observational data then provides for prediction of new system variables. These predictions of system performance are subsequently uploaded into the satellites's on-board memories for transmission in the satellite navigation messages. The errors remaining in this process are considered to be random with dominate systematic errors (biases) removed.

The data flow of the GPS control segment is illustrated in Fig. 4-1. Each GPS Block II/IIA operational satellite carries two caesium (Cs) and two rubidium (Rb) atomic clocks. Each Block IIR satellite carries three Rb clocks. The fundamental clock frequency is 10.23 MHz. The satellite clocks and monitor station clocks contribute to the statistical formation of a continuous system time known as GPS Time, which is specified to be within 1 μs of UTC, except leap seconds are not inserted. After various corrections for ionospheric and tropospheric propagation delays, relativity, and hardware effects are taken into account, GPS can provide a time reference typically with a precision of ≤ 25 ns. However, in practice the precision can be 10 ns or better.

FIGURE 4-1

Control segment data flow

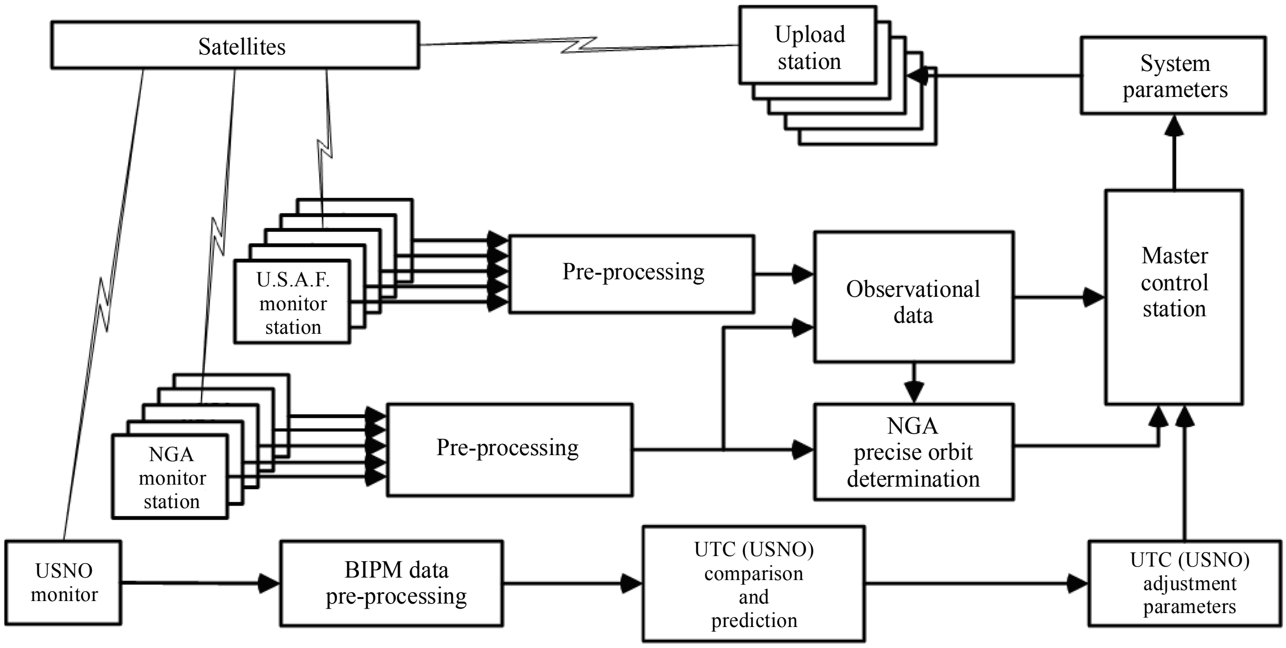

Sat_time_freq-04-01

4.2 Tracking clock measurements and ephemeris determination

Presently (2009), in GPS, the basic measurements are comprised of the pseudoranges and pseudo-carrier phase between the satellite and monitor station clocks. There are five operational control segment (OCS) monitor stations, including the Master Control Station in Colorado Springs, Co. that are operated by the U.S. Air Force. The OCS has been augmented by establishing new direct links with eight monitor stations operated by NGA. The pseudoranges measured by the monitor stations from all of the satellites are processed every 15 min in a Kalman filter containing the relevant constants and models for monitor station coordinates, orbit determination, and clock characteristics. The Kalman filter predicts the ensemble system time

(GPS Time), the individual satellite and monitor-station clock offsets with respect to GPS Time, and the orbital elements of each satellite with respect to the WGS84 geodetic coordinate frame.

The measurement errors are distributed among the Kalman states. The satellite and monitor station clocks are estimated according to a clock model and the errors are expressed in terms of the model covariance matrix.

The orbit determination process for GPS requires knowledge of the difference between UT1 and UTC in order to determine the initial orbit orientation relative to the Earth-centered inertial (ECI) reference frame. The equations of motion are integrated in the ECI reference frame. These coordinates are transformed into the Earth-centered Earth-fixed (ECEF) reference frame via four rotation matrices representing the Earth's polar motion, variable rotation, nutation, and precession. The data from the tracking stations are time-tagged in GPS Time. A Kalman filter at the MCS uses the MS data to generate current estimates of satellite position and clock data and predicts these values for 14 days ahead. These data are then formatted and uploaded to the satellites for transmission to the users as the NAV-MSG along with the ranging signals. Satellite uploads are normally done every 24 h, but can be done more frequently as the system dynamics and data indicate. The NAV-MSG contains satellite ephemeris, clock data, system status and other data needed by the user [IS-GPS-2002 rev D, 2006]. The prediction of accurate satellite positions and the individual satellite's clock deviation from a common time base is the critical function provided by the control segment which enables the GPS concept to perform as it does

4.3 GPS time

The starting epoch of GPS Time is midnight of January 5-6, 1980. Therefore, GPS Time is behind TAI by a constant value of 19 s and in June 2009, GPS Time is ahead of UTC by 15 s. The UTC difference changes every time a leap second is inserted into UTC.

The original concept for synchronization of the system components as GPS was being developed was the master clock approach that has been commonly used in telecommunications systems. All clocks in the system were to be referenced to a single clock in one of the monitor stations (MS). The primary requirement for a satellite navigation system is a uniform system of time that does not contain jumps or discontinuities such that the synchronization of the system elements are consistent. The resulting navigation service will then provide accurate positioning and not be interrupted. In the initial master clock approach that GPS used all the clocks in the system were referenced to a single clock in the Colorado Springs Master Control Station (MCS). For assurance of having a master clock in the face of clock failures the system software could designate any clock in the Monitor Stations to be the master reference clock at any time. Exercising this capability led to significant changes in the overall navigation performance when such a switch occurred. Differences in the clocks, which as the master reference was assumed to be perfect led to an overall system change disrupting navigation performance. Consequently a composite clock approach was developed and incorporated into the system Kalman filter.

This composite clock approach is similar to the traditional clock ensembling concept that produces a "paper clock" that does not depend on any single device [Stein and Filler, 1988]. The Clock ensembling is a well known technique used for long-term timekeeping, but in the case of the composite clock a Kalman estimator technique is used to determine a common reference time representative of the mean value of the clock differences within the system producing a system time synchronized in the short term (less than 10^5 s). Consistent synchronization in the short term is just what is needed for navigation service. The common internal time base is known as GPS Time and represents the basis for synchronization of all clocks in the GPS segments especially the User Equipment.

The Kalman filter estimator that was designed to compute the system parameters for the GPS was originally designed as a partitioned filter. This design was mainly due to computational requirements but also on reliability of the estimates. Each partition of the filter estimated a subset of the satellite clocks and the monitor station clocks. When the composite clock was implemented in the filter an additional state was added so that the individual clock would be differenced from the implicit mean of the measurements. The mean with itself of course produces a residual of zero. The resulting estimates of the actual clock states produced were stable and behaved as expected however the covariance of the solution grows linearly without limit that is a result of the basic unobservability of the system. Also, if a bias was introduced into the clock states the results remained the same. Consequently, a pseudo-measurement was added which would limit the covariance growth without influencing the computed estimates. However, the different filter partitions did not all arrive at the same estimated common time. So it was necessary to reconcile the estimates from the partitions to ensure that GPS Time is consistent across the satellite constellation.

4.3.1 Composite clock implementation

When additional states are added to the Kalman filter in place of the master MS clock the GPS system becomes unobservable. This is because a constant bias shift in all clock states would not affect pseudorange and would therefore be unobservable to the filter. The existence of this unobservable state component causes the clock phase covariance to grow linearly with time even though the system is completely stable with well defined filter gains. See Brown [Brown, 1991] for further discussion of the characteristics. Since a growing covariance matrix will eventually cause numerical problems, a method for reducing the covariance matrix without degrading filter performance was introduced. The method chosen was reduction by pseudo-measurement update [Satin and Leondes, 1990].

4.3.2 Covariance reduction

This pseudo-measurement update takes the standard Kalman form:

$$P' = P - [PH^T (HPH^T + R)^{-1}]HP \tag{4-1}$$

where:

- P': covariance matrix resulting from the update (i.e., the reduced covariance matrix)
- R: pseudo-measurement noise variance
- H: measurement matrix that relates the measurement to the state parameter.

The matrix P in this equation is the full $n \times n$ covariance matrix of n ephemeris and clock states for the satellites and monitor stations in a particular partition. All filter partitions undergo independent covariance reductions ever filter update cycle. The $n \times 1$ column vector H^T is constructed by inserting each element of an $m \times 1$ column vector $\widehat{H}^T$ into the appropriate position in an $n \times 1$ vector of zeros.

$\widehat{H}^T$ is given by:

$$\hat{H}^T = \frac{B^{-1}u}{u^{-1}Bu} \tag{4-2}$$

where:

- B: $m \times m$ submatrix of P corresponding to clock phase states only $m \times 1$ column vector of all zeros
- u: $m \times 1$ column vector of all ones.

Each clock in a partition would then have an ensembling weight in the column vector H (order as P is ordered) where each ephemeris state has weight of zero. The sum of the elements in H is normalized to one. The expression for $\widehat{H}^T$ then assigns to each clock a normalized set of phase and frequency weights that is inversely proportional to the magnitude of the estimation error variance, the diagonals of B. Because of the particular form on H^T, however, the update correction expression will result in some non-zero ephemeris states. Therefore this correction technique is not completely transparent to the ephemeris estimates. In practice however, there appeared to be minimal difference.

4.3.3 Partition reconciliation

Partition reconciliation was required to insure that the composite clock time for each of the filter partitions were consistent. A divergence of the solution time in the partitions would create a direct pseudorange error. The reference time in each partition would have a different bias term that could be estimated from the fact that the monitor station clock values were in each partition. The better solution to the numerical problem caused by the partitions was to use a single partition filter so that the estimates were all processed in the same manner. The GPS system has introduced a single partition filter. The composite clock technique to determine GPS Time will still be used.

4.4 UTC (USNO) from GPS

The GPS satellite atomic clocks are free running with synchronization provided to GPS Time by data correction. GPS Time is not realised within the system in that there is not a physical clock keeping GPS Time as a reference. GPS Time is realized in the output of the GPS receivers and as such is monitored by USNO. They compare these data with their realization of UTC, UTC (USNO), and from these data predict parameters that are provided back to the GPS Master Control Station for transmission in the satellite's NAV-MSG [McKenzie *et al.*, 1989]. The real-time predicted offset of UTC as realized at USNO with respect to GPS Time is available from subframe 4, page 18 of the broadcast NAV-MSG.

References

BROWN, K. [September 1991] The theory of the GPS composite clock. *Proc. Of ION GPS-91*, p. 223–241.

McKENZIE, C.H., *et al.* [28-30 November 1989] GPS-UTC Time Synchronization. *Proc. of the 21st Annual PTTI Applications and Planning Meeting*.

Navstar Global Positioning System Interface Specification IS-200 rev D [2006] Navstar GPS Space Segment/ Navigation User Interfaces, IRN-200D-001, ARINC Engineering Services, LLC, El Segundo, CA 90245.

SATIN, A.L. and LEONDES, C.T. [January 1990] Ensembling Clocks of the Global Positioning System (GPS). IEEE Trans Aerospace and Electronic Systems, Vol. 26, **1**.

STEIN, S. and FILLER, R. [June 1988] Kalman filter analysis for real time applications of clocks and oscillators. *Proc. of the 42nd Annual Symposium on Frequency Control*, p. 447-452.

CHAPTER 5

GLONASS NAVIGATION SATELLITE SYSTEM

Page

5.1 Introduction

The Global Navigation Satellite System (GLONASS) is a government global navigation satellite system (GNSS) which is designed for providing a continuous all-weather support of an unlimited number of aeronautical, maritime, terrestrial and space-born users with high-precision position-fixing and **timing information** at any point of the Earth and in the near-Earth outer-space.

The GLONASS system is as a dual-purpose space facility applied for solving the scientific, industrial, economical, social, defense, security and other relevant problems. The Russian Federal Space Agency (Roscosmos) and the Russian Ministry of Defence are co-customers of the GLONASS system on equal footing [Glotov *et al.*, 2006].

NOTE 1 – The Russian acronym GLONASS stands for **GLO**bal'naya **NA**vigatsionnaya **S**putnikovaya **S**istema, or Global Navigation Satellite System.

5.2 General description and principles of operation

Completely deployed GLONASS system is composed of 24 satellites, orbiting in 3 orbital planes. The orbital planes are spaced at 120° (longitude). In each orbital plane, 8 satellites are evenly spaced in each plane at 45° (phasing). Moreover, the planes themselves are phase shifted with respect to each other by 15°.

The nominal period of the satellite orbit is 11 h 15 min 44 s, that corresponds to circular orbit altitude of 19,100 km. This period ensures the recurrence of satellite track on the Earth surface every 17 orbits. The period was chosen so to reduce the influence of resonant gravity field effects on satellite motion and thus to exclude satellite orbit control maneuvers over its entire lifetime. The nominal orbit inclination is 64.8°. The spacing of the satellites allows providing continuous and global coverage of the terrestrial surface and the near-earth space, [GLONASS, 2008] and (Recommendation ITU-R M.1787).

The GLONASS system operates on the principle of passive triangulation. The system user equipment measures the pseudo-ranges and radial pseudo-velocities from all visible satellites and receives information about the satellites' ephemeris and clock parameters. On the basis of these data, the three coordinates of the user's location and the three velocity vector constituents are calculated and user clock and frequency correction is made (Recommendation ITU-R M.1787).

Each satellite transmits navigation signals in one (GLONASS), two (GLONASS-M) or three (GLONASS-K) frequency bands: L1 (1.6 GHz), L2 (1.2 GHz) and L3 (1.1 GHz) [Dvorking *et al.*, 2009] and (Recommendation ITU-R M.1787).

A unique feature of a GLONASS-type satellite is the availability of an optical retro-reflector system on-board that enables Satellite Laser Ranging. They are used for precise orbit determination and geodetic research [Dvorking *et al.*, 2009].

5.3 GLONASS architecture and development

To provide the required functions sub-systems/elements shown on Fig. 5-1 have been included in the GLONASS system [Polischuk *et al.*, 2002].

FIGURE 5-1

GLONASS architecture

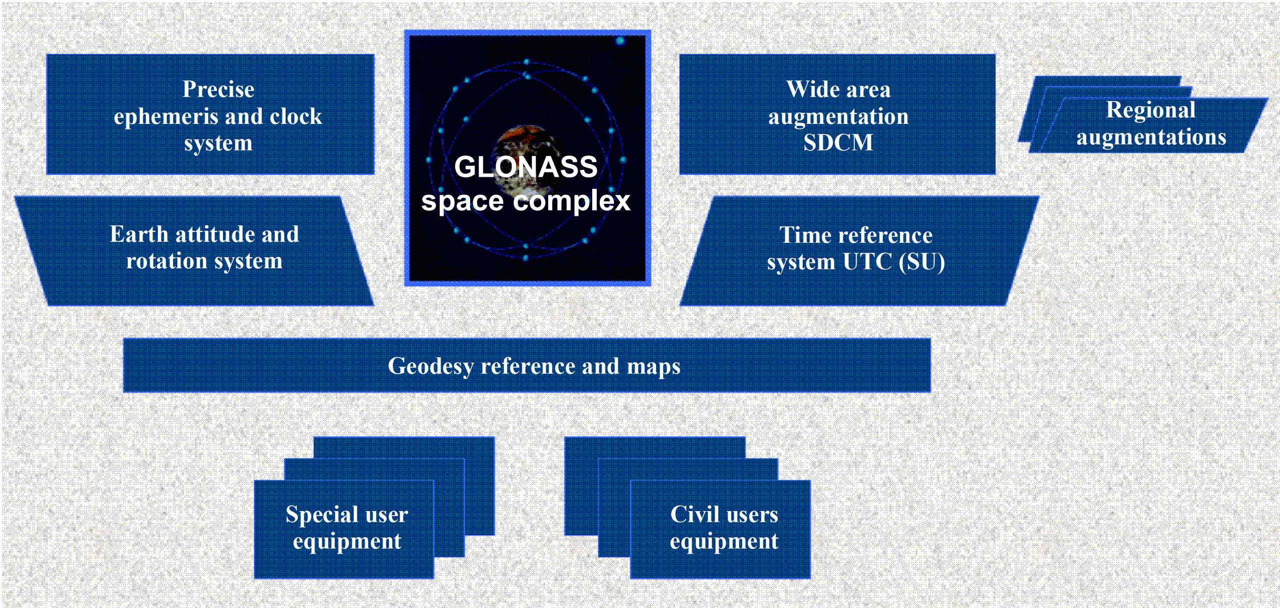

Sat_time_freq-05-01

The GLONASS system is composed of the following segments:

– Orbital constellation of GLONASS satellites (space segment).

– Ground-based control system.

– User equipment (user segment).

Deployment and maintenance of the orbital constellation is provided by two rocket-space systems: one based on the "Proton" launcher and another based on the "Soyuz" launcher from either BAYKONOUR or PLESETSK launch site.

5.3.1 Space segment

In the regular variant, the GLONASS orbital constellation (space segment) includes 24 operational space apparatuses at practically circular 19 100 km orbits at an inclination angle of 64.8° to the equator and an orbital period of approximately 11 h 15 min. They are evenly distributed in 3 orbital planes (spaced along the longitude of the ascending node by 120°), each plane containing 8 satellites (with equal latitude displacements of 45°). The navigation satellites in the neighboring orbit planes have a latitude displacement of 15°. This geometric structure of the orbit constellation ensures global and continuous coverage of the Earth's surface with the navigation field, so that the consumer can see no fewer than 4 satellites at any time moment and at any point of the Earth (the best configuration is when one satellite is at the zenith and the other 3 satellites are near the horizon) [Dvorking *et al.*, 2009].

The first GLONASS satellite was injected into orbit in 1982. In 1993, the system was composed of 12 satellites and operational capability was declared.

The GLONASS system was implemented in 3 phases [Polischuk *et al.*, 2002]:

– Phase 1 (1983 – 1985): Experimental tests. System concept refinement. Orbital constellation of 4-6 satellites.

– Phase 2 (1986 – 1993): Orbital constellation of 12 satellites. Flight test completion. Initial system operation.

– Phase 3 (1993 – 1995): Deployment of nominal orbital constellation of 24 satellites. System operation.

In March 1995, the Russian Federation Government Resolution offered the navigational satellite system GLONASS for civil use by International Organizations ICAO and IMO.

In 1995, the full system deployment was completed. However, due to insufficient funding, the replenishment of the GLONASS system was not performed over the period from 1995 to 1998. And, since 1998, the replenishment of the system has been limited to one launch of 3 satellites per year.

The status of orbital constellation on 4 August 2010 is 21 operational satellites (the current status is indicated on Russian Space Agency Information-Analytical Centre GLONASS,

(http://www.glonass-ianc.rsa.ru/pls/htmldb/f?p=202:1:9296521002007641687).

Since the late 1970 the GLONASS satellite developer JSC "Information Satellite Systems" Reshetnev Company has designed 3 generations of GLONASS satellites: GLONASS, GLONASS-M and GLONASS-K.

Overall views of these satellites are shown on Fig. 5-2.

FIGURE 5-2

Three generations of GLONASS satellites:
a) GLONASS, b) GLONASS-M, c) GLONASS-K

a) b) c)

Sat_time_freq-05-02

Technical characteristics of the GLONASS satellites are presented in Table 5.1.

TABLE 5-1

Comparative performance of GLONASS system satellites

	GLONASS	GLONASS-M	GLONASS-K
First launch	1982	2003	Scheduled for 2010
Lifetime (years)	3	7	10–12
Mass (kg)	1 415	1 415	750
Mass of navigation payload (kg)	180	250	260
Number of satellites per launch:			
– PROTON	3	3	6
– SOYUZ	–	1	2
Power supply (W)	1 000	1 450	1 270
Power consumption by navigation payload (W)	600	580	750
Vertical real time navigation accuracy (95%) (m)	60	30	5–8 (40 – 60 cm, using global differential system)
Number of civil signals	1	3	3
Number of special signals	2	2	3
On-board clocks stability	5×10^{-13}	1×10^{-13}	1×10^{-13}
Root-mean-square error of mutual synchronization of navigation signals (ns)	15	8	3–4
Supplementary functions			Integrity signal Different. Corrections Search and Rescue

GLONASS-K satellite design is based on an unsealed equipment box physically divided into a platform module and payload module.

GLONASS-M Type satellites replace GLONASS satellites. This satellite has improved performance and capability.

The main goals of the performance level of the M-Type satellite are the following:

– Employment of a new frequency band thanks to modernized navigation signal:
  – Frequency band is shifted to the left (instead of frequency letters K = 0 – 12 other frequency letters K = –7...+6 will be used).
  – Previously reserved bytes are used for additional information, including divergence of GPS and GLONASS time scales, navigation frame authenticity (validity) flag, navigation data age.
  – Filters are installed which reduce out- of-band emissions.
  – On both frequencies L1 and L2, dual signals are transmitted which contain digital data and ranging codes for pseudo-range measurements.

– Introduction of an inter-satellite radio-link for distance measurements and data exchange between the satellites orbiting both in the same orbital plane and in different orbital planes.

– Improvement of a navigation signal stability up to 1×10^{-13}. Thanks to the Cs clocks precise temperature stabilization.

– The reduction of solar pressure uncertainty. Thanks to the improvement of the solar array pointing accuracy.

– Satellite lifetime is increased up to 7 years.

A GLONASS-M satellite can be launched both in a tandem launch (3 satellites simultaneously from the BAYKONOUR launch site by a Proton-M Launcher with a Breeze-M Booster) and a single launch (from the PLESETSK launch site by a Soyuz-2 Launcher with a Fregat Booster).

The main part of GLONASS-M satellite's structure is a sealed container, inside which comfortable temperature conditions within the range of 0 – 40ºC are maintained. In the area where the frequency standards are located the temperature stability is ±1ºC.

In the nominal mode, a satellite longitudinal axis is continuously Earth pointed with the accuracy of 0.5º, and a satellite lateral axis coincides with a Sun-satellite-Earth plane with the accuracy of 0.5º, solar arrays are Sun pointed with the accuracy of ±2º. Satellite pointing is provided by momentum wheels that are periodically desaturated by electrical magnetic units.

Propulsion subsystem includes hydrazine (amidol) thrusters and provides generation of control torques in satellite initial modes and orbit control.

It is very important that an orbit control maneuver is only performed during the satellite positioning to its designated orbital slot. High accuracy of orbit parameter control during the Early Orbit Phase and usage of the non-resonant orbits for the orbital constellation enables the exclusion of orbit control maneuvers over the entire satellite mission lifetime.

The electric power subsystem is based on Ni-H batteries and silicon solar arrays. The first launch of a GLONASS-M satellite was in December 2003. This satellite was manufactured by NPO PM.

Further development of the GLONASS system is determined by the Federal Dedicated (Mission Oriented) GLONASS Program approved by Government of the Russian Federation on August 20, 2001. The modernization program was stimulated by:

– (for civil users) the necessity to improve system accuracy, availability and integrity performance to increase system competitive capability in the world market of navigation services;

– (for customers) reduction of the orbit constellation maintenance expense due to increase of satellite lifetime and number of satellites per launch, as well as reduction of ground control segment expenses due to automation implementation;

– (for international cooperation) GLONASS/GPS compatibility and inter-operability.

The Program covers the period from 2002 to 2011. Main Program tasks are:

– Creation and development of space segment and ground infrastructure of navigation satellite system.

– Constellation replenishment and maintenance at the level providing navigation solutions in the interests of different users.

– Development of international cooperation in SATNAV.

– Development and manufacturing of Russian user equipment.

According to the Federal Dedicated (Mission Oriented) Program along with system maintenance using GLONASS-M satellites the development of a new generation GLONASS-K type satellite is envisaged.

Compared to GLONASS-M satellites, a GLONASS-K satellite has the following distinctive features, including:

a) third frequency introduced in L-band to improve reliability and accuracy of user navigation solutions;

b) satellite lifetime increased up to 10 years;

c) satellite mass reduced by a factor of 2;

d) Search and Rescue payload accommodated onboard a satellite.

Up to 2010 NPO PM has completed Phase B and starts Phase C. A GLONASS-K satellite can be launched according to one of the following tandem launch schemes:

– 6 satellites simultaneously from BAYKONOUR launch site by a Proton-M Launcher with a Breeze-M Booster.

– 2 satellites simultaneously from PLESETSK launch site by a Soyuz-2 Launcher with a Fregat Booster.

GLONASS-K satellite design is based on an unsealed equipment box physically divided into a platform module and payload module. In a nominal mode, satellite longitudinal axis is Earth pointed with the accuracy of ±5º, solar arrays are Sun pointed with the accuracy of 1º.

Frequency standards are locally thermally stabilized within the range of ±0.5ºC. For the rest of the equipment the temperature is maintained in the range of –10 to +50ºC.

5.3.2 Control segment

The control segment is composed of:

– System control center (SCC);

– Telemetry, tracking and control stations UT & C;

– One-way monitoring stations;

– Satellite laser ranging stations.

GLONASS ground based control facilities are shown on Fig. 5-3 [Kosenko, 2009].

FIGURE 5-3

GLONASS control segment

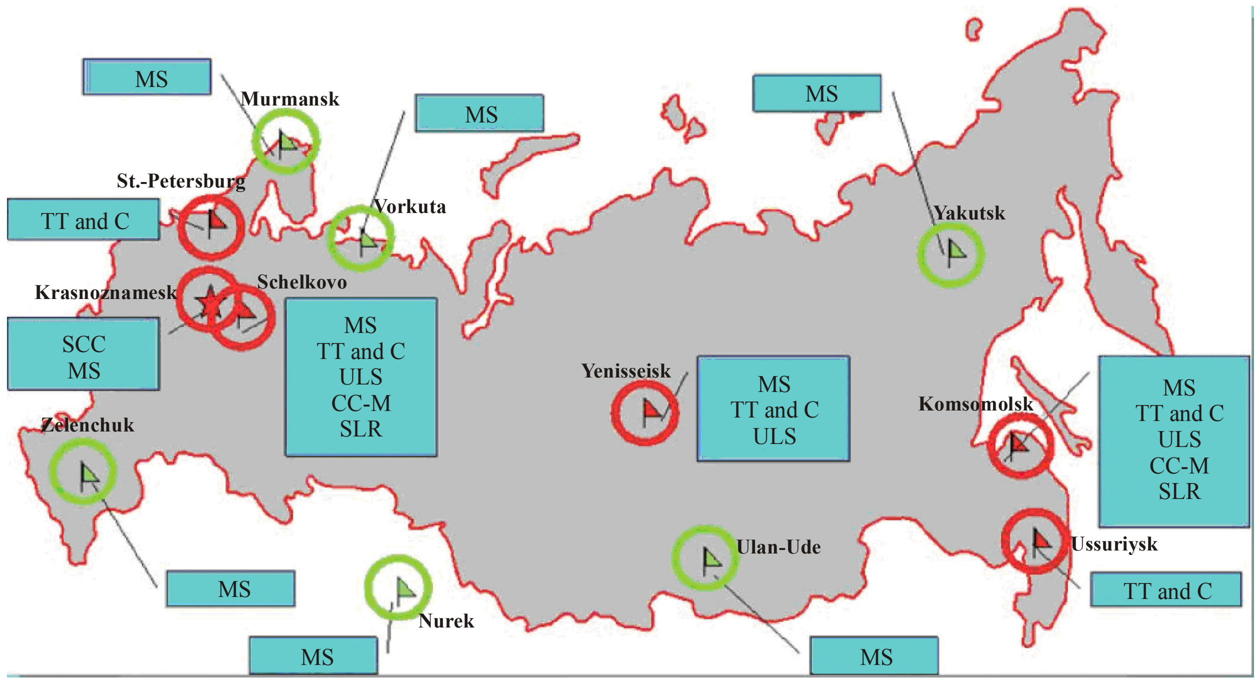

Sat_time_freq-05-03

SSC	– System control centre	MS	– Monitoring and measuring station
TT and C	– Telemetry, tracking, command station	CC	– Central clock
ULS	– Upload station	SLR	– Laser tracking station
(green circle)	– New station (after 2010)	(red circle)	– Operating station

The monitoring stations measure the satellite's orbital parameters and clock shift relative to the main system clock. These data are transmitted to the system control centre. The centre calculates the ephemerides and clock correction parameters and then uploads messages to the satellites through the monitor stations on a daily basis.

5.3.3 User segment

The user segment consists of a great number of user terminals of different types. The user terminal consists of an antenna, a receiver, a processor and an input/output device. This equipment may be combined with other navigation devices to increase navigation accuracy and reliability. Such a combination can be especially useful for highly dynamic platforms.

User equipment performs passive measurements of pseudoranges and pseudorange rate of 4 (3) GLONASS satellites as well as receives and processes navigation messages contained within navigation signals of the satellites. The navigation message describes position of the satellites both in space and in time. Combined processing of the measurements and the navigation messages of the 4 (3) GLONASS satellites allows user to determine 3 (2) position coordinates, 3 (2) velocity vector constituents, and to refer user time scale to the National Reference of Coordinated Universal Time (UTC). The data ensuring of sessions scheduling for navigational determinations, selection of working "constellation" of SVs and detection of radio signals transmitted by them, are transmitted as a part of the navigation message.

These devices are functionally incorporated into GLONASS, just like mobile telephones and user terminals are incorporated into telecommunication systems. Large-scale production of consumer navigation devices (CND) for GPS began in the late 1980s; at present, their serial production, including two-system GPS/GLONASS receivers, is conducted at more than 100 enterprises producing 500 standard types of receivers. Note that CND development and production for non-governmental users is the purpose of private business, especially because at present the world annual sales of products and services in this industry exceed USD 10 billion. Nevertheless, the government supports the development of the element base necessary for creating competitive CND models [GLONASS, 2008].

5.4 GLONASS time

Onboard each satellite, there are caesium time and frequency standards incorporated into the system of the onboard synchronizing device used for forming, storing, and producing the onboard time scale and highly stable navigation signals in frequency ranges of 1 600 MHz and 1 250 MHz. In 2010, it is planned to begin launching new generation satellites GLONASS-K (Fig. 5-1c)) with improved characteristics. Their guaranteed life span will be 10 years. They will also incude the third civilian signal in the frequency range L3 (1 198–1 212 MHz). The time and frequency standards are the onboard synchronizing devices that largely determine the guaranteed life span of the navigation satellites [GLONASS, 2008; Dvorking *et al.*, 2009].

GLONASS time is based on an atomic time scale similar to GPS. This time scale is UTC as maintained by Russia (UTC (SU)). Unlike GPS, the GLONASS time scale is not continuous and must be adjusted for periodic leap seconds. Leap seconds are applied to all UTC time references as specified by the International Earth Rotation and Reference System Service (IERS). Leap seconds are used to keep UTC close to mean solar time. Mean solar time, based on the spin of the Earth on its axis, is not uniform and its rate is gradually changing due to tidal friction and other factors such as motions of the Earth's fluid core.

GLONASS time is maintained within 1 ms, and typically better than 1 μs, of UTC (SU) by the control segment with the remaining portion of the offset broadcast in the navigation message. As well, Moscow offsets GLONASS time from UTC (SU) by plus three hours. The GLOCLOCK log, refer to the OEMV Family Firmware Reference Manual, contains the offset information between GPS and GLONASS time.

The GLONASS satellites are equipped with clocks (time/frequency standards) whose daily instability is not worse than 5×10^{-13} and 1×10^{-13} for the GLONASS-M satellites. An accuracy of mutual synchronization of the satellite time scales is not worse than 20 ns (1 σ) for the GLONASS and 8 ns (1 σ) for the GLONASS-M satellites.

GLONASS time is generated based on GLONASS central synchronizer (CS) time. Daily instability of the central synchronizer hydrogen clocks is not worse than 2×10^{-15}.

The time scales of the GLONASS satellites are periodically compared with the CS time scale. Corrections to each onboard time scale relative to GLONASS time and UTC (SU), are computed and uploaded to the satellites twice a day by control segment. The error of a system using the GLONASS UTC (SU) time scale should not exceed 1 μs.

The GLONASS time scale is periodically corrected to integer number of seconds simultaneously with UTC corrections that are performed according to the Bureau International des Poids et Mesures (BIPM) notification (leap second correction) – see Fig. 5-3. Typically, these corrections (1s) are performed once a year (or 1.5 years) at midnight 00 h 00 min 00 s UTC from December 31 to January 1, 1st quarter (or from March 31 to April 1, 2nd quarter or from June 30 to July 1, 3rd quarter or from September 30 to October 1, 4th quarter) by all UTC users.

FIGURE 5-4

GLONASS time correction accuracy comparison to UTC and GPS time [Kosenko, 2009]

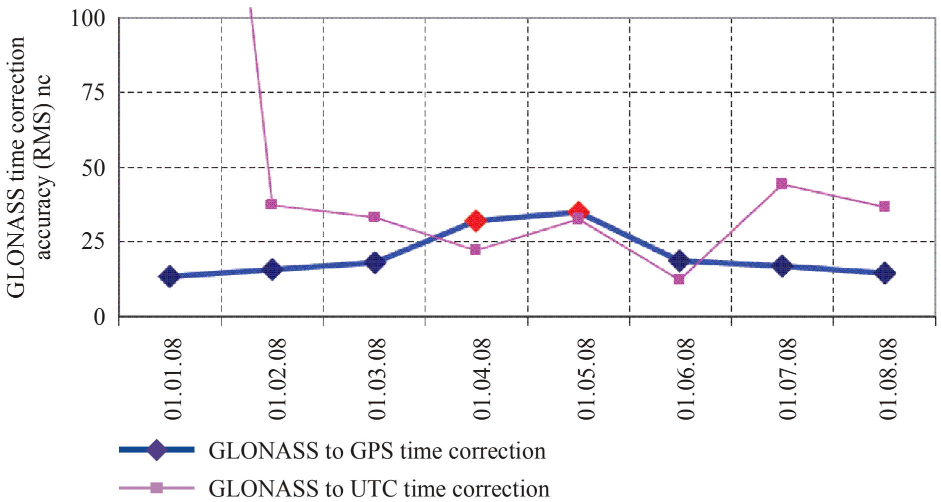

Sat_time_freq-05-04

The GLONASS users are notified in advance (at least three months before) on these planned corrections through relevant bulletins, notifications etc. The GLONASS satellites have not any data concerning the UTC leap second correction within their navigation messages. However, the navigation message of GLONASS-M satellites has provision of advance notice for users on forthcoming UTC leap second correction, its value and sign (see § 4.5 of [GLONASS, 2008]).

Due to the leap second correction there is no integer-second difference between GLONASS time and UTC (SU). However, there is constant three-hour difference between these time scales due to GLONASS control segment specific features:

$$t_{GLONASS} = t_{UTC\ (SU)} + 03\ \text{h}\ 00\ \text{min} \qquad (5\text{-}1)$$

where:

$t_{GLONASS}$: GLONASS time;

$t_{UTC\ (SU)}$: the national scale of Coordinated Universal Time (UTC (SU)).

To re-compute satellite ephemeris at a moment of measurements in UTC (SU) the following equation shall be used:

$$t_{UTC\ (SU)} + 03\ \text{h}\ 00\ \text{min} = t + \tau_c + \tau_n(t_b) - \gamma_n(t_b)\ (t - t_b) \qquad (5\text{-}2)$$

where:

t: time of transmission of navigation signal in onboard time scale

τ_c , τ_n , γ_n, t_b: ephemeris and almanac parameters (given in §§ 4.4 and 4.5).

GLONASS-M satellites also transmit special coefficients B1 and B2 for determination of the difference between Universal Time UT1 and Coordinated Universal Time (UTC) as well as GPS correction to GPS time relative to GLONASS time which shall be not more 30 ns (σ) [GLONASS, 2008].

5.5 Orbit determination and time synchronization (OD & TS) of GLONASS system

In GLONASS system nominal mode, the determination of time corrections and orbit parameters is performed separately. Time corrections are determined twice a day for each satellite using one-way and two-way measurements. The comparison of ranges computed using one-way and two-way measurements enables easy definition of time corrections for onboard clocks. For ephemeris determination only two-way measurements are used.

The frequency-time support system includes radio non-query and query measurement stations (NMS and QMS) and the system's central synchronizer (Shchelkovo in Moscow oblast). Measurements of pseudorange to the navigation satellite using NMS and measurements of distance using QMS produce the values of onboard time scale shifts relative to the system's time scale. The central synchronizer, consisting of several highly stable hydrogen frequency standards with a daily instability of no worse than 5×10^{-14}, acts, in fact, as a system clock, relative to which all the satellite clocks are synchronized and with which the consumer compares his clock.

In turn, the GLONASS system time scale is synchronized with the scale of the National Time and Frequency Standard (Mendeleevo, Moscow oblast), UTC (SU), which is one of the realizations of Coordinated Universal Time (UTC). Correction of the GLONASS system time scale relative to Universal Time (UT1) is determined according to data of radio interferometry with very long baselines and is transmitted to the consumer in a navigation message [Dvorking *et al.*, 2009].

Nowadays (2010) thanks to creation of one-way measuring facilities and completion of Earth gravity field activities, the validation of technology of simultaneous time corrections and ephemeris determination based only on one-way measurements has been started.

The ephemeris transmitted by GLONASS system satellites describes the satellite position in the geocentric reference frame PZ-90. For combined use of GLONASS and GPS systems, satellite coordinates can be converted into the WGS-84 system and a corresponding matrix exists for this purpose. The error of coordinate conversion is less than 1.5 m (1σ) along each axis.

Some tasks of OD & TS for the GLONASS-K satellites are now solved by satellite on-board software that significantly improves satellite autonomy. The main OD & TS tasks performed on-board are as follows:

– generation and delivery of navigation superframes to navigation transmitter;
– preliminary processing of inter-satellite range measurements;
– refinement of satellite reference ephemeris using inter-satellite range measurements;
– calculation of time corrections with respect to a group time scale;
– propagation of ephemeris and time data.

As regards to reference ephemeris refinement using inter-satellite measurements, three methods have been examined:

– The method of orthogonal viewing when only along track components are refined using mutual measurements with line-of-sight orthogonal to satellite motion.
– The method based on "user" principal when every satellite reference ephemeris is refined assuming that the reference ephemerides of other satellites are known exactly.

– The method of planar orbit parameters refinement, which consists in refinement of along track and radial components. The ephemeris of each satellite and of all other satellites in view are refined on-board.

The third method seems to be the most optimum. On-board refinement of the reference ephemeris and onboard refinement of the time corrections using inter-satellite measurements are performed separately. The errors (RMS) of ephemeris transmitted in navigation frame are as follows:

– for GLONASS satellites: along track – 20 m, along binormal – 10 m, along radius – 5 m;

– for GLONASS-M satellites: along track – 7 m, along binormal – 7 m, along radius – 1.5 m.

Since 1999, according to the Russian Government Decree, the GLONASS system became a dual purpose system, that is to say, its usage is foreseen for both military users and civilian ones. Moreover, the GLONASS system is open for international cooperation to create an international navigation system and its usage is envisaged by ICAO and IMO. Combined use of GPS and GLONASS systems will provide users with reliable navigation featuring the high accuracy and availability as well as facilitate the development of world navigation services market.

5.6 GLONASS signals and radio-frequency spectrum

In contrast to the GPS system, which applies signals with coded channel division where all the navigation satellites emit signals at one and the same carrier frequency, the GLONASS system applies frequency division so that each satellite emits the navigation signal at its own carrier frequency. Both methods have their advantages and disadvantages. In particular, the use of coded channel division largely simplifies the creation of mass consumer devices and enables an unlimited increase in the number of satellites. Therefore, with the purpose of balanced development of GLONASS and expansion of the quantity and quality of navigation services, it is planned to introduce new navigation signals with both frequency and phase division on GLONASS-K satellites.

5.6.1 Frequency requirements

The frequency requirements for the GLONASS system were based upon ionosphere transparency, radio link budget, simplicity of user antennas, multipath suppression, equipment cost and RR provisions. The carrier frequencies vary by an integer multiple of 0.5625 MHz in the L1 band, by 0.4375 MHz in the L2 band and by 0.423 MHz in the L3 band.

Since 2006 new satellites in the GLONASS system use 14 to 20 carrier frequencies in different bands. In the L1 band carrier frequencies 1 598.0625 MHz (lowest) to 1 605.3750 MHz (highest) are used, in the L2 band carrier frequencies from 1 242.9375 MHz (lowest) to 1 248.6250 MHz (highest) are used and in the L3 band carrier frequencies from 1201.7430 MHz (lowest) to 1209.7800 MHz (highest) are used. Nominal values of carrier frequencies of radionavigation signals used in the GLONASS system are given in Table 5-1 (Recommendation ITU-R M.1787).

TABLE 5-1

Nominal values of carrier frequencies of radionavigation signals in the GLONASS system

K (No. of carrier frequency)	F_K^{L1} (MHz)	F_K^{L2} (MHz)	F_K^{L3} (MHz)
12	–	–	1 209.7800
11	–	–	1 209.3570
10	–	–	1 208.9340
09	–	–	1 208.5110
08	–	–	1 208.0880
07	–	–	1 207.6650
06	1 605.3750	1 248.6250	1 207.2420

TABLE 5-1 (*end*)

K (No. of carrier frequency)	F_K^{L1} (MHz)	F_K^{L2} (MHz)	F_K^{L3} (MHz)
05	1 604.8125	1 248.1875	1 206.8190
04	1 604.2500	1 247.7500	1 206.3960
03	1 603.6875	1 247.3125	1 205.9730
02	1 603.1250	1 246.8750	1 205.5500
01	1 602.5625	1 246.4375	1 205.1270
00	1 602.0000	1 246.0000	1 204.7040
−01	1 601.4375	1 245.5625	1 204.2810
−02	1 600.8750	1 245.1250	1 203.8580
−03	1 600.3125	1 244.6875	1 203.4350
−04	1 599.7500	1 244.2500	1 203.0120
−05	1 599.1875	1 243.8125	1 202.5890
−06	1 598.6250	1 243.3750	1 202.1660
−07	1 598.0625	1 242.9375	1 201.7430

Two phase-shift keying (by 180° of the phase) navigation signals shifted in phase by 90° (in quadrature) are transmitted at each carrier frequency. They are a standard accuracy (SA) signal and a high accuracy (HA) one.

Each satellite (GLONASS and GLONASS-M) transmits navigation signals in two frequency ranges L1 (1.6 GHz) and L2 (1.2 GHz and use different carriers. The same carriers are used by antipodal satellites in the same plane. The nominal carriers in L1 and L2 frequency bands are defined by the following expressions:

$$f_{K1} = f_{01} + K\Delta f_1 \tag{5-3}$$

$$f_{K2} = f_{02} + K\Delta f_2 \tag{5-4}$$

where:

K: number of the carrier

f_{01} = 1 602 MHz

Δf_1 = 562.5 kHz

f_{02} = 1 246 MHz

Δf_2 = 437.5 kHz.

Before 2005, the values taken for K were integers from 0 to 13, after 2005 – from –7...+6.

For GLONASS-K satellites the third frequency L3 is introduced.

5.6.2 Signal power and spectra

Spectrum of GLONASS signals in L1, L2 bands is shown on Fig. 5-4 and spectrum of GLONASS-K satellite signal in L3 band on Fig. 5-5 [Revnivykh, 2005].

FIGURE 5-5

GLONASS spectrum: b) L1 band, a) L2 band

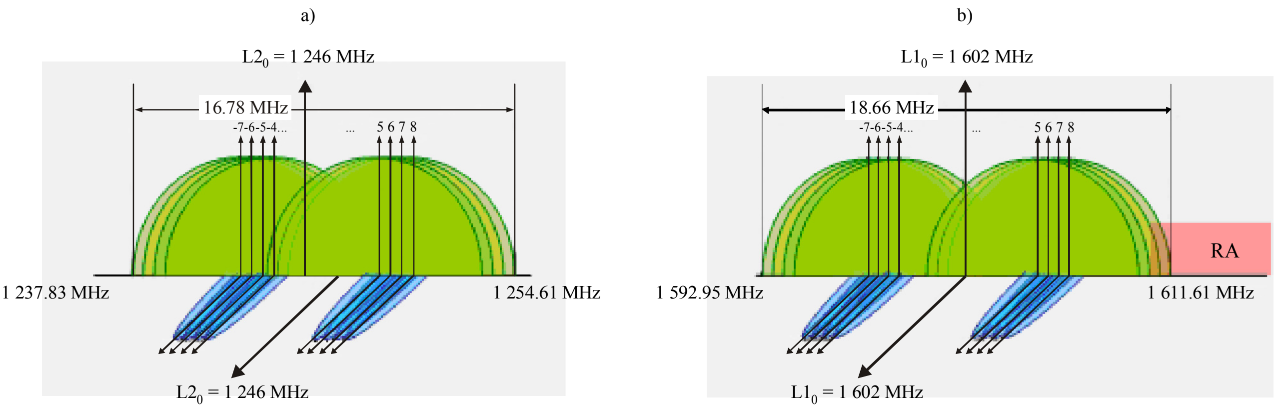

Sat_time_freq-05-05

FIGURE 5-6

GLONASS spectrum: signal L3 (GLONASS-K)

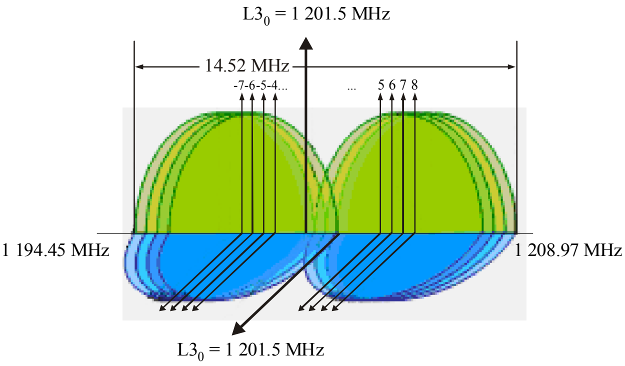

Sat_time_freq-05-06

Transmitted signals are elliptically right-hand polarized with an ellipticity factor no worse than 0.7 for L1, L2 and L3 bands. The minimum guaranteed power of a signal at the input of a receiver (assumes a 0 dBi gain antenna) is specified as −161 dBW (−131 dBm) for both SA and HA signals in the L1, L2 and L3 bands (Recommendation ITU-R M.1787).

Three classes of emissions are used in the GLONASS system: 8M19G7X, 1M02G7X, 10M2G7X. Characteristics of these signals are given in Table 5-2.

TABLE 5-2

Characteristics of GLONASS signals

Frequency range	Emission class(1)	Tx bandwidth (MHz)	Maximum peak power of emission (dBW)	Maximum spectral power density (dB(W/Hz))	Antenna gain (dB)
L1	10M2G7X 1M02G7X	10.2 1.02	15 15	−52 −42	11
L2	10M2G7X 1M02G7X	10.2 1.02	14 14	−53 −43	10
L3(2)	8M19G7X 8M19G7X	8.2 8.2	15 15	−52.1 −52.1	12

(1) Radio Regulations, Edition of 2008. Volume 2, Appendix 1.

(2) Two GLONASS L3 signals are shifted relative to each other by 90° (in quadrature).

The power spectrum envelope of the navigation signal is described by the function $(\sin x/x)^2$, where:

$$x = \pi(f - f_c) / f_t \tag{5-5}$$

where:

f: frequency considered

f_c: carrier frequency of the signal

f_t: chip rate of the signal.

The main lobe of the spectrum forms the signal's operational spectrum. It occupies a bandwidth equal to $2f_t$. The lobes have a width equal to f_t.

5.7 GLONASS and GPS combined use features

It is obvious that combination of GPS and GLONASS will ultimately produce a 48 satellite system. With such a system, satellite blockage will become less of a limiting factor, allowing for increased measurement redundancy.

Modern digital signal processing methods make it possible to process the signals of GPS and GLONASS using the same receiver architecture despite the differences between the systems. GPS and GLONASS frequency ranges are close, thus allowing the use of a combined antenna and common input preamplifier in the user equipment. Optimal receiver design and appropriate signal-processing software should allow the development of a combined receiver at a price only slightly higher than that of a GPS or GLONASS receiver. The differences in the ephemeris information and almanac representation of GPS and GLONASS do not pose an obstacle for user equipment operation. Navigation processor software provides appropriate corrections and permits the processing of both data flows.

User equipment, the most flexible part of the entire system, continuously improves. Most existing receivers are multi-channel, and are capable of simultaneously tracking pseudo-ranges and pseudo-velocities for a number of visible satellites. Thus they provide maximum accuracy and integrity of navigation observations. Technological progress in the field of digital signal processing provides the means for a very high degree of integration that already permits a discrete conversion and digital processing of the satellites' signals at a stage near the front-end input.

Combined application of GLONASS and GPS provides significant advantages versus stand-alone use any of these systems:

Enhanced Availability: For operations in obstructed environments, like mountainous terrain or urban “canyons”, the doubling of the number of available satellites often means a valid solution versus no solution for GPS-or GLONASS-only receivers.

Improved Accuracy: The increased number of satellites will usually lead to better user-to-satellite geometry (PDOP).

Faster Cold Start: When no position or time information is assumed by the receiver, the probability of acquiring a satellite is increased when the number of satellites in view is increased, thereby reducing acquisition time.

Robust System Integrity: The ability to detect and isolate a malfunctioning satellite is greatly enhanced by the increased number of satellite in view. Also, reliance on two independent systems provides an added level of integrity against a system-wide malfunction.

On the market, there is equipment available using the signals of navigation satellites of the GLONASS and GPS systems simultaneously in topological and geodetic survey on the land, at the sea and in the air. This equipment when operating in a differential mode guarantees the precision of geodetic fixing for earth stations 1-3 cm + $10^{-6} L$ ($L = 1\,000$ km), where L is the distance between geodetic stations, cars, aircrafts, vessels [ITU-R Handbook, 2002].

Recognizing the above-mentioned GPS–GLONASS advantages delegations of the United States of America and the Russian Federation met in Washington D.C. on December 9-10, 2004 and established working groups to deal with matters of development and use of GPS and GLONASS. Maintaining compatibility of radio frequencies between each other’s satellite-based navigation and timing signals is a primary focus of continuing cooperative efforts. Both sides reiterated their commitment to continuing these talks and reaffirmed that the United States of America and the Russian Federation intend to continue to provide the GPS and GLONASS civil signals appropriate for commercial, scientific and safety of life use on a continuous, worldwide basis, free of direct user fees. Since that time GPS-GLONASS Working Group is meeting on regular basis.

5.8 Conclusion

Based on the above information, the following can be pointed out:

– GLONASS is a Global Navigation Satellite System currently (2010) providing almost global coverage (to be completed in few years).

– GLONASS system is a dual (civil and military) use system.

– GLONASS is coordinated by the civil agency ROSCOSMOS (Russian Federal Space Agency).

– The use of GLONASS in combination with GPS will improve the quality of navigation and precise time dissemination services.

– GLONASS is open for international cooperation.

References

DVORKING,V. V., NOSENKO,YU. I. URLICHICH, YU. M., FINKEL'STEIN, A. M. [2009] The Russian Global Navigation, Satellite Program. Vestnik Rossiiskoi Akademii Nauk. Vol. 79, **1**, (http://www.springerlink.com/content/180m3184w46747u5/fulltext.pdf).

GLOTOV, V. D., REVNIVYKH, S. G., MITRIKAS, V. V. [October 2006] GLONASS status update. MCC activity in GLONASS program. 15th International Workshop on Laser Ranging, Canberra, Australia, (http://cddis.gsfc.nasa.gov/lw15/docs/papers/GLONASS%20Status%20Update%20and%20MCC%20Activity%20in%20GLONASS%20Program.pdf).

KOSENKO V. [3-9 May, 2009] Satellite System GLONASS Status and Plans. Proceedings of European Navigation Conference - Global Navigation Satellite Systems (ENC-GNSS), Naples, Italy, (http://www.enc-gnss09.it/proceedingsPDF/04_Kosenko.pdf).

POLISCHUK G., M., KOZLOV, V. I., ILITCHOV, V. V., KOZLOV, A. G., BARTENEV V. A., KOSSENKO, V. E., ANPHIMOV, N. A., REVNIVYKH, S. G., PISAREV, S. B., TYULYAKOV, A. E. [2002] Global navigation satellite system GLONASS: development and usage in the 21st century. 34th Annual Precise Time and Time Interval (PTTI) Meeting, Reston, Virginia, USA, (http://tycho.usno.navy.mil/ptti/ptti2002/paper13.pdf).

REILLY, J. P. [2004] A review of the evolution of the Russian GLONASS system, http://www.topconpositioning.com/uploads/tx_topconfilearchive/POB_Magazine_takes_an_in-depth_look_at_GLONASS - Click here for article.pdf.

REVNIVYKH, S. G. [14-15 March, 2005] GLONASS: Status and Perspectives. Civil GPS Service Interface Committee International Information Subcommittee, Prague, Check Republic, (http://radio.feld.cvut.cz/satnav/CGSIC/).

RISDE [2008] Global Navigation Satellite System GLONASS Interface Control Document Navigational radio signals in bands L1, L2, Ed. 5.1, Russian Institute of Space Device Engineering (RISDE), (http://rniikp.ru/en/pages/about/publ/ikd51en.pdf).

ITU-R texts

ITU-R Handbook on Spectrum Monitoring, Edition 2002, (http://www.itu.int/publ/R-HDB-23/en).

Radio Regulations, Edition of 2008, Volume 2, Appendix 1 – Classification of emissions and necessary bandwidth, (http://www.itu.int/publ/R-REG-RR-2008/en).

Recommendation ITU-R M.1787 – Description of systems and networks in the radionavigation-satellite service (space-to-Earth and space-to-space) and technical characteristics of transmitting space stations operating in the bands 1 164-1 215 MHz, 1 215-1 300 MHz and 1 559-1 610 MHz, (http://www.itu.int/rec/R-REC-M.1787-0-200908-I/en).

CHAPTER 6

COMMUNICATION SATELLITE SYSTEMS

Page

6.1 Introduction

The principal function of communications satellites is to transfer RF signals for communications purposes. Therefore, time and frequency transfer via communications satellites is usually accomplished by piggybacking off the communications functions. Some satellite systems, especially those utilizing time-division multiple access systems (TDMA), require precise time for their communications functions [ITU-R Handbook, 2002; Ha, 1990]. In the majority of TDMA cases, the satellite just passes through precise timing signals from the ground, and the satellite payload itself does not require precise time for its operation. Time transfer capability is required in the satellite bus telemetry, tracking, and command system, for ranging and time tagging purposes. However, this part of the satellite system is generally not available to the leasing user. Frequency accuracy and stability requirements for commercial satellites are in general limited to that required for maintaining band allocations and for performing ranging functions. Government communications satellites tend to have much more accurate on-board frequency sources, because they are also used for navigation or other purposes that require precise time.

Two parts of a communications satellite can be used for time transfer, the communications payload and the bus tracking, telemetry, and command (TT & C) system. The following sections will describe the principles of operation of each of these systems with emphasis on the issues for time transfer.

Structure, main technical and operational characteristics of communication satellites are described in [ITU-R Handbook, 2002].

6.2 The communication payload

Communications satellites are used for a variety of communications services. Uplink and downlink frequency bands are used to communicate through the satellite payload. These bands are often further broken down into sub-bands, often called channels. The purpose of a communications payload is to receive signals from the uplink bands or channels, to transpond the signals to new frequencies and further process them, and to retransmit the processed signals at the downlink bands or channels.

A satellite's bands or channels are either utilized by a single user in single access (SA) mode, such as a broadcast application, or multiple users in various multiple access (MA) modes. The various MA modes are spatial domain multiple access (SDMA), time-division multiple access (TDMA), code-division multiple access (CDMA), frequency-division multiple access (FDMA) and random multiple access (RMA).

These MA modes are often used in combination to expand the capacity of the band or channel.

Communications payloads consist of two general types of architectures, bent-pipe or regenerative, and two types of implementations, analog or digital. These architectures and implementations are discussed in the sections that follow.

6.2.1 Analog bent-pipe architecture

The most common payload architecture in use is the analog bent-pipe architecture. In this architecture, multiple bent-pipe transponders simply translate one or more signals in an uplink frequency band to a downlink frequency band and rebroadcast the aggregate signal at the downlink band. This type of architecture is the most useful for time transfer since the signal path is relatively straightforward. Commercial satellites using this architecture tend to utilize individual free running local oscillators (LOs) to translate the frequency bands. Government satellites utilizing this architecture often use LOs that are coherently derived from a single master oscillator (MO) on the satellite. In some cases, the satellite MO is phase locked to a ground reference at the satellite control station. The phase error characteristics of the LOs used to perform this frequency translation are an important limitation for time transfer applications.

Figure 6-1 shows the block diagram of a typical bent-pipe architecture [ITU-R Handbook, 2002; Ha, 1990]. In the diagram, an uplink antenna followed by a wideband band filter (BPF) and low noise amplifier (LNA) to determine the uplink antenna gain to noise temperature ratio (G/T) that is the primary figure of merit for the satellite for the uplink. The received signal is then amplified and translated to the downlink band by a receiver or converter (that sometime includes the LNA).

FIGURE 6-1

Typical bent-pipe repeater architecture

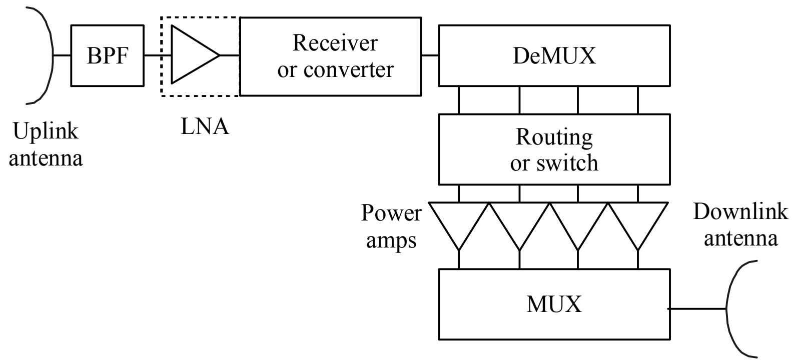

Sat_time_freq-06-01

As mentioned previously, commercial converters or receivers tend to use individual free running crystal controlled oscillators for the LO used to translate the frequency while government converters tend to use synthesized LOs that are phase coherent with a single MO. Figure 6-2 shows a typical commercial receiver [Ha, 1990]. Note the LO multiplier chain that is derived from a free running oven controlled crystal oscillator.

FIGURE 6-2

Typical commercial C-band receiver

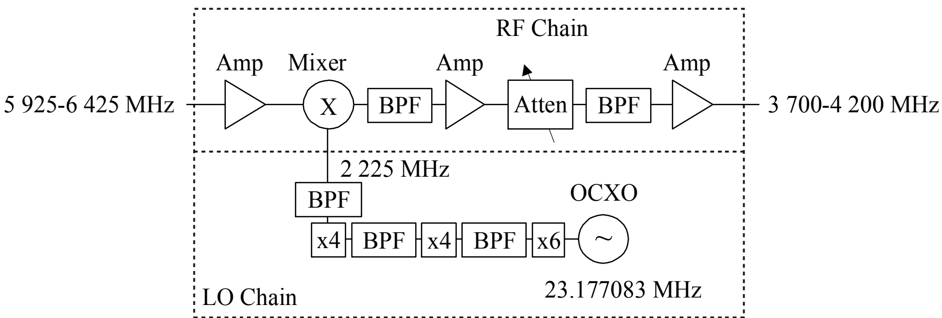

Sat_time_freq-06-02

In Fig. 5-1, a demultiplexer (DEMUX), that separates the full uplink band into individual bands or channels, follows the converter. In some payloads, the de-multiplexing is accomplished in the converters using synthesized LOs to allow individual channel frequency conversations to be selectable. The individual channels are then routed to output power amplifiers, and sometimes a switch is used to select routing paths. The signals from individual power amplifiers are then combined in an output multiplexer (MUX) for rebroadcast by the downlink antenna.

In most bent-pipe payloads, precise time is not required for their operation and frequency accuracy and stability are limited to that required to meet band allocations. This is also true when TDMA switching is accomplished through the ground or earth stations [ITU-R Handbook, 2002]. The exception is satellite switched TDMA (SS-TDMA), where the switch between the DEMUX and the MUX is used to aid the TDMA operation. In this case, the timing requirement for the switch can be at the sub-microsecond level [Ha, 1990].

In payloads that are used for satellite-to-satellite ranging as well as communications signals, there is a higher requirement for frequency accuracy and stability. These payloads often use synthesized LOs locked to a master oscillator.

6.2.2 Regenerative architecture

Regenerative payload architectures demodulate the uplink signals to produce base-band data and remodulate this data onto downlink carriers. Because there is no direct path between uplink and the downlink, time transfer through these payloads must take into account data latencies through the satellite digital processing system.

6.2.3 Digital implementation

Some new satellite systems utilize digital processing even when they are of the bent-pipe type. Time transfer through these systems must also take into account digital latencies. It is difficult to generalize about the time transfer characteristics of these payloads, and often the detailed nature of these payloads is proprietary. The reader is referred to the specific payload manufacturer.

6.2.4 The tracking, telemetry and command system

The telemetry, tracking, and command (TT & C) system in a satellite is part of the bus housekeeping system and the details of operation are generally proprietary. The system utilizes time codes, but this capability is usually limited to accuracies required for diagnostic time tagging purposes unless satellite switched TDMA is used or there are other requirements such as navigation. The tracking system is designed to determine the position and orientation of the satellite. It consists of angular tracking systems to determine orientation and ranging systems to determine position. The ranging systems can be used for time transfer purposes. Ranging systems utilize coherent side-tone or pseudo-random code modulated signals to measure the one-way or round trip delay from the ground station to the satellite in a fashion similar to that used in the GPS system (one-way ranging). The ranging data is time tagged with sufficient accuracy to make orbit calculations and is thus sufficiently accurate for precision time transfer purposes.

6.3 Timing and synchronization for satellite operation

Timing and synchronization in commercial communications satellites is usually a simple matter. Master oscillators are usually manually steered to keep them within a frequency tolerance or allowed to free run for the life of the mission. Independent transponder LOs used in commercial satellites are not frequency controlled, but are designed to meet an accuracy requirement for band allocation purposes over the life of the satellite. The timing system is usually updated manually via ground command if necessary. Government satellites can use more sophisticated timing systems because of navigation and other requirements. Government master oscillators are sometimes locked to ground references and sometimes are free running, with steering through frequency updates.

6.4 Impact of link noise and satellite imperfections in bent-pipe payloads

The noise and imperfections of the link through a bent-pipe payload affects the ability to perform satellite time transfer. The contributors to the noise and imperfections are white noise, and phase noise, and systematic phase variations.

6.4.1 White noise contribution

A general expression for the white noise contribution to satellite time transfer error can be derived from basic satellite link noise equations and time error equations as follows. If a signal of angular frequency ω (rad/s) is utilized for time transfer, the clock reading error x of the time transfer (seconds) can be related to the phase error ϕ of the signal (in radians) by the well-known equation:

$$x = \varphi/\omega \tag{6-1}$$

This time transfer signal may either be the carrier signal itself or various modulation components that reside on the carrier. For white noise, the standard variance of ϕ (for a single phase measurement) is given by:

$$\sigma_{\varphi}^{2} = P_{noise} / P_{signal} \tag{6-2}$$

where:

- P_{signal}: received signal power
- P_{noise}: received noise power.

Thus, from equations (6-1) and (6-2), the standard variance of x (for a single measurement) becomes:

$$\sigma_{x-std}^{2} = P_{noise} / (P_{signal} \omega^{2}) \tag{6-3}$$

Using well-published link and white noise equations [ITU-R Handbook, 2002], one can derive the following expression for the received signal to white noise ratio (for either the satellite uplink or downlink) in terms of basic link parameters:

$$P_{noise} / P_{signal} = kB(2r\omega_{car} / (c\omega))^{2} / P_{eirp}(G/T)) \tag{6-4}$$

where:

- P_{eirp}: transmit effective isotropically radiated power
- G/T: receive gain over temperature ratio
- B: limiting (smallest) bandwidth of the link
- ω_{car}: carrier angular frequency for the link
- k: Boltzman's constant, r is the range and c is the speed of light.

Thus for either link:

$$\sigma_{x-std}^{2} = kB(2r\omega_{car} / (c\omega))^{2} / P_{eirp}(G/T)) \tag{6-5}$$

Since the white noise contributions from the uplink and downlink are statistically independent, the combined variance for both the uplink and downlink is given by:

$$\sigma_{x-std-tot}^{2} = 4\, kB(\omega_{car} / (c\omega))^{2} [r_{uplink}^{2} / P_{eirp-ground}(G/T)_{satellite}) + r_{downlink}^{2} / (P_{eirp-satellite}(G/T)_{ground})] \tag{6-6}$$

where:

- B: limiting bandwidth for the complete link.

Equation (6-6) represents the clock reading error for a single-phase measurement. A fractional frequency estimate over averaging time τ can be made by differencing two clock-reading measurements and dividing by τ. The standard variance or Allan variance (the same for white noise) of the fractional frequency estimates for this averaging time τ is thus given by:

$$\sigma_{y}^{2} = 8\, kB(\omega_{car} / (c\omega))^{2} [r_{uplink}^{2} / P_{eirp-ground}(G/T)_{satellite}) + r_{downlink}^{2} / (P_{eirp-satellite}(G/T)_{ground})] \tag{6-7}$$

The variance of the second difference of the clock reading error over time τ:

$$\sigma_{X}^{2} = \tau^{2} \sigma_{y}^{2} \tag{6-8}$$

and is therefore given by:

$$\sigma_x^2 = 8\,kB(\omega_{car}/(c\omega))^2[r_{uplink}^2 / P_{eirp-ground}(G/T)_{satellite}) + r_{downlink}^2/(P_{eirp-satellite}(G/T)_{ground})] \qquad (6\text{-}9)$$

Equations (6-7) and (6-9) apply to both one and two-way (for each transfer) satellite time transfer since there is no cancellation of white noise by a two-way system. Thus the above equations represent the best one can do for a satellite link. Note also that time transfer utilizing the carrier has lower time jitter than that utilizing modulation because the modulation frequency is always lower than ω_{car}.

6.5 Satellite phase noise and systematic errors

Phase noise is added to the communications signal by the LOs in the frequency converters. Phase noise and frequency drifts of the LOs directly contribute to the transponder signal carrier and modulation phase instability. Near in-phase noise and drifts are generally higher in commercial transponders that utilize individual crystal oscillators. The group and phase delay and delay variations of filters and active components in the system impact both the modulation and the carrier phase, though these instabilities are bounded. The principal source of these instabilities is changes with temperature, bus voltages, and power levels through the channel links. For specific values, one must contact the satellite service provider.

In two-way time transfer through the same transponder, there is a high degree of cancellation of LO drifts and delay variations. For simultaneous two-way time transfer using two different frequencies, the principal issue is delay variation across the channel band due to frequency dispersion. For sequential two-way time transfer, the principal issue is the phase change in the LOs over the time between transfers.

6.6 Conclusion

In order to properly utilize satellite communications systems for time transfer, it is important to understand the structure, operation, and limitations of the system one is utilizing. Time transfer through various types of satellite communications systems has been successfully accomplished by developing methods to take advantage individual system strengths and minimizing the impact of system weaknesses.

References

HA, T. T. [1990] Digital Satellite Communications. McGraw-Hill, 1990.

ITU-R [2002] Handbook on Satellite Communications, Third Edition, International Telecommunication Union, Wiley & Sons, Inc.

MORGAN, W. L. and GORDON, G. D. [1989] Communications Satellite Handbook. Wiley & Sons, Inc.

CHAPTER 7

TIME SCALES

Page

7.1 Introduction

Three primary methods of measuring time have been used. These are:

1. time based on the rotation of the Earth;
2. time based on the celestial motions of the Earth, and Moon and planets;
3. time based on the quantum mechanics of the atom.

Each of these methods has had a variety of refinements as the precision and sophistication of measurement methods have evolved.

Definitions of time scales and related terms are provided in Recommendation ITU-R TF.686-2 – Glossary and definitions of time and frequency terms.

7.2 Universal time

Time as measured by the rotation of the Earth is called mean solar time. When reckoned from midnight on the Greenwich meridian it is called Universal Time (UT). The mean solar day is nominally defined as the time interval between successive transits of the fictitious mean Sun over a given meridian. The mean solar second is defined as 1/86400 of a mean solar day.

The true measure of the Earth's angle of rotation with respect to the celestial reference system is the form of UT known as UT1. In practice, UT1 is determined, not by the position of the Sun, but rather by the diurnal motion of the vernal equinox on the celestial sphere in accordance with a conventional relation specifying UT1 in terms of Greenwich Mean Sidereal Time (GMST). In the past, UT1 was measured from star transits. Today, it is measured by Very Long Baseline Interferometry (VLBI) measurements of selected compact radio point sources, satellite laser ranging (SLR), and tracking of GPS satellites.

The defining expression for UT1 in terms of GMST is [Aoki *et al.*, 1982]:

$$\mathrm{GMST} = 24\,110.''548\,41 + 8640184.''812\,866\,T + 0.''093\,104\,T^2 - 0.''000\,0062\,T^3 \tag{7-1}$$

where:

T: Universal Time elapsed since January 1, 2000, 12 h UT measured in Julian centuries of 36 525 days.

The conventional celestial reference system adopted by the International Astronomical Union (IAU) [General Assembly, 1997] based on positions of extragalactic objects observed with VLBI has changed the basis for UT1 and removed the need for the equinox.

Due to irregularities in the Earth's rotation, UT1 is not uniform. There are three sources of variation: a steady increase in the length of day due to tidal friction, a periodic seasonal variation, and random fluctuations. UT2 is UT1 corrected for the seasonal variation and is defined in seconds by [Seidelmann, 1992]:

$$\mathrm{UT2} = \mathrm{UT1} + 0.''022 \sin 2\pi t - 0.''012 \cos 2\pi t - 0.''006 \sin 4\pi t + 0.''007 \cos 4\pi t \tag{7-2}$$

where:

t: fraction of the Besselian year.

However, UT2 is no longer used in practice.

7.3 Ephemeris time

Ephemeris time (ET) is a uniform timescale defined by the Newtonian gravitational theory of the Earth's motion around the Sun as represented by Newcomb's *Tables of the Sun*. According to Newcomb, the geometric mean longitude of the Sun for the epoch 1900 is given by [NewComb, 1895]:

$$L = 279^{\circ}41'48.''04 + 129\,602\,768.''13\,T + 1.''089\,T^2 \tag{7-3}$$

where:

T: Ephemeris time measured in centuries from 1900.

The linear coefficient of this expression defines the ephemeris second. Thus the tropical year of 1900 contained [360 × 60 × 60/129 602 768.13] × 36 525 × 86 400 = 31 556 925.9747 s.

In 1956, the International Committee for Weights and Measures (CIPM) defined the second of ET as 1/31 556 925.9747 of the tropical year 1900 January 0 12 h ET.

This definition was ratified by the General Conference on Weights and Measures (CGPM) in 1960.

Reference to the year 1900 does not imply that it is the epoch of a mean solar day of 86 400 s. Rather, it is the epoch of a tropical year of 31 556 925.9747 s.

Although ET was defined in terms of the position of the Sun, it was realized indirectly by observation of the Moon. ET may be defined as the independent variable that brings the positions of the astronomical bodies constructed from the Newtonian dynamical laws of motion into accord with observation. It is thus based solely on Newtonian mechanics, which assumes a universal coordinate time, and no provision is made for relativity.

ET replaced UT1 for astronomical ephemerides in 1960.

7.4 Atomic time

The first caesium beam atomic standard became operational at the National Physical Laboratory, United Kingdom, in 1955. Atomic time scales were established in the United States of America by the U.S. Naval Observatory and the National Bureau of Standards in 1956, soon followed by several other observatories and laboratories. Only seven years after the adoption of the ephemeris second in 1960, the CGPM adopted the atomic second as the fundamental unit of time in the International System of Units (SI). The second was defined as "the duration of 9 192 631 770 periods of the radiation corresponding to the transition between the two hyperfine levels of the ground state of the caesium-133 atom". This value was determined by a comparison of ET based on observations of the Moon with the atomic time scale.

Atomic time has become the basis of all modern time scales and has been maintained continuously in various laboratories since 1955 although not formally adopted until 1971 as an international time scale. From the creation of the Bureau International de l'Heure (BIH) in 1920 at the Paris Observatory (OP), the international time scales were based wholly upon astronomical observations. The unit of time was the second and it was likewise based on astronomical observations. The advent and operation of caesium atomic standards in the 1950's, and broadcast systems such as LORAN that enabled accurate international comparison of these standards, lead to an initial form of Atomic Time (AT).

The formation of International Atomic Time (TAI) was recommended by the International Astronomical Union (IAU) in 1967, the International Union of Radio Science (URSI) in 1969 and the International Radio Consultative Committee (CCIR) of the ITU in 1970. The 14th General Conference on Weights and Measures (CGPM) approved the establishment of TAI in 1971 as the coordinate time scale whose unit interval is the second of the International System of Units (SI) as realized on the rotating geoid.

More detailed information on the International Atomic Time implementation (TAI) is provided in § 7.6.1.

7.5 Relativistic time scales

Ephemeris time (ET) was a timescale defined by the Newtonian dynamical laws of motion. However, it made no distinction among dynamical time scales defined with respect to the Earth's surface, the centre of the Earth, or the centre of the solar system. More precise definitions are therefore required for relativistic time scales historically derived from ET. These additional time scales are the arguments of relativistic ephemerides used in astronomy and celestial mechanics. Discussion of relativistic effects in satellite time and frequency transfer and dissemination is provided in Chapter 9.

In 1976 the IAU adopted time scales for relativistic ephemerides such that they differ from TAI by only periodic terms [Muller *et al.* 1977]. In 1979 these time scales were given the names Terrestrial Dynamical Time (TDT) and Barycentric Dynamical Time (TDB). In 1991 TDT was renamed simply Terrestrial Time (TT). In addition, the IAU adopted new time scales that all have the SI second as their unit. Geocentric Coordinate Time (TCG) and Barycentric Coordinate Time (TCB) are time scales for coordinate systems that have their origins at the centre of the Earth and the barycentre of the solar system, respectively [Bergeron, 1992]. These time scales were further clarified by resolutions adopted by the IAU in 2000.

7.5.1 Terrestrial time

Terrestrial time (TT) is the time coordinate that is represented by the proper time readings of clocks on the geoid. In practice, TT is realized in terms of International Atomic Time (TAI), whose unit is the second of the International System of Units (SI). TT can be considered to be equivalent to TDT, which has its origin on 1 January 1977 0 h TAI and maintains continuity with Ephemeris Time (ET). TDT replaced ET in 1984 as the tabular argument of the fundamental geocentric ephemerides.

Since TT is a theoretically uniform time scale, while TAI is a statistically derived atomic time scale, TT and TAI are not rigorously identical. However, to within a tolerance of about ± 10 μs, their difference is constant. A practical realization of TT is:

$$\mathrm{TT} = \mathrm{TAI} + 32.184\ \mathrm{s} \tag{7-4}$$

The constant offset is an estimate of the difference between ET and UT1 at the defining epoch of TAI on 1 January 1958. TT may be regarded as an ideal form of TAI.

7.5.2 Geocentric coordinate time

Geocentric coordinate time (TCG) is the coordinate time scale for ephemerides with respect to the centre of the Earth whose unit is the SI second. The coordinate time Δt at the geocentre TCG is related to the proper time $\Delta\tau$ on the geoid (TT) by:

$$\Delta t = (1 + W_0 / c^2)\, \Delta\tau.$$

Thus TCG differs from TT by the scaling factor:

$$\mathrm{TCG} - \mathrm{TT} = L_G\, \Delta T \tag{7-5}$$

where:

$L_G =$ $W_0 / c^2 = 6.969\ 290\ 134 \times 10^{-10}$ (approximately 60.2 μs/d)

ΔT : time elapsed since 1 January 1977 0 h TAI (JD 244 3144.5)

In 2000, the IAU redefined TT such that it differs from TCG by the constant rate $\mathrm{dTT} / \mathrm{dTCG} = 1 - L_G$. The value of L_G was the best estimate of (W_0 / c^2) in 2000, but it is now considered a defining constant not subject to future revision [Rickmand, 2001].

7.5.3 Barycentric coordinate time

Barycentric coordinate time (TCB) is the coordinate time scale for ephemerides with respect to the centre of the solar system whose unit is the SI second. The coordinate time Δt_B in a barycentric coordinate system corresponding to the proper time $\Delta\tau$ maintained by a clock on the geoid is:

$$\Delta t_B = \int_{\tau_0}^{\tau} \left(1 + \frac{1}{c^2} U(\mathbf{r}) + \frac{1}{2} \frac{1}{c^2} v^2 \right) \mathrm{d}\tau \tag{7-6}$$

where:

r and **v**: barycentric position and velocity of the clock

$U(\mathbf{r})$: gravitational potential of all the bodies in the solar system (including the Earth) evaluated on the geoid.

The coordinate time t_B is identified with TCB and the proper time τ is identified with TT.

The integral depends on the position and velocity of the clock in the barycentric coordinate system. Thus it is desirable to separate the clock–dependent part from the clock–independent part.

In this approximation, one may express **r** and **v** as:

$$\mathbf{r} = \mathbf{r}_E + \mathbf{R} \text{ and } \mathbf{v} = \mathbf{v}_E + \dot{\mathbf{R}}$$

where:

$\mathbf{r}_E$ and $\mathbf{v}_E$: the barycentric position and velocity of the Earth's centre of mass

$\mathbf{R}$ and $\dot{\mathbf{R}} = \boldsymbol{\omega} \times \mathbf{R}$: the geocentric position and velocity of the clock.

The total potential is:

$$U(\mathbf{r}) = U_E(\mathbf{r}) + U_{ext}(\mathbf{r})$$

where:

U_E: Newtonian potential of the Earth

U_{ext}: the external Newtonian potential of all of the solar system bodies apart from the Earth.

Also, $U_{ext}(\mathbf{r}) \approx U_{ext}(\mathbf{r}_E) + \nabla U_{ext} \cdot \mathbf{R}$ and $\mathbf{v}_E \cdot \dot{\mathbf{R}} = (d/dt_B)(\mathbf{v}_E \cdot \mathbf{R}) - \mathbf{a}_E \cdot \mathbf{R}$

where:

$\mathbf{a}_E = \nabla U_{ext}$ is the Earth's acceleration.

Thus [Thomas, 1975; Moyer 1971 and 1981]:

$$\Delta t_B \approx \Delta\tau + \frac{1}{c^2}\int_{t_{B0}}^{t_B}\left(U_{ext}(\mathbf{r}_E) + \frac{1}{2}v_E^2\right)\mathrm{d}t_B + \frac{1}{c^2}W_0\,\Delta\tau + \frac{1}{c^2}\mathbf{v}_E\cdot(\mathbf{r}-\mathbf{r}_E) \qquad (7\text{-}7)$$

where:

– The first term is the proper time measured by a clock on the geoid.

– The second term is due to the combined redshift and time dilation effects at the geocentre with respect to the barycentre and is independent of the clock.

– The third term is the time difference between a clock at the geocentre and a clock on the geoid.

– The fourth term depends on the clock's location.

In the limit of flat space-time, it corresponds to the special relativity clock synchronization correction in the moving geocentric frame when observed from the barycentric frame. For a clock on the geoid, it varies diurnally with an amplitude of 2.1 μs. The cancellation of the two acceleration terms is a manifestation of the *Principle of Equivalence* for a freely falling frame of reference.

The integral may be calculated by numerical integration of the planetary and lunar ephemerides or it may be represented by an analytical formula. It is expressed as the sum of a secular term $L_C\,\Delta T$ and the remaining periodic terms P.

Thus the relation between TCB and TT is (Recommendation ITU-R TF.686-2):

$$\begin{aligned}\mathrm{TCB}-\mathrm{TT} &= \frac{1}{c^2}\int_{t_{B_0}}^{t_B}\left(U_{ext}\left(\mathbf{r}_E\right)+\frac{1}{2}v_E^2\right)dt_B + L_G\,\Delta T + \frac{1}{c^2}\mathbf{v}_E\cdot\left(\mathbf{r}-\mathbf{r}_E\right)\\ &= L_C\,\Delta T + P + L_G\,\Delta T + \frac{1}{c^2}\mathbf{v}_E\cdot\left(\mathbf{r}-\mathbf{r}_E\right)\end{aligned} \tag{7-8}$$

The relation between TCB and TCG is:

$$\mathrm{TCB} - \mathrm{TCG} = (\mathrm{TCB} - \mathrm{TT}) - (\mathrm{TCG} - \mathrm{TT})$$

Thus:

$$\mathrm{TCB}-\mathrm{TCG} = \frac{1}{c^2}\int_{t_{B_0}}^{t_B}\left(U_{ext}\left(\mathbf{r}_E\right)+\frac{1}{2}v_E^2\right)\mathrm{d}t_B + \frac{1}{c^2}\mathbf{v}_E\cdot\left(\mathbf{r}-\mathbf{r}_E\right) = L_C\,\Delta T + P + \frac{1}{c^2}\mathbf{v}_E\cdot\left(\mathbf{r}-\mathbf{r}_E\right) \tag{7-9}$$

where:

$L_C =$ 1.480 826 867 41 $\times 10^{-8}$ (approximately 1.28 ms/d) [Irwin and Fukushima, 1999].

More than one hundred periodic terms must be included to achieve an accuracy of 100 ns [Fairhead *et al.*, 1998]. In the first approximation:

$$\frac{1}{c^2}\int_{t_{B_0}}^{t_B}\left(U_{ext}\left(\mathbf{r}_E\right)+\frac{1}{2}v_E^2\right)\mathrm{d}t_B \approx \frac{3}{2}\frac{1}{c^2}\frac{GM_S}{a_E}\Delta T + \frac{2}{c^2}\sqrt{GM_S\,a_E}\;e\sin E \tag{7-10}$$

where:

GM_S: the gravitational constant of the Sun

a_E and e: the Earth’s orbital semimajor axis and eccentricity.

The first term is an approximation to $L_C\,\Delta T$. The second term is the principal periodic term P, which has an amplitude of 1.7 ms.

7.5.4 Barycentric dynamical time

Barycentric Dynamical Time (TDB) is also a barycentric coordinate time. However, according to the 1976 IAU resolution, the difference between TDB and TT (then called TDT) must contain only periodic terms. Thus the rate of coordinate time is rescaled as:

$$\Delta t'_B = (1 - L_B)\,\Delta t_B$$

where:

$\Delta t'_B$: is identified with TDB

Δt_B: is identified with TCB.

The difference between TCB and TDT is:

$$\mathrm{TCB}-\mathrm{TDB} = L_B\,\Delta T \tag{7-11}$$

The relation between TDB and TT is TDB – TT = (TCB – TT) – (TCB – TDB). Thus:

$$\begin{aligned}\mathrm{TDB}-\mathrm{TT} &= \frac{1}{c^2}\int_{t_{B_0}}^{t_B}\left(U_{ext}\left(\mathbf{r}_E\right)+\frac{1}{2}v_E^2\right)\mathrm{d}t_B + L_G\,\Delta T + \frac{1}{c^2}\mathbf{v}_E\cdot\left(\mathbf{r}-\mathbf{r}_E\right) - L_B\,\Delta T\\ &= L_C\,\Delta T + P + L_G\,\Delta T + \frac{1}{c^2}\mathbf{v}_E\cdot\left(\mathbf{r}-\mathbf{r}_E\right) - L_B\,\Delta T\end{aligned} \tag{7-12}$$

which contains no secular terms if $L_B \approx L_C + L_G$. Another time scale for relativistic ephemerides, called T_{eph}, is used by JPL [Standish, 1998] and is close to TDB. If the integral is computed using planetary ephemeredes expressed in terms of T_{eph} as an argument, it should be divided by the factor $1 - L_B$.

The rate of TDB with respect to TCB is:

$$\left\langle \frac{\mathrm{dTDB}}{\mathrm{dTCB}} \right\rangle = \left\langle \frac{\mathrm{dTDB}}{\mathrm{dTT}} \right\rangle \frac{\mathrm{dTT}}{\mathrm{dTCG}} \left\langle \frac{\mathrm{dTCG}}{\mathrm{dTCB}} \right\rangle \tag{7-13}$$

where:

< > denotes long-term average taken at the geocentre;

the value of L_B is obtained by using the relation:

$1 - L_B = (1 - L_G)(1 - L_C)$

since $\langle \mathrm{dTDB/dTCB} \rangle = 1 - L_B$

$\mathrm{dTT/dTCG} = 1 - L_G$

$\langle \mathrm{dTCG/dTCB} \rangle = 1 - L_C$

$\langle \mathrm{dTDB/dTT} \rangle = 1.$

Thus: $L_B = 1.550\ 519\ 767\ 72 \times 10^{-8}$ (approximately 1.34 ms/d).

The factor $1 - L_B$ relates ephemeris units of time and distance in ephemeredes expressed in terms of TDB to the corresponding SI units.

7.6 International time scales

Development of international telecommunication and computer networks and, especially, global electronic navigation systems require high precision, synchronized international time scales. As a result the relevant international organizations developed and approved the following major international time scales:

– the International atomic time (TAI);

– the Coordinated universal time (UTC).

7.6.1 International atomic time

The epoch of International atomic time (TAI) is 1 January 1958. TAI is defined as the atomic time scale established by the BIPM based on readings of some 400 atomic clocks maintained in approximately 60 laboratories. It is further specified as [BIPM, 1981] a coordinate time scale defined in a geocentric reference frame with the SI second as realized on the rotating geoid as the scale unit. TAI was an extension of an atomic time scale maintained by the BIH that had been in continuous existence back to 1955.

The formation of TAI was recommended by the International Astronomical Union (IAU) in 1967, the International Union of Radio Science (URSI) in 1969 and the International Radio Consultative Committee (CCIR) of the ITU in 1970. The 14th General Conference on Weights and Measures (CGPM) approved the establishment of TAI in 1971.

TAI is the actual time scale established from the clock comparison data supplied to the BIPM by participating laboratories and a particular algorithm known as ALGOS. TAI has been further defined as a coordinate time scale in a geocentric reference frame with the SI second as the scale unit realized on the rotating geoid. The fact that TAI is a coordinate time scale was determined by the Consultative Committee for the Definition of the Second (CCDS) in 1980. The CCDS was renamed the Consultative Committee for Time and Frequency (CCTF) in 1997. The CCDS also provided the necessary correction information for the establishment of TAI in relativistic terms and for its use in non-terrestrial reference frames. The accuracy of TAI is a primary consideration in maintaining the SI second and providing a reliable scale in the long term. The optimization of the long term stability is done at the expense of short term accessibility. The calculation of TAI uses data over an extended period. Clock data are provided to the BIPM on days with the Modified Julian Date ending in 4 and 9.

Two techniques of time transfer are in use for clock comparison:

a) comparison via GPS satellite tracking of the local UTC to GPS time, or

b) comparison of two local UTC (§ 7.6.2) via TWSTFT.

The time links for clock comparisons are organized by the BIPM following the scheme presented in Fig. 7-1. Blocks of data covering 30 days are used in the calculation of the scale. A period of 30 days was chosen to place the effective integration time of the scale at the transition between the flicker floor and the random walk frequency modulation of caesium clocks. Stability would therefore not be improved by a longer integration time. The period of 30 days is enough to smooth out the noise contributed by the time links and the white frequency modulation noise of the clocks.

FIGURE 7-1

International time links between participating centres

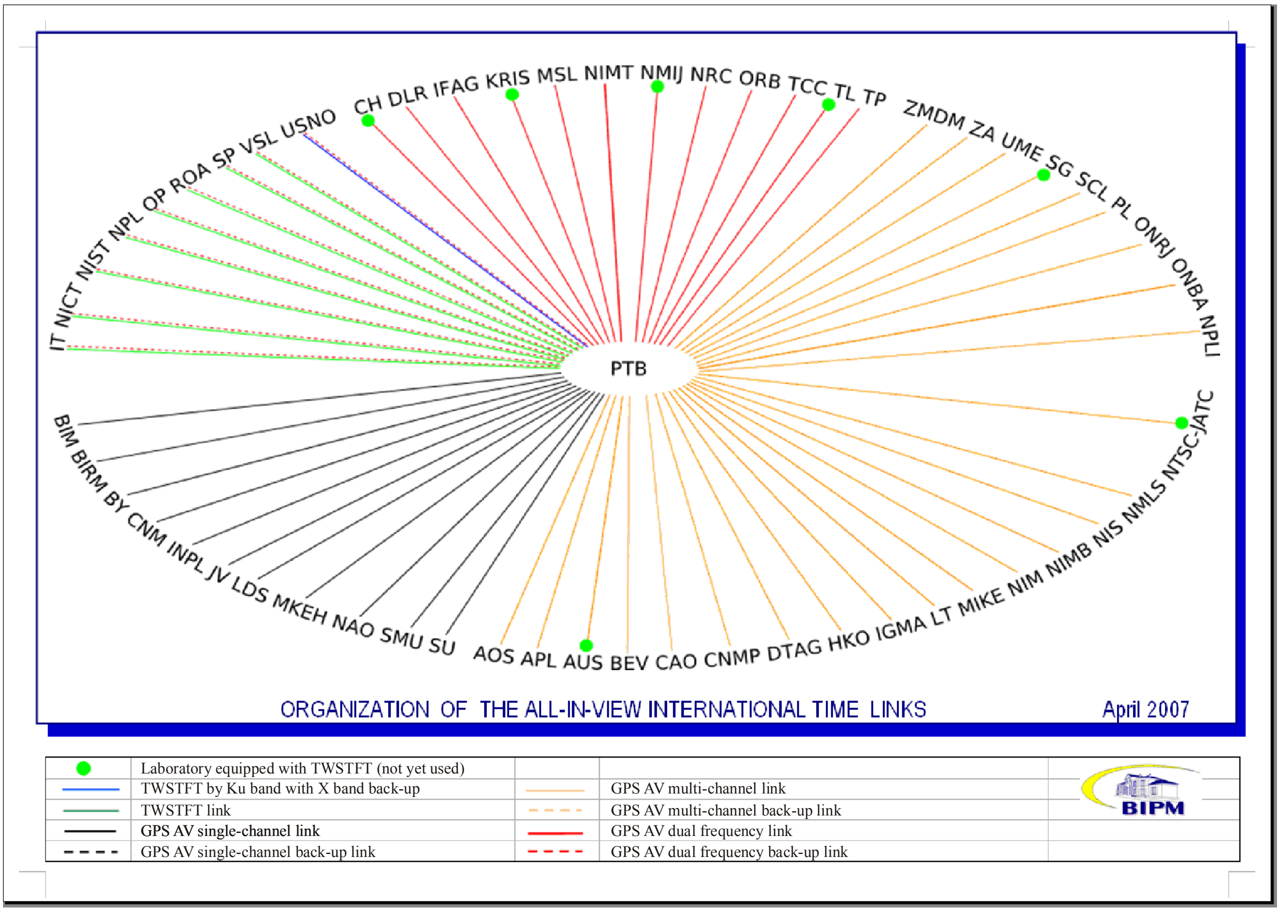

Sat_time_freq-07-01

The determination of TAI is performed in 3 steps:

Step 1: Calculation using a post processing, iterative procedure of an intermediate scale, known as echelle atomique libre (EAL) or free atomic scale, using the clock comparison data and ALGOS.

Step 2: Evaluation of the duration of the scale unit of EAL using data from primary frequency standards and an optimum filter.

Step 3: Production of TAI from EAL by applying, if necessary, a correction to the scale interval of EAL to give a value as close as possible to the SI second. Correcting the scale unit is known as "*frequency* *steering*" and is done if deemed necessary every month by applying a variable correction with a maximum step size from month to month of 7×10^{-16} or lower.

How TAI is established is briefly outlined below. Refer to [Azoubib, *et al.*, 1977] for more details.

1. *Structure of TAI*: The time, t, of EAL $f(t)$ is defined in terms of the readings $h_i(t)$ of a group of N clocks, H_i, by:

$$\mathrm{EAL}(t) = \frac{\sum_{i=1}^{N} p_i \left[\mathrm{h}_i(t) + h'_i(t) \right]}{\sum_{i=1}^{N} p_i} \tag{7-14}$$

where:

p_i : statistical weight assigned to clock H_i:

$h'_i(t)$: time correction designed to ensure time and frequency continuity of the scale when either the weighting of individual clocks or the total number of clocks is changed.

This expression cannot be used directly because the measured quantities that provide the basic data are not the readings of individual clocks but are the results of comparisons between pairs of clocks. At time t, the slowly varying differences $\zeta_{ij}(t)$ between the readings of clocks H_i and H_j are written as:

$$\zeta_{ij}(t) = \mathrm{h}_i(t) - \mathrm{h}_j(t) \tag{7-15}$$

The output of EAL is then a set of N values of the differences $x_i(t)$ defined by:

$$x_i(t) = \mathrm{EAL}(t) - \mathrm{h}_i(t) \tag{7-16}$$

where:

x_i: differences between readings of the individual clocks and the time defined by EAL.

The difference can then be expressed as:

$$x_i(t) - x_j(t) = -\zeta_{ij}(t) \tag{7-17}$$

and equation (7-14) can be transformed into:

$$\sum_{i=1}^{N} p_i x_i(t) = \sum_{i=1}^{N} p_i h'_i(t) \tag{7-18}$$

In practice a non-redundant system of $N - 1$ time links is employed to solve for these last two expressions.

2. *Weighting Procedure:* The weight assigned to each clock is calculated in such a way as to favour the long term stability of the resulting scale and to minimize the annual fluctuations and frequency drift with respect to the primary frequency standards. An important feature of ALGOS is that the evaluation of the weight of the clock although based upon data covering a whole year, takes into account the 30 days of data for which EAL is being computed. It is thus possible to judge clocks on their actual performance during the interval of time along which EAL is being established. It is also possible to take into account any abnormal behaviour observed in an individual clock by adjusting its weight, if necessary to zero. This has proved useful on many occasions.

The weight is normally based on the variance $\sigma^2(6,\tau)$ of the mean rate [Thomas and Azoubib, 1996] with respect to EAL calculated over one month samples. This variance, instead of the usual pair variance, was chosen because it gives greater reduction in the weight of clocks showing a frequency drift. The weights are obtained directly from:

$$p_i = \frac{1\,000}{\sigma_i^2(6,\tau)} \tag{7-19}$$

(σ_i is expressed in ns/day) provided the current 30 day period shows no abnormal behaviour. In the case of abnormal behaviour a weight of zero is assigned. A maximum weight of 2.5/N (N being the number of participating clocks in the month of computation) is fixed. The maximum weight is chosen to ensure that the scale is heavily biased in favour of the best clocks without allowing any one of them to become predominant [Thomas and Azoubib, 1996].

3. *Rate prediction*: The time correction term $h'_i(t)$ is made up of two components:

$$h'_i(t) = a_i(t_0) + \mathrm{B}_{ip}(t)(t - t_0) \tag{7-20}$$

where:

$a_i(t_0)$: simply the time differences between clock H_i and EAL at time t_0, which is the beginning time of the 30 day period

$B_{ip}(t)$: predicted difference in rate between H_i and EAL for the period t_0 to t, where the rate of clock H_i is defined by:

$$\text{rate} = \frac{a_i(t_0 - t) - a_i(t_0)}{(t - t_0)} \tag{7-21}$$

The prediction of $B_{ip}(t)$ is obtained by a one step linear prediction based upon the previous value. This is justified by the fact that for the 30 day period the dominant clock noise is random walk for which the most probable estimated value over the next period is simply that of the preceding period.

Having established the best estimate of EAL the transformation to TAI is made by the determining if the rate of EAL differs sufficiently from that of the best primary standards and thereby warrant a «steering» correction. From 2005 to 2008 frequency changes of maximum value 0.6×10^{-15} each were applied almost every month.

Finally, the output of these calculations is published in the monthly *Circular T* which is distributed to participating laboratories. An excerpt from one is shown in Fig. 7-2. The values of [UTC-UTC(k)] for contributing laboratories k are published every five days, together with the respective uncertainties, whose values remain constant for one month of calculation.

7.6.2 Coordinated universal time

The measure of Universal Time based on the atomically defined SI second is called UTC. Coordination of the international atomic timescales was entrusted to the BIH in 1961. In 1988, this responsibility was transferred from the BIH to the BIPM.

Initially, both rate offsets and periodic step adjustments were applied to broadcast time signals to keep UTC within 0.1 s from UT2. The present form of UTC was introduced in 1972, in which rate offsets were discontinued and integer "leap second" steps replaced the steps of 100 ms or 200 ms then being used because they were too frequent and too small [Nelson, 2001]. UTC is equal in rate to TAI but differs by an integral number of seconds, such that it is always within 0.9 s of UT1.

FIGURE 7-2

Excerpt from *BIPM Circular T*

CIRCULAR T 208 ISSN 1143-1393
2005 MAY 12, 17h UTC

BUREAU INTERNATIONAL DES POIDS ET MESURES
ORGANISATION INTERGOUVERNEMENTALE DE LA CONVENTION DU METRE
PAVILLON DE BRETEUIL F-92312 SEVRES CEDEX TEL. +33 1 45 07 70 70 FAX. +33 1 45 34 20 21 tai@bipm.org

1 - Coordinated Universal Time UTC and its local realizations UTC(k). Computed values of [UTC-UTC(k)].
From 1999 January 1, 0h UTC, TAI-UTC = 32 s.

Date 2005 0h UTC	MAR 30	APR 4	APR 9	APR 14	APR 19	APR 24	APR 29	Uncertainty/ns			
MJD	53459	53464	53469	53474	53479	53484	53489				
Laboratory k				[UTC-UTC(k)]/ns				uA	uB	u	(1)
AOS (Borowiec)	8.2	12.1	17.1	22.7	19.0	16.0	16.8	1.6	5.2	5.4	
APL (Laurel)	-18.6	-23.3	-13.6	-2.0	4.6	39.3	26.5	1.6	5.3	5.5	(2)
AUS (Sydney)	-541.1	-547.9	-556.5	-561.7	-574.0	-590.8	-608.2	3.2	6.4	7.2	
BEV (Wien)	97.8	88.7	80.6	70.6	63.0	58.2	46.3	1.6	5.2	5.4	
BIRM (Beijing)	-145.0	-170.1	-192.3	-217.0	-238.1	-260.8	-288.4	2.8	20.4	20.6	
CAO (Cagliari)	-2890.4	-2883.7	-2871.8	-2865.4	-2845.1	-2819.2	-2794.1	1.6	7.2	7.4	
CH (Bern)	-21.7	-24.4	-24.6	-21.4	-14.6	-9.4	-0.7	0.8	5.2	5.3	
CNM (Queretaro)	36.7	44.2	47.2	52.2	52.6	59.5	78.3	5.0	20.3	20.9	
CNMP (Panama)	-2514.2	-2543.1	-2584.6	-2629.9	-2655.4	-2690.8	-2721.4	4.0	7.2	8.2	
CSIR (Pretoria)	-3393.0	-3468.5	-3548.2	-3628.6	-3718.2	-3800.9	-3891.4	3.0	20.1	20.3	
DLR (Oberpfaffenhofen)	-40.4	-46.1	-44.7	-46.1	-62.1	-62.9	-71.4	0.8	5.2	5.3	
DTAG (Darmstadt)	254.6	274.3	283.9	273.2	267.7	271.2	273.3	3.0	10.1	10.5	
HKO (Hong Kong)	93.7	71.6	68.9	55.1	45.9	45.2	51.0	3.2	6.4	7.2	
IEN (Torino)	-116.2	-116.2	-109.3	-104.5	-99.3	-98.1	-100.5	0.7	1.9	2.0	
IFAG (Wettzell)	-348.7	-340.9	-340.6	-340.4	-332.8	-324.9	-314.8	0.8	5.2	5.3	
IGMA (Buenos Aires)	351.7	353.5	346.2	354.1	361.3	366.9	367.4	5.0	19.9	20.5	
INPL (Jerusalem)	-264.7	-311.1	-347.5	-387.4	-432.2	-478.0	-523.6	4.0	10.1	10.9	
JATC (Lintong)	-10237.5	-10227.2	-10209.8	-10197.3	-10180.0	-10167.2	-10155.8	2.7	21.0	21.2	
JV (Kjeller)	-6316.2	-6310.2	-6252.7	-6243.4	-6219.6	-6173.5	-6177.2	5.0	20.1	20.7	
KRIS (Daejeon)	-3.8	-4.2	0.9	2.5	3.4	5.7	6.0	2.8	6.4	7.0	

Sat_time_freq-07-02

Thus, time signals now provide both the unit interval of the SI second and an approximation to UT1 in the same emission. An additional correction DUT1, having integral multiples of 0.1 s, may be embodied in a broadcast time signal by means of double ticks or pulses, such that, when added to UTC, provides a better approximation to UT1. UTC has been recognized as the basis of civil time as identified in resolutions of various treaty organizations and scientific unions, such as the CGPM, the ITU, and the IAU, and by most national legal codes.

The SI second now defined in terms of the period of the caesium transition was chosen to be in agreement with the ephemeris second within the limits of experimental uncertainty. However, studies based on records of ancient eclipses and modern telescopic observations indicate that the length of the day has been slowly increasing. Over the past 1000 years it has been increasing at a rate of about 1.4 ms per day each century. Thus, the ephemeris second, based on Newcomb's Tables of the Sun, was, in effect, equal to the average mean solar second over the eighteenth and nineteenth centuries.

According to the long-term trend, the mean solar second was equal to the SI second in approximately 1820 [Stephenson, 1997]. This date is also the approximate mean epoch of the data analyzed by Newcomb, which covers the period from 1750 to 1892. Since 1820, the length of the day has increased by roughly 2.5 ms. Thus the mean solar day is currently about 86 400.0025 s, which exceeds the civil day of exactly 86 400 s. Over one year, the difference of 0.0025 seconds accumulates to about one full second, which is compensated by the insertion of a leap second. However, due to the random fluctuations in the Earth's rotation, a leap second cannot be predicted in advance, and its frequency of occurrence is variable.

UTC was developed by the CCIR of the ITU (CCIR was merged with the IFRB and named the ITU-R) which recommended its formation in 1972 as a compromise timescale between UT and TAI. This time scale serves to coordinate the local time kept by the various timing centres and nations and provides a reasonably close agreement to UT1. Coordination was needed due to the development of electronic navigation systems, such as Loran, that could provide reasonable accurate timing measurements over global distances. The specific definition of UTC is in Recommendation ITU-R TF.460 – Standard frequency and time-signal emissions. Since UTC was adopted, its use has grown considerably within the radio- and telecommunications community as electronic navigation and communication systems grew to provide highly accurate timing measurements worldwide and need highly accurate coordinated time in turn (Recommendations ITU-R TF.535-2 and ITU-R TF.767-2).

UTC has been recognized as the international reference of time in resolutions of several scientific unions and treaty organizations, such as the IAU, ITU, URSI, CGPM and standardization bodies as ISO. The CCIR in 1978 approved a new version of CCIR Recommendation 486 (now Recommendation ITU-R TF.486-2 – Use of UTC frequency as reference in standard frequency and time signal emissions) and the WARC-79 decided that UTC should be used to designate the time in all international telecommunication activities [Final Acts, 1980].

The RR (Edition 2008) define UTC as follows:

"**1.14** *Coordinated Universal Time (UTC):* Time scale, based on the second (SI), as defined in Recommendation ITU-R TF.460-6. (WRC-03)

For most practical purposes associated with the Radio Regulations, UTC is equivalent to mean solar time at the prime meridian (0° longitude), formerly expressed in GMT."

The reference for satellite time and frequency applications today is generally accepted to be UTC.

7.6.2.1 Realization of coordinated universal time

UTC is a version of TAI that is adjusted by either adding or subtracting one second steps, known as leap seconds. To maintain a close relationship of UTC to UT1, illustrated in Fig. 7-3, an adjustment known as DUT1 was to be broadcasted or communicated along with UTC. DUT1 was to be the *predicted* value of the difference UT1 – UTC in integral multiples of 0.1 s. A user of UT1 could then adjust a broadcast value of UTC to UT1 with an accuracy of < 0.1 s. UT1 is a version of Universal Time corrected for polar motion, following the irregular rotation of the Earth. UT1 was determined in the past by the transit time of stars corrected for seasonal variations Today the determination of UT1 relies on space satellite techniques and provides a measure of the Earth's rotation rate and relations Earth orientation with the UT1 time of day. More of the history and development of these timescales is discussed in the publication – The Leap Second: Its History and Possible Future [Nelson *et al*., 2001].

Consequently UTC is an atomic time scale that agrees in rate with TAI, but differs by an integral number of seconds. As on June 2008, UTC is behind TAI by 33 s. The decision to insert a leap second is determined by the change in the rotation rate of the Earth such that it accumulates an error of at most 0.9 s. The International Earth Rotation and Reference Systems Service (IERS) monitors the Earth's rotation and determines when the threshold is to be exceeded and advises the BIPM who maintains UTC ever since responsibility for TAI was transferred from the BIH in 1988. In Fig. 7-3, the deviation of UTC from UT1 is depicted for the last ten years. Note the insertion of leap seconds at the end of 2005 and 2008, respectively.

The initial form of UTC attempted prior to 1972 was to keep close to UT1 by adjusting both the frequency offset and fractional-second step adjustments to match broadcast of atomic time signals with the Earth's rotation. Close coupling to the Earth's rotation was considered necessary to aid celestial navigation, however the system was difficult to coordinate between broadcast stations and provide a uniform accurate reference time. The present UTC system of integral leap second steps without frequency offsets was adopted so that an approximation to the epoch of UT1 and the interval of the SI second would be provided by a single scale.

FIGURE 7-3

UT1 – UTC offset over the period 2000 to 2009

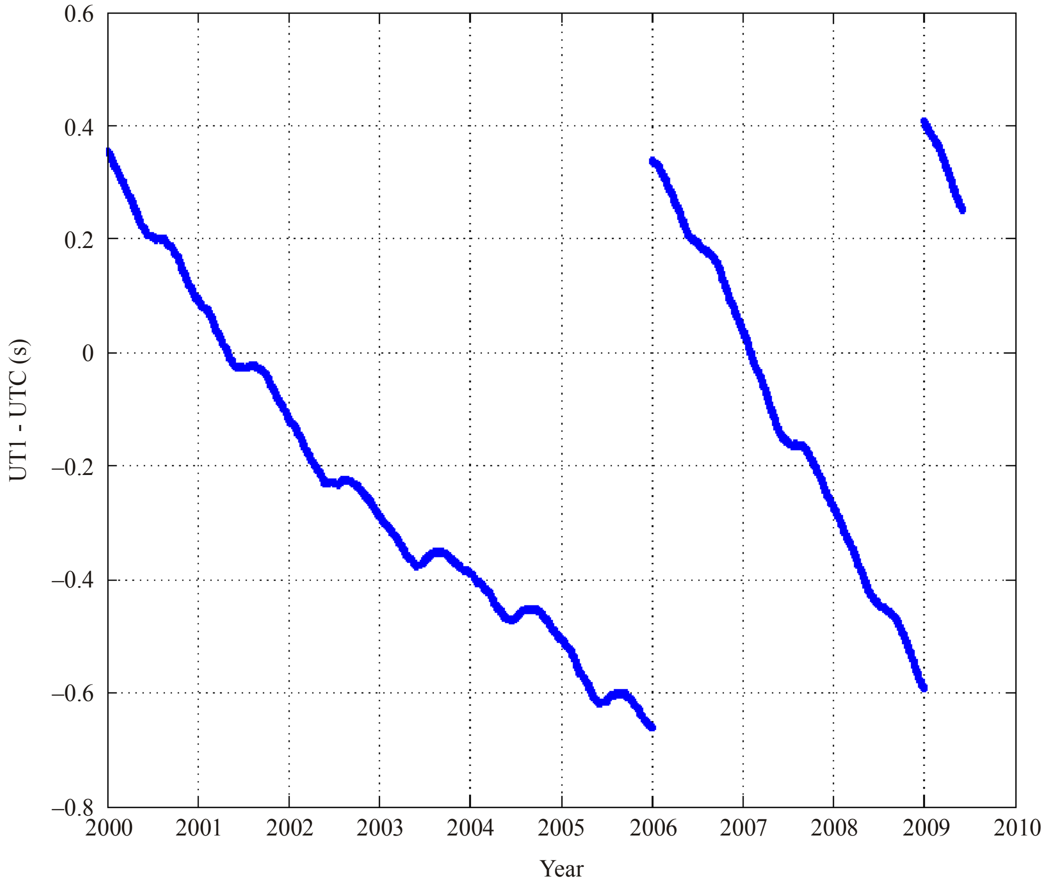

Sat_time_freq-07-03

As the needs of broadcast services require the generation and transmission of signals from the same clocks and oscillators that produce the time keeping signals, a "real-time" or immediate time scale is required. To provide for these "real-time" signals a timing centre may produce a local representation of UTC provided that measurements of the clock signals are reported to the BIPM and considered in the determination of the international time scale. The notation UTC(k) is used for such a local approximation to UTC in a laboratory k contributing data to the formation of TAI and UTC at the BIPM. For example, UTC (USNO) is the delivered real-time prediction of UTC as currently maintained by the U.S. Naval Observatory.

Similar real-time realizations for other timing centres, such as the Observatory of Paris (OP), Physikalisch-Technische Bundesanstalt (PTB) and the U.S. National Institute of Standards and Technology (NIST), contribute to the weighted clock measurement data used by the BIPM [Quinn, 1991]. UTC used without the following qualifying parentheses identifies reference to the final international value determined by the BIPM. These procedures and definitions are described in Recommendation ITU-R TF.536-2 – Time-scale notations. The final determination of UTC does not have a physical output and is available after a delay of two to four weeks in the form of an offset from the representations maintained by the participating laboratories. Values for both TAI and UTC are disseminated by a monthly publication of the BIPM known as *Circular T*. The differences between UTC(k) values of the institutes mentioned above and UTC as reported in the BIPM Circular T are shown in Fig. 7-4.

FIGURE 7-4

UTC - UTC(k) difference reported in BIPM Circular T (daily values)

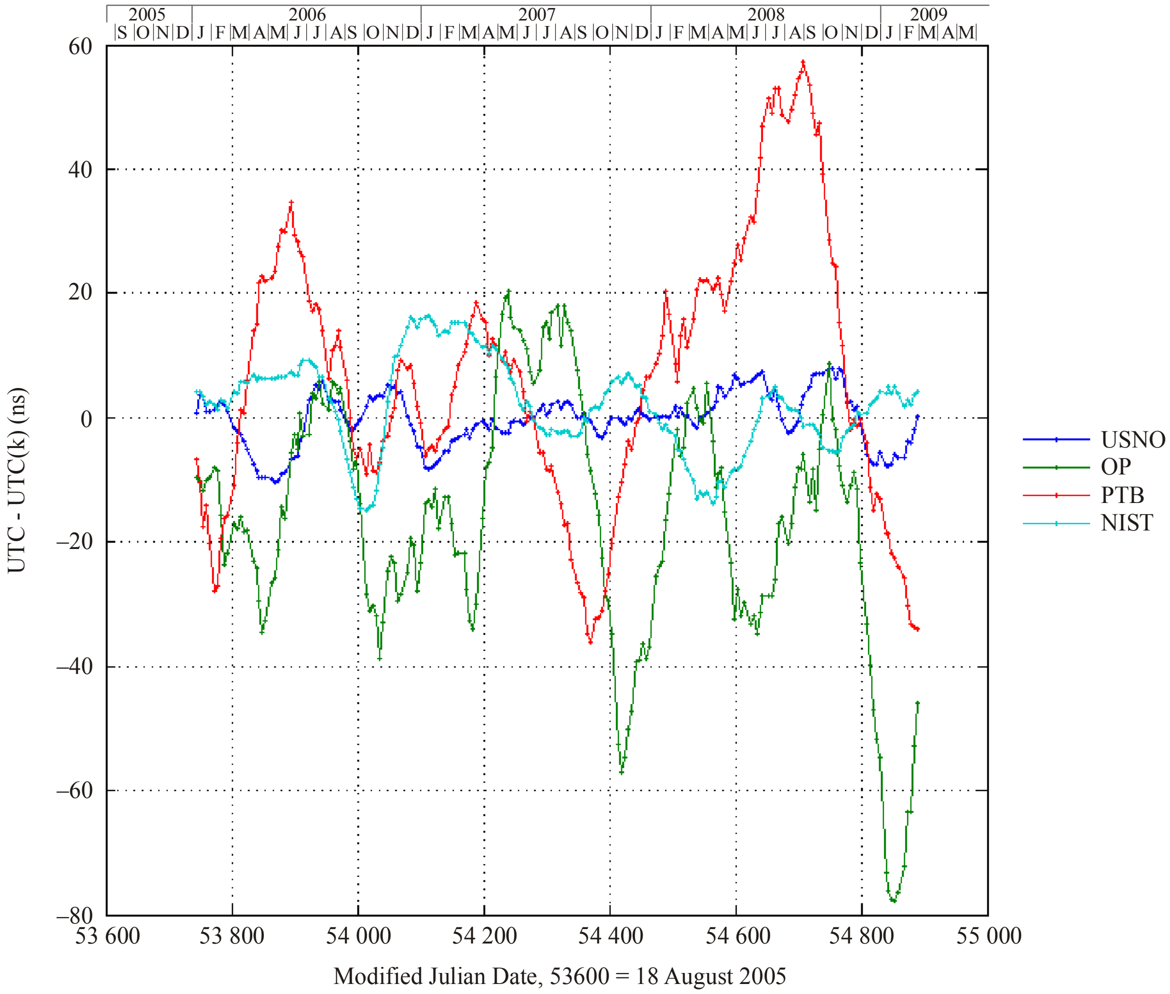

Sat_time_freq-07-04

References

AOKI, S., GUINOT, B., KAPLAN, G. H., KINISHITA, H., MCCARTHY, D. D. and SEIDELMANN, P. K. [1982] The New Definition of Universal Time. Astron. Astrophys. 105, p. 359-361.

AZOUBIB, J. [2001] A revised way of fixing an upper limit to clock weights in TAI computation. *Report to the 15th meeting of the CCTF*, available on request to the BIPM.

AZOUBIB, J., GRANVEAUD, M., GUINOT, B. [1977] Estimation of the scale unit duration of time scales. *Metrologia*, Vol. 13, p. 87-93.

BERGERON, J. (editor) [1992], Trans. Int. Astron. Union, Vol. XXIB, Proc. 21st General Assembly, Buenos Aires, 1991, Reidel, Dordrecht, p. 41-52.

BIPM *Com. Cons. Déf. Seconde* **9**, 15 (1980), *Metrologia* **17**, 70, 1981.

FAIRHEAD, L., BRETAGNON, P. and LESTRADE, J.-F. [1998] The Time Transformation TB – TT: An Analytical Formula and Related Problem of Convention, in *The Earth's Rotation and Reference Frames for Geodesy and Geophysics*, edited by A. K. Babcock and G. A. Wilkins, Kluwer, Dordrecht, p. 419-426.

FUKUSHIMA, T. [1995] Time Ephemeris. *Astron. Astrophys.* **294**, p. 895-906.

IRWIN, A. W. AND FUKUSHIMA, T. [1999] A Numerical Time Ephemeris of the Earth. *Astron. Astrophys.* **348**, p. 642-652.

MOYER, T. D. [1971/1981] Transformation from Proper Time on Earth to Coordinate Time in Solar System Barycentric Space-Time Frame of Reference. *Celestial Mech.* **23**, p. 33-68.

MULLER, E. A. and JAPPEL, A. (editors) [1977], Trans. Int. Astron. Union, Vol. XVIB, Proc. 16th General Assembly, Grenoble, 1976, Reidel, Dordrecht, p. 60.

NELSON, R. A., MCCARTHY, D. D., MALYS, S., LEVINE, J., GUINOT, B., FLIEGEL, H. F., BEARD, R. L. and BARTHOLOMEW, T. R. [2001] The Leap Second: Its History and Possible Future. *Metrologia* **38**, p. 509-529.

NEWCOMB, S. [1895] Astronomical Papers Prepared for the Use of the American Ephemeris and Nautical Almanac. Vol. VI, Part I: *Tables of the Sun*, U. S. Govt. Printing Office, Washington, D.C, p. 9.

QUINN, T. J. [July 1991] The BIPM and the Accurate Measurement of Time. *Proc. IEEE*, 79(7), p. 894-905.

RICKMAND, H. (editor) [2001], Trans. Int. Astron. Union, Vol. XXIVB, Proc. 24th General Assembly, Manchester, 2000, Astron. Soc. Pacific, San Francisco, p. 37-49.

SEIDELMANN P. K. (editor) [1992] Explanatory Supplement to the Astronomical Almanac. University Science Books, Mill Valley, CA.

STANDISH, E. M. [1998] Time Scales in the JPL and CfA Ephemerides. *Astron. Astrophys.* **336**, p. 381-384.

STEPHENSON, F. R. [1997] Historical Eclipses and Earth's Rotation. Cambridge, New York, p. 28.

The XXIIIrd International Astronomical Union General Assembly [1997] Resolution B2 On the International Celestial Reference System (ICRS). Kyoto, Japan.

THOMAS, C. and AZOUBIB, J. [1996] TAI computation: study of an alternative choice for implementing an upper limit of clock weights. *Metrologia*, **33**, p. 227-240.

THOMAS, J. B. [1975] Reformulation of the Relativistic Conversion between Coordinate Time and Atomic Time. *Ap. J.* **80**, p. 405-411.

ITU-R texts

ITU-R [1979] Final Acts of the World Administrative Radio Conference (WARC-79), Geneva.

Radio Regulations, Edition of 2008, Volume 1, International Telecommunication Union, 2008, (http://www.itu.int/publ/R-REG-RR-2008/en).

Recommendation ITU-R TF.458-3 – International comparisons of atomic time scales, (http://www.itu.int/rec/R-REC-TF.458-3-199802-I/en).

Recommendation ITU-R TF.460-6 – Standard-frequency and time-signal emissions, (http://www.itu.int/rec/R-REC-TF.460-6-200202-I/en).

Recommendation ITU-R TF.486-2 – Use of UTC frequency as reference in standard frequency and time signal emissions, (http://www.itu.int/rec/R-REC-TF.486-2-199802-I/en).

Recommendation ITU-R TF.535-2 – Use of the term UTC, (http://www.itu.int/rec/R-REC-TF.535-2-199802-I/en).

Recommendation ITU-R TF.536-2 – Time-scale notations, (http://www.itu.int/rec/R-REC-TF.536-2-200305-I/en).

Recommendation ITU-R TF.686-2 – Glossary and definitions of time and frequency terms, (http://www.itu.int/rec/R-REC-TF.686-2-200202-I/en).

Recommendation ITU-R TF.767-2 – Use of global navigation satellite systems for high-accuracy time transfer, (http://www.itu.int/rec/R-REC-TF.767-2-200103-I/en).

CHAPTER 8

NATIONAL TIMING CENTRES

Page

8.1 Introduction

As it has been described previously, UTC is established at the BIPM by a post-processing computation based on the data of about 350 atomic frequency standards maintained in about 60 timing laboratories distributed worldwide. These laboratories, operating in many cases inside the National Metrology Institutes (NMIs), in addition to a local realisation of the UTC time scale, usually acknowledged as the national reference of time, also perform activities in several if not all of the following fields:

- development of primary frequency standards and clocks,
- participation in international synchronization experiments,
- dissemination of time and frequency standard signals,
- development of accurate time and frequency transfer techniques,
- research on clocks characterization and time scale algorithms,
- calibration of time and frequency equipment.

At least two of these activities, namely the participation in synchronization links and the dissemination activity can be found in all the NMIs who have signed since 1999 the Mutual Recognition Arrangement of the CIPM (CIPM MRA) to comply with its requirements regarding the establishment of the degree of equivalence of national standards, through the participation in key comparisons (KC), and the mutual recognition of the calibration and measurement certificates issued [CIPM/BIPM/OIML, 1999].

As a first duty, every national metrology laboratory contributing with clock data to the formation of UTC at the BIPM, maintains a local real-time representation of UTC which is called UTC(k), kept in close agreement with UTC that may be based on the reading of a single master clock or on an ensemble of clocks. Secondly, each timing laboratory, to be able to participate in the formation of UTC and in key comparisons identified by the CCTF [CCTF Report, 2001; CCTF Report, 2006] needs to operate at least one synchronization system, primarily GPS, to provide regularly to the BIPM the (UTC(k) – GPS time] data that will be used in the realization of the international references for frequency and time (TAI and UTC); Circular T provides monthly the values of [UTC- UTC(k)] to be published by BIPM in the key comparison data base for the equivalence of the national standards. An important issue related to this task is the evaluation of the accuracy of the uncertainty of the synchronization links used, for which regular circulation of calibrated GPS, GLONASS or TWSTFT equipment takes place. Calibration campaigns of GPS equipment in contributing laboratories are regularly organized by the BIPM.

Besides the equipment needed for these core activities, a time and frequency reference laboratory shall have dedicated devices for the generation and monitoring of the standard time and frequency signals to be distributed locally or to remote users by different means, such as dedicated LF, HF and TV transmissions, telephone lines and computer networks. These features, together with the instrumentation suitable to calibrate the time and frequency devices as regards their specifications (time, frequency and drift, frequency stability) complete the traceability chain foreseen in the CIPM MRA.

In the countries where a system of accredited calibration laboratories has been established, the NMI laboratory is also supplying its expertise to the accreditation body and can be involved in the organization of national and international inter-laboratory comparisons which are instrumental in assessing the measurement capabilities of secondary calibration laboratories, that are the end level of the traceability chain devised by the CIPM MRA

8.2 Timing laboratory layout

In Fig. 8-1 is represented a typical example of implementation of the core activities outlined, leaving apart the equipment devoted to the research on standard frequency sources, on caesium standards and the calibration facilities. All the equipment, with the exception of the receiving antennas for the synchronization systems, is installed in temperature and humidity controlled rooms and a redundant power continuity system, not depicted, is available; this facility is very important for the reliability of the metrological activities.

On the left side of the figure, a separate room for the clocks ensemble, usually regulated for a temperature of (23±1)°C, can be seen; this solution is recommended if one needs to get the best performances of the caesium clocks versus the environmental changes, but even better results can be obtained keeping the clocks in small chambers with tight (±0.1°C) temperature and humidity control. This solution is especially appropriate in the case of hydrogen maser to get the utmost frequency stability in case of time scale generation or when it is used as local oscillator for a primary caesium standard.

FIGURE 8-1

Typical layout of a timing centre

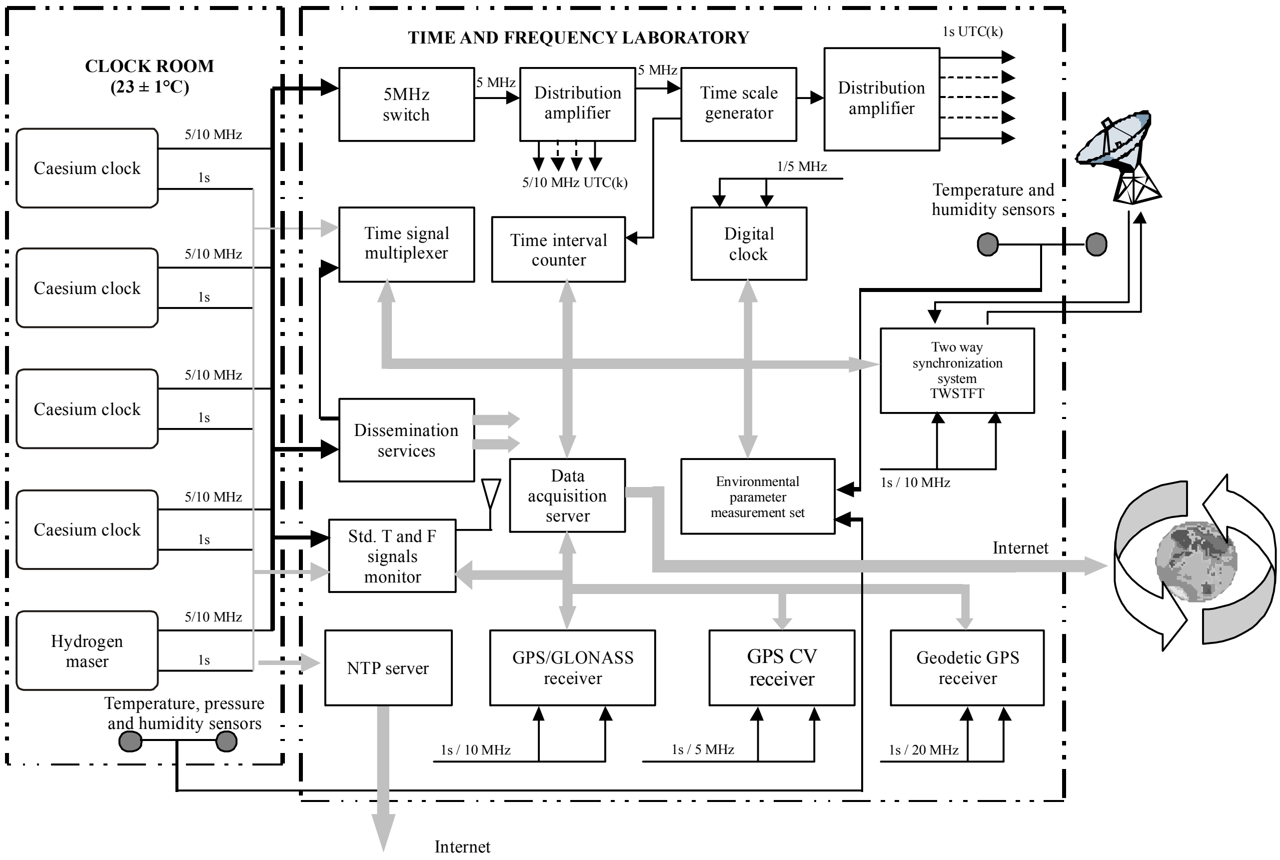

Sat_time_freq-08-01

According to the proposed architecture, at least 4 atomic clocks are suggested for a robust realisation of the local UTC; this configuration also allows generation of a paper time scale improving the long term behaviour of the time scale and its reliability. The most followed approach anyway is the selection of a single clock from the ensemble, according to its accuracy and stability performances, and its use as master clock for the real time generation of UTC(k). To improve the reliability of the time scale generation, an automatic switch (e.g. 5 MHz switch) can be inserted between the caesium clocks and the time scale generator (TSG), receiving at its inputs all the standard frequencies available and checking their amplitudes and phase changes, to detect any anomaly in the system, and thus avoiding discontinuities in the time scale.

Information on possible incoming anomalies can be obtained from the observation of some physical parameters whose values are available from the caesium clock serial ports; it then is advisable to have a permanent monitoring of some readings in the laboratory server.

To be compliant with the recommendations of the Consultative Committee for Time and Frequency, CCTF (which suggest a maximum deviation of 100 ns of the local realisation of UTC (CCDS Report, 1993 from UTC), a micro-phase stepper should be inserted between the master clock and the TSG to adjust its frequency to UTC, according to the corrections published by BIPM in Circular T or to accuracy evaluation versus a laboratory primary standard. Some types of caesium standards have the microstepper feature included and no additional device is required in the time scale generation path.

The standard signals supplied by the reference clocks are distributed in the time and frequency laboratory by means of high quality coaxial cables or optical fibre lines.

Distribution amplifiers for the UTC(k) standard frequencies and 1 s signals are also needed to perform traceable measurements inside the laboratory.

8.3 Local measurement system

The time and frequency laboratory houses the equipment devoted to the time scale generation and the clocks comparisons, the dissemination services, the satellites receivers, the data acquisition systems and the auxiliary monitoring equipment.

The setting up and operation of a local measurement system, inside the laboratory, has the double aim of providing clock data for the computation of the time scale and for the internal time and frequency comparisons between the UTC(k) and all the clocks and frequency standards which are maintained in the laboratory. Dedicated measurement systems are usually necessary to perform the routine measurements on GPS satellites or other synchronization systems prescribed for the international traceability.

The local measurement system consists of a high resolution time interval counter (TIC) that measures for an appropriate time the clock differences with a repetition rate of 1 s and repeats the cycle every hour. The optimum solution concerning measurement rate is strongly dependent on the activities performed by the laboratory. As the measurement accuracy is related to the time base, the UTC(k) external reference frequency is supplied to the TIC. Other factors such as the trigger instant, the quantisation error and the differential delay of the start and stop channels contribute to the uncertainty of the clocks comparisons. Therefore a careful calibration has to be carried out regularly to assess the stability of the measurement system. All the measurements performed by the TIC shall be referred to UTC(k), meanwhile the “stop” signals coming from the diverse clocks are sent through a Time Signal Multiplexer. A Digital Clock provides the necessary time tagging to every measurement. The measurement cycles are controlled by a computer where all the results coming from the TIC, from the synchronization systems and from the environment monitoring are stored. The external connection with the BIPM and other NMIs can also be managed trough a dedicated network server which allows a safe access to the Internet.

8.4 International traceability

The time comparison links routinely used in timing laboratories to establish the traceability of UTC(k) to the international references of time and frequency UTC and TAI, are based on GPS receivers operated according to the BIPM requirements and on two-way satellite time and frequency transfer (TWSTFT) using communication satellites. The same measurement link allows the atomic clocks maintained in each laboratory to contribute to the computation of those references. Time transfer equipment has been upgraded in most laboratories, and other synchronization techniques are replacing the basic GPS like e.g. the reception of GPS and GLONASS satellites with multichannel receivers, many of them with dual-frequency reception, the increased performance of TWSTFT or GPS carrier-phase measurements with geodetic-type receivers. The last two techniques are especially valuable for the more stringent requirements in frequency and time comparisons also for intercontinental baselines. All these instruments need to receive external UTC(k) time and frequency references and particular care is needed in choosing the place of installation of their antenna systems and in realising the signal connections with the time and frequency laboratory.

The measurement data, in the case of the GPS and GLONASS devices, are usually stored inside the receivers and are automatically transferred afterwards into the data acquisition system, meanwhile in the case of TWSTFT an auxiliary measurement system can be needed.

To evaluate the accuracy of any synchronization link, the reference receiver of a timing laboratory should participate in the periodic calibration campaigns, organised either by BIPM or by the regional metrological organizations through the circulation of a calibrated GPS receiver, to monitor the stability with time of the delay of the receiver used in the laboratory. In the case of the TWSTFT, the use of a portable VSAT station and of a satellite simulator can also serve the scope. A complete characterization of the uncertainty of the links used in the construction of UTC, as well as the information on their calibrations are published in BIPM Circular T; an excerpt of the table providing this information is shown in Fig. 7-2 of the previous section. At present, the uncertainty level that can be attained is in the region of a few nanoseconds.

8.5 Time dissemination services

To satisfy the needs of scientific and industrial users and to make available to the national community the legal time information, a national timing centre can implement several time and time dissemination services based on dedicated broadcast on VLF, LF, HF and TV bands, on satellites, on telephone networks and on the internet.

Exhaustive information about the techniques used and the uncertainty levels obtainable from the users can be found in the ITU-R Handbook – Selection and Use of Precise Frequency and Time Systems, meanwhile an updated list of the time signals and frequency standards emissions is reported in the Recommendations ITU-R TF Series (http://www.itu.int/rec/R-REC-TF/en). Description of time signals and time dissemination services are also provided in the BIPM Annual Report on Time Activities.

In the block diagram of Fig. 8-1, this type of activity has been represented with two boxes, namely "Dissemination services" and "NTP server"; to document the traceability to UTC(k) of these services for the users, some monitoring system must be implemented by the laboratory and the time or frequency deviations and the uncertainties of the disseminated time and frequency signals should be made periodically available to the public in paper or electronic form.

The traceability to a national standard can also be provided by the timing centre through the publication of the results of the measurements performed on the GPS, that can be considered as a transfer standard, to allow the secondary laboratories to refer their local standards, mostly GPS disciplined oscillators, to the international time references.

References

BIPM Annual Report on Time Activities, Bureau International des Poids et Mesures, Available upon request from the BIPM.

CCDS – Report on the 14th Meeting, 1993.

CCTF – Report of the 15th Meeting, June 2001, (http://www.bipm.org/cc/AllowedDocuments.jsp).

CCTF – Report of the 17th Meeting, 2006, (http://www.bipm.org/utils/common/pdf/CCTF17.pdf).

CIPM/BIPM/OIML – Mutual recognition of national measurement standards and of calibration and measurement certificates issued by national metrology institutes. Paris, October 1999.

CHAPTER 9

RELATIVISTIC EFFECTS IN SATELLITE TIME AND FREQUENCY TRANSFER AND DISSEMINATION

Page

9.1 The space-time interval

The theory of space, time, and gravitation according to the general theory of relativity is founded upon the notion of an invariant Riemannian space-time interval of the form:

$$\mathrm{d}s^2 = g_{\mu\nu}\,\mathrm{d}x^\mu\,\mathrm{d}x^\nu = g_{00}\,c^2\,\mathrm{d}t^2 + 2\,g_{0j}\,c\,\mathrm{d}t\,\mathrm{d}x^j + g_{ij}\,\mathrm{d}x^i\,\mathrm{d}x^j \tag{9-1}$$

where:

Greek index assumes the range 0, 1, 2, 3

Latin index assumes the range 1, 2, 3.

A repeated index (one in a raised position and one in a lowered position) implies summation on that index. The fundamental mathematical object is the metric tensor $g_{\mu\nu}$, whose components are functions of the coordinates $x^\alpha = (c\,t, x^i)$ and are symmetric in the indices μ, ν (that is, $g_{\mu\nu} = g_{\nu\mu}$). The reciprocal metric tensor $g^{\mu\nu}$ is defined by the relation $g^{\mu\alpha}\,g_{\alpha\nu} = \delta^\mu{}_\nu$, where $\delta^\mu{}_\nu$ is the Kronecker delta ($\delta^\mu{}_\nu = 1$ if $\mu = \nu$, 0 otherwise). In the sign convention adopted here, $-g_{00} > 0$.

In the measurement of length and time, time is the only fundamental quantity; length is a derived concept. Therefore, clocks and light signals are the only fundamental instruments of measurement. There are two distinct methods for the transfer of time between two remote clocks:

1. transport of an intermediate portable clock;
2. an electromagnetic signal.

For relativistic time transfer, it is necessary to distinguish between coordinate time and proper time. The coordinate time t of an event is the same everywhere throughout the space-time coordinate system. The proper time τ is the reading of a clock in its own rest frame. The proper time depends on the clock's state of motion and its position in the gravitational potential. For a transported clock, the space-time interval is:

$$\mathrm{d}s^2 = g_{\mu\nu}\,\mathrm{d}x^\mu\mathrm{d}x^\nu \equiv -c^2\mathrm{d}\tau^2 \tag{9-2}$$

For an electromagnetic signal, the space-time interval satisfies the condition:

$$\mathrm{d}s^2 = g_{\mu\nu}\,\mathrm{d}x^\mu\mathrm{d}x^\nu = 0 \tag{9-3}$$

9.2 The principle of relativity

According to the special theory of relativity, formulated by Einstein in 1905, the laws of physics should have the same form in every inertial frame of reference. This postulate is known as the Principle of Relativity. Thus, in addition to the laws of mechanics, Maxwell's equations of electromagnetism should be valid in all inertial frames. A fundamental prediction of Maxwell's equations is the existence of electromagnetic waves that propagate in vacuum at the speed of light, uniquely given by:

$$c = 1/\sqrt{\mu_0\,\varepsilon_0}$$

where:

μ_0 and ε_0: are electrical constants representing the permeability and permittivity of free space, respectively.

Therefore, the speed of light c must be the same in every inertial frame.

In 1908 Minkowski recognized that this property could be expressed by the invariance of a four-dimensional space-time interval having the form:

$$\mathrm{d}s^2 = -c^2\mathrm{d}t^2 + \mathrm{d}x^2 + \mathrm{d}y^2 + \mathrm{d}z^2 = -c^2\mathrm{d}t'^2 + \mathrm{d}x'^2 + \mathrm{d}y'^2 + \mathrm{d}z'^2 \tag{9-4}$$

such that for a light signal the equation $\mathrm{d}s^2 = 0$ represents an expanding spherical wavefront in either the inertial frame $S(ct, x, y, z)$ or the inertial frame $S'(ct', x', y', z')$. The coefficients of the coordinate differentials are given by the Minkowski metric, $g_{\mu\nu} = \eta_{\mu\nu} \equiv \mathrm{diag}(-1, 1, 1, 1)$.

The coordinate transformation that preserves the invariance of this expression is the Lorentz transformation. If S' moves with velocity V along the x-axis of S, the Lorentz transformation is:

$$x = \gamma(x' + V\,t'); \quad y = y'; \quad z = z' \tag{9-5}$$

$$t = \gamma(t' + V\,x'/c^2)$$

where:

$$\gamma \equiv (1 - V^2/c^2)^{-1/2}$$

Two events are simultaneous if their coordinate times are equal. Thus the second term in the transformation of coordinate time implies the relativity of simultaneity: events that are simultaneous in S are not necessarily simultaneous in S'.

A fundamental tenet of general relativity, stated by Einstein in 1916, is that “the laws of physics must be of such a nature that they apply to systems of reference in any kind of motion”. Therefore, in general relativity the coordinate transformation between any two reference frames is arbitrary and the space-time interval assumes a quadratic differential form whose metric components are functions of the coordinates. By its invariance under an arbitrary coordinate transformation $x^\alpha \to x^\alpha(x'^0, x'^1, x'^2, x'^3)$, the space-time interval is:

$$\mathrm{d}s^2 = g_{\mu\nu}\,\mathrm{d}x^\mu\,\mathrm{d}x^\nu = g'_{\alpha\beta}\,\mathrm{d}x'^\alpha\,\mathrm{d}x'^\beta \tag{9-6}$$

The transformation of the coordinate differentials is:

$$\mathrm{d}x^\mu = \frac{\partial x^\mu}{\partial x'^\alpha}\,\mathrm{d}x'^\alpha \tag{9-7}$$

Thus by substitution of this expression into $\mathrm{d}s^2$, it follows that the transformation of the metric is:

$$g'_{\alpha\beta} = \frac{\partial x^\mu}{\partial x'^\alpha}\frac{\partial x^\nu}{\partial x'^\beta}\,g_{\mu\nu} \tag{9-8}$$

The coordinate differentials and the metric are examples of certain quantities called “tensors”. A tensor in any coordinate system is characterized by its law of transformation to a new coordinate system. The transformation is linear and homogeneous, so that if a tensor equation is valid in one coordinate system, it is also valid in any other coordinate system. Therefore, in general relativity the frame-invariance of physical laws is realized by expressing the equations in terms of tensors.

9.2.1 The metric tensor

The geometrical properties of space-time are determined by the Riemann tensor $R^\alpha{}_{\beta\gamma\delta}$, which is constructed entirely from the metric tensor and its first and second derivatives. A transformation of coordinates that brings a given metric $g_{\mu\nu}$ into the form of the Minkowski metric $\eta_{\mu\nu}$ of special relativity exists if and only if the Riemann tensor is zero. In that case, the space-time is flat. In the presence of matter, the space-time is curved and the metric cannot be reduced to the Minkowski metric over all space-time under any coordinate transformation. However, it is always possible to find a system of coordinates, represented by a freely falling frame of reference, where the first derivatives of the metric vanish at a selected point and the metric is given by the Minkowski metric in the neighborhood of that point. This property is embodied in the *principle of equivalence*, which states that a freely falling frame of reference is locally equivalent to an inertial frame of reference in the absence of gravitation. Alternatively, it states that a noninertial reference frame is locally indistinguishable from a reference frame at rest in a gravitational field. The *principle of equivalence* is based on the experimental observation that all bodies fall with the same acceleration, regardless of their composition or internal structure, and is expressed in the Newtonian theory of gravitation by the equivalence of inertial and gravitational mass.

For a given distribution of matter, the metric tensor is determined by the Einstein field equation:

$$R_{\mu\nu} - \frac{1}{2} g_{\mu\nu} R = \frac{8\pi G}{c^4} T_{\mu\nu} \tag{9-9}$$

where:

- $R_{\mu\nu} = R^{\alpha}{}_{\mu\,\alpha\,\nu}$: Ricci tensor, obtained by contracting (summing) the Riemann tensor on its first and third indices
- $R = g^{\mu\nu} R_{\mu\nu}$: scalar curvature P
- $T_{\mu\nu}$: energy-momentum tensor, and G is the Newtonian gravitational constant. In free space, the field equation reduces to $R_{\mu\nu} = 0$.

However, this equation does not imply the stronger condition $R^{\alpha}{}_{\beta\gamma\delta} = 0$, which implies the space-time is flat.

In the first approximation, to order $1/c^2$, the Einstein field equation reduces to Poisson's equation, $\nabla^2 U = -\,4\pi\, G\, \rho$, where U is the Newtonian gravitational potential and ρ is the density of matter.

In free space, the field equation becomes Laplace's equation, $\nabla^2 U = 0$.

For the analysis of clock transport in this approximation, the metric in an Earth-Centered Inertial (ECI) frame of reference is:

$$-g_{00} = 1 - 2\,U/c^2, \quad g_{0j} = 0, \quad g_{ij} = \delta_{ij} \tag{9-10}$$

where:

- δ_{ij}: the Kronecker delta.

By a transformation of coordinates, the metric in a rotating, Earth-Centered Earth-Fixed (ECEF) frame of reference becomes:

$$-g_{00} = 1 - 2\,U/c^2 - (\boldsymbol{\omega} \times \mathbf{r})^2/c^2 = 1 - 2\,W/c^2, \quad g_{0j} = (\boldsymbol{\omega} \times \mathbf{r})_j/c, \quad g_{ij} = \delta_{ij} \tag{9-11}$$

where:

- $\boldsymbol{\omega}$: Earth's rotational angular velocity
- $W \equiv U + ½\,(\boldsymbol{\omega} \times \mathbf{r})^2$: Earth's geopotential.

For the analysis of light signals it is necessary to include terms in g_{ij} to the same order as terms in g_{00}. Thus for light signals in an inertial frame of reference:

$$-g_{00} = 1 - 2\,U/c^2, \quad g_{0j} = 0, \quad g_{ij} = (1 + 2U/c^2)\,\delta_{ij} \tag{9-12}$$

and in a rotating frame of reference:

$$-g_{00} = 1 - 2\,U/c^2 - (\boldsymbol{\omega} \times \mathbf{r})^2/c^2 = 1 - 2\,W/c^2, \quad g_{0j} = (\boldsymbol{\omega} \times \mathbf{r})_j/c, \quad g_{ij} = (1 + 2U/c^2)\,\delta_{ij} \tag{9-13}$$

These approximations for the components of the metric tensor are sufficient for practical problems involving clocks and light signals.

NOTE 1 – Following an IAU recommendation, the sign of the Newtonian gravitational potential is positive.

9.2.2 The gravitational potential of the Earth

The Earth's gravitational potential U at radial distance r, geocentric latitude ϕ, and longitude λ is a solution to Laplace's equation, $\nabla^2 U = 0$, that may be expressed as a series expansion in spherical harmonics as:

$$U(r,\phi,\lambda) = \frac{GM}{r}\left\{1 + \sum_{n=2}^{\infty}\sum_{m=0}^{n}\left(\frac{R}{r}\right)^2 P_{nm}(\sin\phi)\left(C_{nm}\cos m\lambda + S_{nm}\sin m\lambda\right)\right\}$$

$$= \frac{GM}{r}\left\{1 - \sum_{n=2}^{\infty} J_n\left(\frac{R}{r}\right)^n P_n(\sin\phi) - \sum_{n=2}^{\infty}\sum_{m=1}^{n}\left(\frac{R}{r}\right)^n P_{nm}(\sin\phi)(J_{mn}\cos m\lambda + K_{mn}\sin m\lambda)\right\} \quad (9\text{-}14)$$

where:

G:	the gravitational constant
M:	the mass of the Earth
R:	the equatorial radius of the Earth
$P_n(\sin\phi)$:	The legendre polynomials of degree n
$P_{nm}(\sin\phi)$:	the associated Legendre functions of degree n and order m.

The first term is the potential for a spherical Earth. The terms in the single summation are called zonal harmonics and are associated with Earth oblateness. The terms in the double summation are called tesseral harmonics and are associated with the elliptical shape of the Earth's equator. When it is sufficient to consider only the first oblateness harmonic, the gravitational potential may be approximated by the expression:

$$U(r,\phi) = \frac{GM}{r}\left[1 + \frac{1}{2}J_2\left(\frac{R}{r}\right)^2\left(1 - 3\sin^2\phi\right)\right] \quad (9\text{-}15)$$

where:

J_2: the lowest degree oblateness coefficient
$P_2(x) = ½\,(3\,x^2 - 1)$.

For terrestrial measurements, it is necessary to account for both the Earth's gravitational potential and the Earth's rotation. The sum of the gravitational potential U and the rotational potential $½\,(\boldsymbol{\omega} \times \mathbf{r})^2 = ½\,\omega^2 r^2 \cos^2\phi$ is the geopotential:

$$W = U + \frac{1}{2}(\boldsymbol{\omega}\times\mathbf{r})^2 = U + \frac{1}{2}\omega^2 r^2\cos^2\phi \quad (9\text{-}16)$$

which is a solution of $\nabla^2 W = -\,4\pi\,G\,\rho + 2\,\omega^2$, where $\boldsymbol{\omega}$ is the angular velocity of the Earth's rotation. Retaining only the first oblateness correction, the geopotential may be expressed:

$$W(r,\phi) \approx \frac{GM}{r}\left[1 + \frac{1}{2}J_2\left(\frac{R}{r}\right)^2\left(1 - 3\sin^2\phi\right)\right] + \frac{1}{2}\omega^2 r^2\cos^2\phi \quad (9\text{-}17)$$

The surface of constant geopotential is called the geoid, which is closely approximated by mean sea level. Since the geopotential W_0 over the surface of the geoid is constant, it may be evaluated on the equator and is given by:

$$W_0 \equiv U_0 + \frac{1}{2}(\boldsymbol{\omega} \times \mathbf{R})^2 \approx \frac{GM}{R}\left(1 + \frac{1}{2}J_2\right) + \frac{1}{2}\omega^2 R^2 \tag{9-18}$$

where:

U_0: the Newtonian gravitational potential on the geoid at position **R**.

In the WGS-84 model of the Earth (NIMA Technical Report, 1997), the gravitational constant of the Earth is:

$$GM = 3.986\,004\,418 \times 10^{14}\ \mathrm{m^3/s^2}$$

the equatorial radius of the Earth is R = 6 378 137.0 m, and

the rotational angular velocity of the Earth is $\omega = 7.292\ 1150 \times 10^{-5}$ rad/s.

Also, the speed of light is 299 792 458 m/s exactly.

NOTE 1 – This value defines the meter in the International System of Units (SI). The permittivity of free space is $\varepsilon_0 = 1/(\mu_0 c^2)$, where the permeability of free space is $\mu_0 \equiv 4\pi \times 10^{-7}$ N/A^2 by definition of the ampere. Thus, as they both are now defined constants, c and ε_0 are no longer subject to experimental measurement.

The Earth's second degree oblateness coefficient is approximately J_2 = 0.001 0826.

Thus: $W_0 = 6.2637 \times 10^7$ m^2/s^2 and $W_0 / c^2 = 6.9693 \times 10^{-10}$ approximately.

The local acceleration of gravity **g** is the gradient of the geopotential. Thus:

$$\mathbf{g} = \nabla W = \nabla U - \boldsymbol{\omega} \times (\boldsymbol{\omega} \times \mathbf{r}) \tag{9-19}$$

The difference in geopotential over height h is approximately $\Delta W \approx \mathbf{g} \cdot \Delta\mathbf{r} = -\,g\,h$.

The magnitude of the acceleration of gravity over an oblate, rotating Earth is given in closed form by the Somigliana gravity formula [Heiskanen and Moritz, 1967]:

$$g = g_0 \frac{1 + k \sin^2 \phi'}{\sqrt{1 - \mathrm{e}^2 \sin^2 \phi'}} \tag{9-20}$$

where:

ϕ': the geodetic latitude

$e^2 = 2f - f^2$: the square of the first eccentricity

f: the flattening

g_0: the value of g at the equator.

The geodetic latitude ϕ' and the geocentric latitude ϕ are related by the exact equation:

$$\tan\phi = (1 - f)^2 \tan\phi' = (1 - e^2)\tan\phi'.$$

In the WGS-84 model of the Earth:

– k = 0.001 931 852 652 41

– f = 1/298.257 223 563

– e^2 = 0.006 694 379 990 14, and

– g_0 = 9.780 325 3359 m/s^2.

NOTE 1 – By convention, ΔW is negative when the clock is above the geoid.

9.2.3 Time dilation

In special relativity, the space-time interval for a clock moving with velocity v with respect to an inertial frame of reference is given by:

$$\mathrm{d}s^2 = -c^2\mathrm{d}t^2 + \delta_{ij}\,\mathrm{d}x^i\mathrm{d}x^j = -c^2(1-\mathrm{v}^2/c^2)\mathrm{d}t^2 = -c^2\,\mathrm{d}\tau^2 \tag{9-21}$$

where:

$\mathrm{v}^2 = \delta_{ij}\,(\mathrm{d}x^i/\mathrm{d}t)(\mathrm{d}x^j/\mathrm{d}t)$. For two clocks having velocities v_1 and v_2

$$\mathrm{d}\tau_1 = \sqrt{1-\mathrm{v}_1^2/c^2}\;\mathrm{d}t \tag{9-22}$$

and

$$\mathrm{d}\tau_2 = \sqrt{1-\mathrm{v}_2^2/c^2}\;\mathrm{d}t \tag{9-23}$$

Since the proper time intervals $\mathrm{d}\tau_1$ and $\mathrm{d}\tau_2$ correspond to the same coordinate time interval *dt*:

$$\frac{\mathrm{d}\tau_2}{\mathrm{d}\tau_1} = \sqrt{\frac{1-v_2^2/c^2}{1-v_1^2/c^2}} \approx 1 - \frac{1}{2}\frac{1}{c^2}(\mathrm{v}_2^2 - \mathrm{v}_1^2) \tag{9-24}$$

Therefore, a clock having a higher velocity with respect to an inertial frame of reference will run more slowly than a clock having a lower velocity with respect to the inertial frame.

If $v_1 = 0$, then $\mathrm{d}\tau_2 = \sqrt{1-\mathrm{v}_2^2/c^2}\;\mathrm{d}\tau_1$ and conversely $\mathrm{d}\tau_1 = \mathrm{d}\tau_2/\sqrt{1-\mathrm{v}_2^2/c^2}$.

Thus the proper time interval $\mathrm{d}\tau_1$ recorded by the stationary clock is longer than the proper time interval $\mathrm{d}\tau_2$ recorded by the moving clock. This property is called time dilation.

The time dilation effect has been extensively verified by the measured lifetimes of elementary particles. For example, high velocity muons produced by cosmic rays in the upper atmosphere appear to live longer, as judged by their path lengths before they decay, than the measured proper lifetimes of muons at rest in the laboratory [Frish and Smith, 1963].

Time dilation is also observed in clock transport. Consider the difference between the proper time τ_2 recorded by a clock carried with relative velocity v' around the equator of the rotating Earth and the proper time τ_1 of a reference clock that remains at one location on the equator. With respect to an inertial frame of reference, the velocity of the reference clock is:

$\mathrm{v}_1 = \omega\,R$, and

the velocity of the transported clock is:

$v_2 = \omega\,R + v'$

where:

ω: the Earth's angular velocity of rotation

R: the Earth's equatorial radius.

The difference in the proper times (transported clock – reference clock) is approximately:

$$\tau_2 - \tau_1 \approx -\frac{1}{2}\frac{1}{c^2}(\mathrm{v}_2^2 - \mathrm{v}_1^2)\,\tau_1 = -\frac{1}{c^2}\left(\frac{1}{2}\mathrm{v}'^2 + \omega R\mathrm{v}'\right)\tau_1 = -\frac{2\,\pi\,R}{c^2}\left(\frac{1}{2}\,|v'| \pm \omega\,R\right) \tag{9-25}$$

For an eastward trip, the relative velocity v' is positive and the two terms are additive, but for a westward trip the relative velocity is negative and the two terms tend to cancel. In the Earth's rotating frame, the second term on the right represents the Sagnac effect. In 1971 physicists Joseph Hafele and Richard Keating [Pound and Rebka, 1960] demonstrated time dilation with macroscopic atomic clocks for the first time. They carried a set of four caesium clocks around the world on commercial jet aircraft, once in the eastward direction and once in the westward direction, and quantitatively verified the asymmetry of the clock differences for the eastward and westward flights.

9.2.4 Gravitational redshift

In general relativity, the space-time interval for a clock is given by:

$$ds^2 = g_{\mu\nu}\,dx^\mu\,dx^\nu = g_{00}\,c^2\,dt^2 + 2\,g_{0j}\,c\,dt\,dx^j + g_{ij}\,dx^i\,dx^j = -c^2 d\tau^2 \tag{9-26}$$

In the special case of a clock at rest, $dx^i = 0$ and $d\tau = \sqrt{-g_{00}}\;dt$.

For two clocks A and B at rest in a gravitational potential at points x_A and x_B , the proper time intervals are:

$$d\tau_A = \sqrt{-g_{00}(x_A)}\;dt \tag{9-27}$$

and

$$d\tau_B = \sqrt{-g_{00}(x_B)}\;dt \tag{9-28}$$

Since the proper time intervals $d\tau_A$ and $d\tau_B$ correspond to the same coordinate time interval dt:

$$\frac{d\tau_B}{d\tau_A} = \frac{\sqrt{-g_{00}(x_B)}}{\sqrt{-g_{00}(x_A)}} \tag{9-29}$$

If the clocks are separated by height $h = r_B - r_A$ in the gravitational potential of the rotating Earth, then:

$$-g_{00} = 1 - 2\,U/c^2 - (\boldsymbol{\omega}\times\mathbf{r})^2/c^2 = 1 - 2\,W/c^2 \text{ and} \tag{9-30}$$

$$\frac{d\tau_B}{d\tau_A} \approx \frac{1 - W_B/c^2}{1 - W_A/c^2} \approx 1 - \frac{1}{c^2}(W_B - W_A) = 1 - \frac{\Delta W}{c^2} \approx 1 + \frac{g\,h}{c^2} \tag{9-31}$$

where:

W: the geopotential, g is the local acceleration of gravity;
$\Delta W \approx -g\,h$.

Then the difference in proper time clock readings is:

$$\tau_B - \tau_A = -\frac{1}{c^2}\Delta W\;\tau_A \approx \frac{1}{c^2} g\,h\,\tau_A \tag{9-32}$$

Therefore, due to the difference in gravitational potential, the proper time recorded by clock B at a higher elevation (i.e., in a weaker gravitational potential) will be longer than the proper time recorded by clock A at a lower elevation (i.e., in a stronger gravitational potential). If clock A transmits a periodic signal upward that is received by clock B, the relative frequency difference is:

$$\frac{f_B - f_A}{f_A} = \frac{f_B}{f_A} - 1 = \frac{d\tau_A}{d\tau_B} - 1 = -\frac{g\,h}{c^2} \tag{9-33}$$

The received frequency f_B measured by clock B is thus less than the transmitted frequency f_A measured by clock A. That is, the same number of signal pulses are observed over a longer interval of proper time[1]. This effect is called the gravitational redshift. (In practice, the term "redshift" is generic and applies to a change in frequency of either sign.)

The gravitational redshift was first measured directly in an experiment performed by Robert Pound and Glen Rebka [Pound and Rebka, 1960] at Harvard University in 1960. They precisely measured the extremely small fractional change in frequency of gamma-ray photons rising or falling over a known vertical distance. In the experiment, an Fe^{57} emitter was moved very slowly to produce a Doppler effect that exactly compensated the gravitational redshift to permit resonant absorption over a narrow frequency range by a stationary Fe^{57} absorber. The precision was made possible by using the newly-discovered Mössbauer effect, a phenomenon of recoilless emission and absorption that occurs when the isotope is embedded in an appropriate crystal.

In 1975, a research group led by Carroll Alley [Alley, 1983] at the University of Maryland performed a series of aircraft atomic clock experiments that were specifically designed to test the gravitational redshift at three different altitudes and found complete agreement with theory. The effect of the Earth's gravitational potential was also measured as part of the Hafele-Keating around-the-world atomic clock experiment in 1971.

The most precise test of the redshift to date was performed by Robert Vessot [Vessot and Levine, *et al,*, 1980] of the Smithsonian Astrophysical Observatory in 1976 using a hydrogen maser raised to an altitude of 10 000 km by a Scout D rocket. A two-way signal transponded through the rocket communications payload was mixed with a one-way signal to extract the relativistic frequency change. The gravitational effect exactly cancels on the uplink and downlink, so the transponded signal undergoes twice the Doppler shift, but the one-way signal is affected by both the gravitational and Doppler effects. This test agreed with theory to within 0.01%.

NOTE 1 – From the point of view of quantum mechanics, the kinetic energy of a photon is $E = h\,f$, where h is Planck's constant. As the photon rises, it loses kinetic energy and the observed frequency decreases.

9.2.5 Time transfer by clock transport

For a transported clock, the space-time interval is:

$$\mathrm{d}s^2 = g_{00}\,c^2\,\mathrm{d}t^2 + 2\,g_{0j}\,c\,\mathrm{d}t\,\mathrm{d}x^j + g_{ij}\,\mathrm{d}x^i\,\mathrm{d}x^j = -c^2\mathrm{d}\tau^2 \qquad (9\text{-}34)$$

The coordinate time is defined by the proper time of a standard clock at rest at infinity, since:

$$\text{if } \mathrm{d}x^i = 0 \text{ and } -g_{00} = 1 \text{ then } \mathrm{d}t = \mathrm{d}\tau.$$

This is a quadratic algebraic equation for dt.

Thus the elapsed coordinate time during the transport of a clock corresponding to the measured proper time is:

$$\Delta t = \pm \int_{path} \frac{1}{\sqrt{-g_{00}}}\sqrt{1+\frac{1}{c^2}\left(g_{ij}+\frac{g_{0i}\,g_{0j}}{-g_{00}}\right)\frac{\mathrm{d}x^i}{\mathrm{d}\tau}\frac{\mathrm{d}x^j}{\mathrm{d}\tau}}\;\mathrm{d}\tau \;+\; \frac{1}{c}\int_{path}\frac{g_{0j}}{-g_{00}}\frac{\mathrm{d}x^j}{\mathrm{d}\tau}\,\mathrm{d}\tau \qquad (9\text{-}35)$$

Therefore, when transferring time from point A to point B by means of an intermediate portable clock, the elapsed coordinate time is in the first approximation:

$$\Delta t = \int_A^B \left[1-\frac{1}{2}(-g_{00}-1)+\frac{1}{2}\frac{1}{c^2}g_{ij}\frac{\mathrm{d}x^i}{\mathrm{d}t}\frac{\mathrm{d}x^j}{\mathrm{d}t}\right]\mathrm{d}\tau \;+\; \frac{1}{c}\int_A^B g_{0j}\frac{\mathrm{d}x^i}{\mathrm{d}t}\mathrm{d}\tau \qquad (9\text{-}36)$$

The second term is the Sagnac effect for the transported clock. In an inertial frame of reference, $g_{0j} = 0$ and this term does not occur.

9.2.6 Earth-Centered Inertial coordinate system

Through terms of order $1 / c^2$, the components of the metric tensor in an ECI coordinate system are:

$$-g_{00} = 1 - 2\,U / c^2,\ g_{0j} = 0,\ \text{and } g_{ij} = \delta_{ij}.$$

To this order, the space-time interval is:

$$ds^2 = -\left(1 - \frac{2U}{c^2}\right)c^2 dt^2 + \delta_{ij}\,dx^i dx^j = -c^2\left(1 - \frac{2U}{c^2} - \frac{1}{c^2}\mathrm{v}^2\right)dt^2 = -c^2 d\tau^2 \quad (9\text{-}37)$$

where:

- U: the gravitational potential at the position of the clock
- v: the velocity of the clock relative to the inertial frame of reference.

Therefore, the coordinate time elapsed during the motion of the clock is:

$$\Delta t = \int_A^B \left(1 + \frac{1}{c^2}U + \frac{1}{2}\frac{1}{c^2}\mathrm{v}^2\right)d\tau \quad (9\text{-}38)$$

The corrections under the integral are the effects of gravitational redshift due to the Earth's potential and time dilation due to the clock's velocity. The coordinate time t represented by this prescription is Geocentric Coordinate time (TCG), which is the geocentric coordinate time scale as realized with respect to an ECI coordinate system whose unit is the SI second.

For a clock at rest at position $\mathbf{R}$ on the rotating geoid in a gravitational potential U_0 and with velocity $\boldsymbol{\omega}\times\mathbf{R}$ with respect to the ECI frame of reference, the elapsed coordinate time is:

$$\Delta t = \int_A^B \left\{1 + \frac{1}{c^2}U_0 + \frac{1}{2}\frac{1}{c^2}(\boldsymbol{\omega}\times\mathbf{R})^2\right\}d\tau = (1 + W_0 / c^2)\,\Delta\tau \quad (9\text{-}39)$$

where:

- W_0: is the geopotential over the surface of the geoid.

Since W_0 is a constant, while coordinate time t is a global coordinate, clocks everywhere on the geoid maintain the same proper time $\Delta\tau$. The coordinate time can be made equal to the proper time of a clock on the geoid by rescaling the coordinate time as:

$$\Delta t' \equiv \left(1 - W_0 / c^2\right)\Delta t = \Delta\tau \quad (9\text{-}40)$$

Therefore, the elapsed coordinate time, as measured by the proper time of a reference clock on the geoid, that corresponds to the proper time of a clock in a potential U with velocity v with respect to the ECI frame is:

$$\Delta t' = \int_A^B \left\{1 + \frac{1}{c^2}(U - W_0) + \frac{1}{2}\frac{1}{c^2}v^2\right\}d\tau \quad (9\text{-}41)$$

Note that W_0 includes the effect of the Earth's rotation but U does not. This equation can be used both for clocks near the surface of the Earth and for clocks on satellites up to the altitude of the geostationary orbit (35 786 km). The coordinate time t' represented by this prescription is TT, defined as the coordinate time scale as realized by clocks on the rotating geoid whose unit is the SI second.

Therefore, $t' \equiv$ TT differs from $t \equiv$ TCG uniquely by a constant rate, such that dTT / dTCG = $1 - L_G$;

where:

$L_G \equiv \quad W_0 / c^2 = 6.969\,290\,134 \times 10^{-10}$ (approximately 60.2 μs/d).

TT is an ideal form of TAI.

9.2.7 Earth-Centered Earth-Fixed coordinate system

Through terms of order $1/c^2$, the components of the metric tensor in the rotating Earth-Centered Earth-Fixed (ECEF) coordinate system are:

$$-g_{00} = 1 - 2\,U/c^2 - (\boldsymbol{\omega}\times\mathbf{r})^2/c^2 = 1 - 2\,W/c^2,\ g_{0j} = (\boldsymbol{\omega}\times\mathbf{r})_j/c \text{ and } g_{ij} = \delta_{ij}.$$

To this order, the space-time interval is:

$$ds^2 = -\left[1 - 2\frac{1}{c^2}U - \frac{1}{c^2}(\boldsymbol{\omega}\times\mathbf{r})^2\right]c^2dt^2 + 2\,(\boldsymbol{\omega}\times\mathbf{r})_j\,dx^j c\,dt + \delta_{ij}\,dx^i dx^j = -c^2 d\tau^2 \tag{9-42}$$

Thus the elapsed coordinate time is:

$$\Delta t = \int_A^B \left\{1 + U/c^2 + \frac{1}{2}(\boldsymbol{\omega}\times\mathbf{r})^2/c^2 + (\boldsymbol{\omega}\times\mathbf{r})\cdot\mathbf{v}'/c + \frac{1}{2}v'^2/c^2\right\}d\tau \tag{9-43}$$

where:

$\mathbf{v}'$: the clock velocity with respect to the rotating Earth. This result also follows from the equation for Δt with respect to an inertial frame by the substitution $\mathbf{v} = \mathbf{v}' + \boldsymbol{\omega}\times\mathbf{r}$ to the same approximation.

To make this coordinate time correspond to the proper time recorded by a clock at rest on the geoid, it is multiplied by the scaling factor $1 - W_0/c^2$, yielding:

$$\Delta t' = \left(1 - \frac{1}{c^2}W_0\right)\Delta t = \int_A^B \left\{1 + \frac{1}{c^2}\left[U + \frac{1}{2}(\boldsymbol{\omega}\times\mathbf{r})^2 - W_0\right] + \frac{1}{2}v'^2\right\}d\tau + \int_A^B (\boldsymbol{\omega}\times\mathbf{r})\cdot\mathbf{v}'\,d\tau \tag{9-44}$$

The term in brackets in the first integral may be expressed:

$$U + \frac{1}{2}(\boldsymbol{\omega}\times\mathbf{r})^2 - W_0 = W - W_0 = \Delta W = -g\,h \tag{9-45}$$

where:

W: the geopotential at height h

W_0: the geopotential on the surface of the geoid

g: the local acceleration of gravity.

Therefore, the elapsed coordinate time becomes:

$$\Delta t' = \int_A^B \left(1 - \frac{1}{c^2}g\,h + \frac{1}{2}\frac{1}{c^2}v'^2\right)d\tau + \frac{1}{c^2}\int_A^B (\boldsymbol{\omega}\times\mathbf{r})\cdot\mathbf{v}'d\tau \tag{9-46}$$

The second integral is the Sagnac effect for the transported clock. The Sagnac effect is a kinematic property intrinsic to the rotating frame of reference. This term may be expressed:

$$\Delta t_{Sagnac} = \frac{1}{c^2}\int_A^B (\boldsymbol{\omega}\times\mathbf{r})\cdot\mathbf{v}'\,d\tau = \frac{1}{c^2}\int_A^B \boldsymbol{\omega}\cdot(\mathbf{r}\times d\mathbf{r}) = 2\frac{1}{c^2}\int_A^B \boldsymbol{\omega}\cdot d\mathbf{A} = \frac{2\omega A}{c^2} \tag{9-47}$$

where:

A: the area swept out by the position vector with respect to the center of the Earth projected onto the equatorial plane (positive for the eastward direction and negative for the westward direction).

The Sagnac effect may also be expressed:

$$\Delta t_{Sagnac} = \frac{1}{c^2}\int_A^B (\boldsymbol{\omega}\times\mathbf{r})\cdot\mathbf{v}'\,\mathrm{d}\tau = \frac{1}{c^2}\int_A^B (\omega R\cos\phi)(v'\cos\theta)\,\mathrm{d}\tau \frac{\omega}{c^2}\int_A^B R^2\cos^2\phi\,\mathrm{d}\lambda \tag{9-48}$$

where:

R: radius of the Earth, ϕ is the latitude

λ: longitude

$v'\cos\theta$: eastward component of the velocity. The heading θ, measured relative to east, is the complement of the azimuth Az, measured relative to north, so that $\cos\theta = \sin Az$.

The Sagnac correction to the elapsed coordinate time is positive for a clock travelling east and is negative for a clock travelling west; it is zero for a clock north or south.

Therefore, when transferring time from point A to point B by means of a portable clock, the elapsed coordinate time is:

$$\Delta t' = \int_A^B \left(1 - \frac{1}{c^2}g\,h + \frac{1}{2}\frac{1}{c^2}v'^2\right)\mathrm{d}\tau + \frac{\omega}{c^2}\int_A^B R^2\cos^2\phi\,\mathrm{d}\lambda \tag{9-49}$$

According to this formula, there are three relativistic effects to be taken into account. The corrections under the first integral are the gravitational redshift and time dilation terms. The correction given by the second integral is the Sagnac effect. In general, the coordinate time must be integrated numerically over the specified path.

For a clock that is transported completely around the equator in the eastward direction and returned to the starting point, the Sagnac correction is 207.4 ns.

For a closed path bounding a small area S on the Earth's surface:

$A \approx S\sin\bar{\phi}$, where $\bar{\phi}$ is the mean latitude evaluated at the center of S.

If a clock is transported back and forth between two points over the same path, the Sagnac corrections cancel and the net Sagnac effect is zero.

If the path is a great circle, then $\cos\phi\cos\theta = \cos i$, which is a constant, where i is the inclination of the great circle plane relative to the equator.

The projected area is $A = ½\, R^2\,\gamma\cos i$, where γ is the great circle arc from point 1 to point 2 at the beginning and end of the path.

Thus the Sagnac correction is:

$$\Delta t_{Sagnac} = \frac{2\omega A}{c^2} = \frac{\omega R^2}{c^2}\gamma\cos i \tag{9-50}$$

By spherical trigonometry, γ is given by:

$$\cos\gamma = \sin\phi_1\sin\phi_2 + \cos\phi_1\cos\phi_2\cos(\lambda_2 - \lambda_1) \tag{9-51}$$

where:

ϕ and λ: latitude and longitude of each point.

The inclination of the great circle plane is given by:

$$\tan i = \begin{cases} \tan\phi_1 \csc\beta\,, & \beta \neq 0, \quad \phi_1 \neq 0 \\ \tan\phi_2 \csc(\lambda_2 - \lambda_1)\,, & \beta = \phi_1 = 0 \end{cases} \tag{9-52}$$

such that point 1 is taken to be west of point 2. The angle β is the difference in longitude between the point of intersection of the great circle with the equator and point 1 given by:

$$\cot\beta = \frac{\tan\phi_2}{\tan\phi_1}\csc\left(\lambda_2 - \lambda_1\right) - \cot\left(\lambda_2 - \lambda_1\right) \tag{9-53}$$

At any point on the great circle, the latitude may be expressed in terms of the longitude as:

$$\tan\phi = \tan i \sin\left(\lambda_2 - \lambda_1 + \beta\right) \tag{9-54}$$

Using this expression and the identity $\cos^2\phi = 1/(1+\tan^2\phi)$, and also noting that $\tan(\lambda_2 - \lambda_1 + \beta) = \cos i \tan(\gamma + \psi)$ and $\tan\beta = \cos i \tan\psi$ where ψ is the great circle arc from the point of intersection with the equator to point 1, one may alternatively show that:

$$\Delta t_{Sagnac} = \frac{\omega}{c^2}\int_A^B R^2 \cos^2\phi \, d\lambda = \frac{\omega R^2}{c^2}\gamma \cos i \tag{9-55}$$

as above.

As an example, consider a time transfer measurement between the National Physical Laboratory and the U. S. Naval Observatory by means of a transported atomic clock. Assume that the clock is carried on an aircraft over a great circle route from London to Washington, D.C at an average altitude of 10 000 m and an average velocity of 220 m/s with a flight time of approximately 7.5 h. The proper time interval recorded by the flying clock is $\Delta\tau$ and the proper time interval recorded by a reference clock on the geoid is $\Delta\tau' = \Delta t'$. Then the proper time difference $\Delta\tau - \Delta\tau'$ (flying clock – reference clock) is + 29 ns due to the gravitational redshift and – 7 ns due to time dilation. For the westward flight, the Sagnac effect is + 18 ns. The flying clock would therefore gain a total of 40 ns relative to the reference clock.

On the other hand, for an eastward flight from Washington, D.C to London, the Sagnac effect is – 18 ns and the flying clock would gain only a net 4 ns. Over the round trip, the Sagnac corrections cancel if the flight paths are the same and the resulting net change is + 44 ns (= 2 × 29 ns – 2 × 7 ns) due entirely to the gravitational redshift and time dilation.

9.3 Clock onboard a satellite

For a clock onboard a satellite, the elapsed coordinate time with respect to an ECI frame of reference is:

$$\Delta t = \int_A^B \left(1 + \frac{1}{c^2}U + \frac{1}{2}\frac{1}{c^2}v^2\right) d\tau \tag{9-56}$$

If the satellite follows an unperturbed, Keplerian orbit, the gravitational potential is:

$$U = \frac{GM}{r} \tag{9-57}$$

and the satellite velocity is given by conservation of energy E (per unit mass):

$$E = \frac{1}{2}v^2 - U = \frac{1}{2}v^2 - \frac{GM}{r} = -\frac{GM}{2a} \tag{9-58}$$

where:

a : the orbital semimajor axis.

Therefore, the elapsed coordinate time is:

$$\Delta t = \int\limits_{orbit} \left(1 - \frac{1}{c^2}\frac{GM}{2a} + \frac{1}{c^2}\frac{2GM}{r}\right) d\tau = \left(1 - \frac{1}{c^2}\frac{GM}{2a}\right)\Delta\tau + \frac{2\,GM}{c^2}\int_{\tau_0}^{\tau} \frac{1}{r}\,d\tau \tag{9-59}$$

For a Keplerian orbit, the radial distance is:

$$r = a\,(1 - e\cos E)$$

where:

e: the orbital eccentricity

E: the eccentric anomaly.

Also, by Kepler's equation:

$$M \equiv n\,(\tau - \tau_0) = E - e\sin E$$

where:

M: the mean anomaly

$n \equiv 2\pi / T = \sqrt{GM / a^3}$: the mean motion

T: the orbital period

τ_0: the time of perigee.

Thus the integral is:

$$\int_{\tau_0}^{\tau} \frac{1}{r}\,d\tau = \frac{1}{na}E = \frac{1}{a}\Delta\tau + \sqrt{\frac{a}{GM}}\; e\sin E \tag{9-60}$$

where:

$$\Delta\tau = \tau - \tau_0\,.$$

Therefore:

$$\Delta t = \left(1 + \frac{3}{2}\frac{1}{c^2}\frac{GM}{a}\right)\Delta\tau + \frac{2}{c^2}\sqrt{GM\,a}\; e\sin E \tag{9-61}$$

It is convenient to apply the change of scale:

$$\Delta t' = \left(1 - \frac{1}{c^2}W_0\right)\Delta t = \int_A^B \left\{1 + \frac{1}{c^2}(U - W_0) + \frac{1}{2}\frac{1}{c^2}\mathrm{v}^2\right\} d\tau \tag{9-62}$$

so that the coordinate time will correspond to the proper time registered by clocks on the geoid. Thus a clock on the geoid becomes a coordinate clock. Then the elapsed coordinate time is:

$$\Delta t' = \left(1 + \frac{3}{2}\frac{1}{c^2}\frac{GM}{a} - \frac{1}{c^2}W_0\right)\Delta\tau + \frac{2}{c^2}\sqrt{GM\,a}\; e\sin E \tag{9-63}$$

The first term represents a constant rate offset between the satellite clock and a clock on the geoid. The correction to the satellite clock proper time interval is:

$$k \equiv 1 + \frac{3}{2}\frac{1}{c^2}\frac{GM}{a} - \frac{1}{c^2}W_0 = \frac{3}{2}\frac{1}{c^2}\frac{GM}{a} - \frac{1}{c^2}\frac{GM}{R}\left(1+\frac{1}{2}J_2\right) - \frac{1}{2}\frac{1}{c^2}\omega^2 R^2 \tag{9-64}$$

The value of k is zero for a semimajor axis of approximately 9 545 km.

At this distance, the gravitational redshift and time dilation effects cancel. For a lower orbit, time dilation is greater and k is positive, while for a higher orbit the gravitational redshift is greater and k is negative.

The second term is a small relativistic periodic correction due to the orbital eccentricity and may be expressed without approximation as:

$$\Delta t_r = \frac{2}{c^2}\sqrt{GM\,a}\; e \sin E = \frac{2\,\mathbf{r}\cdot\mathbf{v}}{c^2} \tag{9-65}$$

where:

r and **v**: the position and velocity of the satellite.

Since $\mathbf{r}\cdot\mathbf{v}$ is a scalar, it may be evaluated in either the ECI coordinate system or the ECEF coordinate system. Therefore, the coordinate time interval may be expressed in the form:

$$\Delta t' = (1 + k)\,\Delta\tau + \Delta t_r\,.$$

The satellite clock proper time is:

$$\Delta\tau = (1 - k)\,\Delta t' + \Delta\tau_r$$

where:

the correction to the proper time is the negative of the correction to the coordinate time, $\Delta\tau_r \equiv -\Delta t_r$.

By adjusting the satellite clock rate according to $\Delta\tau' = (1 + k)\,\Delta\tau$, the satellite clock can be made to have the same average rate as a clock on the geoid. Consequently, the proper time becomes:

$$\Delta\tau' = \Delta t' + \Delta\tau_r\,.$$

Therefore, apart from a small periodic correction, the satellite clock also becomes a coordinate clock.

For a GPS satellite with an orbital semimajor axis of 26 562 km, the secular rate offset is:

$$k = -\,4.464\,733 \times 10^{-10} = -\,38.575\,293\ \mu\text{s/d}.$$

Thus a GPS satellite clock runs fast by approximately 38 µs/day with respect to a standard clock on the geoid, comprising 45 µs/day fast due to difference in gravitational potential and 7 µs/day slow due to difference in velocity.

This effect is substantial compared to the nominal clock precision of 10 ns over a few hours. To compensate for the rate difference, a GPS satellite clock is given a fractional offset prior to launch of $\Delta f / f = -\,4.464\,733 \times 10^{-10}$, equivalent to a change in the 10.23 MHz clock rate of $\Delta f = -\,0.004\,5674$ Hz.

The resulting frequency is equal to 10 229 999.995 4326 Hz, so that, as it appears to an observer on the geoid, the frequency remains unchanged. If the maximum orbital eccentricity is 0.02, the periodic term $\Delta\tau_r$ has an amplitude of 46 ns at the orbital period of 11.967 hours. This relativistic correction is applied in the user receiver.

The rate difference was first measured in signals received from GPS prototype satellite NTS-2 in 1977, in agreement with general relativity to within 0.7% [Buisson, *et al.*, 1977]. Relativistic frequency steps have also been observed during orbit repositioning maneuvers [Epstein, *et al.*, 2001]. The amplitude of the periodic term can be significant for a highly elliptical orbit. For example, in a 12-hour Molniya orbit having eccentricity 0.722, the amplitude is 1.7 µs.

These relativistic corrections are sufficient for the measurement of time at the nanosecond level of precision. For sub-nanosecond time measurement, the next most important factor is the contribution to the gravitational redshift due to the Earth's J_2 oblateness perturbation in the potential $U(r, \phi)$ given above. The perturbed semimajor axis a and radial distance r are [Kozai, 1959]:

$$a = \bar{a}\left[1 + \frac{3}{2}J_2\left(\frac{R}{\bar{a}}\right)^2 \sin^2 i\,\cos(2\mathrm{u})\right] \tag{9-66}$$

and

$$r = \bar{a}\left[1 - e\cos E + \frac{1}{4}J_2\left(\frac{R}{\bar{a}}\right)^2 \sin^2 i\,\cos(2\mathrm{u})\right] \tag{9-67}$$

where:

- $\bar{a}$: mean semimajor axis
- e : eccentricity (assumed to be small)
- E: eccentric anomaly
- i: inclination
- u: argument of latitude.

The perturbed semimajor axis a is thus a periodic function of u. The total energy E (which may be regarded as defining a) is:

$$E = \frac{1}{2}\mathrm{v}^2 - U(r,\phi) = \left(\frac{GM}{r} - \frac{GM}{2a}\right) - U(r,\phi) = -\frac{GM}{2\bar{a}}\left[1 + J_2\left(\frac{R}{\bar{a}}\right)^2\left(1 - \frac{3}{2}\sin^2 i\right)\right] \tag{9-68}$$

and is a constant as required.

Therefore, on substituting ½ v^2 and $U(r, \phi)$ into the expression for the elapsed coordinate time $\Delta t'$, noting that $\sin\phi = \sin i \sin u$ and $u \approx n\,\Delta\tau$ where $\Delta\tau$ is the proper time from the ascending node as measured by the satellite clock, one finds (NIMA Technical Report, 1997):

$$\Delta t_{oblateness} = \frac{1}{2}\frac{1}{c^2}\frac{GM}{\bar{a}}J_2\left(\frac{R}{\bar{a}}\right)^2\left[\left(1 - \frac{3}{2}\sin^2 i\right)\Delta\tau + \frac{\sin^2 i}{n}\sin(2n\,\Delta\tau)\right] \tag{9-69}$$

For a GPS orbit with inclination 55°, the periodic term has an amplitude of 24 ps.

By the *Principle of Equivalence*, the gravitational potentials of the Moon and Sun do not directly affect a clock on a satellite in orbit about the Earth because the Earth constitutes a freely falling frame of reference in those potentials.

Thus they appear instead as tidal effects. The tidal potential due to an external third body is approximately given by:

$$U_{tidal} = \frac{1}{2}\frac{\partial^2 U_{ext}}{\partial x^i\,\partial x^j}x^i x^j \approx \frac{GM_{ext}}{r_E^3}(r_S - r_E)^2 \tag{9-70}$$

where:

r_S and r_E: the distances of the third body from the satellite and the Earth, respectively.

$$r_S - r_E \approx r\cos i\,\sin(n\,\Delta\tau)$$

where:

- r: the orbital radius
- i: the orbital inclination relative to the third body, which is variable.

Thus the correction to the coordinate time interval is:

$$\Delta t_{tidal} \approx \frac{1}{2}\frac{1}{c^2}\frac{GM_{ext}}{r_E}\left(\frac{r}{r_E}\right)^2 \cos^2 i\left[\Delta\tau - \frac{1}{2n}\sin(2n\,\Delta\tau)\right] \tag{9-71}$$

Tidal effects on a GPS clock are small. Apart from the inclination factor, for the Moon the secular drift rate is 15 ps per revolution and the amplitude of the periodic term is 1 ps. For the Sun the values are 7 ps per revolution and 0.5 ps, respectively. Although the Sun's mass is about 30 million times that of the Moon, it is about 400 times farther away. Since the tidal potential varies inversely as the cube of the distance, the tidal effect of the Sun is about one-half that of the Moon.

9.4 Time transfer by an electromagnetic signal

In special relativity, the equation for light propagation in an inertial frame of reference is:

$$ds^2 = \eta_{\mu\nu}\, dx^\mu dx^\nu = -c^2 dt^2 + dx^2 + dy^2 + dz^2 = 0 \tag{9-72}$$

where:

$\eta_{\mu\nu}$: the Minkowski metric.

The propagation time between two points *A* and *B* is simply:

$$\Delta t_{AB} = \Delta t_{BA} = \frac{1}{c}\int_A^B \sqrt{\delta_{ij}\, dx^i dx^j} = \frac{1}{c}\int_A^B \sqrt{dx^2 + dy^2 + dz^2} \tag{9-73}$$

The Einstein prescription is a convention in special relativity used to synchronize clocks in an inertial frame of reference via an electromagnetic signal, such as a light pulse or a radar pulse. Suppose that a signal is transmitted at point *A* and is received at point *B*, where it is reflected back to a receiver at point *A*. If the coordinate times of transmission, reflection, and reception as measured by clocks at *A* and *B* are respectively t_1, t_2, and t_3, then by definition the clocks are synchronized if $t_2 - t_1 = t_3 - t_2$. Since $\Delta t_{AB} = t_2 - t_1$ and $\Delta t_{BA} = t_3 - t_2$, then:

$$t_2 \equiv \frac{1}{2}\left[(t_1 + \Delta t_{AB}) + (t_3 - \Delta t_{BA})\right] = \frac{1}{2}(t_1 + t_3) \tag{9-74}$$

Thus the coordinate time of reflection t_2 is identified with the midpoint in time between t_1 and t_3. Clock *A* is assigned the proper times $\tau_1 = t_1$ and $\tau_3 = t_3$, while clock *B* is assigned the proper time $\tau_2 = t_2$. By this method a coordinate time scale may be established that is given by the readings of a spatially distributed network of standard clocks. If clock *A* is synchronized with clock *B* and clock *B* is synchronized with clock *C*, then clock *A* is also synchronized with clock *C*.

In general relativity, the light propagation equation is:

$$ds^2 = g_{\mu\nu} dx^\mu dx^\nu = g_{ij}\, dx^i dx^j + 2 g_{0j} dx^j c\, dt + g_{00}\, c^2 dt^2 = 0 \tag{9-75}$$

This is a quadratic equation for the increment in coordinate time *dt*. Therefore, the elapsed coordinate time of propagation is:

$$\Delta t = \pm\frac{1}{c}\int_{path} \frac{1}{-g_{00}}\sqrt{(-g_{00}\, g_{ij} + g_{0i}\, g_{0j})\, dx^i dx^j} + \frac{1}{c}\int_{path} \frac{g_{0j}}{-g_{00}}\, dx^j \tag{9-76}$$

The two roots correspond to light propagation in the forward and backward directions. Consequently, defining Δt_{AB} and Δt_{BA} as the propagation times in each direction (with limits of integration from A to B and from B to A, respectively), one obtains:

$$\Delta t_{AB} = \frac{1}{c}\int_A^B \frac{1}{\sqrt{-g_{00}}}\sqrt{\left(g_{ij} + \frac{g_{0i}\, g_{0j}}{-g_{00}}\right)\mathrm{d}x^i\,\mathrm{d}x^j} + \frac{1}{c}\int_A^B \frac{g_{0j}}{-g_{00}}\mathrm{d}x^j \tag{9-77}$$

and

$$\Delta t_{BA} = -\frac{1}{c}\int_B^A \frac{1}{\sqrt{-g_{00}}}\sqrt{\left(g_{ij} + \frac{g_{0i}\, g_{0j}}{-g_{00}}\right)\mathrm{d}x^i\,\mathrm{d}x^j} + \frac{1}{c}\int_B^A \frac{g_{0j}}{-g_{00}}\mathrm{d}x^j \tag{9-78}$$

The first term is the propagation time over the path with spatial interval $\mathrm{d}\rho^2 \equiv \gamma_{ij}\ \mathrm{d}x^i\ \mathrm{d}x^j$, where $\gamma_{ij} \equiv g_{ij} + g_{0i}\, g_{0j}/(-g_{00})$ is the three-dimensional metric. The second term is the Sagnac effect.

Suppose a pulse is sent out from a reference clock at point A at time t_1, reflected at a distant clock at point B at time t_2, and received by the reference clock at point A at time t_3. The coordinate time of reflection at point B is:

$$t_2 = \frac{1}{2}\left[\left(t_1 + \Delta t_{AB}\right) + \left(t_3 - \Delta t_{BA}\right)\right] = \frac{1}{2}\left(t_1 + t_3\right) + \frac{1}{c}\int_A^B \frac{g_{0j}}{-g_{00}}\mathrm{d}x^j \tag{9-79}$$

In general, the coordinate time of reflection will depend on the metric components g_{0j} and $-g_{00}$ and on the light path from A to B. Therefore, when g_{0j} is not equal to zero, it is not possible to synchronize clocks in the Einstein sense uniquely. This will be the case in a rotating frame of reference, where there is a Sagnac effect given by the second term.

9.4.1 Earth Centered Inertial coordinate system

One may neglect the gravitational potential in the first approximation. Thus in an ECI coordinate system the metric becomes $-g_{00} \approx 1$, $g_{0j} = 0$, and $g_{ij} \approx \delta_{ij}$.

Integrating the equation $\mathrm{d}s^2 = 0$ along the path, one obtains the signal propagation time:

$$\Delta t = \frac{1}{c}\int_{path} \sqrt{\delta_{ij}\ \mathrm{d}x^i \mathrm{d}x^j} = \frac{\rho}{c} \tag{9-80}$$

where:

ρ: the propagation path length in the ECI frame.

This is simply the non-relativistic propagation time over a path with the Euclidean spatial interval $\mathrm{d}\rho^2 \approx \delta_{ij}\ \mathrm{d}x^i\ \mathrm{d}x^j$.

If a signal is transmitted from a satellite at coordinate time t_T to a moving receiver at coordinate time t_R, the coordinate time elapsed over the path length in the ECI frame is:

$$\Delta t = \frac{\rho}{c} = \frac{1}{c}\left|\mathbf{r}_R(t_R) - \mathbf{r}_T(t_T)\right| = \frac{1}{c}\left|\Delta\mathbf{r} + \mathbf{v}_R\ (t_R - t_T)\right| \approx \frac{1}{c}\left|\Delta\mathbf{r}\right| + \frac{1}{c^2}\Delta\mathbf{r}\cdot\mathbf{v}_R \tag{9-81}$$

where:

$\Delta\mathbf{r} \equiv \mathbf{r}_R(t_T) - \mathbf{r}_T(t_T)$: the difference between the position of the receiver and the satellite at the coordinate time of transmission t_T and $\mathbf{v}_R$ is the velocity of the receiver in the ECI frame.

Thus the correction to the coordinate time due to the receiver velocity is:

$$\Delta t_v \approx \Delta \mathbf{r} \cdot \mathbf{v}_R / c^2 \tag{9-82}$$

If the receiver has position $\mathbf{R}$ and velocity $\mathbf{v}'_R$ relative to the rotating geoid, $\Delta\mathbf{r} = \mathbf{R}(t_T) - \mathbf{r}_T(t_T)$ and $\mathbf{v}_R = \mathbf{v}'_R + \boldsymbol{\omega} \times \mathbf{R}$.

Then the receiver velocity correction becomes the sum of two terms:

$$\Delta t_v = \Delta \mathbf{r} \cdot \mathbf{v}'_R / c^2 + \boldsymbol{\omega} \cdot [\mathbf{r}_T(t_T) \times \mathbf{R}(t_T)] / c^2 = |\Delta \mathbf{r}|\, v'_R \cos\theta / c^2 + 2\,\omega\, A / c^2 \tag{9-83}$$

where:

- $|\Delta \mathbf{r}|$: the range
- θ: the angle between the receiver velocity and the line joining the satellite and the receiver, and A is the area of the triangle with vertices at the satellite, receiver, and center of the Earth projected onto the equatorial plane at the coordinate time of transmission t_T.

In the Earth's rotating frame of reference, the first term is a range rate, or integrated Doppler shift, correction and the second term is the Sagnac correction.

The propagation time Δt is the time measured by a standard clock at rest at infinity. To determine the propagation time with respect to a clock on the Earth's surface, the effect of the geopotential must be included. Thus by the change of scale $\Delta t' = (1 - W_0 / c^2)\, \Delta t$, the propagation time becomes $\Delta t' = (1 - W_0 / c^2)\, \rho / c$.

For a GPS satellite, the maximum signal propagation time is 86 ms and the correction is – 60 ps.

To consider the effect of the gravitational potential U on the light signal, it is necessary to include the potential in both the spatial and time parts of the metric. The components of the metric tensor are:

$$- g_{00} = 1 - 2\, U / \mathrm{I}^2 ,\ g_{0j} = 0,\ \text{and}\ g_{ij} = (1 + 2\, U / c^2)\, \delta_{ij} .$$

Therefore, by the equation $\mathrm{d}s^2 = 0$, the elapsed coordinate time of propagation, as measured by a clock at infinity, is:

$$\Delta t = \frac{1}{c} \int_{path} \sqrt{\frac{g_{ij}}{-g_{00}}\, \mathrm{d}x^i \mathrm{d}x^j} \approx \frac{1}{c} \int_{path} \left(1 + 2\, U / c^2\right) \sqrt{\delta_{ij}\, \mathrm{d}x^i \mathrm{d}x^j} = \frac{\rho}{c} + \frac{2}{c^3} \int_{path} U\, \mathrm{d}\rho \tag{9-84}$$

where:

the gravitational potential: $U = GM / r$.

The first term is the Euclidean propagation time and the second term is the gravitational time delay Δt_{delay}. For a straight line path in the radial direction, one obtains:

$$\Delta t_{delay} = \frac{2}{c^3} \int_R^r \frac{GM}{r}\, dr = \frac{2\, GM}{c^3} \ln \frac{r}{R} \tag{9-85}$$

In general, however, the range ρ, elevation angle θ, and radial distance r are related by the law of cosines $r^2 = R^2 + \rho^2 + 2\, R\, \rho \sin\theta$.

The range may be expressed in terms of the elevation angle as:

$$\rho = \sqrt{r^2 - (R\cos\theta)^2} - R\sin\theta$$

Therefore, the gravitational time delay is:

$$\Delta t_{delay} = \frac{2}{c^3} \int_0^{\rho} \frac{GM}{\sqrt{R^2 + \rho^2 + 2\,R\rho\,\sin\theta}}\,d\rho \;=\; \frac{2GM}{c^3} \ln\left[\frac{r + \sqrt{r^2 - (R\cos\theta)^2}}{R(1+\sin\theta)}\right] \tag{9-86}$$

An alternative formula may be derived that involves the distances r, R, and ρ in a symmetric manner. Since $\sqrt{r^2 - (R\cos\theta)^2} = \rho + R\sin\theta$ and $R\sin\theta = (r^2 - R^2 - \rho^2)\,/\,2\,\rho$, the argument of the logarithm is:

$$\frac{2r\rho + \rho^2 + r^2 - R^2}{2R\rho + r^2 - R^2 - \rho^2} = \frac{(r+\rho)^2 - R^2}{r^2 - (\rho - R)^2} = \frac{(r+\rho+R)(r+\rho-R)}{(r+\rho-R)(r-\rho+R)} = \frac{R+r+\rho}{R+r-\rho} \tag{9-87}$$

Thus the gravitational time delay with respect to a clock at infinity may be expressed:

$$\Delta t_{delay} = \frac{2\,GM}{c^3} \ln\left(\frac{R+r+\rho}{R+r-\rho}\right) \tag{9-88}$$

When $\rho = r - R$, this equation reduces to the time delay for a straight line path.

The total relativistic correction with respect to a clock on the geoid is thus:

$$\Delta t'_{delay} \;=\; -\frac{W_0\,\rho}{c^3} + \frac{2\,GM}{c^3} \ln\left(\frac{R+r+\rho}{R+r-\rho}\right) \tag{9-89}$$

The first term is the contribution of the geopotential due to the change of scale and the second term is the gravitational time delay. These terms tend to cancel in the vicinity of the Earth.

The predicted gravitational time delay was verified by Irwin Shapiro [Shapiro, 1980] in 1967 and 1971 using radar ranging to the planets Mercury and Venus. The round trip time delays at superior conjunction are approximately 240 μs and 180 μs, respectively. More precise ranging to the Viking lander on Mars at superior conjunction had a gravitational delay of approximately 250 μs.

For a GPS satellite with orbital radius 26 562 km and an elevation of 40°, the relativistic path delay is 48 ps with respect to a clock at infinity and −3 ps with respect to a clock on the geoid. For the LAGEOS satellite, with an orbital radius of 12 270 km, the maximum delay is 38 ps with respect to a clock at infinity and 14 ps with respect to a clock on the geoid. For a signal sent from the equator to a geostationary satellite at an orbital radius of 42 164 km, the correction is 56 ps with respect to a clock at infinity and − 27 ps with respect to a clock on the geoid.

9.4.2 Earth-Centered Earth-Fixed coordinate system

In the rotating ECEF coordinate system, the coordinate time of propagation of an electromagnetic signal is:

$$\Delta t \;=\; \frac{\rho'}{c} + \frac{1}{c} \int_{path} \frac{g_{0j}}{-g_{00}}\,\mathrm{d}x^i \tag{9-90}$$

where:

ρ': propagation path length in the ECEF frame.

If the receiver has a velocity $\mathbf{v}'_R$, then $\rho' = |\,\mathbf{R}(t_R) - \mathbf{r}_T(t_T)\,| \approx |\,\Delta\mathbf{r}\,| + \Delta\mathbf{r}\cdot\mathbf{v}'_R\,/\,c$ and there is a range rate correction $\Delta t_{v'} = \Delta\mathbf{r}\cdot\mathbf{v}'_R\,/\,c^2$, where $\Delta\mathbf{r} = \mathbf{R}(t_T) - \mathbf{r}_T(t_T)$.

The integral term in the equation for Δt is the Sagnac effect.

The metric components are:

$$-g_{00} \approx 1\,,\; g_{0j} = (\boldsymbol{\omega} \times \mathbf{r})_j / c\,,\text{ and } g_{ij} \approx \delta_{ij}$$

Therefore, the Sagnac effect is:

$$\Delta t_{Sagnac} \approx \frac{1}{c^2}\int_A^B (\boldsymbol{\omega}\times\mathbf{r})\cdot d\mathbf{r} = \frac{1}{c^2}\int_A^B \boldsymbol{\omega}\cdot(\mathbf{r}\times d\mathbf{r}) = \mathbf{2}\frac{1}{c^2}\int_A^B \boldsymbol{\omega}\cdot d\mathrm{A} = \frac{2\omega A}{c^2} \tag{9-91}$$

where:

- A: the perpendicular projection of the area formed by the center of rotation and the endpoints of the light path.

The path as seen from the rotating frame is approximately a straight line. For endpoints at (x_A , y_A) and (x_B , y_B), the Sagnac effect may be expressed:

$$\Delta t_{Sagnac} = \frac{2\,\omega\, A}{c^2} = \boldsymbol{\omega}\cdot(\mathbf{r}_A \times \mathbf{r}_B) = \frac{\omega}{c^2}\left(x_A\, y_B - y_A\, x_B\right) \tag{9-92}$$

In the case of a receiver at rest on the Earth, an observer in the ECEF frame regards the receiver as stationary and applies a Sagnac correction, but an observer in the ECI frame sees that the receiver has moved due to the Earth's rotation and instead applies a velocity correction. The total propagation time is:

$$\Delta t = |\,\Delta\mathbf{r}\,| / c + \Delta\mathbf{r}\cdot\mathbf{v'}_R / c^2 + 2\,\omega\, A / c^2 = |\,\mathbf{r}_R(t_R) - \mathbf{r}_T(t_T)\,| / c$$

NOTE 1 – The term "Sagnac effect" is part of the vocabulary of only the observer in the rotating reference frame. The corresponding correction applied by the inertial observer should be called a "velocity correction."

As specified in the GPS documentation [Navstar GPS, 2000], the total propagation time correction for a GPS signal is applied in the user receiver. The maximum Sagnac effect is 133 ns, which occurs when the receiver is on the equator and the satellite is on the horizon. From the point of view of an inertial observer, this correction is due to the motion of the receiver with a velocity of 465 m/s relative to the ECI frame of reference during the 86 ms signal propagation time. The self-consistency of this correction has been demonstrated by closure of simultaneous common view GPS measurements between pairs of timing centers distributed around the world [Allen *et al.*, 1985].

The Sagnac effect must also be considered for time transfer by means of an electromagnetic signal via a geostationary satellite. This property has been confirmed routinely by comparison with synchronization by clock transport [Saburi, 1976]. Assume that the Earth is a sphere of radius R and that the satellite orbit is exactly circular with radius r in the equatorial plane. The coordinates of an Earth station at latitude ϕ_E and east longitude λ_E are:

$$x_E = R\cos\phi_E\cos\lambda_E \text{ and } y_E = R\cos\phi_E\sin\lambda_E$$

where:

R = 6 371 km is the mean radius of the Earth.

The coordinates of the satellite are:

$$x_S = r\cos\lambda_S \text{ and } y_S = r\sin\lambda_S$$

where:

r = 42 164 km is the radius of the geostationary orbit.

Then for an uplink signal path in the eastward direction from Earth station A to the satellite:

$$\Delta t_1 = \frac{\omega}{c^2}\left(x_{EA}\, y_S - y_{EA}\, x_S\right) = \frac{\omega}{c^2} R\, r\cos\phi_{EA}\sin\left(\lambda_S - \lambda_{EA}\right) \tag{9-93}$$

Similarly, for a downlink signal path in the eastward direction from the satellite to Earth station *B*:

$$\Delta t_2 = \frac{\omega}{c^2}\left(x_S\, y_{EB} - y_S\, x_{EB}\right) = \frac{\omega}{c^2} R\, r \cos\phi_{EB} \sin\left(\lambda_{EB} - \lambda_S\right) \tag{9-94}$$

The total Sagnac correction is the sum of these two terms, $\Delta t = \Delta t_1 + \Delta t_2$. For a signal path in the westward direction, the correction has the same magnitude but opposite sign.

For example, consider a two-way satellite time transfer (TWSTT) measurement from the National Institute of Standards and Technology in Boulder, Colorado (latitude 40.0°, longitude 105.3° W) to the U. S. Naval Observatory in Washington, D.C (latitude 38.9°, longitude 77.1° W) via a geostationary satellite at 97.0°W. The Sagnac corrections are 24.1 ns for the uplink and 57.7 ns for the downlink and the total correction is 81.8 ns. For the signal path in the opposite direction the correction is − 81.8 ns.

However, in practice, the Earth is not a perfect sphere. In addition, the satellite orbit is perturbed, so that it is neither perfectly circular nor precisely in the equatorial plane. The error in the Sagnac correction is about 0.1 ns for a 300 m error in Earth station position, a 1° error in satellite longitude, or a 0.2° error in satellite latitude. For more precise calculations, one must evaluate the Earth station and satellite coordinates by taking into account the figure of the Earth and the satellite orbital elements.

9.4.3 Inter-satellite link

The analysis of electromagnetic signals used in cross-link ranging, time transfer among satellites and ground stations, and interoperability across satellite constellations involves three steps:

1. a relativistic transformation from the proper time reading of the clock at the transmitter to the coordinate time of transmission in the adopted coordinate system;
2. calculation of the coordinate time of signal propagation, including both relativistic and nonrelativistic effects;
3. a relativistic transformation from the coordinate time of reception in the adopted coordinate system to the proper time reading of the clock at the receiver.

In addition, all proper times must be corrected for "hardware" effects, such as processing noise and clock environment.

Consider the relativistic time transfer between atomic clocks *A* and *B* onboard two satellites by means of an inter-satellite link. Assume that the proper time τ of each clock has been adjusted by the prescription $\Delta\tau' = (1 + k)\,\Delta\tau$, so that the resulting proper time τ' is on average equal to the coordinate time t' as realized by atomic clocks on the geoid. If each clock has position $\mathbf{r}$ and velocity $\mathbf{v}$ in an ECI frame of reference, then $\Delta\tau' = \Delta t' + \Delta t_r$ where the relativistic correction is:

$$\Delta t_r = -2\,\frac{1}{c^2}\sqrt{GM\,a}\; e \sin E = -\frac{2\,\mathbf{r}\cdot\mathbf{v}}{c^2} \tag{9-95}$$

Thus the proper time of clock *A* at the coordinate time of transmission is:

$$\tau'_T = t'_T - 2\,\mathbf{r}_T \cdot \mathbf{v}_T / c^2$$

and the proper time of clock *B* at the coordinate time of reception is:

$$\tau'_R = t'_R - 2\,\mathbf{r}_R \cdot \mathbf{v}_R / c^2 + \Delta\tau_R$$

where:

$\Delta\tau_R$: the synchronization offset of clock *B* with respect to clock *A*.

The coordinate time of signal propagation as measured by a clock at infinity is:

$$t_R - t_T = \frac{\rho}{c} + \Delta t_{delay} \tag{9-96}$$

where:

ρ: the path distance from the first satellite at the time of transmission to the second satellite at the time of reception;

Δt_{delay}: the gravitational time delay.

The path distance is:

$$\rho = |\mathbf{r}_R(t_R) - \mathbf{r}_T(t_T)| = |\Delta\mathbf{r} + \mathbf{v}_R\ (t_R - t_T)| \approx |\Delta\mathbf{r}| + \frac{1}{c}\,\Delta\mathbf{r}\cdot\mathbf{v}_R \tag{9-97}$$

where:

$\Delta\mathbf{r} = \mathbf{r}_R - \mathbf{r}_T$: the separation of the two satellites at the coordinate time of transmission.

The gravitational time delay is:

$$\Delta t_{delay} = \frac{2\,GM}{c^3}\ln\left(\frac{r_T + r_R + \rho}{r_T + r_R - \rho}\right) \tag{9-98}$$

The coordinate time of signal propagation as measured by clocks on the geoid is:

$$t'_R - t'_T = (1 - W_0 / c^2)(t_R - t_T)$$

Therefore, the difference in the ideal proper times is:

$$\tau'_R - \tau'_T = \Delta\tau_R + \frac{|\Delta\mathbf{r}|}{c} + \frac{\Delta\mathbf{r}\cdot\mathbf{v}_R}{c^2} - \frac{2\,\mathbf{r}_R\cdot\mathbf{v}_R}{c^2} + \frac{2\,\mathbf{r}_T\cdot\mathbf{v}_T}{c^2} - \frac{W_0\,|\Delta\mathbf{r}|}{c^3} + \frac{2GM}{c^3}\ln\left(\frac{r_T + r_R + \rho}{r_T + r_R - \rho}\right) \tag{9-99}$$

The actual clock readings are "hardware" proper times affected by noise and environmental biases. There may also be a nonrelativistic path delay due to the residual atmosphere.

9.4.4 Relativistic Doppler effect

Consider a transmitter with position $\mathbf{r}_T$ and velocity $\mathbf{v}_T$ that transmits an electromagnetic signal at coordinate time t_T and an Earth station with position $\mathbf{r}_R$ and velocity $\mathbf{v}_R$ that receives the signal at coordinate time t_R with respect to an ECI frame of reference. The ratio of the proper frequency f_T of the transmitted signal to the proper frequency f_R of the received signal is inversely proportional to the ratio of the proper periods.

Therefore:

$$\frac{f_R}{f_T} = \frac{\mathrm{d}\tau_T}{\mathrm{d}\tau_R} \tag{9-100}$$

This expression can be written in terms of the increments of coordinate time as:

$$\frac{f_R}{f_T} = \frac{(\mathrm{d}t_R / \mathrm{d}\tau_R)}{(\mathrm{d}t_T / \mathrm{d}\tau_T)}\frac{\mathrm{d}t_T}{\mathrm{d}t_R} \tag{9-101}$$

The range from transmitter to receiver is:

$$\boldsymbol{\rho} \equiv \mathbf{r}_R(t_R) - \mathbf{r}_T(t_T)$$

The difference in coordinate times between reception and transmission is:

$$t_R - t_T = \rho / c = |\mathbf{r}_R(t_R) - \mathbf{r}_T(t_T)| / c$$

Differentiating both sides with respect to t_R, one obtains:

$$1-\frac{dt_T}{dt_R}=\frac{1}{c}\left(\frac{\partial\rho}{\partial t_R}+\frac{\partial\rho}{\partial t_T}\frac{dt_T}{dt_R}\right)=\frac{1}{c}\left(\mathbf{n}\cdot\mathbf{v}_R-\mathbf{n}\cdot\mathbf{v}_T\frac{dt_T}{dt_R}\right) \tag{9-102}$$

where the unit normal in the direction of propagation from transmitter to receiver is:

$$\mathbf{n}\equiv\frac{1}{\rho}\boldsymbol{\rho}=\frac{\mathbf{r}_R-\mathbf{r}_T}{|\mathbf{r}_R-\mathbf{r}_T|} \tag{9-103}$$

Therefore:

$$\frac{dt_T}{dt_R}=\frac{1-\mathbf{n}\cdot\mathbf{v}_R/c}{1-\mathbf{n}\cdot\mathbf{v}_T/c} \tag{9-104}$$

For measurements analyzed in an ECI frame of reference with a gravitational potential U, the metric tensor components are:

$-g_{00}=1-2U/c^2$, $g_{0j}=0$, and $g_{ij}=\delta_{ij}$ and the space-time interval is:

$$ds^2=-c^2(1-2U/c^2-v^2/c^2)\,dt^2=-c^2\,d\tau^2.$$

Therefore:

$$\frac{dt_R}{d\tau_R}=\frac{1}{\sqrt{1-2U_R/c^2-v_R{}^2/c^2}} \tag{9-105}$$

and

$$\frac{dt_T}{d\tau_T}=\frac{1}{\sqrt{1-2U_T/c^2-v_T{}^2/c^2}} \tag{9-106}$$

Thus

$$\frac{f_R}{f_T}=\frac{\sqrt{1-2U_T/c^2-v_T{}^2/c^2}}{\sqrt{1-2U_R/c^2-v_R{}^2/c^2}}\;\frac{(1-\mathbf{n}\cdot\mathbf{v}_R/c)}{(1-\mathbf{n}\cdot\mathbf{v}_T/c)} \tag{9-107}$$

This is the relativistic Doppler effect equation. The first factor is the relativistic correction and the second factor is the classical Doppler effect. Expanding terms through order v^2/c^2, one obtains:

$$\frac{\Delta f}{f_T}=\frac{1}{c}\left(1+\frac{1}{c}\mathbf{n}\cdot\mathbf{v}_T\right)\left[\mathbf{n}\cdot(\mathbf{v}_T-\mathbf{v}_R)\right]+\frac{1}{c^2}(U_R-U_T)+\frac{1}{2}\frac{1}{c^2}\left(v_R^2-v_T^2\right) \tag{9-108}$$

where:

$$\Delta f\equiv f_R-f_T$$

Two properties of this equation should be noted. First, there is a term of order v^2/c^2 that is nonrelativistic in origin. Second, there are no mixed terms of the type $\mathbf{v}_T\cdot\mathbf{v}_R/c^2$.

A case of special interest is when the transmitter is on a satellite and the receiver is on the rotating Earth. The velocity of the satellite with respect to the ECI frame is given by the vis viva equation and the radial coordinate is:

$$r=a\,(1-e^2)/(1+e\cos\nu)$$

where:

a and e are the orbital semimajor axis and eccentricity, and

ν is the true anomaly.

Also, the velocity of the receiver at latitude ϕ_R is:

$$v_R = \omega R \cos \phi_R .$$

The gravitational potential at the satellite transmitter is: $U_T = GM / r$ and the gravitational potential at the Earth station receiver is: $U_R = GM / R$.

Therefore, neglecting terms of order e^2:

$$\frac{\Delta f}{f_T} = \frac{1}{c}\left(1 + \frac{1}{c}\,\mathbf{n}\cdot\mathbf{v}_T\right)\left[\mathbf{n}\cdot(\mathbf{v}_T - \mathbf{v}_R)\right] + \frac{GM}{c^2}\left(\frac{1}{R} - \frac{3}{2a}\right) - \frac{2GM}{c^2 a}e\cos\nu + \frac{1}{2}\frac{1}{c^2}\omega^2 R^2 \cos^2\phi_R \qquad (9\text{-}109)$$

The first term is the classical Doppler shift. The second term is the secular part of the combined time dilation and gravitational redshift effects. The third term is a residual relativistic periodic effect. The first evidence of this effect was reported by R. E. Jenkins [Jenkins, 1969] in 1969. The fourth term is due to the velocity of the Earth station. For a GPS satellite with an orbital eccentricity of 0.02, the amplitude of the periodic effect is 6.7×10^{-12}. This implies that the GPS L1 carrier frequency of 1.57542 GHz would undergo a modulation due to relativity of amplitude 0.011 Hz and period equal to the satellite orbital period of 11.967 h.

9.5 Conclusion

The general theory of relativity provides the foundation for modern concepts of space, time, and gravitation. Over the past four decades, a wide range of precision experiments have confirmed a rich variety of its predictions. Thus relativity has become an important practical consideration for precise timekeeping systems in engineering, physics, and astronomy.

The three principal effects are time dilation, the gravitational redshift, and the Sagnac effect. The Global Positioning System is an example of an engineering system in which these effects are important. The combined effect of time dilation and redshift produces a secular rate offset of 38 μs per day and a residual periodic variation with an amplitude of up to 46 ns, while the Sagnac effect is typically on the order of 100 ns. The GPS has served as a laboratory for relativistic time measurement at the one-to-ten nanosecond level. The successful application of relativity to GPS time and position measurements has been demonstrated by the operational precision of the system and by numerous experiments designed to test these individual effects over a wide range of conditions. For time measurement by clocks in space at the picosecond level of precision, additional effects will need to be considered, including the redshift contribution due to Earth oblateness, the tidal potentials of the Sun and Moon, and the effect of gravitation on the speed of propagation of light itself.

Far from being merely of theoretical scientific interest, the corrections imposed by the general theory of relativity are required for the consistent measurement and dissemination of precise time by terrestrial and space-borne atomic clocks.

References

ALLEY, C.O. [1983] Proper Time Experiments in Gravitational Fields With Atomic Clocks, Aircraft, and Laser Light Pulses. Quantum Optics, Experimental Gravitation, and Measurement Theory, edited by P. Meystre and M. O. Sculley, Plenum, New York, p. 363-427.

ALLEN, D. W., WEISS, M. A. and ASHBY, N. [1985] Around-the-World Relativistic Sagnac Experiment. Science **228**, p. 69-70.

ASHBY, N. [2001] Relativistic Effects on SV Clocks Due to Orbit Changes, and Due to Earth's Oblateness. Proc. 33rd Annual Precise Time and Time Interval (PTTI) Meeting, U. S. Naval Observatory, Washington, D.C, p. 509-524.

BUISSON, J. A., EASTON, R. L. and MCCASKILL, T. B. [1977] Initial Results of the Navstar GPS NTS-2 Satellite. Proc. 9th Annual Precise Time and Time Interval (PTTI) Applications and Planning Meeting, U. S. Naval Observatory, Washington, D.C, p. 177-200.

DEPARTMENT of DEFENSE WGS 84 [1997] NIMA Tech. Rep.TR8350.2, 3rd edition. National Imagery and Mapping Agency, Bethesda, MD.

EPSTEIN, M., STOLL, E. and FINE, J. [2001] Observable Relativistic Frequency Steps Induced by GPS Orbit Changes. Proc. 33rd Annual Precise Time and Time Interval (PTTI) Meeting, U. S. Naval Observatory, Washington, D.C, p. 493-508.

FRISCH, D. H. and SMITH, J. H. [1963] Measurement of the Relativistic Time Dilation Using μ-Mesons. *Am. J. Phys.* **31**, p. 342-355.

HAFELE, J. C. and KEATING, R. E. [1972] Around-the-World Atomic Clocks: Predicted Relativistic Time Gains; Observed Relativistic Time Gains. *Science* **177**, p. 166-170.

HEISKANEN, W. A. and MORITZ, H. [1967] Physical Geodesy. Freeman, San Francisco, p. 70.

JENKINS, R. E. [1969] A Satellite Observation of the Relativistic Doppler Shift. *Astron. J.* **74**, p. 960-963.

KOZAI, Y. [1959] The Motion of a Close Earth Satellite. *Astron. J.* **64**, p. 367-377.

NAVSTAR GPS Space Segment/Navigation User Interfaces, ICD-GPS-200C-004 [2000] Arinc Research Corporation, El Segundo, CA.

POUND, R. V. and REBKA, Jr .G. A. [1960] Apparent Weight of Photons. Phys. Rev. Lett. **4**, 337-341.

SABURI, Y. [1976] Observed Time Discontinuity of Clock Synchronization in Rotating Frame of the Earth. J. Radio Research Laboratories **23**, p. 255-265.

SHAPIRO, I. I. [1980] Experimental Tests of General Relativity, in General Relativity and Gravitation, edited by A. Held, Plenum, New York, , Vol. II, p. 469-489.

VESSOT, R. F. C. and LEVINE, M. W. *et al.* [1980] Tests of Relativistic Gravitation With a Space-Borne Hydrogen Maser. Phys. Rev. Lett. **45**, p. 2081-2084.

CHAPTER 10

EARTH ORIENTATION AND GEODETIC SYSTEM

Page

10.1 Introduction

Reference systems are composed of:

1. a specified origin;
2. the directions of fundamental axes;
3. a set of conventional models and procedures that are used to realize the system.

A reference frame, then, is the realization of that system through a list of coordinates to be given to the defining elements. Earth orientation refers to the procedure and models used to relate a terrestrial geodetic reference system to a celestial system.

The rigorous details are outlined in the International Earth Rotation and Reference System Service (IERS) Conventions available electronically at: http://www.iers.org/iers/products/conv/.

Celestial reference systems are specified by astronomers, and most modern systems are usually considered to have their origins at the barycentre of the solar system, and their polar axes related in some way to the axis of the Earth. The third axis then lies in the equatorial plane perpendicular to the polar axis and is directed toward a fiducial point in that plane. A list of the positions and possible motions of astronomical objects then comprises the related celestial reference frames. The International Astronomical Union has designated a standard celestial reference system and frame called the International Celestial Reference System (ICRS) and the International Celestial Reference Frame (ICRF) respectively. The ICRF is made up of the designated positions of distant radio sources.

Analogously, terrestrial reference systems generally have their origins at the centre of mass of the Earth with their polar axes related to the direction of an axis fixed with respect to the Earth's crust. The origin of longitudes in the equatorial plane provides the third direction. As was the case with the celestial frames, the terrestrial frames are comprised of a list of site coordinates and possible motions. The International Terrestrial Reference System (ITRS) and the International Terrestrial Reference Frame (ITRF) maintained by the IERS are accepted as the international standards.

10.2 Earth orientation

Earth orientation is specified by five angles. Three would ordinarily be sufficient, but five angles are used in order to describe the physical processes involved and to make the transformations easier to apply.

Two angles are used to model the changing direction of the Earth's axis in a conventional celestial system. This axis is called the Celestial Intermediate Pole (CIP) and its motion is due to the precession and nutation of the Earth. These phenomena are driven by the gravitational attraction of the solar system bodies, principally the Sun and the Moon, on the non-spherical Earth. Precession refers to the aperiodic portion of the motion and nutation refers to the periodic portion. Both motions depend on the positions of the solar system bodies and the internal structure of the Earth, but they can be modelled mathematically with reasonable accuracy.

Two more angles are used to describe the motion of the CIP over the Earth's crust. This phenomenon is called "polar motion" and is driven by geophysical and meteorological variations within the Earth and its atmosphere. The principal components are a linear drift and two periodic motions with periods of 365 and 435 days. Polar motion is difficult to model because the forces driving the motion are difficult to predict. As a result these angles must be observed astronomically and reported to users routinely.

The CIP is a conventionally defined pole separating the motion of the pole of the terrestrial reference system (TRS) in the celestial reference system (CRS) into the celestial motion of the CIP (precession/nutation), including all the terms with periods greater than 2 days in the CRS (frequencies between -0.5 cycles per sidereal day (cpsd) ((in the T+F community – and the ITU the use of negative frequency values is unusual and should be explained)) and +0.5 cpsd), and the terrestrial motion of the CIP (polar motion), including all the terms outside the retrograde diurnal band in the TRS (frequencies lower than -1.5 cpsd or greater than -0.5 cpsd).

The last of the five angles characterizes the rotation angle of the Earth and is expressed as the time difference [UT1 - UTC], where UT1 is an astronomical time determined by observations of distant radio sources and

UTC is the uniform time scale, Coordinated Universal Time. Principal variations in the rotation speed of the Earth include a constant deceleration due to tidal deceleration and deglaciation, decadal variations due to changes in the internal distribution of the Earth's mass, largely seasonal meteorologically driven variations and tidally driven periodic variations. As with polar motion, UT1 - UTC is difficult to model and predict, and must be observed astronomically and reported to users routinely.

Resolution B1.8, adopted by the XXIVth General Assembly of the International Astronomical Union in August 2000, recommends using the "non-rotating origin" [Guinot, 1979] both in the geocentric celestial reference system (GCRS) and the ITRS and that these origins be designated as the celestial ephemeris origin (CEO) and the terrestrial ephemeris origin (TEO). The *earth rotation angle* is defined as the angle measured along the equator of the CIP between the CEO and the TEO. This resolution further recommends that UT1 be linearly proportional to the earth rotation angle and that the transformation between the ITRS and GCRS be specified by the position of the CIP in the GCRS, the position of the CIP in the ITRS, and the earth rotation angle.

Mathematically, the procedure to transform from TRS to CRS at the epoch t is written:

$$\left[CRS(t)\right] = Q(t)\,R(t)\,W(t)\left[TRS(t)\right] \tag{10-1}$$

where *Q(t), R(t) and W(t)* are the transformation matrices describing the motion of the celestial pole in the celestial system (precession/nutation), the rotation of the Earth around the axis of the pole, and polar motion respectively. The parameter t, used in this and all of the following expressions, is defined by:

$$t = \left[\mathrm{TT} - 2000 \text{ January } 1, 12\mathrm{h}\ \mathrm{TT} - \text{in days}\right]/36525 \tag{10-2}$$

Note that 2000 January 1.5 TT = Julian Date 2451545.0 TT.

In the following discussion of the rotation matrices to be used in the transformations, we use the notation R_1, R_2, and R_3 to indicate rotations about the x, y, and z axes of the reference system respectively. That is:

$$\mathrm{R}_1(\theta) = \begin{bmatrix} 1 & 0 & 0 \\ 0 & \cos\theta & \sin\theta \\ 0 & -\sin\theta & \cos\theta \end{bmatrix} \tag{10-3}$$

$$\mathrm{R}_2(\theta) = \begin{bmatrix} \cos\theta & 0 & -\sin\theta \\ 0 & 1 & 0 \\ \sin\theta & 0 & \cos\theta \end{bmatrix} \tag{10-4}$$

$$\mathrm{R}_3(\theta) = \begin{bmatrix} \cos\theta & \sin\theta & 0 \\ -\sin\theta & \cos\theta & 0 \\ 0 & 0 & 1 \end{bmatrix} \tag{10-5}$$

10.2.1 Precession/nutation

Gravitational forces exerted by solar system bodies act on the non spherical Earth to cause its direction in the celestial reference system to move. In 26,000 years the axis moves to describe a cone in space. This motion is called precession. Nutation causes a much smaller periodic nodding of the axis in addition to the precessional motion. The principal period of the nutational motion is 18.6 years. The IAU has recommended that beginning on 1 January 2003, the precession-nutation model IAU 2000A, or the shorter version IAU 2000B for those who need a model accurate to the level of 1 milliarcsecond (mas), be used to describe this motion.

Referring to equation (10-1) the precession/nutation matrix *Q(t)* can be written as:

$$Q(t) = \begin{bmatrix} 1-aX^2 & -aXY & X \\ -aXY & 1-aY^2 & Y \\ -X & -Y & 1-a\left(X^2+Y^2\right) \end{bmatrix} \bullet \mathrm{R}_3(s) \tag{10-6}$$

with

$$a = \tfrac{1}{2} + \tfrac{1}{8}\left(X^2+Y^2\right)$$

where:

X and *Y*: the "coordinates" of the CIP in the CRS, and are provided by the conventional IAU 2000A or IAU 2000B models, which are based on geophysical and astronomical theory.

This formulation models the motion of the pole due to luni-solar and planetary motions. It does not include what has been called "planetary precession" in the literature, which is the motion of the ecliptic (the path of the Earth's orbital motion) caused by planetary gravitation. Before the IAU adopted this procedure in 2000 to describe the Earth's precession and nutation, the ecliptic was used as a fundamental reference plane and its motion was described by a conventional expression based on astronomical theory. The combined precession/nutation of the Earth's pole and the ecliptic was called general precession.

The quantity s specifies the position of the celestial ephemeris origin on the equator of the celestial intermediate pole. It is given by:

$$\begin{aligned} s = -XY/2 + \sum_{i=0}^{i=3} \mathrm{c}_i t^i + \sum_k \mathrm{C}_k \ \sin \alpha_k + 1.71t \sin \Omega + 3.57t \cos 2\Omega \\ +743.53t^2 \ \sin \Omega + 56.91t^2 \ \sin\left(2\mathrm{F}-2\mathrm{D}+2\Omega\right) + 9.84t^2 \ \sin\left(2\mathrm{F}+2\Omega\right) - 8.85t^2 \ \sin 2\Omega \end{aligned} \tag{10-7}$$

The tables and software to implement the algorithm described above can be found in the IERS Conventions [McCarthy and Petit, 2003].

10.2.2 Polar motion

The CIP also moves within the TRF, but this motion is not able to be modelled. Instead this motion must be observed and accounted for appropriately in the transformation between coordinate systems. The motion is represented as polar coordinates x and y expressed in angular units. x is directed along 0º longitude, and y and is directed along 90º west longitude. The longitude system is defined implicitly by the adopted positions of the sites in the TRF.

Polar motion is made up principally of an approximately linear drift plus two periodic terms. The first is a free motion of the pole called the Chandler wobble after its discoverer, Seth C. Chandler. Its period is 435 days and corresponds to the free motion of a non-rigid Earth that was originally predicted by L. Euler for a rigid Earth in 1758. The second principal component of the polar motion is an annual motion driven by the seasonal redistribution of the Earth's atmospheric mass.

The size of these motions is small but very significant for precise transformation between reference frames. The linear drift is a few centimeters per year in the direction of 75º W longitude. The periodic motions move the CIP with amplitudes of a few tens of meters.

Mathematically, referring again to equation (10-1) this rotation is given by:

$$W(t) = \mathrm{R}_3(-s')\mathrm{R}_1(y)\mathrm{R}_2(x) \tag{10-8}$$

The polar coordinate information must be observed and reported. The data are available from the International Earth rotation and Reference system Service (IERS). They provide a series of files containing the latest data and predictions for the future. See http://www.iers.org/iers/products.

s' can be approximated for the 21st Century as a function of the time by:

$$s' = -47\ \mu\text{as}\ t \qquad (10\text{-}9)$$

10.3 Universal Time (UT)

Solar time is based on the rotation of the Earth with respect to the Sun. Mean solar time was designed to eliminate the irregularities in solar time caused by the obliquity of the ecliptic and the varying speed of the Earth in its orbit around the Sun. It is the hour angle of a fictitious point moving uniformly along the celestial equator at the same rate as the average rate of the Sun along the ecliptic. In practice, it is intervals of sidereal time that are directly observed astronomically and afterward converted into intervals of mean solar time by division by 1.00273790935.

The mean solar time determined for the meridian of 0° longitude is called UT1. Astronomical observations are made to determine the difference between this time and Coordinated Universal Time (UTC). The raw observations of time are referred to as UT0 and must be corrected for the polar motion of the Earth in order to obtain UT1. The effect of polar motion may amount to several hundredths of a second. The IERS receives these data and maintains a UT1 time scale.

These observations show the Earth to have variations in rotational speed that may be classified into three types: secular, irregular, and periodic. The secular variation of the rotational speed refers to the apparently linear increase in the length of the day due chiefly to tidal friction. This effect causes a slowing of the Earth's rotational speed resulting in a lengthening of the day by about 0.0005 to 0.0035 s/century. The irregular changes in speed appear to be the result of random accelerations, but may be correlated with physical processes occurring on or within the Earth. They include decade fluctuations with characteristic periods of 5 – 10 years as well as variations, which occur at shorter time scales.

Periodic variations are associated with periodically repeatable physical processes affecting the Earth. Tides raised in the solid Earth by the Moon and the Sun produce periodic variations in the length of the day of the order of 0.0005 s with periods of 1 year, 1/2 year, 27.55 days and 13.66 days.

Referring again to equation (10-1) this rotation is given by:

$$R(t) = \mathrm{R}_3(-\theta) \qquad (10\text{-}10)$$

θ being the Earth Rotation Angle between the CEO and the TEO at date t on the equator of the CIP. It is obtained from the conventional relationship to UT1 [Capitaine *et al.*, 2000]:

$$\theta(T_u) = 2\pi(0.7790572732640 + 1.00273781191135448\,T_u) \qquad (10\text{-}11)$$

where:

T_u = (Julian UT1 date - 2451545.0), and UT1 = UTC + (UT1 - UTC), or equivalently

$$\theta(T_u) = 2\pi(\text{UT1 Julian Days elapsed since 2451545.0 } + 0.7790572732640 + 1.00273781191135448\,T_u)$$

NOTE 1 – See further details in Chapter 7 – Time scales.

10.4 Geodetic systems

As explained above, terrestrial reference systems have their origins at the center of mass of the Earth with their polar axes related to the direction of an axis fixed with respect to the Earth's crust. The origin of longitudes in the equatorial plane provides the third direction. Terrestrial reference frames are comprised of a list of site coordinates and possible motions. These coordinates can be expressed as a set of Cartesian (x, y, z) coordinates of a site. Often they are described by the latitude, longitude and height of the location above some reference surface. This surface can be a reference ellipsoid or a geopotential surface.

10.5 Reference surfaces

10.5.1 Geoid

The Earth can be considered as being made up of a series of surfaces each having the same gravity potential. This potential includes not only the gravitational potential but also the potential due to the centrifugal force. These surfaces are called geops, and the one that approximates the mean sea surface is called the geoid. It is a natural reference surface because a plumb line is perpendicular to this surface, and it is easy to measure heights along a plumb line. The geoid is the surface usually referred to as mean sea level. It is defined by describing its height above a reference ellipsoid, called geoid undulation, along the line perpendicular to the ellipsoid.

The height of the surface topography above the geoid measured along the plumb line is called the mean sea level height or the orthometric height.

10.5.2 Ellipsoid

A reference ellipsoid is used to describe an approximate shape of the Earth for reference purposes. It is specified by a semi-major (equatorial radius) and flattening (the relationship between equatorial and polar radii). Flattening is defined by:

$$f = \frac{a-b}{a} \tag{10-12}$$

where:

a and b: equatorial and polar radii, respectively.

The height of the surface topography above the ellipsoid along the line perpendicular to the ellipsoid is called the ellipsoidal height. For example, for the WGS 84 ellipsoid a = 6378137.0 m and f = 1.0/ 298.2572235630.

10.5.3 Types of coordinates

10.5.3.1 Geocentric coordinates

Geocentric coordinates are referred to the center of the Earth. These can be given in a vector format, *i.e.* (x, y, z) Cartesian coordinates of a site or as geocentric latitude ϕ' and longitude λ. The relationship between the two is given by:

$$\begin{bmatrix} x \\ y \\ z \end{bmatrix} = r \begin{bmatrix} \cos\phi' \cos\lambda \\ \cos\phi' \sin\lambda \\ \sin\phi' \end{bmatrix} \tag{10-13}$$

The geocentric latitude of a location refers to the angle between the equator of a reference ellipsoid and a line from the center of the ellipsoid to the location. The geocentric longitude is the angle between the reference meridian of the ellipsoid and the meridian of the location.

10.5.3.2 Geodetic coordinates

Geodetic coordinates are determined with reference to a reference ellipsoid. These are usually given in terms of the geodetic latitude ϕ and the geodetic longitude λ. The geodetic latitude is the angle between the ellipsoidal equator and the normal to the ellipsoid that passes through the site. The difference between geocentric and geodetic latitude is shown in Fig. 10-1. The geodetic longitude is the angle between the reference meridian of the ellipsoid and the meridian of the site. It is the same as the geocentric longitude if the reference ellipsoid in each case has the same axes and reference meridian. The geocentric Cartesian coordinates can be related to the geodetic coordinates by:

$$\begin{bmatrix} x \\ y \\ z \end{bmatrix} = r \begin{bmatrix} \left(N_\phi + h\right)\cos\phi\cos\lambda \\ \left(N_\phi + h\right)\cos\phi\sin\lambda \\ \left[\left(1-e^2\right)N_\phi + h\right]\sin\phi' \end{bmatrix} \tag{10-14}$$

where:

h: ellipsoidal height

e: eccentricity of the ellipsoid given by:

$$e = \frac{\sqrt{a^2 - b^2}}{a} = \sqrt{2f - f^2}$$

N_ϕ: ellipsoidal radius of curvature in the meridian given by:

$$N_\phi = \frac{a}{\sqrt{1 - e^2 \sin^2 \phi}} \tag{10-15}$$

Height is specified by the ellipsoidal height, h, which is the distance of the site above the reference ellipsoid measured along the line passing through the site perpendicular to the ellipsoid.

FIGURE 10-1

The difference between geocentric latitude ϕ' and geodetic latitude ϕ

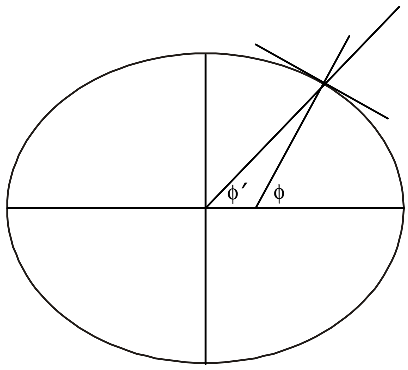

Sat_time_freq-10-01

10.5.3.3 Astronomical coordinates

Astronomical coordinates are measured by referring to the direction of the local vertical or plumb line. The local vertical is perpendicular to the gravitational equipotential surface at the site. These surfaces are called geops, and the geop having the potential of the Earth at sea level is called the geoid. The astronomical latitude, then, is the angle between the direction of the vertical and the plane of the Earth’s equator. The astronomical longitude is the angle between the plane containing the vertical and the plane of the reference meridian. The deflection of the vertical is the angle between the ellipsoidal normal and the vertical, and is described by specifying the angle components in the north-south direction and in the east-west directions. The height of the site above the geoid is called the mean sea level height or orthometric height, H. It is measured along the direction of the vertical. The height of the geoid above a reference ellipsoid is called the geoid undulation, N, and is measured along the normal to the ellipsoid.

FIGURE 10-2

Geodetic reference surfaces

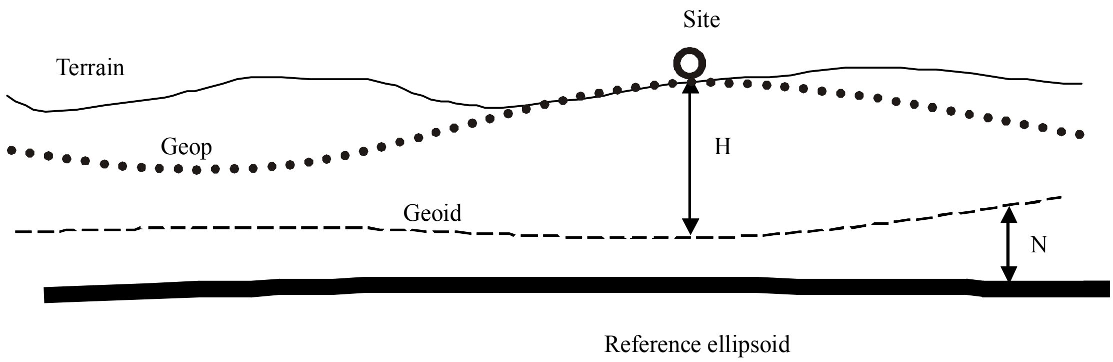

Sat_time_freq-10-02

10.5.3.4 Geodetic datums

A geodetic datum is used to provide an overall geodetic model of the Earth and is defined classically by a reference ellipsoid and the specification of an initial point. Modern space geodesy has now made it possible to provide a reference system directly related to the center of the Earth without using a reference ellipsoid. These observations are often used to provide a datum consisting of a set of parameters and defining site coordinates that can be used to extend the system through differential measurements with respect to the defining sites. Transformations between datums can be expressed by the expression:

$$\begin{bmatrix} x \\ y \\ z \end{bmatrix}_2 = \begin{bmatrix} x \\ y \\ z \end{bmatrix}_1 - \begin{bmatrix} T_1 \\ T_2 \\ T_3 \end{bmatrix} - \begin{bmatrix} D & -R_3 & R_2 \\ R_3 & D & -R_1 \\ -R_2 & R_1 & D \end{bmatrix} \begin{bmatrix} x \\ y \\ z \end{bmatrix}_1 \tag{10-16}$$

where:

the translation parameters (T_1, T_2, T_3) , the rotation parameters (R_1, R_2, R_3) and the scale parameter are determined empirically by comparing the coordinates of sites in two different datums.

10.5.3.5 International terrestrial reference frame

The International Earth rotation and reference (IERS) provides the International terrestrial reference system (ITRS) as the international standard. The origin of the system is the geocenter of the Earth's mass including oceans and atmosphere and it is defined to have no global residual rotation with respect to horizontal motions on the Earth's surface. The unit of length is the meter (SI) providing a scale consistent with the TCG time coordinate for a geocentric local frame, in agreement with international recommendations.

The realization of the ITRS produced by the IERS ITRS Product Center is called the International terrestrial reference frame (ITRF). It is derived from space geodetic observations. Currently, ITRF solutions are published nearly annually by the ITRS-PC in the IERS Technical Notes. The numbers (yy) following the designation "ITRF" specify the last year whose data were used in the formation of the frame. Hence ITRF97 designates the frame of station positions and velocities constructed in 1999 using all of the IERS data available until 1998.

The Report of the ITRF Working Group on the ITRF Datum [Ray *et al.*, 1999], contains useful information related to the history of the ITRF datum definition. It also details technique-specific effects on some parameters of the datum definition, in particular the origin and the scale.

References

CAPITAINE, N., GUINOT, B. and MCCARTHY, D. D. [2000] Astronomy & Astrophysics. p. 355-398.

GUINOT, B. [1979] Time and the Earths Rotation, IAU Symp. 82, ed. D. D. McCarthy & J. D. H. Pilkington, D. Reidel Publ. Co., Dordrecht, 7.

MCCARTHY, D. D. and PETIT, G. (editors) [2003] *IERS Conventions (2003)*, *IERS Technical Note* 32, International Earth Rotation Service.

RAY, J. , BLEWITT, G., BOUCHER, C., EANES, R., FEISSEL, M., HEFLIN, M., HERRING, T., KOUBA, J., MA, C., MONTAG, H., WILLIS, P., ALTAMIMI, Z., EUBANKS, T. M., D. GAMBIS, PETIT,G. , RIES, J., SCHERNECK, H. G., SILLARD, P. and P. [1999] Report of the Working Group on ITRF Datum.

CHAPTER 11

PROPAGATION AND ENVIRONMENTAL FACTORS

Page

11.1 Introduction

The transfer of precise time via satellite has as its largest potential error source the propagation delays of the Earth's neutral atmosphere and the ionosphere. In this section these range delays will be outlined and various techniques for compensating for them will be presented and discussed. The range delays of the troposphere and of the ionosphere differ in several important aspects. The range delay of the earth's troposphere is not dispersive; that is, it is not a function of frequency, at least not over the normal radio frequency range used for ranging to artificial Earth satellites. The range delay of the ionosphere, on the other hand, is dispersive; it varies inversely with frequency. Thus, by measuring the relative range delay at two, suitably spaced, frequencies the absolute range delay can be computed directly along the satellite to user path. The range delay of the Earth's troposphere cannot be measured directly, but several models, or indirect measurement techniques can be used to infer the tropospheric time delay contribution for time transfer via satellite to high accuracy.

11.2 Comparative range delay of the Earth's troposphere and the ionosphere

Figure 11-1 illustrates typical range delay values versus elevation angle for the Earth's troposphere and for the mid-latitude ionosphere at the GPS L1 frequency, under different conditions of solar activity. There are several important things to note in Fig. 11-1. First, the tropospheric range delay at high elevation angles is similar to that of the mid-latitude ionosphere during solar minimum conditions. Second, the variation of range delay with elevation angle, from the zenith to 5° elevation, varies by an approximate factor of 3 for the ionosphere, but by a factor greater than 10 for the troposphere. This is, of course, due to the fact that the troposphere is much nearer to the Earth's surface than the ionosphere, and, at low elevation angles it is viewed more obliquely than viewing through the ionosphere, which is at a greater height.

FIGURE 11-1

Comparative range delay of the troposphere and the mid-latitude ionosphere versus elevation angle

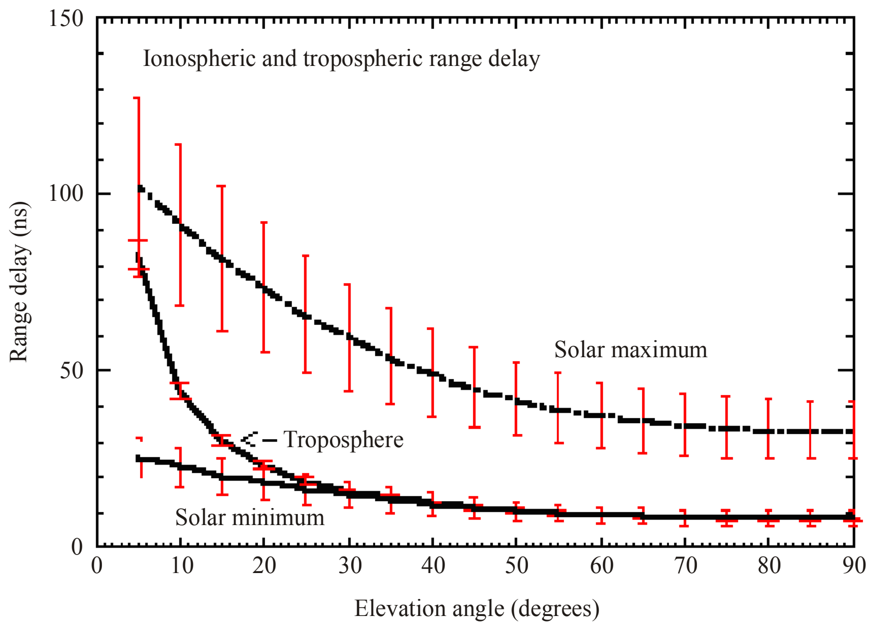

Sat_time_freq-11-01

Finally, note the approximate 1σ error bars in Fig. 11-1. The errors for average ionospheric range delay are approximately ±25% during all conditions of solar activity, while the 1σ error bars of the troposphere are less than approximately ±5%. Also, the range delay due to the Earth's troposphere is much more constant, varying by less than 20% over the entire Earth. This is due to the fact that approximately 90% of the tropospheric range delay is due to the so-called "dry component" of the Earth's troposphere, proportional to absolute pressure and absolute temperature, which, fortunately for us who live on the Earth, typically does not vary more than a few percent from nominal values. Since most of the troposphere is due to the "dry component" its range delay is easier to model than that of the Earth's ionosphere.

11.3 Modeling the range delay of the Earth's troposphere

There are many models of the Earth's troposphere, some of which have been reviewed by Spilker [1996]. The basis for most tropospheric models is simply an elevation angle function that relates the zenith range delay to the delay at lower elevation angles. While each elevation angle function is somewhat different, most of them simply require that the zenith range delay be specified, and then be multiplied by a number that is a function of elevation angle to obtain the equivalent required delay at the elevation angle of the satellite being observed. There are climatological methods of specifying the vertical range delay, and methods of determining the actual vertical delay by near-real-time measurements using precise dual frequency data from a number of GPS satellites at different elevation angles and fitting the range delay to the best fit elevation angle function at the time. Accuracies of approximately 1-2 cm of range delay correction are claimed by using this curve fitting technique.

The vertical range delay due to the troposphere is given approximately by:

$$\Delta r = 10^{-6} c \int N(h)\mathrm{d}l \tag{11-1}$$

where:

c: the velocity of light in m/s:

$N(h)\mathrm{d}l$: the total refractivity of the troposphere, given in refractivity units.

One of the many forms of zenith range delay, in which the dry, or hydrostatic, term, and the so-called "wet" term are separated, and, in which the local temperature, pressure and water vapor can be taken into account, is:

$$\Delta r_{Vtotal} = \Delta r_{Dry} + \Delta r_{Wet} \tag{11-2}$$

$$\Delta r_{dry} = \frac{0.62 \times P_{millibars}}{T_{Kelvin}} \qquad \text{(m)} \tag{11-3}$$

where:

P: total pressure, in millibars.

$$\Delta r_{wet} = \frac{8.3 \times 10^2 \times P_{WV}}{T^2} \qquad \text{(m)} \tag{11-4}$$

where:

P_{WV}: partial pressure of the water vapor.

Using typical numbers for pressure, 1 013 millibars, and temperature , 15° Centigrade, or 288° K, and a partial water pressure equivalent to 8.5 millibars, corresponding to 50% relative humidity, the total vertical tropospheric range delay is then:

$$\Delta r_{\mathrm{V}total} = 2.18 + 0.08 = 2.26 \qquad \text{(m)} \tag{11-5}$$

For this typical case the "wet" component due to the water vapor in the atmosphere is only 0.08/2.26 = 3.5 % of the total vertical tropospheric range delay.

Users requiring only an average tropospheric range delay for various latitudes can use a single worldwide constant value, given approximately by:

$$\Delta r = \frac{2.47}{\sin E + 0.0121} \quad \text{(m)} \tag{11-6}$$

where:

E: elevation angle.

A simplified mapping function is:

$$\mathrm{m}(E) = \frac{1.0121}{\sin E + 0.0121} \tag{11-7}$$

A climatological tropospheric range delay model that has been extensively tested against actual radiosonde data from many stations in North America, has been developed by Collins and Langley [Collins and Langley, 1999]. They described their results in terms of deviations from normal, or Gaussian, residuals. Their model, called UNB3, closely follows a Gaussian distribution from approximately the –5 σ to the + 4σ points, impressive performance for a climatological model with no real-time inputs. Limiting factors to the model have been described in [Collins and Langley, 1996].

11.3.1 Variability of the ionospheric and the tropospheric range delay

As shown above the variability of the Earth's tropospheric range delay is primarily due to the water vapor content in the atmosphere. However, the absolute magnitude of the zenith range delay due to water vapor is only of the order of a few centimeters, and, even at low elevation angles, it may not be a major factor in overall range error. The absolute variability of the range delay of the earth's ionosphere is much larger, but it can be nearly completely eliminated by using a dual frequency GPS receiver as described below.

Those who need the highest precision corrections for both ionospheric and tropospheric range delay corrections should use a dual frequency correction to eliminate the first-order ionospheric range delay, and then should consider using one of the "fitting" functions to the residual range errors versus elevation angle to independently determine the tropospheric range delay. If only a single frequency GPS receiver is available then the residual ionospheric range delay, even after using one of the various ionospheric correction methods, likely will still be larger than the residual range delay of the troposphere using even a climatological model of the range delay, such as the UNB3 model.

11.4 The time delay of the ionosphere, its worldwide behavior, day-to-day variability and solar cycle variability

The range delay of the ionosphere is dispersive; that is, it varies inversely with frequency in the following manner:

$$\Delta t = \frac{40.3}{cf^2} \int_0^{Sat.} N dl \quad \text{(s)} \tag{11-8}$$

where:

$\int_0^{Sat.} N\mathrm{d}l$: integrated number of free electrons along the radio wave path from the ground measurement point to the satellite, commonly called the slant Total Electron Content, (TEC) along this path

c: the velocity of light in m/s

f: the system operating frequency (Hz).

Since the ionospheric range delay is a function of frequency the best method of correcting for its effects on time transfer is simply to measure it at two frequencies that are spaced sufficiently far apart, and thus measure the ionospheric time delay directly. Other methods are all less direct, and are necessarily of lower accuracy.

Typical numbers for the TEC of the Earth's ionosphere vary from 10^{16} to $10^{19}\,\mathrm{el/m^2}$ column. Corresponding one-way ionospheric time delay values versus frequency for TEC values from 10^{16} to 10^{19} el/m^2 column are illustrated in Fig. 11-2. The GPS L1 frequency of 1.57542 GHz is shown by a vertical line in Fig. 11-2. The large variation in TEC of approximately 3 orders of magnitude is due to many factors, among them being the time of day, season, station location, and solar ultraviolet ionizing flux.

FIGURE 11-2

One way ionospheric range delay as a function of frequency for different values of TEC from 10^{16} to 10^{19} el/m^2 column. The GPS L1 frequency is indicated by a vertical line at 1.575 GHz

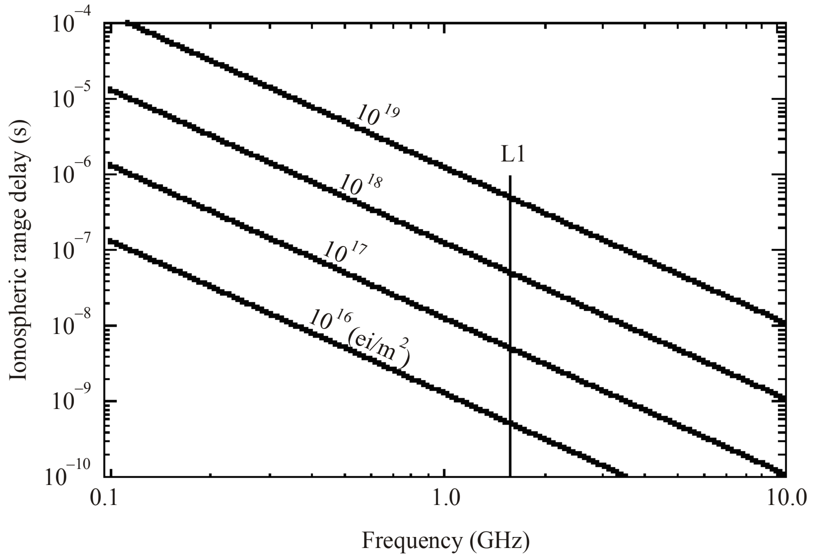

Sat_time_freq-11-02

Figure 11-3 illustrates worldwide monthly mean ionospheric vertical range delay, in units of meters at the GPS L1 frequency, for solar maximum equinox conditions. Note that the maximum range delays occur, not at the geographic equator, but at latitudes of approximately ± 15º either side of the magnetic equator. While this model representation of average range conditions shows maximum values of only 24 m at L1 the absolute values can be much larger and the day-to-day variability also normally is high.

Figure 11-4 illustrates the day-to-day, seasonal and solar cycle variability of the northern mid-latitude ionosphere by plotting range delay values for each day of the four months, January, March, June and September of the years 1986 through 1990 for a station located near Boston, Massachusetts, a period of increasing solar activity in the solar cycle that peaked in the 1989-90 time period. Note the large day-to-day variability in diurnal range delay curves within any given month, as well as the seasonal effects with the equinoctial months having larger absolute values than those in the solstice months, with especially low values in the month of June. Note that large changes in absolute range delay as the solar cycle increases from 1986 to 1989 and 1990. Models of ionospheric range delay that are not updated with a timely nearby measurement can only hope to replicate the monthly average range delay; hence, leaving the residual approximate 25% r.m.s. day-to-day variability in ionospheric range delay uncorrected.

FIGURE 11-3

Worldwide median ionospheric range delay, in units of meters at the GPS L1 frequency, for solar maximum equinox conditions

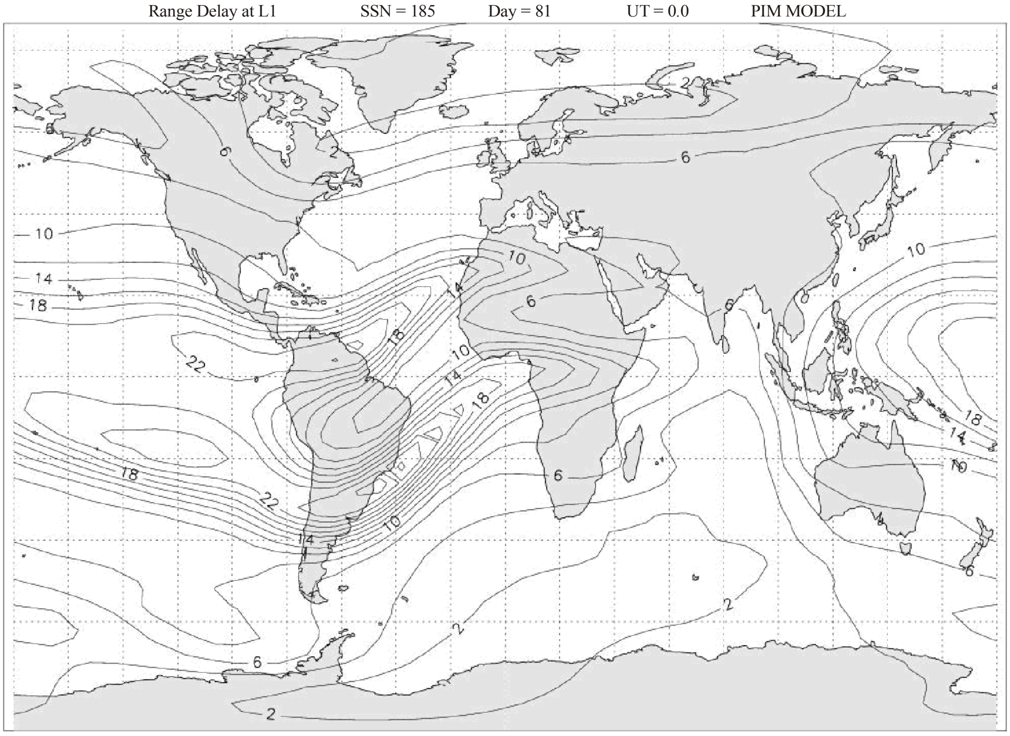

Sat_time_freq-11-03

FIGURE 11-4

Monthly overplot of diurnal curves of equivalent vertical ionospheric range delay at the GPS L1 frequency for four months of five years of increasing solar activity. Monthly mean sunspot numbers for each month, (SSN) are indicated by the large arrows on the right hand side of each monthly overplot

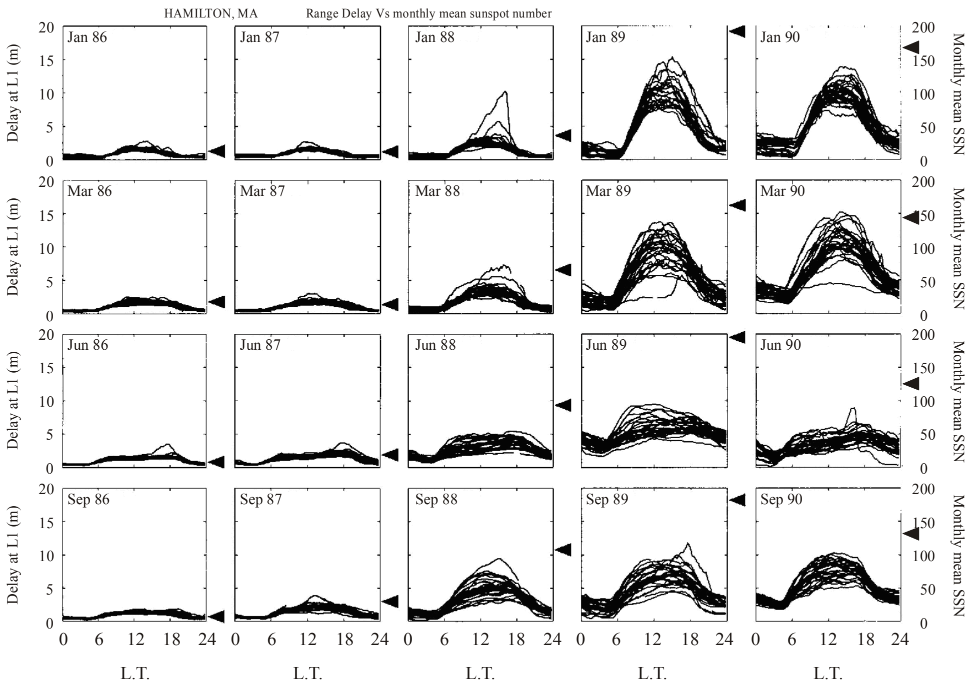

Sat_time_freq-11-04

11.4.1 Methods of correcting for ionospheric time delay, monthly mean models, updated models, use of SBAS/WAAS/IGS ionospheric real-time data, two-frequency corrections

Left uncorrected, typical GPS vertical pseudorange errors due to TEC can be on the order of 10-25 m. In fact, the *vertical* ionospheric range delay just south of the southeastern continental United States of America reached over 40 m during two recent large geomagnetic storms, a region where monthly average *vertical* range delay values are typically of the order of only 10 m. Fortunately, there are several methods of correcting for the effects of the ionosphere on time transfer. These are given below, beginning with the (trivial) case of no attempt to make a correction, and progressing to the dual frequency correction technique that provides the best correction, albeit with a moderate increased cost in initial equipment, but eliminates the ionosphere from consideration, at least down to the few centimeter level of correction.

There are at least five different methods of correcting for the effects of ionospheric range delay. Each of these methods will be discussed, along with the relative difficulty in implementing the correction. The methods yield the following approximate corrections:

0 % – No attempt to correct for ionospheric range delay. This is a trivial case, but is included for the sake of completeness. Even a "constant" correction for each "season" and location, with no diurnal dependence, would be a considerable improvement over this "do nothing" case.

50% – Use the Ionospheric Correction Algorithm (ICA) designed to correct for approximately one half (r.m.s.), of the ionospheric range delay. This is the standard correction used by virtually all single frequency GPS receivers. The coefficients for the ICA are transmitted as part of the satellite message and are updated at least once each ten days by the GPS Master Control Facility, or more often if there are significant changes in the five-day running mean solar radio flux during the ten-day period. The ICA is limited to only 8 coefficients due to GPS message length limitations [Klobuchar, 1987].

75% – Use a state-of-the-art ionospheric model, requiring thousands of coefficients, but which will fit the monthly average behavior of ionospheric range delay to within a residual bias of approximately 10%. Typical models are the International Reference Ionosphere, (IRI) [Bilitza, 2000], and the Bent model. Both models are available over the Internet. Use of such models still leaves the GPS user to contend with the remaining day-to-day variability of approximately 20-25%, and the consequent approximate 22-27%, one σ error when the bias in knowledge of the monthly mean is included. Note that this level of correction still does not use any near-real-time inputs, but relies only on a state-of-the-art model to more accurately describe the monthly average ionospheric behavior than the ICA that only uses 8 coefficients. Thus, by increasing the number of coefficients from 8 to several thousand, the improvement goes from approximately 50% to approximately 75%, r.m.s.

90% – Use the Space based augmentation systems (SBAS) ionospheric corrections that are transmitted as part of the SBAS augmentation messages. Such messages are provided by e. g. WAAS and EGNOS as was described in chapter 2 on augmentation systems. This greatly improved correction provides near-real-time ionospheric range delay data obtained from a network of SBAS Reference Stations that are used to generate a grid of equivalent ionospheric range delay corrections at 5° by 5° latitude and longitude grid points over the coverage region. Of course, this correction technique can only be used in regions where a SBAS exists and where there are adequate ground reference stations to measure the ionospheric range delays. The improvement by using actual near-real-time ionospheric data comes at a cost of requiring a single frequency GPS receiver that is also capable of receiving the SBAS message. The estimated correction of only 90% using e. g. WAAS, even with using near-real-time range delay data, is due to the need to interpolate from the 5° by 5° grid values of vertical ionospheric range delay provided by WAAS to the equivalent slant range delays along the line of sight to each GPS satellite being monitored by the user.

99% – Use a dual frequency receiver as described in Chapter 1 on GPS and in the chapters concerning time transfer to remove essentially all the ionospheric range delay along the path to each GPS satellite being monitored. This method directly measures the line of sight slant ionospheric range delay along each GPS satellite path, and involves no model computations, and no interpolation from range delay values measured along another path. It is by far the best correction technique to use, and should become the standard for all civilian GPS users when the new L5 frequency is fully implemented on future GPS and Galileo satellites, likely by sometime early in the second decade of the 21st century.

Each of the above percentage correction levels comes with a penalty of some sort. The zero correction, of course, has the penalty of having the largest errors, and the 99% correction has the obvious higher cost of requiring a dual frequency GPS receiver. Using the ICA to correct for approximately 50% r.m.s. of the ionospheric range delay error has only a small penalty as the equations for its implementation are given in the Interface Control Document ICD-200, and it is the standard procedure used in single frequency GPS user receivers.

11.4.2 Higher order ionospheric effects on time delay

Equation 11-1 relating ionospheric time delay to TEC uses the first-order form of the refractive index of the ionosphere. The complete form of the refractive index, neglecting those terms whose magnitude is less than 10^{-9} [Brunner and Gu, 1991], consists of several additional terms that include:

$$n = 1 - \left(X/2\right) \pm (XY/2)\cos\theta - (X^2/8) \tag{11-9}$$

where:

1:	the free-space term
X/2:	the first-order term, proportional to $1/f^2$
XY/2 cosθ:	proportional to $1/f^3$
$X^2/8$:	proportional to $1/f^4$.

If these terms are called A, B, and C, respectively, the magnitude of the higher-order terms at GPS frequencies, for maximum worldwide ionospheric conditions are:

$$B \approx 2 \times 10^{-4},\ C \approx 2 \times 10^{-7},\ D \approx 2 \times 10^{-8}$$

The ratios of the higher-order terms, C and D, to the first-order term, B, again under worst-case ionospheric conditions, is:

$$C/B \approx 10^{-3},\ D \approx 10^{-4}$$

Thus, these higher-order terms are 0.1% and 0.01% of the first-order term at GPS frequencies, even for the extremely high ionosphere considered here. Similar conclusions have been reached by Ioannides and Strangeways [Ioannides and Strangeways, 2002], in which the largest contribution to higher order terms was only a few cm.

11.4.3 Scintillation effects

Both amplitude and phase scintillations can effect the short-term performance of various GPS receivers. However, the occurrence of significant scintillation fading or phase scintillation "jitter" effects is very small in the mid-latitude regions. Even in the near-equatorial region, where some time averaging of the signal is used, scintillation effects should not be a problem. In the equatorial region deep amplitude fading effects generally only occur during the post-sunset hours until local midnight, and then only during equinoctial months of years of relatively high solar activity. A pictorial representation of the times and regions of the world having various scintillation levels is illustrated in Fig. 11-5. Various reviews of scintillation effects have been made, including one by Goodman and Aarons [Goodman and Aarons, 1990] in which the morphology of amplitude scintillation is described for various frequencies commonly used in satellite communication and time transfer. Scintillation can be a limitation to precise time transfer by satellite, but scintillation effects can be minimized simply by avoiding times and periods of the day when it normally occurs. For instance, although deep amplitude fading that can produce signal outages on the GPS frequencies is rare in the auroral latitudes, if possible avoid performing time transfer during magnetically disturbed periods. Similarly, avoid time transfer after local sunset in the near-equatorial regions, especially during years of high solar activity. Finally, it is always best to monitor the receiver carrier-to-noise density ratio C/N_0 in real time for each GPS satellite to continuously have a reliable method of determining if there deep amplitude scintillation may be affecting the received signal.

FIGURE 11-5

Map of the world in magnetic coordinates and local time, showing where regions of scintillation normally occurs

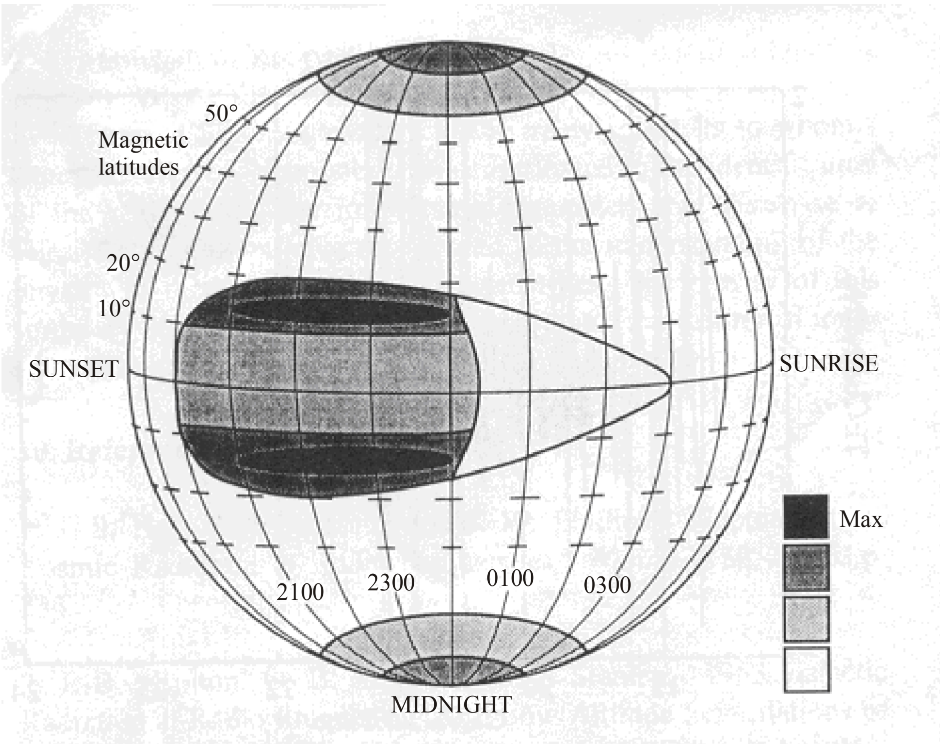

Sat_time_freq-11-05

11.5 Conclusion

The best advice that could be given to the time transfer community concerning ionospheric delay effects on time transfer would be to run, not walk, to the nearest location where a dual-frequency GPS receiver is sold and purchase one for each end of the satellite time transfer link. Using a dual-frequency GPS receiver is simply the absolute best method of guaranteeing that over 99% of the ionospheric range delay will automatically be removed from all satellite paths. If a dual frequency GPS receiver cannot be used, then use the SBAS (WAAS, EGNOS) ionospheric corrections to provide ionospheric time delay values if such corrections are available in the regions of the world where the time transfer is to be done. If no SBAS ionospheric corrections are available, then TEC values from a nearby IGS station should provide a better correction than any of the non-updated ionospheric models.

References

BILITZA, D. [2001] The International Reference Ionosphere 2000. Radio Science, Vol. 236, p. 261-275.

BRUNNER, F. K. and GU, M. [1991] An Improved Model for the Dual Frequency Ionospheric Correction of GPS Observations. Manuscripta Geodaetica, Vol.16, p. 205-214.

COLLINS, P. and LANGLEY, R. B. [July 1999] Tropospheric Delay Prediction for the WAAS User. GPS World, p. 52-58.

COLLINS, P., LANGLEY, R. and LAMANCE, J. [19th-21 June, 1996] Limiting Factors in Tropospheric Propagation Delay Error Modelling for GPS Airborne Navigation. Presented at The Institute of Navigation 52nd Annual Meeting, Cambridge, Massachusetts, USA.

GOODMAN, J. M. and AARONS, J. [1990] Ionospheric Effects on Modern Electronic Systems. Proc. of the IEEE, Vol. 78, p. 512-528.

IOANNIDES, R. T. and STRANGEWAYS, H. J. [August 2002] Improved Ionospheric Correction for Dual Frequency GPS. Proceedings of the XXVIIth General Assembly of URSI, Maastricht, Netherlands.

KLOBUCHAR, J. A. [May 1987] Ionospheric Time-Delay Algorithm for Single-Frequency GPS Users. *IEEE Trans*. on Aerospace and Electronic Systems, Vol. AES-23, No. 3, p. 325-331.

SPILKER, Jr. J. J. [1996] Tropospheric Effects on GPS. Chapter 12 in Global Positioning System: Theory and Applications. Edited by B. W. Parkinson and J. J. Spilker, Jr., publ. by the American Institute of Aeronautics and Astronautics, Inc. ,Washington, DC. Vol. 1, p. 517-546.

CHAPTER 12

GLOBAL NAVIGATIONAL SATELLITE SYSTEMS – AS A PRIMARY TOOL FOR TIME TRANSFER

Page

12.1 Introduction

Over the years, the clocks by which we have kept time have become not only more precise but also more accurate. Figure 12-1 depicts the performance levels of different forms of clocks over a wide range of time intervals. There is a progression from least accurate to more accurate from top to bottom. The lower part of this graph is representative of more recent history. Today, we are on the verge of using clocks that are capable of frequency accuracy of 1×10^{-16}. This corresponds to a clock having the capability to maintain a level of performance corresponding to 10 ps/day.

FIGURE 12-1

Clock time-keeping ability
(This Figure courtesy of D. W. Allan)

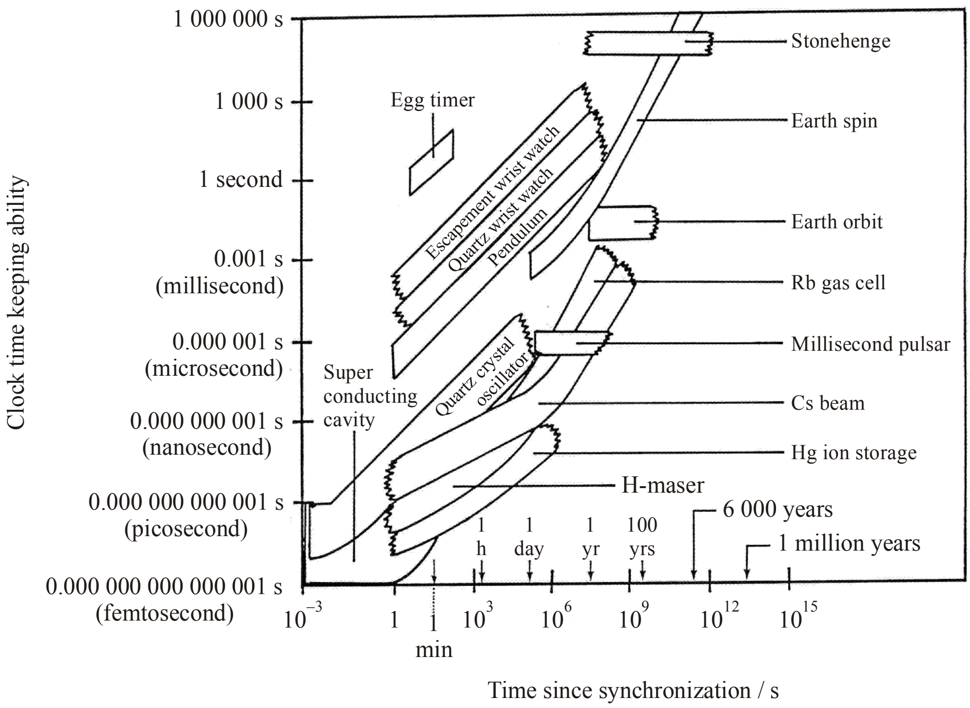

Sat_time_freq-12-01

Over the years, the timekeeping community has used many different techniques and systems to help them with the task of synchronizing clocks or time transfer. Figure 12-2 shows the performance level of some of these systems. They include the use of:

– terrestrial communications systems, such as television and telephones (MODEMS);

– direct radio broadcasts (WWV and WWVH);

– navigation systems, such as Loran-C and GPS;

– satellite communications systems such as two-way satellite time and frequency transfer (TWSTT).

As clocks have become more precise and accurate, the timekeeping community has sought more precise and more stable systems to help them with synchronization. For the timekeeping community, GPS is a significant contributor to solving the traditional problems of timekeeping. It is a reliable source of time and it is a reliable time-transfer system.

FIGURE 12-2

Performance of different techniques for time transfer
(This Figure courtesy of D. W. Allan)

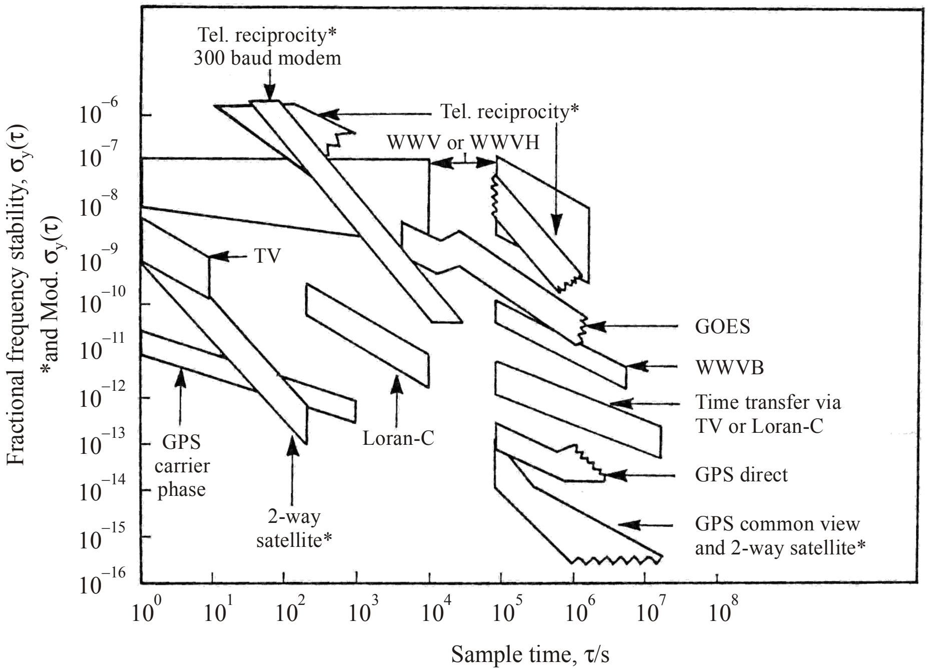

Sat_time_freq-12-02

12.2 GPS and time

GPS is a navigation system that has proven to be a reliable source of positioning for both the military and civilian communities. But it is a little-known fact that GPS has proven itself to be an important and valuable utility to the timekeeping community [Klepczynski *et al.*, 1996]. GPS is a versatile and global tool that can be used to both distribute time to an arbitrary number of users and synchronize clocks over large distances with a high degree of precision and accuracy. This paper will discuss briefly how GPS is used by the timing community for these purposes and will highlight the most recent developments in this field.

12.2.1 How does GPS distribute time?

As part of the navigation solution, the computer contained within the GPS receiver can determine the difference between the clock that is contained within the user receiver and either GPS time or the reference time for GPS, which is UTC(USNO), i.e., UTC as determined at the U.S. Naval Observatory. The clock contained within a user's GPS receiver is usually a quartz crystal clock. However, in some cases, an external clock such as a rubidium frequency standard or a caesium beam frequency standard can be the local reference for a GPS receiver. The local receiver can be programmed to display UTC(USNO), as broadcast by GPS, or GPS time since the navigation solution yields the difference between the local receiver clock and GPS time. It should be pointed out that UTC(USNO) is steered to UTC as determined by the BIPM. UTC(USNO) is usually kept to within about 10 ns of UTC.

One advantage the timing community has over the navigation community is the number of GPS satellites that it needs. The navigators need four satellites to determine their position; three to get their position and one to determine the offset of their local clock from GPS time. Since the timekeepers are in fixed locations and know their position, they only need one GPS satellite to get the offset of their local clock from GPS time. Consequently, they have modified the algorithms in their timekeeping receivers to take advantage of this fact.

As part of the navigation solution, the computer contained within the GPS receiver can determine the difference between either GPS Time or the reference time for GPS, which is UTC(USNO), and the clock that is contained within the user receiver. The clock contained within a user's GPS receiver is usually a quartz crystal clock. However, in some cases, an external clock such as a rubidium frequency standard or a cesium beam frequency standard can be the local reference for a GPS receiver. The local receiver can be programmed to display UTC since the navigation solution yields the difference between the local receiver clock and GPS Time.

One advantage the timing community has over the navigation community is the number of GPS satellites that it needs. The navigators need four satellites to determine their position; three to get their position and one to determine the offset of their local clock from GPS Time. Since the timekeepers are in fixed locations and know their position, they only need one GPS satellite to get the offset of their local clock from GPS Time. Consequently, they have modified the algorithms in their timekeeping receivers to take advantage of this fact.

12.2.2 How does GPS synchronize clocks over large distances?

It does this through a technique that is known as GPS Common View. In the Common View Technique, two stations simultaneously observe the same GPS satellite. Each of the users at both stations must record the difference between his local clock (T) or local time reference and GPS Time at the same instant using the same satellite using a GPS receiver known as a GPS Time Transfer Unit (TTU). A GPS TTU is a special GPS receiver programmed to compute and display items of interest to the timing community.

$$\text{User A Observes: A} = T_a - \text{GPS Time} \qquad (12\text{-}1a)$$

$$\text{User B Observes: B} = T_b - \text{GPS Time} \qquad (12\text{-}1b)$$

It is essential that the two users observe the same satellite at the same instant in order to minimise the effects of some errors [Allan and Weiss, 1980]. By computing the difference between the two sets of numbers:

$$\text{A - B} = (T_a - \text{GPS Time}) - (T_b - \text{GPS Time}) = T_a - T_b \qquad (12\text{-}2)$$

The differences between the two local clocks can easily be calculated because the common GPS clock drops out. This is a very simple but powerful process because it is independent of GPS time.

Over the years, significant progress has been made in improving the precision and accuracy of the time distribution and clock synchronization capabilities of GPS. Presently, we are at the 10-25 ns level in one-way time distribution with a coarse acquisition (C/A) code receiver and at the 2-15 ns level in time synchronization. A range of values is given for these estimates to indicate that experience has shown that what is achievable is dependent on the user and site specific. These values are representative of the results currently obtained by users in different fields such as telecommunications and metrology.

12.3 Applications of GPS time transfer

Within a telecommunications network, the major nodes must be synchronized [Butterline, 1993]. This can be done internally (through synch pulses) or externally (through synchronization). GPS easily provides the capability to allow the external synchronization of clocks at major nodes within a network to better than 100 ns in time and 1×10^{-13} in frequency. This, in the terms of the telecommunications industry, meets their Stratum I level requirements that require an accuracy of 1 ms in time and 1×10^{-11} in frequency.

In some *telecommunications* networks, time and especially frequency are kept by an ensemble of atomic clocks such as rubidium frequency standards, which are synchronized to UTC via GPS. Usually, the rate of each rubidium clock in the ensemble, with respect to UTC, is determined by averaging GPS observations over some interval of time. The interval chosen depends on the requirements of the particular system in question. One needs to know the difference between the rate of each rubidium clock and UTC with the best precision and accuracy attainable in order to ensure that if contact is lost with the GPS system for some reason, the rate offset of the rubidium clock with respect to UTC can be extrapolated using the last observed values until contact is re-established with GPS. If contact is lost, this may or may not mean an immediate problem for the telecommunication system in question. It all depends on how long it takes for synchronization among nodes to deteriorate to the point where they can no longer communicate coherently, among themselves. This could take 1 h to several weeks, depending on the particular system involved.

The *electric power industry* is relying more and more on GPS for time. Power companies are now using GPS to synchronize the clocks at their monitor stations in order to locate faults in electric service within their area of concern. They locate the source of a fault (break in a power line) by triangulation, i.e., by knowing the time of its occurrence at three stations whose clocks are synchronized. The power industry also needs to have synchronized clocks among different regional service providers. Synchronization is important if one wants to transfer power efficiently from one grid to another. Out-of-phase transfer of electric power fro m one grid to another reduces the total available power.

Time metrology began to use GPS signals about 15 years ago at the National Bureau of Standards (NBS, now National Institute of Standards and Technology, NIST). A system using CV observations of GPS satellites for accurate time and frequency transfer was suggested [Allan and Weiss, 1980] and receivers specially designed for this purpose were built first at NBS and then in several commercial companies. These were single-channel one-frequency C/A-code receivers capable of tracking only one satellite at a time. To operate them it was essential to issue periodic schedules of CV observations. The CV method was clever and far-reaching: it not only reduced some uncertainties of physical origin but went on to cancel the deliberate degradation of GPS time introduced in 1990 under the name of Selective Availability (SA) [Lewandowski and Thomas, 1991].

The introduction of GPS brought about a significant improvement in time and frequency transfer. With uncertainties ranging from 10 to 20 ns for time comparisons during early stages of the use of GPS, it was possible, for the first time, to compare the best atomic standards in the world at their full level of performance using integration times of about ten days. Since then a number of improvements have been introduced, including the use of ultra-accurate antenna coordinates, precise ephemerides, and measurements of the ionosphere [Lewandowski and Thomas, 1991]. These led at the beginning of 1990's to time comparison uncertainties of about 3 ns. This paralleled improvements in atomic standards that advanced by an order of magnitude and made possible the comparison of the new clocks (e.g., HP5071A caesium beam frequency standards) at their full level of performances for averaging times of several days.

Today in metrology we are witnessing the birth of a number of new and innovative frequency standards. These devices seem to be approaching 1×10^{-15} in accuracy and seem to have short-term instability approaching 1×10^{-16}. The performance of a frequency standard is very often described in terms of the variances of its frequency variations over a wide range of time intervals ranging from 1 second to several months. There are many different mathematical variations of these statistical formulations used to describe the performance of a clock. Figure 12-3 shows one of them: $\sigma^2_y(\tau)$, or, as it is sometimes called, the Allan variance [1987], for several different kinds of frequency standards, e.g., quartz, rubidium, caesium, and hydrogen maser. Such a graphical representation of the performance of a frequency standard exhibits different characteristics that are a function of the noise processes that occur within the frequency standard. In fact, the slope of the curve can be used to identify the type of noise. A slope of zero, or the curve being parallel to the ordinate, indicates that the limiting performance in stability of a standard has been reached (flicker floor). The type of noise that is identified with this process is flicker frequency modulation.

Since the newest devices are not transportable and do not operate continuously, it is important to compare them in a reasonable time in order to determine the existence of systematic differences among them. A measurement with a precision of 1 ns over a 24-hour period corresponds to 1×10^{-14} in frequency. Therefore, at today's present levels it would take weeks to compare two such devices. That is why it is important to develop and improve time-transfer methods to allow these comparisons to be made within a reasonable amount of time.

The time scales, TAI and UTC, are based on data from some 220 atomic clocks located around the world in about 50 time laboratories. The time section of the BIPM computes these time scales. The sole operational means of comparing these clocks is the GPS CV technique based on C/A-code single-channel measurements. For this reason, the timing community is engaged in the development of new approaches to time and frequency comparisons. Among them are techniques based on multi-channel GPS C/A-code measurements, GPS carrier phase measurements, temperature-stabilized antennas, and standardization of receiver software.

As an additional resource, other developments use GLONASS C/A-code and P-code measurements. This paper focuses mainly on the progress that has resulted from the use of GPS multi-channel observations and specially protected receiver antennas. It also points out some of the difficulties experienced with other current techniques. It describes the delay instabilities of current GPS timing receivers, and compares GPS C/A-code time transfer with other satellite time-transfer techniques.

FIGURE 12-3

Stability ranges of various frequency sources

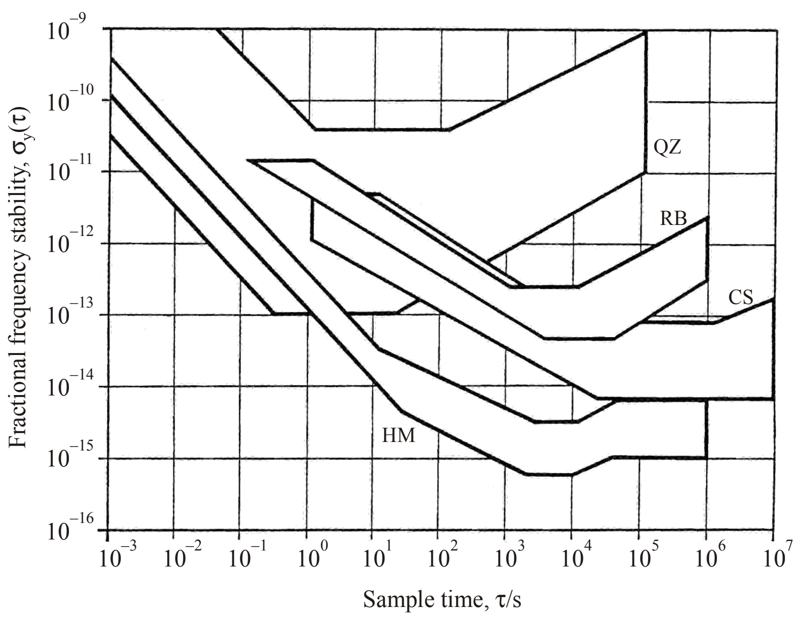

Sat_time_freq-12-03

12.3.1 GPS C/A-code single-channel common-view time transfer

Many users rely on single frequency (C/A-code) receivers which track only one satellite (single channel) for synchronizing clocks via the OPS CV technique. Over the last 15 years, the performance of GPS C/A-code CV time transfer has improved by one order of magnitude. At present, the estimated uncertainty of operational single-channel GPS C/A-code time transfer is about 7 ns for a single CV observation and about 3 ns for a daily average, which corresponds to a few parts in 10^{14} in terms of frequency transfer. However, this performance is barely sufficient for the comparison of current atomic clocks and needs to be improved rapidly to meet the challenge of the clocks now being designed. Over the past 45 years the performance of atomic clocks has improved on average by an order of magnitude every seven years. The stability of TAI and UTC, which are reference international time scales, is currently about two parts in 10^{15} over a period of a few weeks. Thus, it is reasonable to predict that by the year 2005 the stability of TAI and UTC will attain a few parts in 10^{16}.

12.3.2 One-site comparisons (zero baseline)

One-site comparisons are comparisons in which CV's are computed between two GPS time receiving systems located at the same site, connected to the same clock, and with antennas distant by no more than a few meters. Comparisons at short distances allow the cancellation of common clock errors and a number of other errors. If the receivers being compared use identical software, no error should arise from satellite broadcast ephemerides, antenna coordinates, or imperfect modeling of the ionosphere and troposphere. Any constant bias measured arises from delay differences in the two compared pieces of equipment, including receiver itself, antenna, cables, etc. Considerable data are now available which describe such comparisons [Kirchner *et al.*, 1993; Buisson *et al.*, 1985]. All show similar behavior: a short term (one day) and sometimes a long-term (seasonal) dependence on external temperature. The diurnal change is likely to be a few nanoseconds and seasonal change about 10 ns. It must be emphasized that the phenomenon observed is a differential effect so the actual delay changes caused by the temperature dependence could be larger.

12.3.3 GPS differential calibration

Differential calibration of remote GPS time equipment, based on the principle of the one-site technique described above, has progressed over the last few years. In this case, one of the two receivers being compared is a local receiver. The other is a portable receiver, which is shipped between the sites to be calibrated. By supposing that the receiver delays of the traveling GPS time equipment (including cables and antennas) are constant, a differential time correction can be calculated for each of the sites compared. The stated uncertainty of such a differential calibration, if performed under ideal conditions, is about 2 ns. Differential calibration of GPS time equipment allows accurate comparison of remote atomic clocks. Uncertainties in the differential calibration and noise in the CV link limit this accuracy.

Over the last 15 years a number of differential calibrations have been performed [Lewandowski, 1996] by the BIPM. The GPS time equipment located at NIST and the Paris Observatory (OP) have been compared about ten times; differential time corrections determined during these calibrations differ by no more than a few nanoseconds. This gives an idea of the reproducibility that can be obtained when calibrations are performed under ideal conditions in laboratories where the GPS time equipment, including cables, is maintained carefully. It also gives some ideas of the long-term stability of the GPS time equipment. Again, it must be emphasized that, as for a one-site comparison, these are differential comparisons. Seasonal effects may have been cancelled since both receivers are located in the northern hemisphere. As of now, repeated calibrations have not been carried out between sites located in the northern and southern hemispheres.

A clear consistency between repeated calibrations is not found for all sites. In some cases discrepancies of about 10 ns have been found. These may be attributed to a different response of the receivers being compared to seasonal changes of temperature or unrecognized multipath. In others the discrepancy was large, sometimes tens of nanoseconds; such changes probably arise from unrecorded intentional changes or from non-intentional changes in the GPS time equipment hardware.

12.3.4 Closure around the world

As mentioned earlier, GPS CV time transfers occur between pairs of stations. In some instances, it is possible to circle the globe, in one direction, with a number of pairs of stations. The closure condition implies a cancellation of all clocks errors and, in the ideal case of noiseless time links, we should obtain zero. Several tests have been performed in the past. One test, performed over a period of about one- year on the data from NIST, OP, and the Communications Research Laboratory (CRL), used post-processed precise ephemerides and ionospheric measurements and showed a bias of several nanoseconds that changed with time [Lewandowski, 1993]. As hardware delays are also cancelled by the closure condition the remaining sources of uncertainty are linked only to the path of the GPS signal through the space or multipath. It seems that the observed bias may arise from the limited accuracy of ionospheric measurements. A part of this bias can be also due to an error in antenna coordinates in one of involved laboratories. Variation of the bias with time also points towards ionospheric measurements because these can be affected by changing conditions from day to night as sidereal GPS orbits “move” by 4 min each day throughout the year. The troposphere correction may also play a part in the observed variation of delays.

Closure around the world seems to provide a good test of the accuracy with which atmospheric refraction delays may be calculated, as CV’s over such long baselines necessarily are performed at very low elevations.

12.4 Comparison of GPS with other time transfer techniques

12.4.1 Comparison with two-way satellite time and frequency transfer

Two-way satellite time and frequency transfer (TWSTFT) is a technique that utilizes geostationary telecommunications satellites to provide time transfer with precision of several hundred picoseconds. In this technique, each of two stations, A and B, simultaneously sends a coded signal to the other and receives one. The start of the coded signal of A is synchronized to the 1-Hz signal of local clock A. The coded signal of B is also synchronized to local clock B. The received signal, that is encoded, is used to stop a time interval counter that was started by the user's local clock. One needs to bring together the time interval counter readings of Stations A and B before one can compute the difference between the two local clocks. Usually, it takes about 2 min to get sufficient data to compute an average value because of the noise processes involved. These two-minute sessions are usually performed three times a week. In 1991, for about one year, the time scales of Observatoire de la Cote d'Azur (OCA) and the Technical University of Graz (TUG), separated by about 800 km, were compared by means of GPS CV I and TWSTT [Kirchner *et al.*, 1993]. The stated uncertainty of the GPS link is 3 ns.

The data presented in Fig. 12-4 show differences between values of [UTC(TUG)-Clock(OCA)] obtained by TWSTT and GPS CV measurements. The links were calibrated independently at the end of experiment by measuring the differential delays of the GPS receivers and the satellite Earth stations by transporting one GPS receiver and one satellite terminal to the other site. Because the differences between TWSTT and GPS CV values exhibit an apparent systematic (seasonal) variation, the mean value and the standard deviation of the differences (3.6 and 3.9 ns, respectively) are not appropriate measures with which to describe the agreement of the two techniques over the period of comparison. The modified Allan variance of the differences exhibits white-noise PM up to an averaging time of about 50 days, so computation of mean values and corresponding standard deviations is justified for data intervals up to this value. For the time of comparison the average of 50 day means is 3.2 ns and the standard deviation 2.6 ns. The maximum difference of the means is 8 ns and corresponds to a seasonal effect that, again, is likely to be the result of temperature-dependent delays in the GPS receiving equipment used (Fig. 12-4).

FIGURE 12-4

Differences between (UTC(TUG)-Clock(OCA)) obtained by TWSTT measurements, differences between (UTC(TUG)-Clock(OCA)) obtained by GPS Common view measurements, and outside temperature at TUG

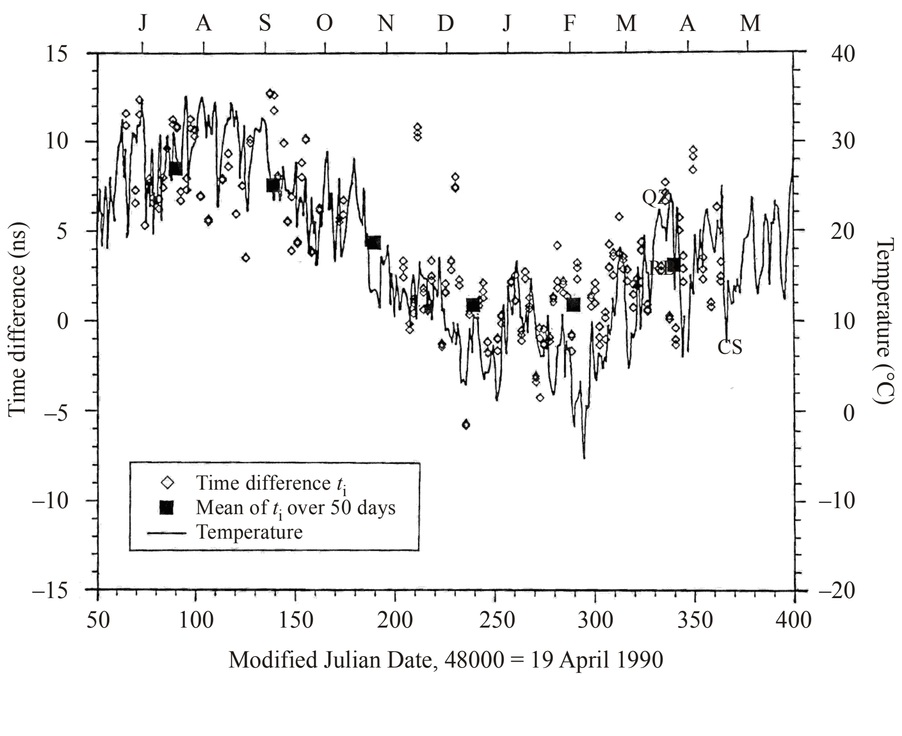

Sat_time_freq-12-04

The TWSTT technique is implemented in eight European and two United States of America time laboratories and has preoperational status. Results of a 1997 exercise, show the same temperature dependence of the differences between TWSTT and GPS CV measurements as in 1991 exercise.

12.4.2 Comparison with laser time transfer

Laser synchronization from stationary orbit (LASSO) was a technique that should allow for comparison of remote atomic clocks with an uncertainty of about 100 ps. During an experiment covering the period from December 8, 1992 to January 28, 1993, two remote atomic clocks in McDonald Observatory, TX, and the OCA, France (separated by 8000 km) were compared using LASSO and GPS CV's [Friedelance, 1994; Baumont *et al.*, 1993]. Because of bad weather conditions only five LASSO sessions were performed. The GPS CV link was computed without applying precise ephemerides or ionospheric double-frequency measurements, so its uncertainty is considered to be 10 ns.

The GPS link was calibrated by means of a portable receiver: the LASSO link had uncertainty believed to be better than 100 ps, but it was not calibrated. This comparison of GPS CV and LASSO time transfer shows consistency within involved uncertainties and a bias of about 192 ns. Measurements of the differences between the two methods reach a peak-to- peak discrepancy of about 15 ns. The root mean square error (r.m.s.) of the residuals to the mean is 6 ns.

A new generation of time transfer with lasers has been upcoming in the recent years with for instance T2L2 (time transfer by laser link, which is expected to provide an uncertainty of 30 ps) or LTT (laser time transfer). These two experiments are flying on board Jason 2 and a Compass satellite respectively since 2008. European laser timing (ELT) is also expected to fly on board the ISS in the frame of the ESA ACES mission.

Although these systems are inherently unsuited for operational duties, because of their sensitivity to weather conditions, they are certainly excellent tools for assessing the accuracy of GNSS and TWSTT time transfers. Moreover, by performing extremely accurate time transfers between state-of-the-art ground clocks, they might also be used for tests of fundamental physics.

12.5 Recent developments in GPS time transfer

12.5.1 Multi-channel common-view GPS time transfer

A renaissance in GPS time transfer has occurred recently because of the development and availability of multi-channel timing receivers that followed completion of the GPS constellation, reductions in receiver prices, and requests from the timing community. For the previous 15 years international time transfer had been carried out using single- channel C/A-code GPS receivers and an international CV schedule of standard 13-min tracks [Allan and Weiss, 1980].

Because older receivers have limited memory, no more than 48 tracks per day could be programmed; in practice, however, the useful number is even smaller. The choice of a single satellite observation over a 13-min integration period results from the transmission speed of GPS navigation message. It can take up to 12.5 min to transmit a complete message (25 transmitted pages). Integrating over 13 min ensures that all CV measures have the same data. In the early days of GPS, some significant discontinuities were observed between consecutive navigation messages. This has changed, so integration periods may perhaps be shortened.

The multi-channel C/A-code receivers considered here observe all GPS satellites in view and use standard 13-min tracks every 16 min at the standard hours. The multi-channel output data is stored in a single file in a standardized format [Allan and Thomas, 1994; Lewandowski, *et al.*, 1996]. The standard hours are displaced each day by 4 min to follow the GPS sidereal orbits.

The standard hours are referenced to October 1, 1997, a reference date adopted by convention [Report on GPS and GLONASS standardization, 1997]. The same standard hours are used in the BIPM international single-channel CV tracking schedule, which is issued every six months. Instruments that use the "all-in-view" procedure also observe the international single-channel schedule. This greatly simplifies their parallel introduction into the present system of single- channel observations. It seems likely that single-channel observations will soon cease to be made, and there will no longer be a need for the periodic BIPM schedule.

Although, in theory, up to 12 GPS satellites can be observed simultaneously, only about five satellites are ob- served above 15^{o} (and thus are of interest for time transfer) at an average urban site. As there are 89 useful 16-min periods in a day, 89 tracks may be observed in each channel. Using all available observations above 15^{o} (about 5 per 16 minute period), we may therefore observe 445 tracks per day. All these tracks may be used for regional CV links. For very large baselines, between continents, about 100 CV tracks may be available using a multi-channel approach.

The increase by a factor of ten in the number of CV's in the GPS multi-channel mode relative to the single-channel mode, should provide a consequent improvement in the quality of time and frequency transfer. A theoretical gain in stability of $(10)^{1/2} = 3.2$ is expected for averaging times where white phase noise is preponderant [Lewandowski *et al.*, 1997].

Multi-channel observations, however, may be subject to systematic variations, mainly caused by environmental effects on the antenna. This should affect all channels in ways similar to those described above for single-channel receivers except for multipath effects. The gain obtained by multi-channel observations, and systematic effects, are illustrated by a trial comparison described below.

The time link between the BIPM and the NMi Van- Swinden Laboratorium (VSL), Delft, the Netherlands, was considered for a trial comparison because it has a baseline of about 400 km [Lewandowski *et al.*, 1997]. Both laboratories are equipped with GPS multi-channel receivers and their ground-antenna coordinates are expressed in the ITRF with an uncertainty of 0.3 m.

At both laboratories, receivers were connected to HP5071A clocks. Both receivers were calibrated using a portable receiver. We used the same receivers (for the same period of 10 days), for single-channel and multi-channel mode time transfer. We had about 38 useful observations per day for single-channel mode and about 350 for multi-channel mode (Figs 12-5 and 12-6). The level of noise of about 3 ns is similar for both links.

Now consider the advantage obtained by increasing the number of daily CV's from 38 to 350. The theoretical gain in stability is $(350/38)^{1/2} = 3.0$. This may be observed on stability curves for averaging times of less than 104 S for time transfer over 400 km, and also for a one-site comparison at the BIPM. Stability curves for a one-site comparison are reported in Fig. 12-7. The multi-channel comparison is affected by a systematic effect that becomes evident at about 3×10^{4} s (trace 2).

This effect is reduced when the temperature-stabilized antennas are activated (trace 3) (§ 12.5.2). Systematic effects are invisible for the single-channel comparison (trace 1) as they are certainly covered by the higher noise level. So, the advantage brought about by multi-channel observations is limited severely by the instability of receiver delays and barely allows comparison of average HP5071A units at their full level of performances for averaging times of five days, this being the standard interval for computation of TAI.

FIGURE 12-5

(BIPM clock-VSL clock) by single-channel GPS common view

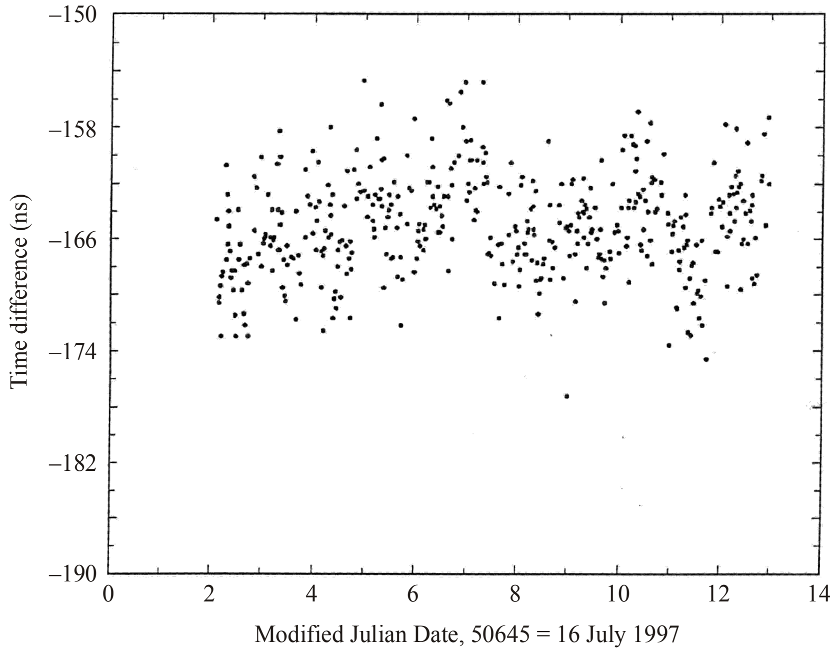

Sat_time_freq-12-05

FIGURE 12-6

(BIPM clock-VSL clock) by multi-channel GPS Common View

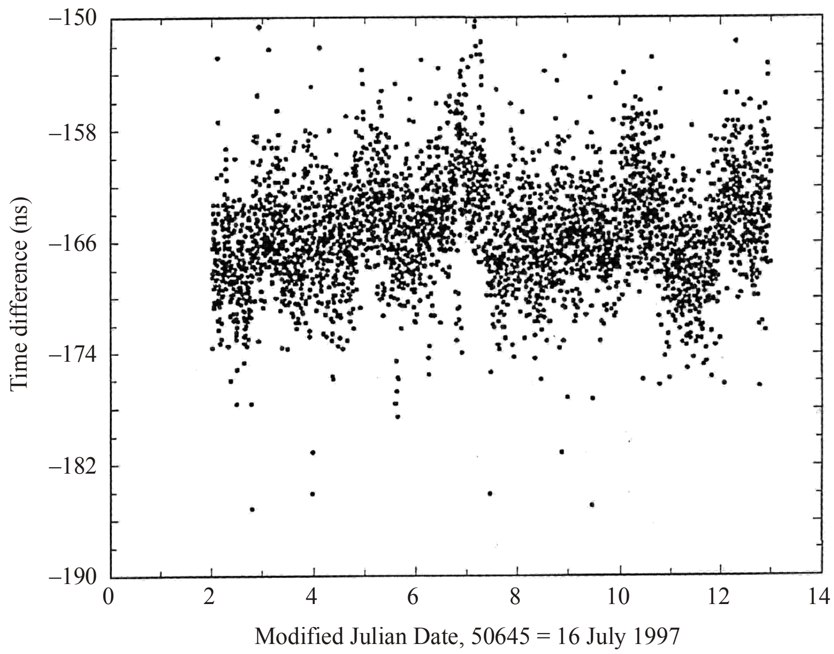

Sat_time_freq-12-06

FIGURE 12-7

One site comparison of two GPS time receivers at the BIPM (two separate antennas on a single site). Modified Allan deviation of:

a) single-channel comparison without stabilizing antenna temperature;
b) multi-channel comparison without stabilizing antenna temperature;
c) multi-channel comparison with temperature stabilized antennas activated

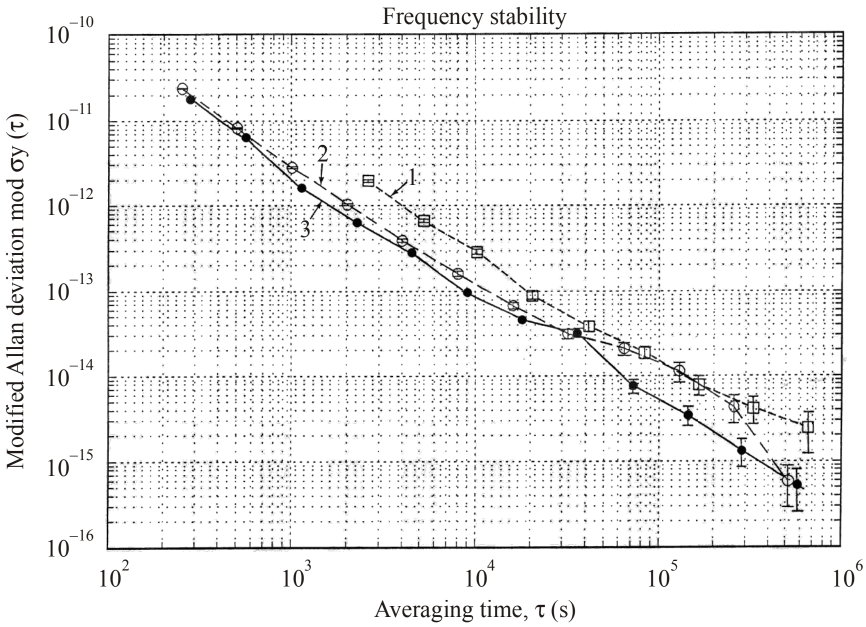

Sat_time_freq-12-07

12.5.2 Temperature stabilized antennas

It is now well documented, and generally admitted, that GPS time-receiving equipment, and more specifically its antenna, is sensitive to environmental conditions [Lewandowski and Tourde, 1990]. For conventional GPS time-receiving system this sensitivity could be expressed by a coefficient of about 0,2 ns/°C and can approach 2 ns/°C. This was a major precluding obstacle, as it did, the goal of 1 ns accuracy announced earlier for GPS time transfer. A comparison of GPS CV with two-way satellite time transfer covering a period of about one year shows a seasonal 8-ns peak-to-peak effect, Fig. 12-4, which is attributed to the instability of the GPS time equipment. The solution to this problem was not found immediately, and even today the quasi-totality of GPS time equipment used in time metrology laboratories is subject to this effect. More importantly, the advantage brought about by the recent introduction of "all-in-view" multi-channel observations is severely limited by the instability of receiver delays.

As no practical way was found to resolve the problem electronically, another approach was suggested [Lewandowski, *et al.*, 1997]: an oven with a stabilized temperature should protect the antenna. The primary objective of the antenna temperature stabilization process is to maintain the critical components at some constant temperature.

First prototypes of the ovens were built at the BIPM. Then very quickly a commercial version, called a temperature- stabilized antenna (TSA), became available commercially. A preliminary one-site comparison of two GPS multi-channel receivers equipped with TSA antennas at the BIPM shows the removal of the systematic, and a fractional frequency stability of a few parts in 10^{15} for averaging times of about one day, Fig. 12-7. This improvement made it possible to take full advantage of multi-channel time transfer and approach the performance expected from the use of GPS carrier phase.

12.5.3 Use of GPS carrier phase

The international GPS service (IGS), which was founded to improve the geodetic applications of GPS, has played a major role in the most recent advances in GPS time transfer. Existing time-transfer receivers typically discard carrier phase and pseudorange data after the time-transfer algorithm is executed. If these data are retained, post-processing with more sophisticated algorithms could lead to a more precise time and frequency transfer. These data are already used in geodesy for differential positioning. Locking on the carrier phase cuts down the effects of multipath. With .the multi-channel receivers now available and using the CV double differencing techniques typical in geodesy, two sites may well be able to maintain a common-carrier phase. If measured ionospheric delays were used in combination with nominally compensated troposphere corrections, a frequency stability of one part in 10^{15} may be attainable with integration times on the order of one day [Schildknecht *et al.*, 1990; Overney *et al.*, 1998]. This performance is about what is required for the comparison of the current primary frequency standards. Continuous measurements, rather than measurements taken once a day, are necessary to achieve this performance.

Already several trials have shown the advantages of using carrier phase measurements for frequency comparisons [Overney *et al.*, 1998; Petit *et al.*, 1996]. The receiver independent exchange format (RINEX) [Gurtner, 1994] provides a convenient format for recording GPS and GLONASS carrier phase and pseudorange data. If the timing receiver has the capability, it is suggested -that a RINEX format carrier phase and pseudorange data file be generated at 15-s intervals for all satellites in view. This data file can then be used for post-processing of precision time and frequency data.

The timing metrologists and geodesists, who possess better understanding of GPS carrier phase signals, have recently joined forces and have undertaken an important initiative known as the “IGS/BIPM Pilot Project”. This project studies accurate time and frequency comparisons using GPS phase and code measurements. An important issue is the resolution of phase ambiguities for timing applications that limits the accuracy of the technique.

It is important to note that carrier phase is also affected by hardware delay instabilities. Here also, in order to take full advantage of this promising technology, the delays of various parts of the receiving equipment must be stabilized and measured.

12.6 Use of GLONASS

In most ways GLONASS [Gouzhva *et al.*, 1992] is similar to the GPS but, until recently, the international time metrology community rarely used it because suitable commercial receivers were not available. This is now changing and the first permanent international time links have been established. GLONASS timing receivers are now available and conform to the same standards as GPS timing receivers. Several studies have been conducted to compare performance of GPS and GLONASS C/A-code single-channel measurements [Lewandowski *et al.*, 1993]. All of them show that the two systems have similar performance for regional links. GLONASS receiver antennas also show temperature dependence similar to that seen with GPS antennas. For intercontinental links, it is necessary to use post-processed precise GLONASS ephemerides.

Some recent studies demonstrate the feasibility of GPS + GLONASS C/A-code multi-channel time transfer [Lewandowski *et al.*, 1997]. The dual-system multi-channel and multi-code receivers operate smoothly with no software problems. They use standard software and format [Lewandowski *et al.*, 1996]. Comparison with other GPS timing receivers has provided a test of their metrological quality. Common use of GPS and GLONASS in multi-channel mode almost doubles (GLONASS constellation is incomplete) number of observations. The stability gain of GPS + GLONASS multi-channel time transfer with respect to single-channel GPS measurements is about four. The GPS multi-channel alone provides a stability gain of about three.

Use of GLONASS P-code presents an obvious advantage. This is the lower noise of the basic code measurement known as pseudorange. The precision of the measurement of pseudorange is of the order of 1/100th of the wavelength of the code considered. This means that the precision of the pseudo-ranges made on GLONASS P-code are 1 ns (wave length of GLONASS P-code is 30 in or about 100 ns), while the GLONASS C/A-code allows the precision of measurement of the pseudorange of only 10 ns (wave length of GLONASS C/A-code is 300 in or about 1 000 ns). Some tests were performed recently using newly available GLONASS P-code timing receivers. Despite difficulties due to different GLONASS frequencies causing different hardware delays, the first results are very promising [Azoubib *et al.*, 1998].

12.7 Conclusion

GPS has become the workhorse of the timekeeping community. It is a source of time and can be used to compare clocks. Currently, GPS is close to being a ns/day time-transfer system. Figure 12-8 compares the newer improved GPS techniques with the standard GPS CV technique now being used and several other techniques. However, there are developments taking place that will dramatically improve that number.

FIGURE 12-8

Comparison of some newer time transfer techniques to classical GPS one-channel Common View time transfer. (Clock data and Loran-C, TWSTFT and GPS Carrier phase data courtesy of D. W. Allan.)

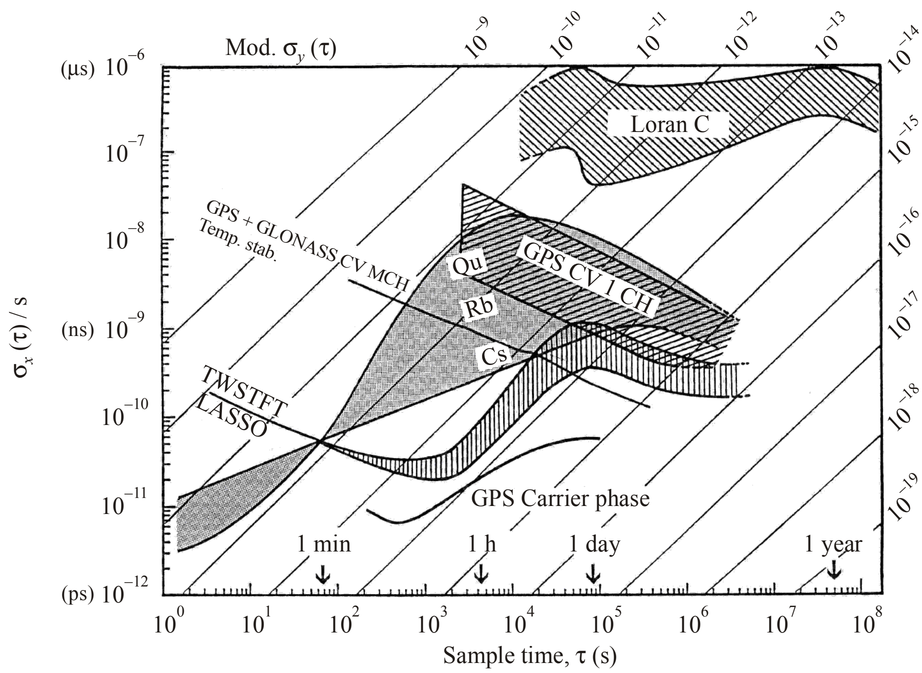

Sat_time_freq-12-08

GPS C/A-code time transfer, as now practiced, is limited mainly by hardware instabilities and, over long distances, by uncertainty in the determination of ionospheric delays. The uncertainty of single-channel comparisons is of 3-4 ns for one-day averaging times, sometimes larger. This is barely sufficient for the comparison of average commercial HP5071A clocks. This technique is obviously insufficient for the comparison of high-performance laboratory frequency standards. GPS carrier phase offers the greatest potential for frequency comparisons because it has greater precision. When operational, it will be used for the comparison of high-performance laboratory frequency standards and may serve for the evaluation of other time and frequency transfer techniques. It should reach stability on the order of 100 ps/day, perhaps even better. If GPS carrier phase ambiguities can be resolved then this technique can be used not only for frequency transfer but also for time transfer.

Also there is the evolution of GPS itself. The "GPS modernization" program will use a second and a third civil coded signal. This will lead to significant progress, as more civil frequencies would allow more accurate measurements of ionosphere and better solution of GPS carrier phase ambiguities. Also, the future GPS constellation may contain more satellites and the satellite signal may have more power. In accordance with the Presidential Directive of March 1996, SA was set to zero. This greatly improved direct time distribution through GPS.

One of the most important steps for improved receiver accuracy is the development of a built-in calibration system for timing receivers. This represents the best solution to resolving the present difficulties with delay instabilities of GPS timing equipment. Until built-in calibration systems are commonly available, antenna electronic assemblies and any outdoor, in-line amplifiers, and probably antenna cables, must be temperature stabilized. The use of temperature-stabilized enclosures should improve not only C/A-code CV time transfer and time dissemination, but also frequency comparisons by carrier phase measurements.

Combining GPS and GLONASS code measurements within timing equipment receivers definitely seems to provide an additional value for international time comparisons. For GLONASS, the possibility of the access of precise code on two frequencies provides a means to measure ionospheric delays. Also, GLONASS signals are broadcast on 48 frequencies (in the future 24 frequencies) in contrast to GPS that are broadcast on two. This provides a robust broadcasting system more resistant to interference. However, GLONASS has to improve its reliability and assure continuity of operations.

What of the future? Over the past 45 years the performance of atomic frequency standards has improved on average by an order of magnitude every seven years. The needs for their future comparison over large distances will require adequate progress in time and frequency transfer. The information detailed in this paper promises that this challenge will be met by advanced GPS time-transfer techniques.

References

ALLAN, D. W. [November, 1987] Time and frequency (time-domain) characterization, estimation and prediction of precision clocks and oscillators. *IEEE Trans. Ultrasonics., Ferroelectrics., Fre . Contr.*, UFFC-34, p. 647-654.

ALLAN, D. W. and LEPEK, A. [1993] Trends in international timing. *Proc. 7th European Frequency and Time Forum*, p. 221-227.

ALLAN, D. W. and THOMAS, C. [1994] Technical directives for standardization of GPS time receiver software. *Metrologia*, Vol. 31, **1**, p. 69-79.

ALLAN, D. W. and WEISS, M. M. [1980] Accurate time and frequency transfer during common-view of a GPS satellite. *Proc. 1980 Frequency Control Symp.*, p. 334-336.

AZOUBIB, J., LEWANDOWSKI, W. and DE JONG, G., [1998] A new approach to international time transfer: multi-channel multi-code GPS+GLONASS common-view observations. *Proc. 12th European Frequency and Time Forum*, 1998, p. 87-93.

BAERISWYL, P., T. SCHILDKNECHT, J. UTZINGER, and G. BEUTLER, [1995] Frequency and time transfer with geodetic GPS receivers: First results. *Proc. 9th European Frequency and Time Forum*, p. 46-51.

BAUMONT, F., FRIEDELANCE, P., GRUDLER, P., VEILLET, C., WIANT, L., LEWANDOWSKI,W and G. PETIT [1993] Preliminary report on the comparison of LASSO and GPS time transfers. *Proc. 7th European Frequency and Time Forum*, p. 641-643.

BIPM [1997] Report of the open forum on GPS and GLONASS standardization. Presented at 6th CGGTTS Meeting, 1997 (available, on request from).

BUISSON, J. A., OAKS, O. J. and LISTER, M. J. [1985] Remote calibration and time synchronization (R-CATS) between major European time observatories and the US Naval Observatory using GPS. *Proc. 17th Annual. P7TI Meeting*, p. 201-222.

BUTTERLINE, E. [January, 1993] Reach out and time someone. *GPS World*, p. 32-40.

FRIEDELANCE, P. [1994] L'expérience LASSO. Ph. D. dissertation, Université de Paris 6, Paris, France.

GOUZHVA, J. *et al.* [July/August, 1992] High-precision time and frequency dissemination with GLONASS. *GPS World*, p. 40-49.

GURTNER, W. [1994] RINEX: The receiver independent exchange format version 2. Astronomical Institute, University of Berne, Berne, Switzerland.

KIRCHNER, D., RESSLER, H., GRUDLER, P., BAUMONT, F., VEILLET, C., LEWANDOWSKI, W., HANSON, W., KLEPCZYNSKI, W. and UHRICH, P. [September, 1993] Comparison of GPS common-view and two-way satellite time transfer over a baseline of 800 km. *Metrologia*, Vol. 30, **3**, p. 183-192.

KLEPCZYNSKI, W. J., [1996] GPS for precise time and time interval measurement. *Global Positioning System: Theory and Applications*, Vol.11. B. W. Parkinson and J. J. Spilker, Jr., Eds. Washington, DC: American Institute of Aeronautics and Astronautics, chapter 17, p. 483-500.

LEWANDOWSKI, W. [1996] Determination of the differential time correction between GPS time equipment located at the Observatoire de Paris, Paris, France, and the United States Naval Observatory, Washington, DC, USA. BIPM, Rep. BIPM-96/10.

LEWANDOWSKI, W., AZOUBIB, J., DE JONG, G., NAWROCKI, J. and DANAHER, J.[…] A new approach to international time and frequency comparisons: "All-in-view" multi-channel GPS+GLONASS observations. *Proc. ION GPS97*, p. 1085-1091.

LEWANDOWSKI, W., AZOUBIB, J., GEVORKYAN, A. G., BOGDANOV, P. P., KLEPCZYNSKI, W. J., MIRANIAN, M., DANAHER, J., KOSHELYAEVSKY, N. B. and ALLAN, D. W. [1996] A contribution to the standardization of GPS and GLONASS time transfers. *Proc. 27th P7TI Meeting*, p. 367-383.

LEWANDOWSKI, W., MOUSSAY, P., CHERENKOV, G. T., KOSHELYAEVSKY, N. B. and PUSHKIN, S. B. [1993] GLONASS common- view time transfer. *Proc. 7th European Frequency and Time Forum*, p. 147-151.

LEWANDOWSKI, W., MOUSSAY, P., DANAHER, J., GERLACH, R. and LEVASSEUR, E. [1997] Temperature-protected antennas for satellite time transfer receivers. *Proc. 11th European Frequency and Time Forum*, p. 498-503.

LEWANDOWSKI, W., PETIT, G. and THOMAS, C. [April 1993] Precision and accuracy of GPS time transfer. *IEEE Trans. Instrum. Meas.*, Vol. 42, p. 474-478.

LEWANDOWSKI , W. and THOMAS, C. [July 1991] GPS time transfer. *Proc. IEEE*, Vol. 79, **7**, p. 991-1000.

LEWANDOWSKI, W. and TOURDE, R. [1990] Sensitivity to the external temperature of some GPS timing receivers. *Proc. 22nd P7TI Meeting*, p. 307-316.

OVERNEY, F., PROST, L., DUDLE, D., SCHILDKNECHT, T., BEUTLER, G., DAVIS, J. A., FURLONG, J. M. and HETZEL, P. [1998] GPS time transfer using geodetic receivers (GeTT): Results on European baselines. *Proc.12th European Frequency and Time Forum*.

PETIT, G., MOUSSAY, P. and THOMAS, C. [1996] GPS time transfer using carrier-phase and P-code measurements. *Proc. 10th European Frequency and Time Forum*, p. 279-285.

SCHILDKNECHT, T., BEUTLER, G., GURTNER, W. and ROTHACHER, M. M. [1990] Toward sub-nanosecond GPS time transfer with geodetic GPS receivers: First results. *Proc. 4th European Frequency and Time Forum*, p. 335-346.

CHAPTER 13

GEODETIC TECHNIQUES USING GPS PHASE AND CODE MEASUREMENTS

Page

13.1 Introduction

GPS methods have been the basis for most high-accuracy time and frequency transfers for more than two decades. The usual approach for maintaining Coordinated Universal Time (UTC) has relied primarily on single-frequency pseudorange (C/A-code) data and simple common-view (CV) data analyses that assume cancellation of most systematic errors [Allan and Weiss, 1980]. With improved data yields thanks to widespread replacement of the earlier single-channel receivers by multi-channel units, intercontinental CV comparisons have achieved uncertainties of a few ns averaged over five-day intervals [Lewandowski *et al.*, 1997]. In contrast, the parallel development of high-accuracy geodetic methods using dual-frequency GPS carrier-phase observables has demonstrated positioning repeatabilities at the cm level for one-day integrations [Zumberge *et al.*, 1997]. Assuming such positioning results can also be realized as equivalent light travel times (~33 ps), the potential for GPS carrier phase-based geodetic techniques to permit sub-ns global time comparisons is evident, as widely recognized by the 1990s. In fact, the method has been shown to have a precision approaching ~100 ps at each epoch in favorable cases for one-day analysis arcs [Ray and Senior, 2003]. The absolute time transfer capability remains limited to >1 ns, however, due to instrumental calibration uncertainties [Petit *et al.*, 2001]. In addition to higher precision (equivalent to frequency stability), the geodetic approach easily lends itself to global time and frequency dissemination. This is consistent with the basic GPS operational design (albeit with replacement of the GPS broadcast message with more accurate information), unlike the point-to-point nature of CV, which furthermore degrades as baseline distances increase.

The essential ingredients of the geodetic method are the availability of dual-frequency GPS observations for both pseudorange (usually “codeless” P-code) and carrier phase, recorded typically every 30 s, coupled with comprehensive analysis modeling of the undifferenced one-way signal propagation accurate to the mm level. Standard errors for phase and code measurements are about 1 cm and 1 m, respectively, at each frequency. For both observables, multipath errors are thought to dominate over thermal noise [Langley *et al.*, 1996]. The phase data are vital for modern geodetic applications because of their higher precision; therefore continuous sampling is required in order to ensure reliable phase continuity throughout a satellite pass. For relative positioning solutions, where double-differencing algorithms are commonly employed to remove all clock-like effects of the satellites and the tracking receivers, code data are not normally used due to their very low weight. However, to analyze undifferenced data and extract clock estimates, it is necessary to add the code data in order to separate the otherwise indistinguishable clock offset and phase cycle ambiguity parameters. The combination of observables in this way effectively smoothes the noisy code data taking advantage of the much more precise phases. For each receiver-satellite pair, the quality of the clock estimates is maximized by ensuring the longest possible spans of continuous phase data free of cycle slips, thus minimizing the number of ambiguity parameters. Modern geodetic receivers track 12 or more satellites simultaneously with individual passes of up to about 4 h each. Apart from viewing obstructions, the most problematic tracking is usually at the lowest elevation angles where the signal strength is weakest and the atmospheric path delay and multipath effects are greatest and most variable.

This chapter reviews the GPS geodetic time transfer method and the status of recent developments. In principle, the same methods can be used with other global navigation satellite systems (GNSSs). While the existing GLONASS constellation has not been widely exploited for this purpose, it is generally anticipated that the European GALILEO system may significantly enhance current capabilities.

13.2 Instrumental and hardware considerations

Any component in the GPS signal path (or even nearby sometimes) can possibly affect time and frequency performance. With respect to time transfer, the hardware considerations that apply for a geodetic installation basically follow the same common-sense rules as for any other timekeeping facility. The overall configuration of receiver equipment should be kept as simple as possible with an utmost concern placed on the stability of the system components and their environment. To the extent feasible, new components should be thoroughly tested before being deployed operationally. When changes are needed, limiting them to a single component at a time allows a clearer assessment of the consequences.

13.2.1 GPS satellite components

The basic information needed to utilize GPS is provided in the interface control document ICD-GPS-200, or the newer interface specification IS-GPS-200. Positions of the satellites are broadcast for the effective phase centers of the transmitter antenna arrays. However, internally the GPS system computes dynamical orbits for the center of mass point of each satellite and transforms the results to the phase centers. The vector offsets used for this are not officially provided, as they are not required by the ICD user.

However, the National Geospatial-Intelligence Agency (NGA) publishes the offsets at their website, (earth-info.nga.mil/GandG/sathtml/).

Users who compute their own satellite ephemerides and clock values must also assume some set of antenna phase center offsets. When comparing satellite clock values from different sources, it is necessary to account for any discrepancies in the radial components of the assumed phase center offsets as these will manifest themselves as biases in the satellite clocks. The situation is complicated by the difficulty of making accurate measurements of the actual antenna offsets [Mader and Czopek, 2002], which has led to the use of different sets of values.

In contrast to the GPS broadcast message, the precise orbits of the International GPS Service (IGS) are referenced to the satellite centers of mass. When the first Block IIR satellite was launched in 1997 it became apparent that its offset in the direction to the Earth differs from earlier spacecraft. In order to ensure that satellite clock determinations from the various IGS Analysis Centers can be compared and combined consistently, the IGS adopted a common set of values for the antenna phase center offset vectors, implemented starting 29 November 1998:

Blocks II & IIA	dx = 0.279 m	dy = 0.000 m	dz = 1.023 m	[IGS]
Block IIR	dx = 0.000 m	dy = 0.000 m	dz = 0.000 m	[IGS]

The usual satellite-fixed coordinate system applies, where the z-axis is directed from the satellite center of mass towards the Earth center, the y-axis is aligned with the solar panels, and the x-axis is orthogonal. Mader and Czopek [Mader and Czopek, 2002] determined the dz offset to be 1.66 m for an unused Block IIA antenna array on the ground. The offsets used by the GPS operational system are similar to those of the IGS for Blocks II and IIA:

Blocks II & IIA	dx = 0.2794 m	dy = 0.0000 m	dz = 0.9519 m	[GPS]

but differ significantly and are distinct for each Block IIR spacecraft, most being around 1.5 to 1.6 m for dz. If a user wishes to compare the IGS satellite clock values with other results using different antenna offsets, then corrections must be applied according to:

$$C_i(\text{user}) = C_i(\text{IGS}) - \{[\, dz_i(\text{user}) - dz_i(\text{IGS})\,] / c\} \tag{13-1}$$

where:

- dz_i(IGS): the IGS value for dz for satellite PRNi
- dz_i(user): the user's value for dz for satellite PRNi
- C_i(IGS): the IGS clock value for PRNi
- C_i(user): the user's clock value for PRNi
- c: the speed of light (299792458 m/s).

GPS broadcasts are currently within two L-bands, having nominal central frequencies of:

$$L_1 = 154\cdot 10.23 = 1575.42 \text{ MHz and } L_2 = 120\cdot 10.23 = 1227.60 \text{ MHz.}$$

The L_1 band contains a 1.023 MHz C/A code modulation as well as an encrypted P1(Y) code (10.23 MHz) and a 50 bit/s message code.

On L_2 only a precise 10.23 MHz P2(Y) code is currently modulated, though a second civilian code is to be added in the near future.

While nominally in phase, the various GPS modulations inevitably have significant non-zero biases with respect to one another. Most important of these is the pseudorange bias between the P1 and P2 modulations. The peak-to-peak dispersion in P1-P2 biases is more than 10 ns. Since the broadcast clocks are determined for the ionosphere-free P1/P2 linear combination (see more below), single-frequency users must compensate for the P1-P2 biases by using the T_{GD} values given in the navigation message (see ICD-GPS-200). In generating its ionospheric map products, the IGS also reports its own observed P1-P2 biases, known as differential code biases (DCBs). For reference, the nominal relationship between broadcast T_{GD} values and IGS DCBs is given by:

$$\mathrm{DCB} = [1 - (77/60)^2] * T_{GD} \quad (+\text{ scale offset}) \tag{13-2}$$

for each individual satellite, except that the two scales differ by a time-varying offset because the mean value for DCBs is set by IGS convention to zero whereas the broadcast T_{GD} values are referenced to an empirical absolute instrumental bias. The scale difference, in T_{GD} units, has gradually been decreasing, from about -4.3 ns at the beginning to 2000 to –7.1 ns in mid-2004. The broadcast T_{GD} values are reviewed and updated quarterly while the IGS monitors and reports its DCBs continuously at daily intervals.

The T_{GD} correction procedure assumes the P1-P2 bias is appropriate for single-frequency users of the C/A-code, the same as for P1. In fact, this is not strictly true because of P1-C/A biases. They have a peak-to-peak range of about 5 ns. While currently ignored in ICD-GPS-200, the IGS has accounted for such biases since 1999. It is necessary because some geodetic receivers track C/A instead of P1 and some report [C/A + (P2-P1)] instead of true P2, which have different biases [Ray *et al.*, 2000]. To avoid mixing data with different satellite biases, which would degrade the IGS satellite clock products (and precise point positioning using them), procedures for handling and analyzing diverse GPS data sets were implemented by the IGS to maintain consistency. As new modulations are added to the GPS signals in the future, it is expected that calibration values for the additional inter-signal biases will be included in the broadcast navigation message and monitored by the IGS.

Another complication of the satellite transmit signals is the phase pattern of the beam. While generally assumed to be perfectly hemispherical, there is strong evidence otherwise [Schmid and Rothacher, 2003]. Neglect of the non-ideal phase patterns, for satellites or tracking antennas (see more below), causes mostly errors in the GPS frame scale (i.e., radial direction) at the level of roughly 10 to 15 ppb. While important for many geodetic applications, this effect is probably not significant for most time comparisons, at least not until instrumental calibrations attain sub-ns accuracy.

A final point to note concerning the GPS satellite clocks is that the intentional degradation of the GPS clock signals by selective availability (SA) was discontinued at 04:00 UTC on 02 May 2000. Prior to that time, the RMS clock variations over a day were at the level of roughly 80 ns. Since then, the clock stability is that intrinsic to each satellite’s timekeeping system, which is more than an order of magnitude better. In addition to allowing civilian access to greatly improved GPS positioning and timing determinations, all users, especially those taking advantage of the much more accurate IGS products, can now interpolate tabulated GPS clock values with far smaller errors than before.

13.2.2 GPS tracking antenna installations

A geodetic installation is normally built about an ultra-stable monument that provides the physical basis for long-term, high-accuracy measurements. Deeply anchored concrete piers, cross-braced metal rod structures, and steel masts are among the monument designs commonly used, although buildings are also used, especially for timing applications.

Information about various monument types is available at: igscb.jpl.nasa.gov/network/monumentation.html.

Permanently and securely embedded into the monument is a geodetic marker with an inscribed point to which the station coordinates are referred. The best practice is to also establish a high-accuracy local geodetic control network to monitor relative motions of the primary GPS station.

In order to distinguish very local monument displacements from larger-scale effects, the control network should include permanent markers covering a range of distances from ~10-100 m out to around 10 km. The local network must be resurveyed periodically to be useful and may be partly formed by other continuously operating GPS stations. The GPS antenna itself should be securely anchored directly over the geodetic marker in such a way that its position is fixed and the eccentricity from the marker reference point to the antenna reference point (ARP) can be measured with an accuracy <1 mm.

A conventional ARP has been designated by the IGS for each antenna model. It must be a physically accessible point, as opposed to the L1 and L2 electrical phase centers, in order that local survey measurements can be made. For most choke ring antennas, the ARP is a point at the base of the preamplifier on the bottom side of the unit. The physical dimensions relating the ARP and the signal phase centers, as well as measured wavefront phase patterns, are maintained in files available from the IGS. The information on marker eccentricity and antenna dimensions is required to analyze the observational data and reduce the results to the reference station coordinates.

In cases where the highest quality geodetic performance is not required, such as many timing installations, a geodetic monument and marker might not be used. In this situation, the station coordinates are referenced directly to the ARP (or sometimes to the phase center). While expedient, this will generally cause a station's coordinates to change whenever the antenna model is changed. It is preferable to follow standard geodetic guidelines whenever practical.

High-quality, dual-frequency antennas are required for geodetic applications, including high-accuracy time transfer. The most common design features a set of concentric choke rings, available from several vendors with slightly different internal dimensions. The design has been tailored for dual-frequency reception while strongly attenuating signals near the horizon and below, where multipath reflections are usually worst [Schupler and Clark, 2001]. For time transfer applications, in particular, it is critical that the antenna be situated in such a way as to minimize multipath signals, especially code multipath. Generally, this means maintaining a clear horizon in all directions and avoiding placement of reflecting objects near the antenna. The L2 signal is particularly sensitive to back-reflections from behind the antenna [Byun *et al.*, 2002] so, if the antenna cannot be placed directly against a non-reflecting surface, then it is usually best to put it as high above any background as practical (keeping in mind stability and access requirements). In any event, the space between the antenna phase center and its backing surface should strictly avoid multiples of the L-band half-wavelength, especially in the near field of the antenna [Elosegui *et al.*, 1995]. A clear view of the sky down to at least 10° elevation, preferably 5°, is needed in order to allow robust geodetic determinations of the antenna position.

There have been some poorly supported claims of strong variations of geodetic clock estimates with temperature changes in some GPS antennas, together with recommendations to use temperature-stabilized units. While this might apply to certain low-end, single-frequency units, direct tests of a standard AOA Dorne Margolin choke ring antenna have failed to detect any sensitivity of the clock estimates to antenna temperature variations. Ray and Senior [2001] placed an upper limit of 2 ps/°C on the short-term (diurnal) temperature sensitivity and later extended this to <10.1 ps/°C for any possible long-term component [Ray and Senior, 2003]. Even smaller sensitivities, 0.17 ps/°C or less, were determined by [Rieck *et al.*, 2003] for an Ashtech choke ring model.

As with the satellite transmitter antennas, and recognized much earlier, the beam patterns of GPS tracking antennas deviate from the perfectly hemispherical ideal [Schupler *et al.*, 1994]. Effectively, this means that the phase center of the antenna, and hence the geodetic reference point, will depend on the direction of the signal from a particular satellite. Azimuthal variations have usually been ignored and only the elevation-angle dependence considered, although this is likely to change in the future. The IGS has developed sets of phase corrections to apply in the data analysis for each particular antenna model. Neglecting these effects can cause systematic errors in station height determinations up to ~10 cm. The present IGS approach uses differential phase corrections relative to the AOA Dorne Margolin T choke ring antenna as a standard reference and most of the measured values follow the methodology of Mader [1998], described at the website (www.ngs.noaa.gov/ANTCAL/).

The phase patterns of the satellite transmitters have been ignored. The IGS has transitioned to using absolute antenna patterns for satellites and tracking stations [Schmid and Rothacher, 2003].

Many permanent GPS antennas have been fitted with radomes for protection of the choke ring elements from filling with snow or miscellaneous rubbish. These invariably affect the performance of the GPS system, mostly by distorting the wavefront phases, which can give rise to apparent shifts in station position, especially height. Differences in position, with and without a radome, can reach the level of several cm.

Tests have shown that conical radomes are usually most problematic; some types of hemispherical radomes seem to show minimal effects. Currently the IGS does not account for the presence of radomes in its published antenna phase center tables – all antennas are treated as radome-free even when phase center corrections have been measured for the radomes. The best general advice is to avoid the use of radomes unless absolutely necessary. Otherwise choose a hemispherical radome whose effect has been measured and found to be minor.

13.2.3 Antenna cables and connections

The cable run from the GPS antenna to the receiver should be as short as feasible and use a single continuous segment. No signal splitters or other components should be inserted in order to ensure the best possible power and impedance matching. While specific tests of the effects of splitters or other such elements on clock performance are very limited, anecdotal evidence indicates degradations whenever additions of this type have been made. [Rieck *et al.*, 2003] report temperature sensitivity results, but did not study multipath or other effects.) The connectors should be well sealed against moisture and exposure. The type of cable should be chosen to have good phase-stability properties, low temperature sensitivity (< 0.1 ps/°C/m), and low loss. Cable runs across open ground should be avoided in favor of a trenched conduit. Generally, any effort to reduce exposure to environmental influences is advisable.

13.2.4 GPS receivers

Geodetic GPS receivers must report pseudorange and carrier phase observables at both the L1 and L2 frequencies. For time comparisons, the receiver must also have the ability to accept reference frequency and 1 PPS inputs from an external standard and use them faithfully for its internal timing functions. Such features are often purchase options for otherwise standard geodetic equipment. At L1, most receivers in the IGS network track the P1 code over the narrower C/A code, so experience with C/A-only models is limited. No side-by-side comparisons of clock performance have been reported for the different types of code tracking. On the other hand, no discernible difference has been seen for the few models in common use [Ray and Senior, 2003]. The essential requirement is that the code multipath susceptibility should be low.

Various studies have shown the detrimental effects of temperature variations on the frequency stability of GPS receivers [Rieck *et al.*, 2003], [Overney *et al.*, 1997], [Petit *et al.*, 1998], [Bruyninx and Defraigne, 1999], [Schildknecht and Dudle, 2000]. Typical sensitivities are of the order of ±100 ps/°C with large variations among individual units, even for the same model. Therefore, for high-performance time and frequency applications, it is essential that the GPS receiver equipment be maintained in an environmentally controlled location, with thermal fluctuations preferably no greater than ~0.1°C.

Many receivers have user-selectable settings for various functions such as enabling onboard code-smoothing or steering of the internal receiver clock to GPS Time. The latter setting must be disabled for useful time comparisons. It is also usually advisable to disable code-smoothing as this is better handled in the subsequent data analysis.

As with any time and frequency distribution system, it is essential that the input reference frequency and 1 PPS signals be kept coherent with one another and well isolated from interference sources. Care should be taken especially with the generation of secondary input frequencies, if required. Furthermore, the 1 PPS ticks must usually be within some small tolerance of GPS Time, such as < 30 ms, in order for the receiver to function properly.

GNSS observational data are universally transmitted using the RINEX (receiver independent exchange) format, which is described at: (ftp://igscb.jpl.nasa.gov/igscb/data/format/rinex210.txt). This document also contains format specifications for navigation messages, meteorological data, and related information. Generally, it is advisable to archive the raw, native data files from the receiver, in addition to the RINEX files, in case a problem in the translation is later discovered. Timing users can derive the file types used for CV ("CGGTTS format") from RINEX files using a tool developed at the Royal Observatory of Belgium [Defraigne *et al.*, 2001].

13.2.5 Evaluating multipath effects and system testing

Once a geodetic station has been established, the data quality should be thoroughly assessed before it is made operational. If problems are found, they should be ameliorated as much as possible. The University Navstar Consortium (UNAVCO) has developed a very informative website (www.unavco.org/facility/facility.html), which contains helpful advice and test reports on equipment for continuously operating GPS stations. They also maintain a range of software tools. In particular, the "teqc" toolset is indispensable for handling and examining raw GPS data, including RINEX file translation, data editing, and quality checking [Estey and Meertens, 1999]. Using teqc output, most fundamental problems with data quality can be spotted, such as excessive cycle slips, incomplete data capture, blockages in sky coverage, and so forth. The teqc diagnostics MP1 and MP2 measure the RMS variations of the code multipath at L1 and L2, respectively, assuming that the effects of phase multipath are negligible. An unknown bias is reset for each satellite pass, so these multipath metrics are insensitive to long-period signals that can be important for timing. Also, because of intrinsically different behavior for different receiver types, the MPi measures generally lack absolute meaning and cannot easily be compared from one site to another. However, unexpectedly large multipath variations with elevation angle and over time can indicate site or configuration problems. In at least one case, MP2 variations were found to correlate strongly with changes in geodetic clock performance [Ray and Senior, 2003].

If precise point positioning solutions (see below) can be generated for the receiver clock behavior using precise orbit and satellite clock products from the IGS, then a code-only solution compared with code+phase can reveal unexpected problems with the pseudorange data. Another useful diagnostic is the level of discontinuities in clock estimates between consecutive 1-day analysis arcs [Ray and Senior, 2003], which mostly reflects variations in pseudorange multipath noise (see below). Other methods for investigating multipath errors – such as the sky distribution of post-fit residuals from a geodetic solution or high-frequency variations in GPS signal-to-noise ratios – usually focus on phase effects, rather than on the pseudorange. The classic test, though, is repetition of a particular error pattern from one day to the next at the nominal period of one sidereal day, 23 h 56 min 4 s, corresponding approximately to the repeat cycle of the satellite-ground geometry.

13.2.6 Calibration of tracking station delays

To compare clock readings at one station with those at another using any intervening system requires that the internal delays within all the instrumental hardware be accurately known. The process of doing so is known as calibration. Generally, we may consider two classes of calibration methods: absolute determinations, where an end-to-end set of bias measurements is made using a GPS signal simulator, which itself must have been accurately calibrated; and differential determinations, where a side-by-side comparison is made against another similar system taken as a standard reference. In practice, both methods are used. A small number of geodetic receivers have been calibrated in an absolute mode. These then are used as traveling standards to differentially calibrate a much larger number of receivers deployed operationally [Petit *et al.*, 2001].

One geodetic GPS receiver type has been calibrated absolutely, the Ashtech Z-XII3T, using a simulator facility at the U.S. Naval Research Laboratory [White *et al.*, 2001], [Petit *et al.*, 2001], [Plumb *et al.*, 2005]. The absolute results agree within their reported uncertainties of about 3.5 ns with a differential measurement relative to a previously calibrated classical CV timing receiver [Petit *et al.*, 2000]. The dominant error source in the absolute calibration procedure is thought to be the GPS simulator itself [Plumb and Larson, 2005]. Subsequent differential calibrations against an absolute standard can be made with smaller uncertainties of about 1.6 ns [G. Petit, private communication].

For the convenience of users, the GPS data from a calibrated receiver can be adjusted to remove the instrumental bias in the process of generating RINEX exchange files. The specified manner of doing this is to write the clock offset correction, dT, into a field reserved on each observation epoch record and modify the reported observables according to the following relations in order to maintain their strict consistency:

$$\text{Time(corrected)} = \text{Time} - \text{Dt} \tag{13-3}$$

$$\text{PR(corrected)} = \text{PR} - (\text{dT*c}) \tag{13-4}$$

$$\text{phase(corrected)} = \text{phase} - (\text{dT*freq}) \tag{13-5}$$

where:

Time: the observation epoch

PR: the pseudorange

phase: the carrier phase for frequency “freq”.

Providing the clock offset correction value for each observation epoch allows the reconstruction of the original observations, if necessary. However, this RINEX feature is limited by the format specification to clock offsets values truncated to the nearest ns. If sub-ns clock calibration corrections are applied without using the RINEX clock offset field, then the clock correction value should be documented as a comment in the RINEX file header.

13.3 Data analysis strategies

The recognition that GPS could be utilized to achieve geodetic accuracies several orders of magnitude better than was originally conceived is usually attributed to Counselman and Shapiro [Counselman and Shapiro, 1979]. Applying astronomical techniques developed for Very Long Baseline Interferometry (VLBI), they proposed using the carrier phase as the main GPS observable rather than the pseudorange. By very precise tracking of changes in the GPS signal phase it was shown how relative position determinations could be made to the cm level rather than to tens of meters. Soon afterwards, Bossler *et al.* [1980] described methods to resolve the integer phase ambiguities of the carrier signal. Developments followed quickly thereafter, drawing heavily on the heritage of VLBI methods and models, most of which apply directly to GPS also. The main analysis differences are the additional orbit-related parameters of GPS and the relative weights of the group delay observables (vital for VLBI, not for GPS except for clock solutions) and the phase observables (vital for GPS, usually included only as low-weight time derivatives in VLBI).

13.3.1 GPS observation equation

The basic steps for reducing GPS observations are outlined in ICD-GPS-200 and many succeeding publications. For a given satellite and tracking station pair, the pseudorange observation equation for each observing frequency, i, can be written as:

$$Pi = R + c\left(C_r - C_s\right) + I_i + T + e_i \qquad (i = 1,2) \tag{13-6}$$

where:

i= 1, 2 correspond to the two frequencies L_1 and L_2

R: distance between the satellite and receiver phase centers

c: vacuum speed of light

C_r: clock synchronization error of the tracking station at the time of signal reception (including all internal delay components)

C_s: clock error of the transmitting satellite at the time of emission

I_i: ionospheric delay

T: delay due to the neutral atmosphere (mostly troposphere)

e_i: measurement error (including both thermal noise and such other sources as multipath).

Thermal noise in the antenna and receiver places a theoretical lower limit on the size of the measurement errors, which depends to some extent on the particular tracking technology employed by the receiver. Zero baseline experiments, where most external effects such as multipath can be removed, show the RMS of the C/A pseudorange and the L1 carrier phase measurement noises to be 4 cm and 0.2 mm, respectively, for a pair of Ashtech Z-12 receivers [Langley, 1996]. However, local environmental effects always dominate actual measurement noise. Standard *a priori* values for geodetic processing are around 1 m and 1 cm for the pseudorange and carrier phase and errors, respectively, based on observed post-fit residuals [Lichten and Border, 1987], [Zumberge *et al.*, 1997].

The ionosphere is dispersive (delay approximately proportional to the inverse of the frequency squared) and is opposite in sign for pseudorange and phase. The linear combination of the two frequencies:

$$P3 = 2.5457 * P1 - 1.5457 * P2 \tag{13-7}$$

is, to first order, free of ionospheric effects (but see [Kedar *et al.*, 2003] for a study of the second-order effect). So:

$$P3 = R + c\left(C_r - C_s\right) + T + e \tag{13-8}$$

where:

e: combined errors of $P1$ and $P2$.

The observation equation for phase observables is the same (expressed in distance units) with the addition of an ambiguity term ($N_i \cdot \lambda_i$) for the unknown number of phase cycles at each carrier frequency. The range, R, is given in terms of the geocentric coordinates of the satellite (X,Y,Z) and the receiver (x,y,z) antenna phase centers by:

$$R = \sqrt{\left(X - x\right)^2 + \left(Y - y\right)^2 + \left(Z - z\right)^2} \tag{13-9}$$

When using coordinates for the satellite center of mass or receiver geodetic marker, rather than phase centers, appropriate eccentricities must be applied based on external measurements. The GPS broadcast message provides values for each satellite position (phase center) and clock reading as a function of time, accurate to a few meters. With simultaneous observations of at least four different satellites and a crude model for the tropospheric delay, the position and clock reading for a user receiver can be determined to < 10 m at each epoch. If the user position is known *a priori* and only the clock is unknown, then just one satellite observation is needed.

Common-view clock comparisons are made by differencing simultaneous data from two receivers with known coordinates. Then the satellite clock error is removed, together with much of the satellite position error and tropospheric delay. For conventional CV measurements, using only single-frequency C/A pseudoranges, ionospheric modeling errors usually limit the accuracy of the determinations of remote clock differences. This can be significantly improved using the linear combination of codeless P1 and P2 observations, as is done in the P3 CV method [Defraigne *et al.*, 2001]. As a rule, the accuracy of CV clock comparisons worsens with increasing distance between the receivers because the common-mode cancellation of the neglected terms becomes progressively less effective. To attenuate these effects, the CV method for UTC has been modified in recent years. The highly accurate IGS orbits and ionosphere maps (igscb.jpl.nasa.gov) are now used to compute corrections for these effects [G. Petit, private communication]. Further refinements can be made, such as better tropospheric modeling and accounting for geophysical motions (e.g., tidal displacements). Such incremental modifications, however, fail to take advantage of the inherent precision of the phase observables, so the CV timing results cannot reach the level of the full geodetic technique, particularly over intervals less than 1 d or so.

In geodetic analyses, the broadcast navigation information is not used except possibly for the first level of data screening and editing. The highest quality *a priori* models are evaluated for all known geophysical effects and the remaining unknowns are adjusted from the data using physically plausible parameterizations. In most cases it is advantageous to fix the satellite clock and orbit values to the very accurate determinations published by the IGS since the general GPS user is unlikely to do as well. This greatly simplifies the estimation of receiver clocks, provided the IGS conventions and models are also strictly followed.

13.3.2 Methods for global solutions

In the case where satellite clocks and orbits are to be determined, rather than taken from an external source, we first consider procedures like those used by the IGS Analysis Centers, where data from a global tracking network are reduced in large simultaneous adjustments. A globally well-distributed network of receivers is required to determine satellite orbits and clocks. Analysis arcs are usually segmented into 24-hour batches, coinciding with the standard RINEX daily files that normally contain observations from 00:00:00 to 23:59:30. (Note that the IGS convention uses GPS Time for time tags in all its data files.) For some solution types, multi-day analysis arcs may be formed by linking together several successive one-day arcs. The initial processing step involves screening the data files from each station. It is necessary to check and edit for potential problem data, repair or flag slips in the carrier phases, adjust for small time tag drifts in some receiver types, and correct for pseudorange biases in cases where P1 and P2 are not available. The screened data are generally reformatted into direct access files appropriate to the chosen analysis system.

All geodetic adjustment methods assume the availability of sufficiently accurate *a priori* information that parameter estimation is linear and thus generalized least-squares methods can be applied. The broadcast navigation message can be used if no better sources are at hand. If necessary, such as for a new station, solution iteration may be used to satisfy the linearity condition. The *a priori* satellite orbits are rotated from an Earth crust-fixed frame (used for orbits distributed in the broadcast message as well as by the IGS) to an Earth-centered inertial (ECI) frame using an assumed set of Earth orientation parameter (EOP) values. Typically, the EOPs are those produced by the IGS or by the International Earth Rotation and Reference Systems Service (IERS); see their website at: (www.iers.org). In the ECI frame, the satellite orbits can be fitted to parameterized models for the dynamical motions and integrated. This step is needed to generate parameter partial derivatives if the orbits will be adjusted in the following data fitting. Various forms have been developed to describe GPS satellite motions, from the finite-element approach of Fliegel *et al.* [1992] to the empirical model of Beutler *et al.* [1994]. Even though a better physical model of the behavior of the satellites would be expected to be superior to a purely empirical approach, experience suggests that any gain is negligible. This is because, for high-accuracy geodetic applications, the orbit parameterization must be intense enough to capture cm-level motions, which is exceedingly difficult to accomplish for real satellites without using at least some empirical parameters. The motions are complicated by variations in acceleration as the exposure to solar radiation pressure changes and especially by micro-thrusting events that are used to maintain the attitude of some older satellites.

The observation equation is evaluated for each data point, using the *a priori* station coordinates also rotated to the ECI frame. In addition to the basic effects already mentioned, contributions due to a number of smaller effects must also be included (see next section). The parameters are adjusted to fit the observations by minimizing the residuals using standard methods, such as batch least-squares, sequential least-squares, or a Kalman filter. Kalman and related filters are particularly adept for handling clock parameters as they easily accommodate stochastic noise processes appropriate for realistic clock variations. For a global network of some tens of tracking stations, the full set of parameters that are usually adjusted includes:

– up to three geocentric coordinates for each station (subject to some specification of the terrestrial datum, such as constraints on the positions of certain reference stations);
– time-varying receiver clock parameters (which must be sufficient to allow nearly arbitrarily large variations from epoch to epoch);
– orbital parameters for each satellite (at least the six Keplerian elements, or equivalent, plus a Y-bias and other empirical terms);
– time-varying satellite clocks;
– time-varying zenith tropospheric delays (as well as possible azimuthal gradients); EOP offsets and rates for polar motion and length of day; and
– carrier phase ambiguities.

Sometimes, additional minor parameters are included for such effects as variations in satellite attitude or net offsets in the tracking network origin from the Earth's center of mass. The set of clock parameters have a rank deficiency of one since there is no absolute information of any clock epoch. Standard geodetic analyses resolve the defect by choosing one specific clock (usually a very stable ground clock) to be unadjusted as a reference in estimation process. Estimates of all other clocks are then determined relative to that fixed clock. Alternatively, the clock datum can be specified by fixing a linear combination of the available clocks to be equal to zero (or any specified value, such as GPS Time).

For the highest quality results, "fixing" of at least some of the phase ambiguity parameters is desirable. Because of the huge difficulty in attempting to do this with undifferenced one-way observations, the normal procedure is to apply tight constraints on the integer values of double-differenced ambiguities for selected station pairs. Successfully doing so for a major fraction of the ambiguity parameters greatly stabilizes the overall solution. In most cases, iteration of the solution can increase the number of ambiguity parameters successfully fixed and improve the data editing.

13.3.3 Reference frames and models for correction terms

In evaluating the basic GPS observation equation, a number of minor effects must also be considered if cm-level results are expected. Most of these are documented in the IERS Conventions [McCarthy and Petit, 2003]. The geocentric coordinate system used for points attached to the Earth's surface is the International Terrestrial Reference Frame (ITRF) [Altamimi *et al.*, 2002]. Transformation from ITRF to the ECI frame takes into account movements of the pole in the Earth frame and rotation about the pole. Movement of the pole in inertial space (i.e., nutation [Altamimi *et al.*, 2002]) is sometimes neglected or handled only approximately as near-Earth satellites are not very sensitive to this effect. So the ECI frame is not always precisely aligned to the International Celestial Reference Frame (ICRF), a nearly inertial system formed by the VLBI positions of extragalactic radio sources and whose origin is the solar system barycenter.

Correction terms for the satellites are the offsets described previously, between the centers of mass and the antenna phase centers, and the phase rotation of the satellite polarization due to changes in perspective. The latter effect, known in astronomy as parallactic angle, arises because the GPS signal is right circularly polarized. As the viewing geometry between the receiver and satellite varies, the polarization phase appears to change correspondingly. A correction must be applied in evaluating the carrier phase observations, but not the pseudoranges, as described by Wu *et al.* [1993].

The receiver position corrections are much more diverse and complex due to geophysical effects [McCarthy and Petit, 2003]. The mostly vertical motions of surface points due to the solid Earth ("body") tide have amplitudes of a few decimeters at mid-latitudes and must be accurately modeled. The corresponding motions of the crust due to ocean tidal loading are nearly an order of magnitude smaller at most places but can be amplified in some coastal areas. If estimating the GPS orbits, then the variations in the geopotential due to the solid Earth and ocean tides should also be included in the *a priori* orbital integrations. The pole tide correction accounts for large-scale rotational deformation due to variations in the pole's position with respect to the Earth's crust. The polar motion itself, and the rate of rotation, undergo rather large diurnal and semidiurnal modulations due to tidal motions of the ocean. When the GPS satellites are expressed in an inertial frame, corrections for these large-scale motions of the Earth frame should be applied. The IGS orbits, in an Earth-fixed frame, have already included the subdaily EOP variations so there is no net effect for a terrestrial observer. Accurate models for all these effects have been given by McCarthy and Petit [McCarthy and Petit, 2003]. In addition, users should apply the antenna-specific phase center corrections recommended by the IGS and described previously.

Even though international scientific unions advocate the use of geocentric coordinate time (TCG) for the analysis of near-Earth satellite data, most (if not all) analysis groups continue to use Terrestrial Time (TT), which differs from UTC and TAI only by an offset. On the other hand, TCG differs in rate (frequency) from TT due to general relativistic effects. Consequently, the clock frequencies from the IGS and other GPS analysis groups should be directly comparable to those measured in timing laboratories. Some physical constants, such as the gravitational constant-Earth mass product, GM, depend on the choice of relativistic reference frame so care should be taken in using the appropriate values.

Three types of relativistic corrections are usually applied in GPS processing:

1. The first-order frequency shift, relative to TT, due to time dilation and gravitational potential difference has already been applied in the GPS system by setting oscillator offsets in the spacecraft, assuming nominal orbital elements. The second-order correction for non-circular GPS orbits must be applied by the user; (see ICD-GPS-200).
2. A "dynamical" correction to the acceleration of near-Earth satellites is given in the IERS Conventions [McCarthy and Petit, 2003].
3. The coordinate time of propagation, including the gravitational delay, is given separately in the IERS Conventions (but is often neglected).

(See Kouba [2004] for further details.)

13.3.4 Precise point positioning

Rather than form large global network GPS solutions, for most applications it is much more economical and efficient to analyze data from individual stations in the precise point positioning (PPP) mode [Zumberge *et al.*, 1997]. In this approach, accurate satellite orbits and clocks are taken from some prior source and applied without adjustment. (In some variations of the PPP method, partial relaxation of the orbits and clocks is permitted.) Applying all the same models as discussed above, the user can determine coordinates, clock variations, and tropospheric delays for an isolated, single receiver [Kouba and Heroux, 2000]. The quality of the results will depend directly on the accuracy and consistency of the *a priori* satellite information. The reference frame and datum of the assumed orbits and clocks will be inherited by the PPP results so it is important that these be well defined and stable. The IGS products (see below) are expressly intended for this purpose. Kouba [2004] provides a guide to the proper use of IGS products for PPP analyses. For one-day solution arcs, typical position repeatabilities should be at the level of about 10 mm in the vertical and 3 to 5 mm in the horizontal. The PPP receiver clock results should be precise to a similar level, < 100 ps, but the accuracy (not including the calibration uncertainty) will normally be larger (see below); the PPP timescale will be that of the *a priori* satellite clocks.

13.3.5 Effects of errors on clock solutions

Errors in the analysis models, *a priori* information, or observational data will influence GPS clock estimates. Dach *et al.* [2003] have used simulations to examine the signatures of various types of input errors. For instance, a station height error will cause a frequency offset for long east-west baselines. In the time domain, a discontinuity is introduced at the boundary between processing arcs due to this error. Satellite orbit errors can have similar effects. In actual practice, these error effects are not likely to be very significant in IGS products since station and satellite positions are adjusted together with the clocks. Probably more important is the confirmation by Dach *et al.* that pseudorange noise at the 0.5 m level, even if assumed to have a white noise distribution, will cause offsets between discrete 1-day processing arcs at levels seen in actual clock results (see below). Colored pseudorange noise presumably has an even more pronounced effect on clock jumps between arcs.

Using more pseudorange data (higher sampling rate and/or longer arcs) would be expected to improve the clock accuracy. Higher sampling rates will only be effective as long as the dominant multipath wavelength is shorter than the sampling period; otherwise the clock errors will not average down with the addition of more data. As shown by Senior *et al.* [1999] for the clock formal uncertainties, longer analysis arcs should average down the code noise effects, although less effectively than $\sqrt{N}$. However, this has not been demonstrated for actual clock results, only for their formal errors. It has also not been determined whether longer arcs differ only by a net clock bias or whether the frequency content is also changed (improved). If longer arcs provide better clock accuracy only in a bias sense, then other analysis approaches should give nearly equivalent results, such as a suitable post-analysis filtering of shorter-arc results. The latter approaches could prove more economical or better suited for some applications.

Discontinuities between independent analysis arcs are natural and expected for all geodetic parameters, including orbits, tropospheric delays, as well as clocks. The offsets should reflect the inherent quality of the GPS data and analysis methods. The magnitude of clock jumps tends to be larger than for most other parameters because only code data contribute, though effectively averaged over the analysis arc. Various approaches have been considered to minimize the day-boundary clock discontinuities. The obvious method would be to avoid discrete analysis batches altogether and to use some type of continuous processing scheme [Petit *et al.*, 1999; Senior *et al.*, 1999].

However, this is difficult to accomplish in practice and can cause some error effects to accumulate [Senior *et al.*, 1999]. Long analysis arcs will also cause clock estimates to be correlated over the same periods (random walk type statistics), which could limit the stability that might otherwise be obtained using independent analysis arcs (white noise behavior). An alternative method to remove analysis discontinuities is to concatenate time series using overlapping arcs to determine the offsets [Bruyninx and Defraigne, 1999], [Larson *et al.*, 2000]. Even if the clock jumps at arc boundaries obey a white noise distribution [Ray and Senior, 2003], the effect on the concatenated series will be the addition of a random walk noise component. In other words, the concatenation process also causes long-term clock correlations and could limit the long-term stability that might otherwise obtain. Dach *et al.* [Dach *et al.*, 2006] consider other more sophisticated methods of generating nearly continuous clock results within the estimation process itself by passing information from one arc to the next. These act much like a filter/smoother to improve the short-term time transfer stability with little effect at longer intervals.

It is difficult to understand the widespread obsession with suppressing clock jumps at arc boundaries, especially when they are small (at the 100 to 200 ps level). Using methods that introduce long-term correlations into the clock time series (such as by concatenation) would seem to be particularly counterproductive. If elimination of the discontinuities is genuinely needed, then a filter/smoother method is probably preferable to avoid the problem of correlated time series, although this can distort the short-term clock behavior. On the other hand, the discontinuities themselves provide valuable diagnostic information on the quality of the station installation (see below). If the jumps are larger than the standard noise level of about 120 ps [Ray and Senior, 2003], then the underlying causes should be identified and ameliorated, not hidden from view by post-analysis manipulations.

13.4 IGS clock products and timescales

From its inception in 1994, the IGS has provided daily files of accurate satellite positions and clock readings, tabulated at 15-min intervals. Since then, new or modified products have been added from time to time. All IGS products (http://igscb.jpl.nasa.gov/components/prods.html) are formed by the weighted averaging of solutions submitted by up to eight contributing Analysis Centers. While the data sets used by the individual groups usually overlap, the effects of differing analysis strategies, modeling, and software are largely independent. So, properly weighted combinations of the individual results are generally superior to any single solution. In this way, the IGS products probably benefit in precision and accuracy, but certainly in stability, reliability, and robustness, compared to the results of any individual analysis group.

13.4.1 Available product sets

The IGS “classical” clock products were changed on 5 November 2000 (GPS Week 1087) when a new combination algorithm was implemented and the clock products were expanded to include many of the receivers in the tracking network, as well as the satellites [Kouba and Springer, 2001]. The tabulation interval of the new clocks (satellites and tracking stations) was reduced to 5 min, compared with the prior 15 min sampling of the satellite clocks.

Three series of product lines are generated based on data latency:

1. the Ultra-Rapid products (with satellite clocks but not receivers), which are intended for real-time users;
2. rapid products, released about 17 h after the end of each day;
3. the definitive Final products, released about 13 days after the end of each week.

Table 13-1 summarizes the IGS orbit and clock products, latencies, and estimated accuracies. (In addition to those shown in the table, the IGS provides ionospheric maps, tropospheric zenith path delays, Earth orientation parameters, and so forth.) All products are available from the IGS data centers or Central Bureau; (igscb.jpl.nasa.gov). Use of the IGS Rapid or Final products instead of broadcast information allows for PPP determinations at the 1 cm level for 24-h arcs.

The IGS tracking network consists of more than 350 globally distributed receiver installations. All stations operate continuously and report daily (at least) RINEX observation files with 30-s samples. Most of the stations use internal crystal oscillators, which are steered by their own observations to track GPS Time, but more than 100 IGS stations are equipped with external frequency standards. Figure 13-1 shows the distribution and type of external standards within the IGS network (as of November 2004). About 51 use H-maser standards, 28 use Cs clocks, and 27 use Rb clocks. A subset of these, about 20, are co-located at timing labs.

TABLE 13-1

IGS combined orbit and clock products and their characteristics compared with broadcast values

GPS Satellite ephemerides and satellite/station clocks		Accuracy estimates	Latency	Update intervals	Sample interval
Broadcast	**Orbits**	~200 cm	Real time	--	Daily
	Satellite clocks	~7 ns			
Ultra-rapid (predicted half)	**Orbits**	~ 10 cm	Real time	Four times daily	15 min
	Satellite clocks	~ 5 ns			
Ultra-rapid (observed half)	**Orbits**	< 5 cm	3 h	Four times daily	15 min
	Satellite clocks	~ 0.2 ns			
Rapid	**Orbits**	< 5 cm	17 h	Daily	15 min
	Satellite and station clocks	~ 0.1 ns			5 min
Final	**Orbits**	< 5 cm	~ 13 days	Weekly	15 min
	Satellite and station clocks	~ 0.1 ns			5 min

Orbit accuracy estimates, except for predicted orbits, are based on comparisons with independent laser ranging results. Precisions are better than the quoted accuracies. Product files are for 24-h periods except that the ultra-rapids span 48 h. The 5-min clock data are available in “clock RINEX” format files, while 15-min clock samples are available in SP3 format files together with the satellite ephemerides.

FIGURE 13-1

Map showing distribution of IGS stations using external frequency standards (as of November 2004). Colors indicate the type of standard: red are H-masers, yellow are cesiums and blue are rubidiums. IGS stations co-located at timing labs are indicated by star symbols

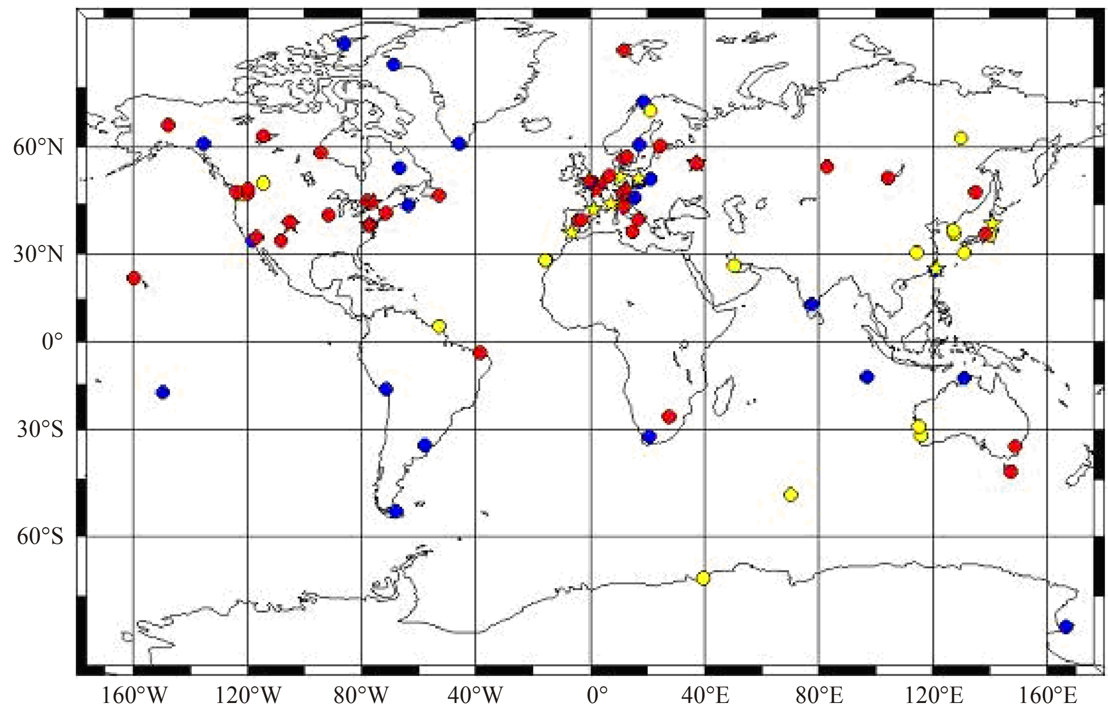

Sat_time_freq-13-01

13.4.2 IGS timescales

There is no specific requirement for the underlying timescale of the clock products when used for geodetic positioning applications, except that it should be reasonably close to GPS Time. An important strength of GPS geodesy is that it does not depend, to first order, on the stability or accuracy of the timescale since the effects of clocks can be removed by double differencing. Nonetheless, it is desirable for the reference timescale to possess other properties, such as being highly stable and accurately traceable to UTC. These qualities enhance the value of the IGS clock products for applications other than pure geodesy, especially for timing operations.

The IGS originally used as a reference for its clock products a simple daily linear alignment of the observed satellite clocks to broadcast GPS Time. However, the instability of GPS Time is comparatively large, about 2×10^{-14} at 1 day, which is at least an order of magnitude poorer than the instability of the best frequency standards in the IGS network. Even some of the newer Block IIR satellites have clocks that are more stable than the ensemble GPS Time due, in part, to the bang-bang steering algorithm used to keep the broadcast timescale aligned to UTC (via the realization maintained by the U.S. Naval Observatory). The old IGS procedure of aligning its clocks each day to GPS Time introduced large day-to-day discontinuities in both time and frequency (Fig. 13-2). There is no impact of this procedure on the usefulness of the products for precise positioning, but the utility for time and frequency dissemination is certainly limited.

FIGURE 13-2

GPS geodetic time transfer estimates for the BRUS station in Brussels, during the period 28 March through 2 April 2004

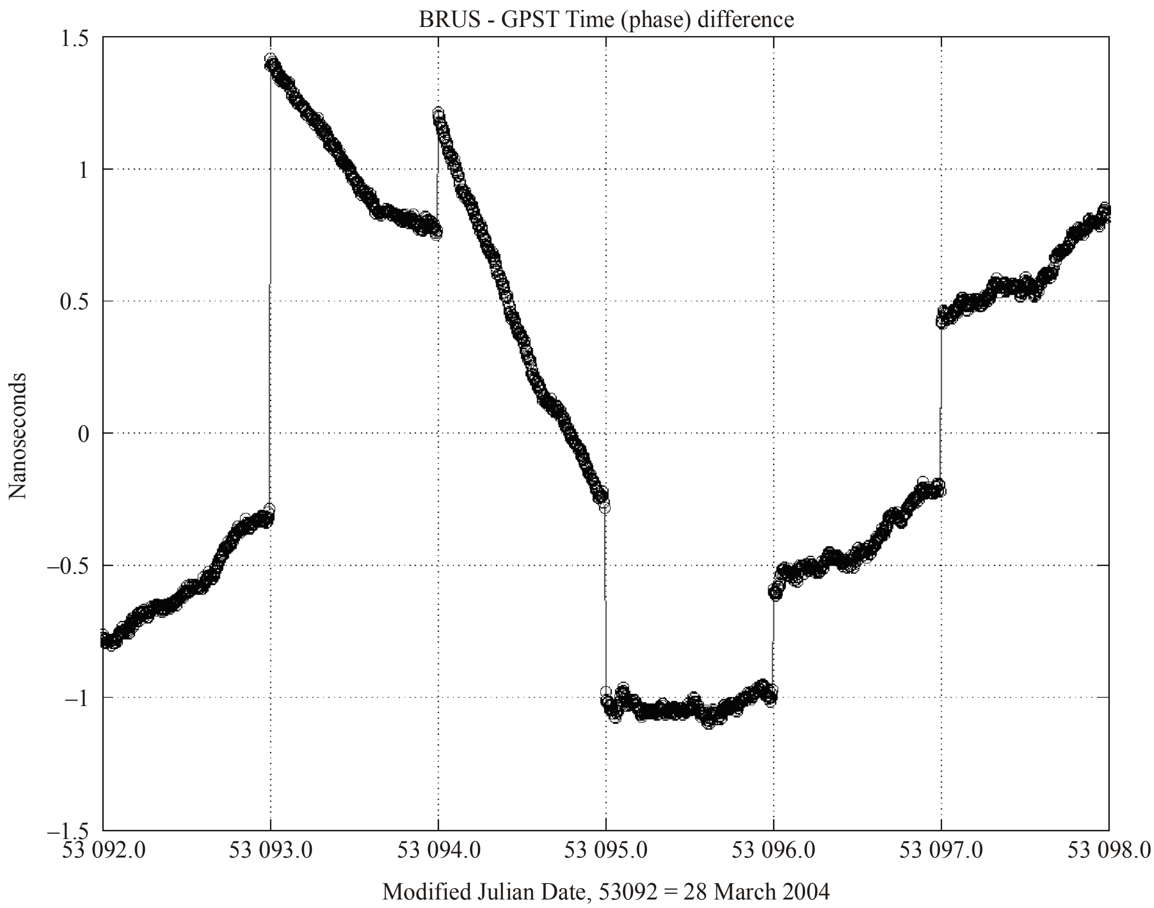

Sat_time_freq-13-02

The time transfer estimates in Fig. 13-2 are referenced to a daily linear alignment to GPS Time. The BRUS instability is dominated by the daily linear timescale alignment to broadcast GPS Time, which is responsible for the large discontinuities in time and in frequency. A linear trend has been removed for plotting.

To improve the instability of its Rapid and Final clock products, new IGS internal timescales were developed. The new timescales are formed as weighted ensembles of the included clocks, for both stations and satellites. A detailed description of the algorithm is given by Senior *et al.* [Senior *et al.*, 2003].

Each timescale ("IGRT" for the Rapids and "IGST" for the Finals) is driven largely by the available H-masers, though lesser clocks can contribute slightly, including the rubidium clocks onboard the Block IIR satellites.

The algorithm is a Kalman filter implementation with a simple polynomial model for each clock followed by a linear quadratic Gaussian (LQG) algorithm for loosely steering the timescales to GPS Time.

Weights for each clock are determined iteratively and dynamically based on the observed instability at several averaging intervals less than 1 day. An upper limit of weights is imposed for each clock to avoid the situation of a single clock overtaking the timescales [Thomas and Azoubib, 1996].

The LQG steering algorithm is critically damped with a time constant of about 30 – 40 days. The results are timescales with instability generally better than about 1×10^{-15} at 1 day, but still limited in the medium and longer terms by the steering to GPS Time. There are periods however when the instability of the timescales can be degraded somewhat, such as when the number H-maser stations in the clock products in unusually small.

Figure 13-3 shows the performance of the BRUS clock after changing the reference to the IGS Finals timescale, IGST. The inter-station clock information is the same as in Fig. 2; only the underlying timescales are different. The much improved stability using the IGS timescale is evident. The remaining small discontinuities at some day boundaries reflect mostly the local BRUS data quality.

It is possible that some effects of individual clocks, including day-boundary jumps, can adversely affect the ensemble timescales, due for instance to undetected data editing problems. However, evidence indicates that any such limitations are minor and that the ensemble timescales are far superior to any single contributing clock.

The new IGS timescales were implemented in the official products in early March 2004 (see IGS Mail No. 4875 at: igscb.jpl.nasa.gov).

Clock products aligned to the same internal timescales are available from November 2000 at: (https://goby.nrl.navy.mil/IGStime).

FIGURE 13-3

Same BRUS clock data as shown in Fig. 13-2 except referenced to the IGS Final clock timescale, IGST. A linear trend has been removed for plotting

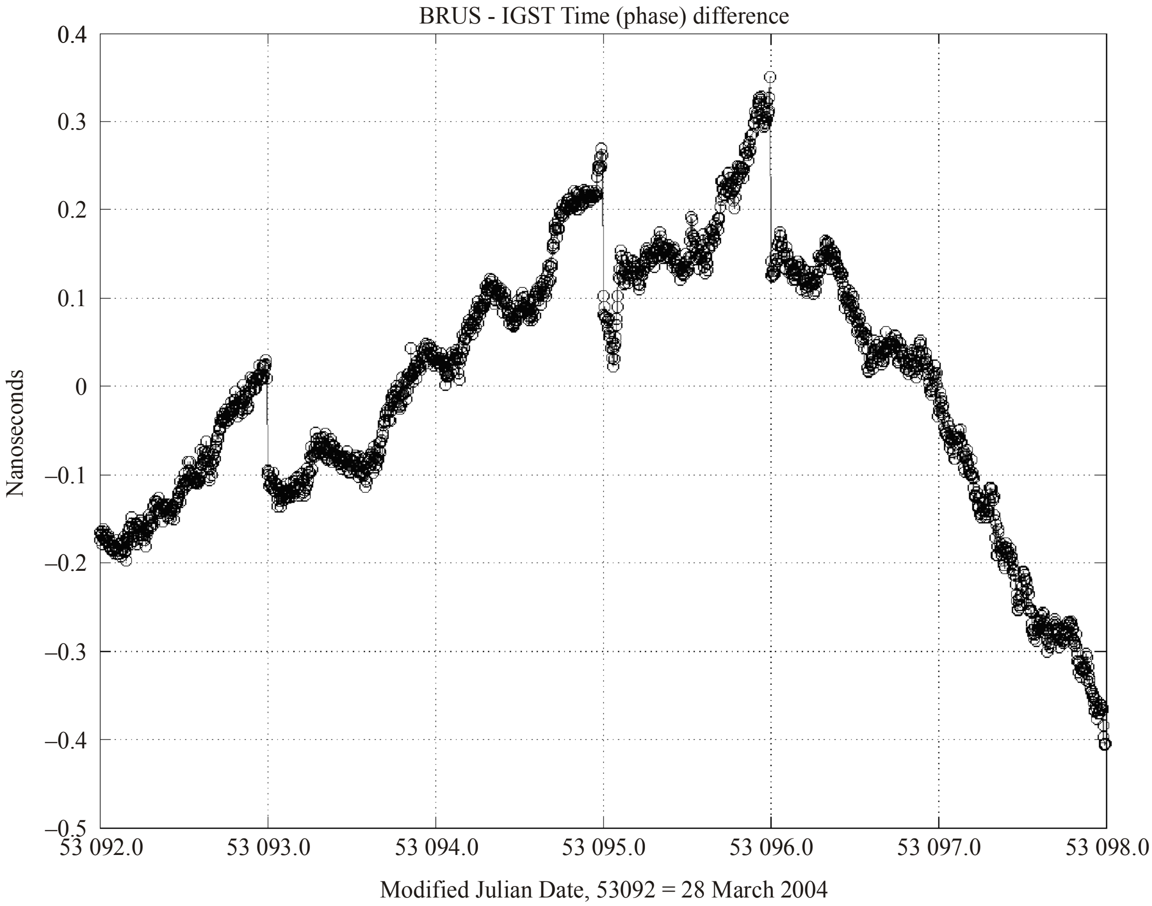

Sat_time_freq-13-03

The long-term variation of each IGS timescale is illustrated in Fig. 13-4 relative to GPS Time and to UTC (approximately). Though the subdaily to daily instability of the IGS timescales is greatly improved over GPS Time, the longer-term instability is similar owing to the continued reliance on GPS Time. Efforts are underway to tie the IGS timescales to UTC more accurately by using data from the BIPM and taking advantage of IGS stations co-located at timing laboratories [Senior *et al.*, 2004].

The top plot on Fig. 13-4 shows UTC minus GPST from the BIPM Circular T series as well as the IGS timescales IGST and IGRT minus GPST. The IGS and BIPM realizations of GPST can differ by several ns due to distinct observational and analysis strategies [Senior *et al.*, 2004]. The middle plot shows UTC-IGST and UTC-IGRT obtained by differencing the time series in the top plot, which assumes that GPST is equivalent from Circular T and the IGS. Deviations from this assumption are responsible for a small portion of the plotted differences, especially at high frequencies. Finally, the bottom plot shows IGRT minus IGST, assuming each observes GPST equivalently. The occasional spikes are due to infrequent misalignment errors of the IGS Rapid clocks to GPST and are not actually present in either timescale.

FIGURE 13-4

Comparison of the IGS timescales IGST and IGRT against GPS Time (GPST) and against UTC (modulo leap seconds) from 5 November 2000 through 28 June 2004

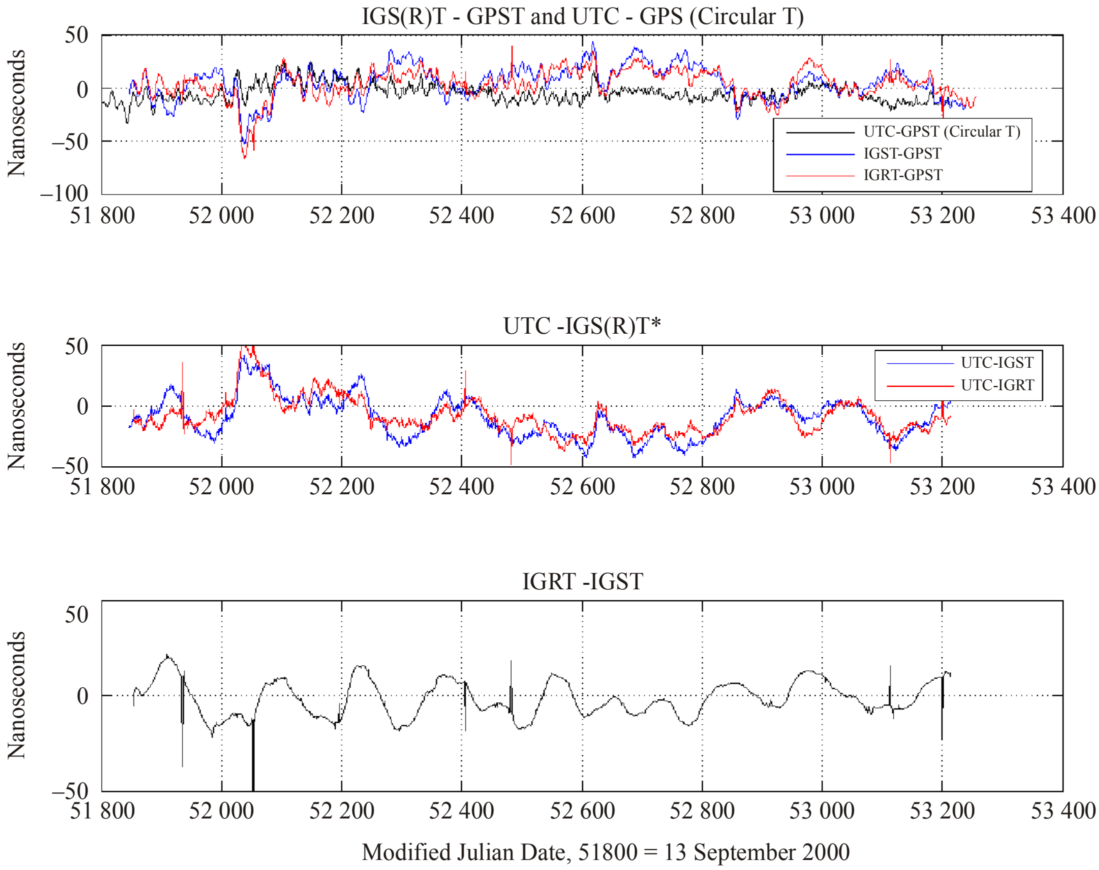

Sat_time_freq-13-04

13.5 Evaluation of performance by day-boundary discontinuity analysis

The "absolute" accuracy of GPS-based clock estimates (modulo the calibration bias) is determined entirely by the pseudorange data, averaged over the analysis interval, usually 24 h. When analyzing 1 day arcs of global data sampled at 5 min intervals, the formal error estimates for the clocks are typically about 120 ps, assuming each pseudorange observation has an uncertainty of 1 m. A more realistic test of actual measurement accuracy can be made by comparing clock estimates at the boundaries between independent analysis arcs for receivers equipped with very stable oscillators. (Less stable clocks can also be tested if overlapping analysis arcs are used to eliminate interpolation errors, but the adjacent clock estimates will then no longer be independent.) This is analogous to the classic geodetic repeatability test for a time series of position determinations.

Day-boundary clock jumps can be analyzed for baseline solutions or for networks where a single station clock has been held fixed as the reference. The results can be difficult to interpret, however, since effects at two stations will be convolved in each clock time series. A superior approach is to use the IGS clock products, with the new highly stable ensemble timescale, for such an analysis [Senior *et al.*, 2003]. By decoupling clock pairs, it was possible to isolate observed behaviors to individual stations. Figure 13-5 is an example of simultaneous time series of IGS clock estimates for eight H-maser stations. Note that the variability in the discontinuities among stations is independent of the stability of the individual clocks as some sites show large jumps but very good subdaily stability and vice versa. The distributions for day-boundary offsets studied by Ray and Senior were found to be zero-mean and Gaussian, but with RMS variations being highly site-specific.

FIGURE 13-5

Clock estimates of nine IGS sites with H-masers during 5 - 15 February 2002

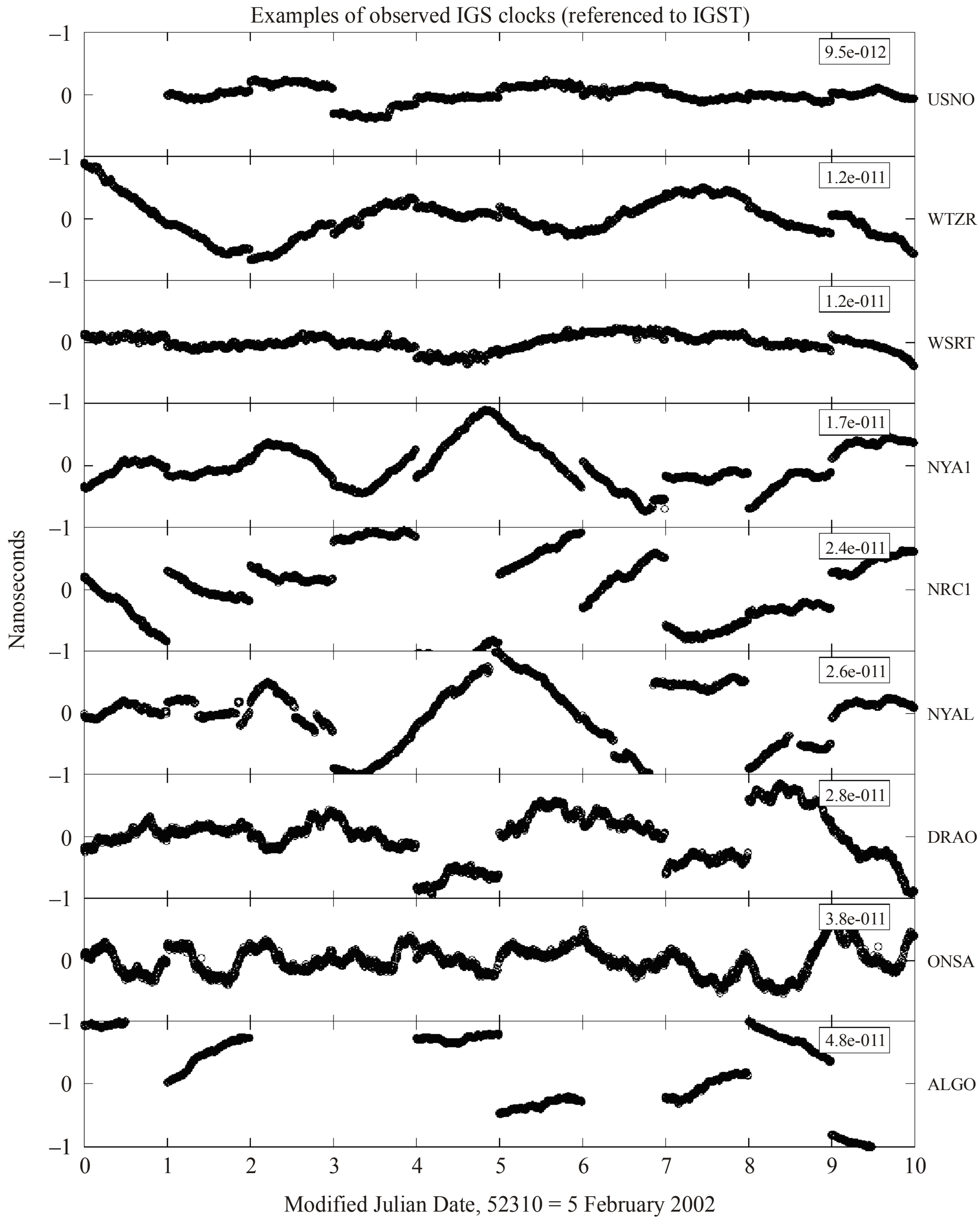

Sat_time_freq-13-05

A separate quadratic trend has been removed from each clock for Fig. 13-5 plotting. The boxed value in each panel gives the Allan deviation at 300 s, neglecting clock jumps at day boundaries. The magnitude of the day-boundary jumps varies greatly among the station and is independent of the subdaily clock stability.

The previous analysis of IGS clock jumps has been updated and extended in Table 13-2. A total of 1 310 days between October 2000 and June 2004 were examined from the IGS Rapid and Final clocks.

The editing and processing criteria were the same as in Ray and Senior [Senior *et al.*, 2003]. The maximum data gap at the day boundary is 30 min (typically 5 min), so the interpolation noise due to instabilities in the H-maser standards should be negligible. Since the RMS statistics are for the differences between pairs of independent days, each daily accuracy estimate should be smaller by √2. Of particular note is the very large dispersion in RMS performance among stations, nearly one order of magnitude. This presumably reflects the wide range in code performance among these stations and, in turn, shows the vast variation in multipath environments, external to the antenna as well as internal to the GPS instrumentation. In some cases the performance has varied markedly with time, sometimes correlated with changes reported in the site logs. Seasonal variations are found in a few cases. The RMS variations were previously shown to be independent of the choice of receiver or antenna models, or the use of radomes.

TABLE 13-2

Summary of day-boundary clock discontinuity statistics for 38 IGS stations with H-maser frequency standards

IGS Site	RMS clock Jump (ps)	Remarks
ONSA	149	Excellent
BREW	152	Excellent
OPMT (TL)	158	New station, so very limited data
BRUS (TL)	165	After changes in summer 2003 improved to 118 ps
MAD2	170	Very limited data, so RMS is not reliable
WTZR (TL)	189	
GODE	205	
USN1 (TL)	225	Station replaced by USN3 in July 2004
WSRT	227	Slight degradation since summer 2003
KHAJ	233	Limited data
CRO1	236	Maser no longer used
USUD	266	Maser no longer used
NPLD (TL)	268	
TID*	269	Appears improved since summer 2003
YEBE	271	
GOL2	271	Very limited data, so RMS is not reliable
AMC2 (TL)	283	Improved after antenna/receiver changes in June 2002
SPT0 (TL)	286	
WES2	296	
PIE1	305	Improved since receiver change in October 2002
STJO	334	
USNO (TL)	354	Appears worse since spring 2003
IRKT	359	
NYAL	363	Much better than NYA1 in 2004
NLIB	368	
MATE	389	Significant time variations; better in 2004
KOKB	460	Large degradation before antenna/cable change in May 2004
FAIR	478	Somewhat improved since summer 2003
DRAO	522	
YELL	564	Large seasonal variations, much worse in winters
ALBH	587	After September 2003 greatly improved to 97 ps
HOB2	631	Variations correlated with station changes

TABLE 13-2 (*end*)

IGS Site	RMS clock Jump (ps)	Remarks
MEDI	703	
FORT	706	
NYA1	750	Large degradation since summer 2003
ALGO	877	Large seasonal variations, much worse in winters
NRC1 (TL)	936	Large seasonal variations, much worse in winters
METS	1 065	Maser no longer used

IGS Rapid and Final clocks from October 2000 till June 2004 were used. Stations co-located at timing laboratories are indicated by (TL).

The best long-term performance among the IGS stations studied is at ONSA (Onsala, Sweden), corresponding to a daily clock accuracy of $(149/\sqrt{2}) = 105$ ps.

BREW (Brewster, WA, United States of America), OPMT (Paris, France), BRUS (Brussels, Belgium), MAD2 (Madrid, Spain), WTZR (Wettzell, Germany), and GODE (Greenbelt, MD, United States of America) have only slightly larger daily clock errors, from 107 to 145 ps.

There is a continuous progression of poorer performance among the other stations, up to 620 to 753 ps for ALGO (Algonquin, ON, Canada), NRC1 (Ottawa, ON, Canada), and METS (Metsahovi, Finland).

The order of magnitude range of clock accuracy reflects variations in local conditions, not an artifact of the IGS timescale, for instance. Strongly supporting this conclusion are the temporal changes in performance seen at a number of stations.

Abrupt changes usually correspond to known changes in configuration or equipment. (Regrettably, not all station changes are publicly reported.) A few stations show large seasonal variations, especially the three Canadian stations at YELL, ALGO, and NRC1 (Fig. 13-6).

We previously speculated that the large increase in clock jumps during wintertime at these sites is caused by a buildup of snow and ice on surfaces below and in the near-field of the antennas.

Figure 13-6 shows the history of the day-boundary clock jumps for those IGS stations at timing labs equipped with H-masers (indicated in Table 13-2 by TL). OPMT has been omitted due to its very sparse data. The BRUS installation, especially since summer 2003, should be considered exemplary and a model for other timing labs.

The study period on Fig. 13-6 is October 2000 to June 2004. Results from the IGS Rapid clocks are shown as black circles; Final clocks are blue “+” symbols.

FIGURE 13-6

Temporal variations in day-boundary clock offsets for eight IGS H-maser stations at timing labs

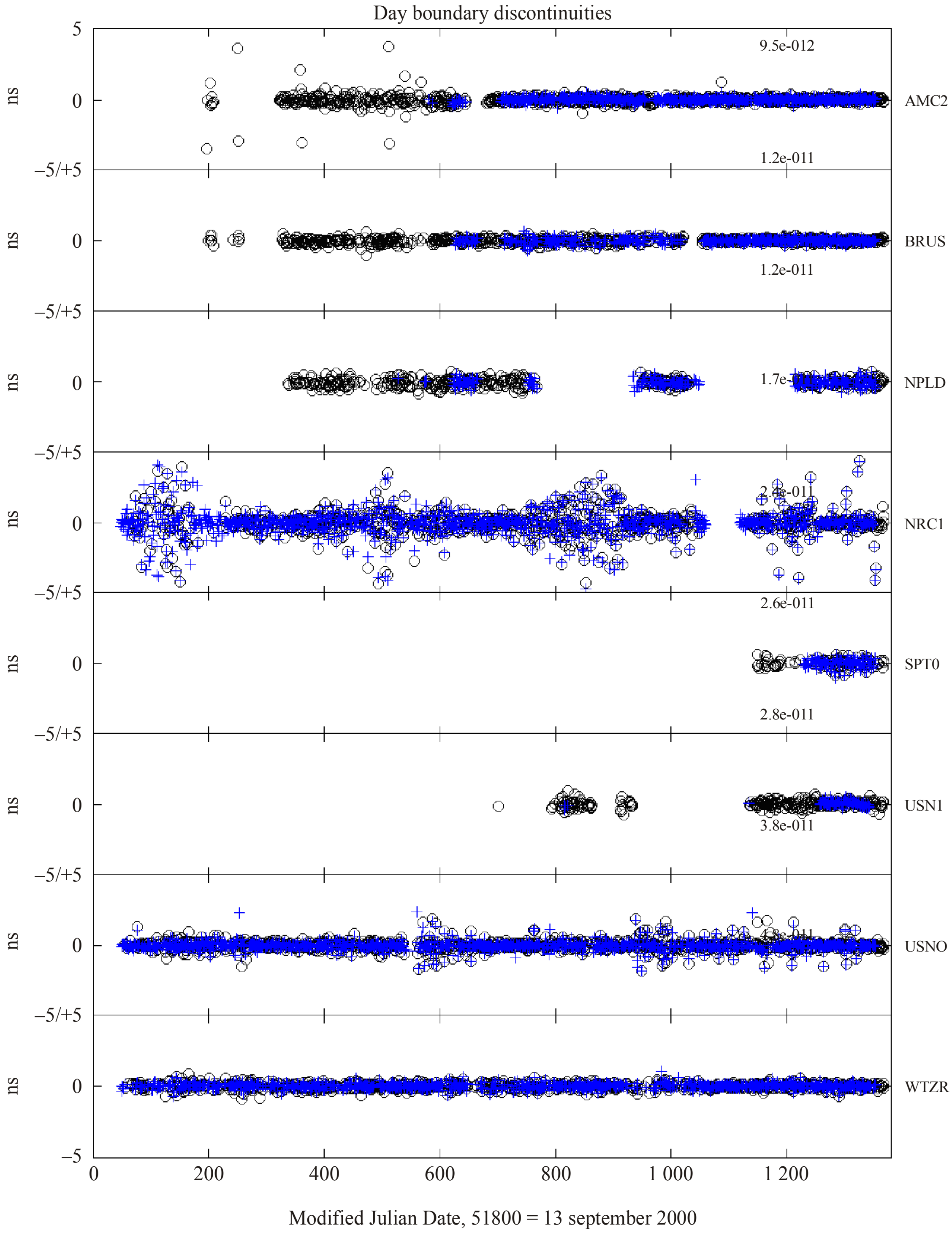

Sat_time_freq-13-06

13.6 Comparisons with independent two-way time transfer results

In addition to the internal assessments discussed above, it is important to compare geodetic clock estimates with those from independent systems. Conventional CV, while widely deployed at timing labs, is not sufficiently accurate to provide very informative comparisons except possibly over the longest averaging intervals. More promising are the P3 CV and TWSTT methods. Some of the best results over inter-continental baselines demonstrate agreements with geodetic clocks to about 0.5 ns RMS or about 0.3 ns TDEV for averaging times up to a few months [Plumb *et al.*, 2005; Petit *et al.*, 2004].

Table 13-3 summarizes results from recent high-quality comparison studies.

TABLE 13-3

Summary of published comparisons between geodetic and P3 CV or TWSTT methods for a number of links of varying lengths

Link	Baseline Length	Method/statistic/value	Data Span	Source
NPL-PTB	749 km	P3 / RMS / 0.48 ns TW / RMS / 0.57 ns	5 months 4 months	Petit & Jiang, 2004
IEN-PTB	835 km	P3 / RMS / 0.49 ns TW / RMS / 0.64 ns	2 months 2 months	Petit & Jiang, 2004
TL-CRL	2 112 km	P3 / RMS / 0.58 ns TW /RMS / 1.27 ns	8 months 8 months	Petit & Jiang, 2004
USNO-NPL	5 695 km	P3 / RMS / 0.48 ns TW / RMS / 0.59 ns	5 months 3 months	Petit & Jiang, 2004
USNO-PTB	6 275 km	P3 / RMS / 0.45 ns TW / RMS / 0.49 ns	5 months 5 months	Petit & Jiang, 2004
USNO-AMC(1)	2 361 km	TW / Difference ± RMS / -2.10 ± 0.69 ns (cal. agreement) TW / TDEV / < 0.1 ns, $300 \leq \tau \leq 2\ 000$ s < 0.34 ns, $2\ 000 \leq \tau \leq 7 \times 10^6$ s TDEV / 0.34 ns at 7×10^6 s	7 months	Plumb & Larson, 2004
USNO-NIST	2 405 km	TW / RMS / 0.83 ns TW / TDEV / < 0.3 ns, $3\ 600 \leq \tau \leq 6 \times 10^6$ s < 0.72 ns, $6 \times 10^6 \leq \tau \leq 7.4 \times 10^6$ s TDEV / 0.72 ns at 7.4×10^6 s	5.5 months	Plumb & Larson, 2004
PTB-NIST	7 532 km	TW / RMS / 0.79 ns TW / TDEV / < 0.5 ns, $2 \times 10^5 \leq \tau \leq 7.5 \times 10^6$ s TDEV / 0.24 ns at 7.5×10^6 s	7 months	Plumb & Larson, 2004
USNO-PTB	6 275 km	RMS / 2 ns	2 years	Dach *et al.*, 2002

(1) TW and geodetic links calibrated separately for instrumental delays.

TWSTT measurements are relatively sparse compared with continuous GPS data, about four times daily in recent years. Differences are computed by interpolation of the geodetic and P3 CV results to the TWSTT epochs. The P3 CV data reductions have used IGS precise orbits and ionosphere maps, as well as applying model displacements for solid Earth tide motions. A Vondrak smoothing has also been applied to the P3 results, equivalent to a low-pass filter with a cut-off period of about 0.4 day. As noted by Petit and Jiang [Petit and Jiang, 2004], the differences between simultaneous time series should be a constant for each clock-pair (equivalent to a calibration bias).

So the standard deviation should be a measure of the relative long-term instability of the two time transfer methods. The geodetic and P3 data are often from the same GPS receiver, so it is expected that some receiver- and antenna-based errors will be common to each and not evident in their differences (such as temperature sensitivity effects). So only the comparisons with TWSTT are fully independent. For all three of the long baselines studied by Plumb and Larson [Plumb and Larson, 2005], the Allan deviations of the TW-geodetic clock differences were dominated by TWSTT instabilities up to intervals of 10^5 to 10^6 s. At longer intervals, clock instabilities dominate over transfer noise from both methods.

Based on the published comparisons with TWSTT, the accuracy of geodetic time transfer results is apparently at least as good as (0.5 ns / $\sqrt{2}$) = 0.35 ns (RMS), assuming that each method contributes equally to the observed differences. This is a good deal larger than the geodetic formal errors for 1 day analyses, of about 0.12 ns, but it is within the range of performance for some poorer GPS stations (Table 13-2). Considering that the comparisons also show consistently better stability for geodetic clocks for up to several-day intervals, the actual RMS noise of TWSTT is almost certainly larger and the typical geodetic accuracy is better than 0.35 ns.

13.7 Assessment of time transfer performance

Figure 13-7 shows the stability floor of 24 h geodetic clock determinations, as inferred by Ray and Senior [Ray and Senior, 2003] from an analysis of IGS clock day-boundary jumps. The behavior is not significantly different from $\tau^{-0.5}$, consistent with a random walk noise process. At an averaging time of 1 day, the inferred instability is 1.4×10^{-15}.

Some of the best IGS stations approach this level of performance, but, as we have seen, others are much poorer. Beyond the 1-day analysis interval, the clock estimates should be nearly independent and the behavior is predicted to be closer to that of a white noise process, τ^{-1}, as illustrated in Fig. 13-7.

However, it has not yet been possible to study this domain so carefully due to instabilities in the frequency standards in common use. When caesium fountain data become more available, the stability of geodetic clocks over intervals longer than 1 day will be exposed. Figure 13-7 plots the design goal for the METAS Cs fountain [Dudle *et al.*, 2001], for instance.

If analysis arcs are extended beyond 24 h, then the stability floor will probably be lower than the level shown here, though this has not been demonstrated. On the other hand, doing so will definitely extend the random walk behavior of geodetic clocks over the same longer intervals and could therefore compromise achieving higher stability over longer times using independent 1-day arcs.

Also shown in Fig. 13-7 is the specified stability (presumably conservative) of the MHM2010 active H-maser from Symmetricon (successor of the former Sigma Tau H-maser). This shows that the geodetic method need not be a limitation to comparing such high-performance clocks over 1-day intervals, though time transfer noise does probably dominate over clock instabilities for intervals less than about 14 000 s. The dispersion in 1 day stabilities seen among the IGS H-maser stations – from the level of our inferred stability floor up to about 10^{-14} – is probably a combination of the inherent stability of the local frequency standard (some are old devices and some are not maintained under strict environmental control) and the local pseudorange multipath conditions.

FIGURE 13-7

The Allan deviation stability floor for geodetic time transfers is shown by the solid black line

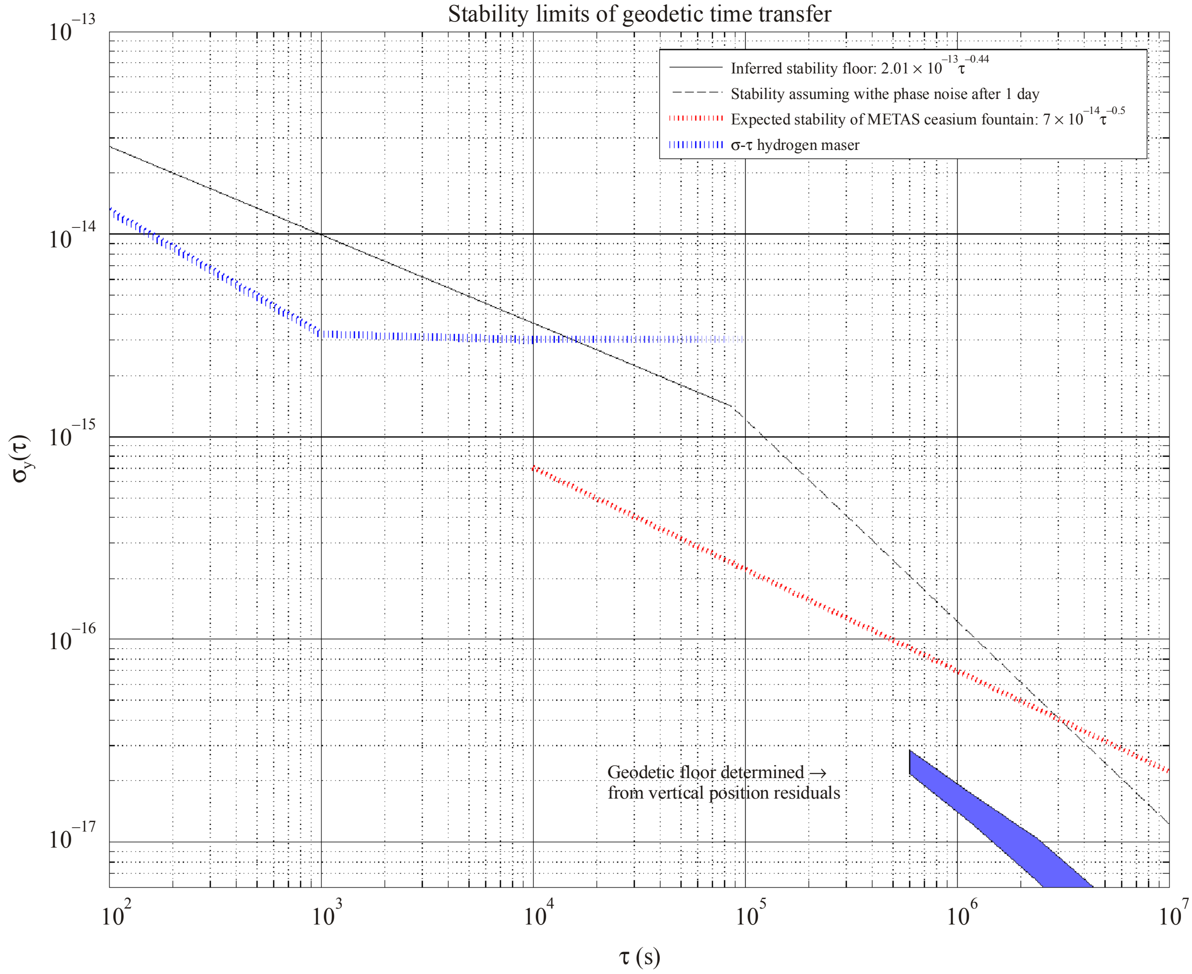

Sat_time_freq-13-07

The limit's behavior on Fig. 13-7 is consistent with a random walk noise process up to 1-day intervals. Beyond that, it is expected that independent daily clock estimates will have white noise-distributed errors and follow a τ Allan deviation, shown by the dashed black line. For comparison, the red trend indicates the design goal for the METAS Cs fountain and the blue trend is for a σ τ H-maser (from symmetricon). The fundamental geodetic limit is represented by the lower blue band, based on the repeatability of station height measurements.

13.8 Future trends

The application of geodetic methods to global time and frequency transfers is only in its infancy. It is not yet widely used within the timekeeping community. We expect much greater adoption of the technique for international time and frequency comparisons in the future, especially in view of its high performance and modest cost. Installation of new, more stable laboratory frequency standards will doubtless spur such a trend. Probably the biggest obstacle to wider usage has been the more complex data analysis required by the geodetic approach. While a number of software packages exist and are very commonly used within the positioning communities, they are less well known among timing groups, which is understandable. Almost certainly, the development of simple generic tools for PPP clock solutions will greatly facilitate broader use of geodetic clock estimates.

As the performance limit for geodetic timing is set by the quality of the pseudorange data, especially multipath effects, any major improvements in the technique will probably be related to reductions in pseudorange and multipath errors. Refinements in GPS receiver tracking technology and in geodetic antenna design may offer some benefits. Better siting and installation of existing equipment would certainly be useful in many cases. But the largest gains will likely come with new GNSS broadcast signals and modulation schemes. Some of the proposed signal designs for GALILEO, for instance, offer the prospect of greatly reduced multipath error [Hein and Pany, 2002]. Generally, proposed signal structures which shift more of the power toward the band edges, including some new GPS modulations, promise the potential of significantly improved multipath mitigation [Weill, 2003].

For time comparisons using any existing method, hardware calibration uncertainty is the dominant absolute error. The calibration errors are at least an order of magnitude larger than the typical errors of the geodetic clock estimates. The prospects for substantial calibration improvements in the future are unclear.

References

ALLAN, D. and WEISS, M. [1980] Accurate time and frequency transfer during common-view of a GPS satellite, *Proc. 1980 IEEE Freq. Contr. Symp*., Philadelphia, PA, p. 334-356.

ALTAMIMI, Z., SILLARD, P. and BOUCHER, C. [2000] ITRF2000: A new release of the International Terrestrial Reference Frame for Earth science application. *J. Geophys. Res*., **107**(B10), 2214, doi: 10.1029/ 2001-JB000561, 2002.

BEUTLER, G., BROCKMANN, E., GURTNER, W., HUGENTOBLER, U., MERVART, L. and ROTHACHER, M. [1994] Extended orbit modeling techniques at the CODE processing center of the International GPS Service for Geodynamics (IGS): Theory and initial results. *Manuscripta Geodaetica*, **19**, p. 367-386.

BOSSLER, J.D., GOAD, C.C. and BENDER, P.L. [1980] Using the Global Positioning System (GPS) for geodetic positioning. *Bull. Geod*., **54**, p. 553-563.

BRUYNINX, C. and DEFRAIGNE, P. [1999] Frequency transfer using GPS codes and phases: Short- and long-term stability. *Proc. 31st Precise Time and Time Interval Meeting*, Washington, DC: The U.S. Naval Observatory, p. 471-480.

BYUN, S.H., HAJJ, G.A. and YOUNG, L.E. [2002] GPS signal multipath: A software simulator. *GPS World*, **July 13**(7), p. 40-49.

COUNSELMAN, C.C. and SHAPIRO, I.I. [1979] Miniature interferometric terminals for Earth surveying. *Bull. Geod*., **53**, p. 139-163.

DACH, R., BEUTLER, G., HUGENTOBLER, U., SCHAER, S., SCHILDKNECHT, T., SPRINGER, T., DUDLE, G. and PROST, L. [2003] Time transfer using GPS carrier phase: Error propagation and results. *J. Geodesy*, **77**, doi 10.1007/s00190-002-0296-z, p. 1-14.

DACH, R., SCHILDKNECHT, T., HUGENTOBLER, U., BERNIER, L.G. and DUDLE, G. [2006] Continuous Geodetic Time Transfer Analysis Methods. *IEEE Trans. Ultrason., Ferroelect., Freq. Contr.*, **53**(7), p. 1250-1259.

DEFRAIGNE, P., PETIT, G., and BRUYNINX, C. [2001] Use of geodetic receivers for TAI, *Proc. 33rd Precise Time and Time Interval Meeting*, Washington, DC: The U.S. Naval Observatory, p. 341-348.

DUDLE, G., JOYET, A., BERTHOUD, P., MILETI, G. and THOMANN, P. [2001] First results with a cold cesium continuous fountain resonator. *IEEE Trans. Instr. Meas.*, **50**(2).

ELOSEGUI, P., J.L. DAVIS, R.T.K. JALDEHAG, J.M. JOHANSSON, A.E. NIELL, and I.I. SHAPIRO [1995] Geodesy using the Global Positioning System: The effects of signal scattering on estimates of site positions. *J. Geophys. Res*., **100**, p. 9921-9934.

ESTEY, L.H. and MEERTENS,C.M. [1999] TEQC: The multi-purpose toolkit for GPS/GLONASS data. *GPS Solutions*, **3**(1), p. 42-49.

FLIEGEL, H., T. GALLINI, and SWIFT, E. [1992] Global Positioning System radiation force model for geodetic applications. *J. Geophys.Res.*, **97**(B1), p. 559-568.

HEIN, G. W. and PANY, T. [December, 2002] Architecture and signal design of the European satellite navigation system Galileo – Status . *J. Global Positioning Systems*, **1**(2), 2002, p. 73-84.

KEDAR, S., HAJJ, G.A., WILSON, B.D. and HEFLIN, M.B. [2003] The effect of the second order GPS ionospheric correction on receiver positions. *Geophys. Res. Lett.*, **30**(16), 1829, doi:10.1029/2003 GL017639.

KOUBA, J. [2004] Improved relativistic transformations in GPS. *GPS Solutions*.

KOUBA, J. and P. HEROUX, [2000] Precise point positioning using IGS orbit products . *GPS Solutions*, **5**(2), p. 12-28.

KOUBA, J. and SPRINGER, T.[2001] New IGS station and satellite clock combination. *GPS Solutions*, **4**(4), p. 31-36.

LANGLEY, R. B. [1996] GPS receivers and the observables. *GPS for Geodesy*, Teunisen, P.J.G. and A. Kleusberg (editors), Berlin: Springer-Verlag, p. 141-173.

LARSON, K.M., LEVINE, J., NELSON, L.M., T.E. and PARKER [2000] Assessment of GPS carrier-phase stability for time-transfer applications. *IEEE Trans. Ultrason., Ferroelect., Freq. Contr.*, **47**(2), p. 484-494.

LEWANDOWSKI, W., AZOUBIB, J., De JONG, G., NAWROCKI, J. and DANAHER, J. [1997] A new approach to international time and frequency comparisons: All-in-view multi-channel GPS+GLONASS observations. *Proc. Institute of Navigation GPS97,* p. 1085-1091.

LICHTEN, S. and BORDER, J. [1987] Strategies for high precision GPS orbit determination. *J. Geophys. Res.*, **92**, 1987, p. 12751-12762.

MADER, G.L. [1998] GPS antenna calibration at the National Geodetic Survey. *GPS Solutions*, **3**(1), p. 50-58.

MADER, G.L. and CZOPEK, F. [2002] Calibrating antenna phase centers. *GPS World*, **13**(5), p. 40-46.

MCCARTHY, D. D. and PETIT, G. [2003] IERS Conventions 2003, IERS Technical Note 32, Frankfurt am Main: Verlag des Bundesamts für Kartographie und Geodäsie, 2003.

OVERNEY, F., Th. SCHILDKNECHT, G. BEUTLER, L. PROST, and U. FELLER, [1997] GPS Time transfer using geodetic receivers: Middle-term stability and temperature dependence of the signal delays. *Proc. 11th European Frequency and Time Forum*, p. 504-508.

PETIT, G. and JIANG, Z. [28 May 2004 and 16 July 2004] Study of time transfer methods: II. TWSTT vs. geodetic clock comparisons, internal BIPM reports.

PETIT, G., JIANG, Z., MOUSSAY, P., WHITE, J., POWERS, E., DUDLE,G. and UHRICH, P. [2001] Progresses in the calibration of "geodetic like" GPS receivers for accurate time comparisons. *Proc. 15th European Frequency and Time Forum*, p. 164-166.

PETIT, G., JIANG, Z., TARIS, T., UHRICH, P., BARILLET, R. and HAMOUDA, F. [1999] Processing strategies for accurate frequency comparison using GPS carrier phase. *Proc. 1999 Joint European Frequency and Time Forum and 1999 IEEE International Frequency Control Symposium*, p. 235-238.

PETIT, G., JIANG, Z., UHRICH, P. and TARIS, F. [2000] Differential calibration of Ashtech Z12-T receivers for accurate time comparisons. *Proc. 14th European Frequency and Time Forum*, p. 40-44.

PETIT, G., JIANG, Z., WHITE, Z., J., BEARD, R. and POWERS, E. [2001] Absolute calibration of an Ashtech Z12-T GPS receiver. *GPS Solutions*, 4(4), p. 41-46.

PETIT, G., THOMAS, C., JIANG, Z., UHRICH,P. and TARIS, F. [1998] Use of GPS Ashtech Z12T receivers for accurate time and frequency comparisons. *Proc. 1998 IEEE International Frequency Control Symposium*, p. 306-314.

PLUMB, J. and LARSON, K. [2005] Long-Term Comparisons Between Two-Way Satellite and Geodetic Time Transfer Systems. *IEEE Trans. Ultrason., Ferroelect., Freq. Contr.*, **52**(11), p. 1912-1918.

PLUMB, J., LARSON, K., WHITE, J. and POWERS, E. [2005] Absolute Calibration of a Geodetic Time Transfer System. *IEEE Trans. Ultrason., Ferroelect., Freq. Contr.*,**52**(11), p. 1904-1911.

RAY, J. R., DRAGERT, H. and KOUBA, J. [2000] Recommendations for handling non-Rogue data. *IGS 1999 Technical Reports*, Jet Propulsion Laboratory Publication, Pasadena, California, p. 445-451.

RAY, J.R. and SENIOR, K. [2001] Temperature sensitivity of timing measurements using Dorne Margolin antennas. *GPS Solutions*, **5**(1), p. 24-30.

RAY, J. R., and SENIOR, K. [2003] IGS/BIPM Pilot Project: GPS carrier phase for time/frequency transfer and time scale formation. *Metrologia*, **40**(3), p. S270-S288.

RIECK, C., JARLEMARK, P., JALDEHAG, K. and JOHANSSON, J. [2003] Thermal influence on the receiver chain of GPS carrier phase equipment for time and frequency transfer. *Proc. 2003 IEEE International Frequency Control Symposium and PDA Exhibition Jointly with the 17th European Frequency and Time Forum,* p. 326-331.

SCHILDKNECHT, Th. and DUDLE, G. [2000] Time and frequency transfer: High precision using GPS phase measurements. *GPS World*, 2000 **11**(2), 2000, p. 48-52.

SCHMID, R. and ROTHACHER, M. [2003] Estimation of elevation-dependent satellite antenna phase center variations of GPS satellites. *J. Geodesy*, **77**, doi: 10.1007/s00190-003-0339-0, p. 440-446.

SCHUPLER, B.R., ALLSHOUSE, R.L. and CLARK, T.A. [1994] Signal characteristics of GPS user antennas. *J. Inst. Navigation*, **41**, p. 277-295.

SCHUPLER, B.R. and CLARK, T.A. [2001] Characterizing the behavior of geodetic GPS antennas. *GPS World*, **12**(2), p. 48-55.

SENIOR, K., KOPPANG, P. and RAY, J. [2003] Developing an IGS time scale, *IEEE Trans. Ultrason., Ferroelect., Freq. Contr.*, **50**(6), p. 585-593.

SENIOR, K., MATSAKIS, D. and POWERS, E. [1999] Attenuating day-boundary discontinuities in GPS carrier-phase time transfer. *Proc. 31st Precise Time and Time Interval Meeting*, p. 481-489.

SENIOR, K., RAY, J. and PETIT, G. [2004] Comparison of instrumental and empirical station timing biases for a set of Ashtech GPS receivers, *Proc. 2004 European Frequency and Time Forum*.

THOMAS, C. and AZOUBIB, J. [1996] TAI computation: Study of an alternative choice for implementing an upper limit of clock weights. *Metrologia*, **33**, p. 227-240.

WEILL, L. R. [2003] How good can it get with new signals? Multipath mitigation. *GPS World*, **14**(6), p. 106-113.

WHITE, J., BEARD, R., LANDIS, G., PETIT, G. and POWERS, E. [2001] Dual frequency absolute calibration of a geodetic GPS receiver for time transfer. *Proc. 15th European Frequency and Time Forum*, p. 167-172.

WU, J.T., WU, S.C., HAJJ, G.A., BERTIGER, W.I. and LICHTEN, S.M. [1993] Effects of antenna orientation on GPS carrier phase. Manuscripta Geodaetica, **18**, p. 91-98.

ZUMBERGE, J.F., HEFLIN, M.B., JEFFERSON, D.C., WATKINS, M.M. and WEBB, F.H. [1997] Precise point positioning for the efficient and robust analysis of GPS data from large networks. *J. Geophys. Res*., **102**(B3), p. 5005-5017.

CHAPTER 14

TWO WAY SATELLITE TIME AND FREQUENCY TRANSFER (TWSTFT)

Page

14.1 Introduction

In Time transfer, one of the primary goals is to compare clocks and/or frequency standards over widely separated distances. There are many reasons for making such comparisons. One can simply be interested in making instantaneous measurements of widely separated clocks to monitor the performance of time scales through the intermediary of the clocks being compared. One can also be interested in making comparisons of advanced frequency standards, such as cesium fountains, and/or checking the long-term stability of such standards. The precision and accuracy with which these measurements can be achieved is of interest for metrology.

The technique known as TWSTFT is a method by which one obtains an estimate of the clock differences between two stations through the active exchange of timing signals through a geostationary communications satellite [Kirchner, 1991]. The 11th meeting of the Consultative Committee on the Definition of the Second (CCDS), now the Consultative Committee for Time and Frequency (CCTF), in 1989 issued a declaration 1989/1 encouraging the use of TWSTFT and suggesting the creation by the BIPM of an *ad hoc* Working Group on TWSTFT.

Following the decision of the 12th CCDS meeting in 1993, the ad hoc Group was converted into a permanent CCTF Working Group. The main achievements of the Working Group are:

– development of a standard format;

– organization of TWSTFT time links;

– choice of modems;

– schedule of observations;

– duration of observation;

– data exchange;

– negotiation for the use of satellites;

– evaluation of TWSTFT links;

– comparison with other time transfer techniques.

The method has been increasing in its popularity as a means to obtain high precision comparisons between timing laboratories. BIPM now utilizes information on clocks that contribute to TAI obtained through this technique (see 20th BIPM TWSTFT Report).

14.2 Description of TWSTFT technique

For carrying out TWSTFT, laboratories have to work in pairs (Fig. 14-1). Both laboratories require receive-and-transmit stations and spread-spectrum modems in order to exchange timing information via communication satellites employing pseudo-noise (PN) coded signals and code-division multiple access (CDMA). At the transmitting site, by means of the modem, a one pulse per second (1 PPS) signal is modulated onto the station's IF, usually at 70 MHz. The signal is then up-converted to the radio frequency (RF), amplified, and transmitted to the satellite. In the satellite transponder it is amplified, offset in frequency by the satellite translation frequency, and again amplified and retransmitted. At the receiving site, the received RF signal is amplified, down-converted to the IF, and demodulated by means of the modem, to produce a received 1 PPS. The measurement consists of simultaneous time-interval measurements at both sites. The 1 PPS generated by the local clock starts both the local time-interval counter, and, after being transmitted via satellite, stops the remote time-interval counter.

FIGURE 14-1

Two-Way Satellite Time and Frequency Technique comparison principle

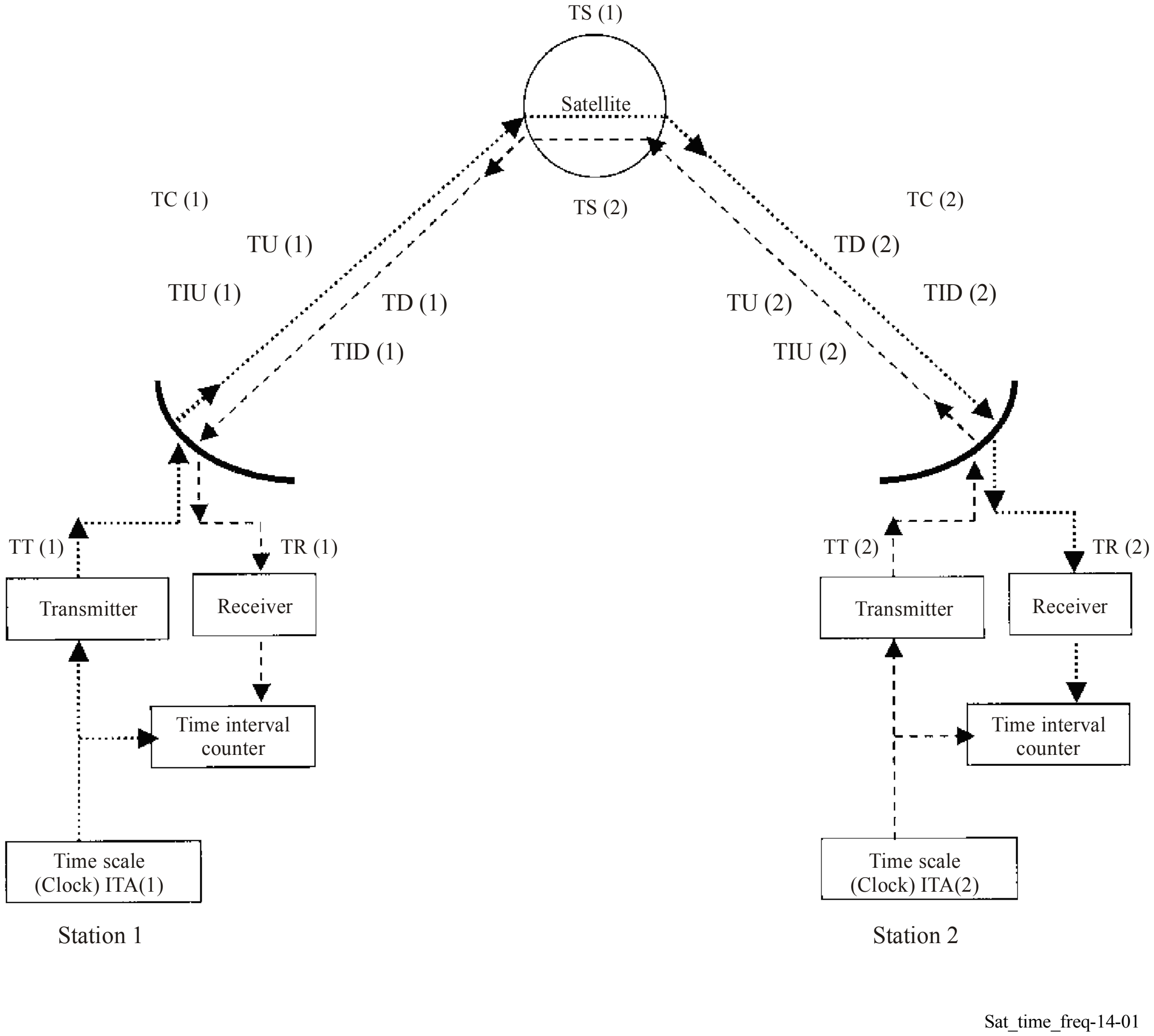

The following parameters for Station 1 and Station 2 (k = 1,2) are shown in Fig. 14-1:

– TA(k): Clock or time scale at station k
– TI(k): Time interval counter reading
– TT(k): Transmitter delay
– TR(k): Receiver delay
– $T_U(k)$: Up-link delay through the atmosphere
– $T_D(k)$: Down-link delay through the atmosphere
– TS(k): Propagation delay through the satellite transponder
– TC(k): Correction for relativistic effects
– $TI_U(k)$: Ionospheric delay up
– $TI_D(k)$: Ionospheric delay down

The difference between the clocks located at Stations 1 and 2 is given by:

$$TA(1)-TA(2)$$

where:

TA(1) is related to TI(1) by:

$$TI(1) = TA(1) - TA(2) + TT(2) + T_U(2) + TS(2) + T_D(1) + TR(1) + TC(1) + TI_U(1) + TI_D(1) \quad (14\text{-}1)$$

and TA(2) is related to TI(2) by:

$$TI(2) = TA(2) - TA(1) + TT(1) + T_U(1) + TS(1) + T_D(2) + TR(2) + TC(2) + TI_U(2) + TI_D(2) \quad (14\text{-}2)$$

The difference between these two expressions gives:

$$TI(1) - TI(2) = 2\,[TA(1) - TA(2) + TT(2) - TT(1) + T_U(2) - {}_{TU}(1) + TS(2) - TS(2)$$
$$+ T_D(1) - T_D(2) + TR(1) - TR(2) + TC(1) - TC(2) + TI_U(1) - TI_U(2) + TI_D(1) - TI_D(2)] \quad (14\text{-}3)$$

This can be rewritten as:

$$TA(1) - TA(2) = \tfrac{1}{2}\,[TI(1) - TI(2) + TT(1) - TT(2) + T_U(1) - T_U(2) + TS(1) - TS(2)$$
$$+ T_D(2) - T_D(1) + TR(2) - TR(1) + TC(2) - TC(1) + TI_U(1) - TI_U(2) + TI_D(1) - TI_D(2)] \quad (14\text{-}4)$$

If the signals pass through the same transponder in the satellite, then TS(1) equals TS(2) and their delays cancel. If the satellite is not moving too fast, then $T_U(1)$ equals $T_D(1)$ and $T_U(2)$ equals $T_D(2)$ and their delays cancel. TC(1) and TC(2) can be calculated but subject to the uncertainty with which the station coordinates are known. If the stations are close to each other than $TI_U(1) = TI_U(2)$ and $TI_D(1) = TI_D(2)$.

14.3 Measurements of TWSTFT

The fundamental measurement that is made with TWSTFT is an estimate of the difference between two clocks. One can compute the standard deviation of the residuals to the measured differences between two clocks obtained with TWSTFT. Under reasonable assumptions of normal clock behavior exhibiting white noise, one can expect that the standard deviation of a linear regression to the clock differences will asymptotically approach a limit, as more measurements are included in the regression.

Figure 14-2 shows the standard deviation as a function of the number of one-second data points included in the curve fit interval [Klepczynski, 1995]. After about 300 s of observing time, a limit of about 125 ps is approached.

FIGURE 14-2

Standard deviation of the residuals to a linear fit of clock differences obtained by TWSTFT

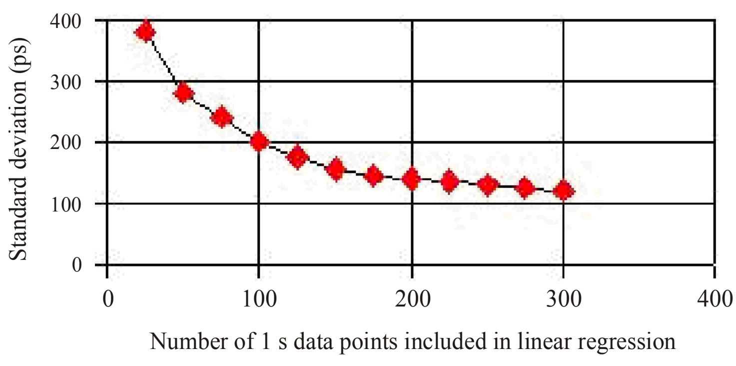

Sat_time_freq-14-02

14.4 Station laboratory equipment

Many investigations have been made on the uncertainties in the TWSTFT equipment used on the ground. They are summarized by Kirchner [Kirchner, 1999]. The primary sources of uncertainty involved in this area are:

– the spread spectrum modem used to generate 1 PPS that is transmitted by one station and received by the other;

– a Time interval counter used to measure the difference between a local clock and the timing pulse that has been reconstructed by the spread spectrum modem;

uncertainty caused by variations in the carrier-to-noise density ratio (C/N_0) within the spread spectrum modem being used.

14.4.1 Spread spectrum modem

The MITREX modem was the first commercially available spread-spectrum modem especially designed for range measurements and point-to-point time transfer of high precision and accuracy, using geostationary communication satellite [Hartl *et al.*, 1983]. It makes use of the so-called direct-sequence or PN technique. Binary phase-shift keying (BPSK) is used for the modulation of the carrier. The resolution of a system employing PN codes depends on the length of a code element (the chip length) and the needed bandwidth is given by its reciprocal value, the chip-rate (f_C). Using codes with low cross correlation, several such codes can be transmitted over the same channel (CDMA) without interfering with one another. The MITREX employs a chip rate of 2.5 MHz, and, depending on signal filtering and the satellite service used, it requires a satellite channel with a bandwidth of typically 3.5 MHz [Veenstra, 1990].

At present, two types of modems are commercially available: the ATLANTIS modem, manufactured by Allen Osborne Associates, USA, and the SATRE modem, manufactured by Time Tech GmbH, Germany. The SATRE modem is fully compatible with the MITREX modem, but the ATLANTIS modem uses its own standard (slightly different chip rate, other codes), thus not providing compatibility. A modem developed at the Communication Research Laboratory (CRL), Japan is not compatible with the MITREX modem.

14.4.2 Time interval counter

Also, as a matter of good practice, Stations use an external counter when employing a modem with internal time-interval measurement capability. An external counter is usually necessary for accompanying measurements.

14.4.2.1 Carrier to noise density ratio (C/N_0)

For TWSTFT stations, the operational parameters of the station are determined by the carrier-to-noise density ratio, C/N_0, of the modem and by the satellite (equivalent isotropic radiated power, EIRP, and figure-of-merit, G/T, of the satellite terminal). The latter parameters are calculated by means of a link budget. The carrier-to-noise density ratio, C/N_0, is necessary to get the required measurement precision of measurement.

14.5 Link dependent measurements (path and equipment)

The primary sources of uncertainty involved in this area are:

– an effect due to the movement around the rotation axis of the Earth, both of the participating stations and of the satellite during the propagation of the signal to and from the satellite (Sagnac effect);

– an effect due to the geostationary satellite's motion relative to the Earth's surface;

– an effect due to the difference in ionospheric retardation of the signal in the up-link and down-link frequencies used to transmit signals by the user and the satellite.

14.5.1 The Sagnac effect

The Sagnac effect results from movement around the rotation axis of the Earth, both of the Earth stations and of the satellite, during the propagation of a signal to and from the satellite [Ashby and Allan, 1979]. It is proportional to the equatorial projection of the area of the quadrangle, the vertices of which are the center of the Earth and the positions of the stations on the surface of the Earth, and the position of the satellite with respect to the Earth's surface. It is thus a function of the positions of stations 1 and 2 and the satellite. The extreme case is about 420 ns for stations 1 and 2 at the equator, with each having an elevation of 6°, caused by a maximal separation in longitude (about 150°). For calculation of the Sagnac effect, the positional accuracy requirements are orders of magnitude below those needed to calculate the signal delay, for one-way methods like GPS. Estimates for the uncertainty arising from errors in station coordinates for the Sagnac effect between TUG – USNO are 150 ps and between TUG-OCA are 16 ps.

14.5.2 Second-order relativistic correction to the Sagnac effect

A second order correction, due to the satellite's motion relative to the Earth's surface, is a function of the satellite's velocity and the satellite's elevations from Stations 1 and 2 [Petit and Wolf, 1993]. The extreme case is one station having an elevation of 6° and the other, of 90°. The difference of the times of arrival (TOA) of simultaneously transmitted signals at the satellite would then be about 17 ms. If we assume a rather high radial satellite velocity of 3 m/s, the resulting error is about 170 ps. By choosing a satellite that is observed by both stations at the same elevation, the effect can be minimized. It can also be eliminated completely by offsetting the transmission times. Estimated effects for experiments carried out between the United States Naval Observatory (USNO) and the Technical University Graz (TUG) are on the order of 100 ps. Between the Observatoire de la Cote d'Azur (OCA), and the Technical University Graz (TUG) they are on the order of 10 ps.

14.5.3 Difference in up-link and down-link frequencies

The ionospheric excess delay of a signal penetrating the ionosphere depends on the frequency (proportional to $1/f^2$), the total electron content (TEC), and the elevation [Flock, *et al.*, 1982; Jespersen, 1989]. The TEC is the Total Electron Content of a vertical column with a cross-sectional area of 1 m^2, given in electrons/m^2. Using a mapping function, the total electron content along a slant path can be calculated. The uncertainty due to the ionosphere is a function of the up-link and down-link frequencies of Stations 1 and 2, of the TECs for Stations 1 and 2, and of the elevations of Stations 1 and 2. The uncertainty in non-reciprocity is about 150 ps in the extreme case:

– having one satellite's elevation at 90° and the other elevation at 6°;

– up-link and down-link frequencies of 14 GHz and 12 GHz, and 14 GHz and 11 GHz;

– TECs of 10^{17} electrons/m^2 and 10^{18} electrons/m^2 (assuming one station at nighttime and the other at daytime).

For C-band frequencies (6/4 GHz), the effect, of course, is substantially higher. The effect can be minimized by choosing a satellite for which both elevations are about the same, and having the same TEC and the same up-link and down-link frequencies at both sites, or by using even higher frequencies (Ka-band: 30/20 GHz).

One effect that is neglected is tropospheric delay. It is frequency independent (negligible) at the frequencies used for satellite communications.

14.6 Calibration methods

Certain uncertainties cannot be statistically measured or estimated. They must be evaluated through a process often called *calibration*. In some cases, this means measuring the delays through individual components of the system being used to make measurements or measuring the delay through the entire system. One can also calibrate by transport of a system that has either exhibited reasonable stability or a system that has been calibrated. This is sometimes called relative calibration. In some cases, one may even make comparisons through an entirely different system.

14.6.1 Station calibration using a satellite simulator

While the delays of some individual components of a system can be measured, the total system uncertainty cannot be simply estimated because of the complicated paths that signals may traverse within it. Two methods could be employed for this purpose. One can either measure the difference of the delays of Stations 1 and 2, or measure the delays of both stations, separately.

In the first method, delays through individual components of the system would be made by the injection of a signal through a satellite simulator whose characteristics are well-documented [De Jong and Polderman, 1994; De Jong and Van Bemmelen, 2001]. The calibration system is automated and one measurement campaign was made in conjunction with a Fly-Away Satellite Terminal (FAST) [De jong *et al.*, 1995]. Such a satellite simulator can also be used to permanently measure the variation of the delays of a station, giving the long-term stability of a station. Figure 14-3 is a schematic of VSL satellite simulator used to make such measurements.

FIGURE 14-3

Schematic of the VSL satellite simulator to measure delays through a TWSTFT Earth station

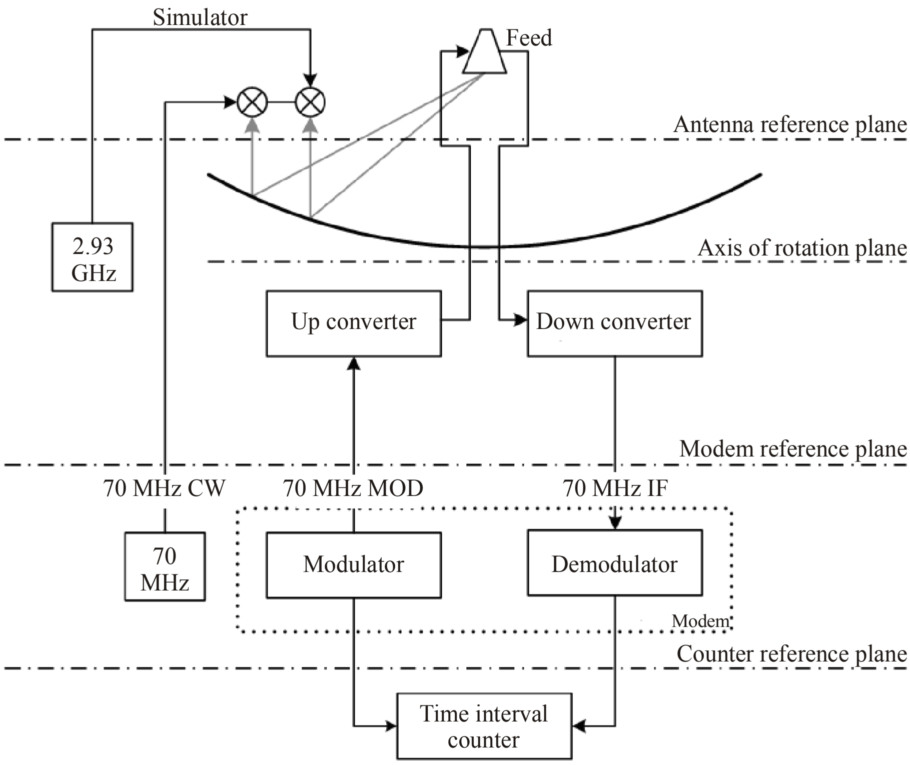

Sat_time_freq-14-03

14.6.2 Station calibration using a transportable Earth station

The second approach can be realized by collocation of an Earth station at two participating stations or by employing a third station as a transfer standard. Measurement campaigns were made in 1993 and 1998 using this technique.

14.6.3 Calibration campaigns of 1993 and 1998

In the first campaign, a TWSTFT Station was transported between the Observatoire de Cote d'Azur, Grasse, France (OCA) and the Technical University of Graz, Austria (TUG), a distance of about 800 km [Kirchner, *et al.*, 1993]. The formal standard deviations of the measurements made during the trip were about 1 ns. Ways to improve on this experiment were discussed and a second campaign was made [Kirchner *et al.*, 1998]. During this campaign, the formal standard deviations were on the order of 200 ps., a significant improvement over the first experiment. During both campaigns, comparisons with GPS Common View were made and systematic differences between the two methods were noted. In the both approaches to external calibration, measurements should be made on a continuing basis. This would allow for the development of a statistical history of the uncertainty.

14.6.4 X-band calibration campaign

An experiment that uses a transportable X-band station was performed between the US Naval Observatory (USNO), Washington, D.C and the National Physical Laboratory (NPL), Teddington, England.

14.7 Problems arising when using different satellite transponders

Unless measurements of the delays through different transponders of the satellite have been made before the satellite was launched, it is very difficult to obtain estimates of the uncertainty of the delays through them. It can only be done through relative calibration by transporting a calibrated system to the participating stations. Such measurements should be repeated as frequently as possible. They should also be done using different independent techniques to verify as best as possible the results obtained by other techniques. The major problem here is that the techniques used to verify other techniques may not be of the same uncertainty as the primary technique. Extreme care needs to be exercised when evaluating the uncertainty in this fashion.

The calibrated independent system may also be a TWSTFT system, if, for this system, the problem of unknown differential satellite delays does not exist. If the differential satellite delay is known (e.g., from measurements before the launch of the satellite), one can employ the methods given in the previous section to calibrate the station delays.

14.8 Problems arising when using different satellite transponders

In addition to the two systems previously mentioned, other methods such as GPS could be used. Of course, the accuracy obtained cannot be better than the accuracy of GPS, itself.

The measurement set-up for GPS C-V is shown in Fig. 14-4. The signals from the navigation satellites (C) are received in the receivers and measured against the time scales of clock A and clock B located at A and B. The measured values (A-C) and (B-C) are subtracted and the result is the difference of the time scales (A - B).

FIGURE 14-4

GPS common-view

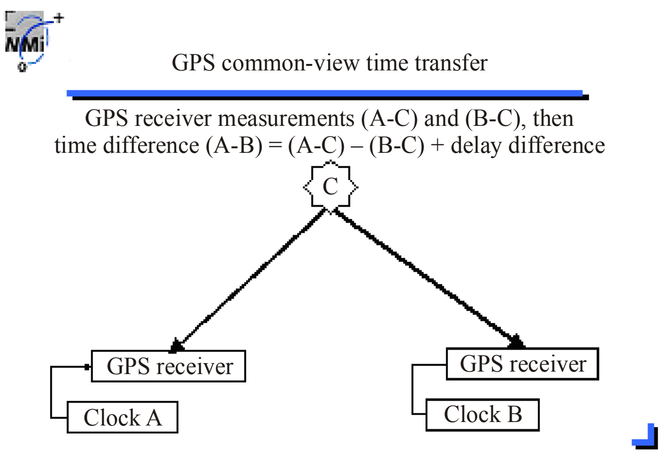

Sat_time_freq-14-04

The common delays in the satellite and its clock cancel. The differences in excess delay in the ionosphere and in the troposphere still have to be taken into account. The delays in the antenna, antenna cable, clock cable and receiver at each site should be known (calibrated), so the result can be corrected for delay differences in the equipment at A and B. These delays should be stable with environmental conditions.

First, a calibrated GPS Time Transfer Unit (TTU) is sent to the Participating Stations so that baseline measurements can be made at the start of the calibration period against a GPS TTU that will be present at the Participating Stations throughout the course of the evaluation period. Then, during subsequent intervals, the calibrated receiver is again sent to the Participating Stations.

Figure 14-5 shows the results of these comparisons made over long periods of time.

FIGURE 14-5

Differences between TWSTFT and GPS C/A-code common-view for NPL/NIST link

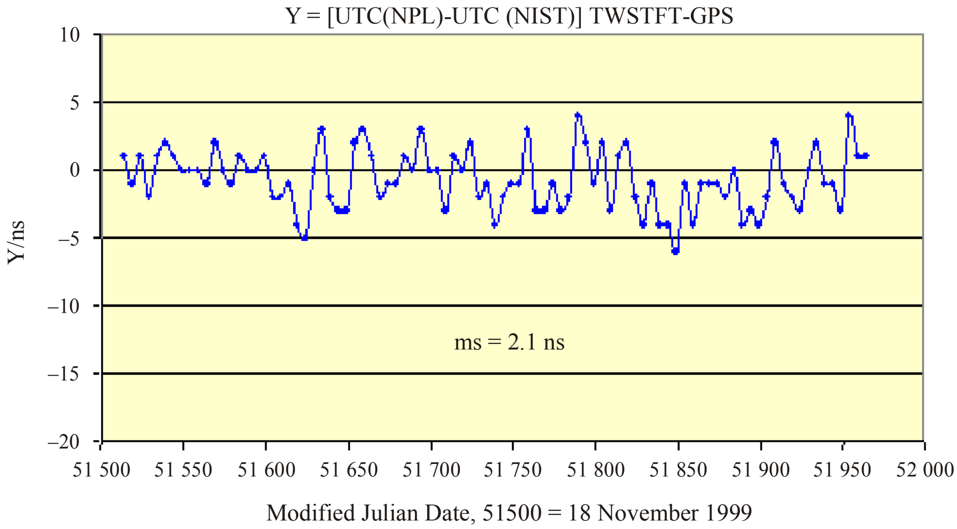

Sat_time_freq-14-05

14.9 Long term stability of TWSTFT

For frequency comparison, 150 ps is probably a good estimate for the uncertainty associated with measurements made using TWSTFT.

14.9.1 Long term comparisons between GPS and TWSTFT

There are in September 2002 twelve operational TWSTFT links in Europe, North America and Pacific Rim. Ten of them are used for the construction of TAI. All these TWSTFT links are compared with GPS Common-View and published in BIPM TWSTFT Reports. This permanent monitoring provides valuable information about long term stability of the two methods: some of these links are operational already since 3 years. A typical comparison for NPL/NIST distant by about 8 000 km for the Modified Julian Day period 51 510-51 970 is given in Fig. 14-5. The NPL/NIST TWSTFT link was calibrated by GPS.

The TWSTFT data collected during three weekly sessions, on Monday, Wednesday and Friday, were linearly interpolated for TAI standards dates (Modified Julian Day ending by 4 and 9). The GPS common views were computed using IGS precise ephemerides and IGS ionospheric maps, then were smoothed and interpolated for standard dates. During the period of comparison we do not observe any departure or seasonal effect. The r.m.s. of the differences between two methods for the period of comparison is 2.1 ns.

An estimated uncertainty of the TWSTFT link is below 1 ns, and the one of GPS is 2.5 ns. This is why it is believed that most of the observed noise in the differences between the two methods is due to GPS Common-

View. This is confirmed by the analysis of frequency stability of [UTC(NPL) – UTC(NIST)] given in Fig. 14-6.

FIGURE 14-6

Modified Allan deviation indicates the frequency stability of the two techniques, GPS Common View (top curve) and TWSTFT (bottom curve)

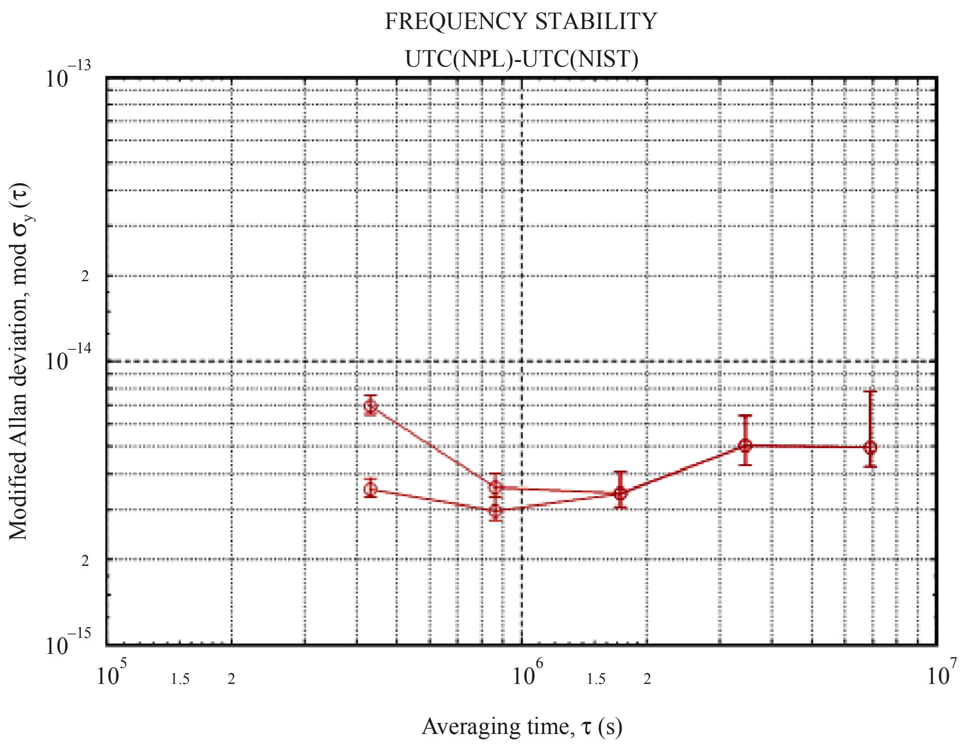

Sat_time_freq-14-06

The GPS Common-View data is showing white phase noise due to method of comparison up to averaging times of 20 days. The TWSTFT data is showing white frequency noise characteristic to behavior of clocks already for averaging times of 5 days. It means that for averaging times of 5 days we do not have any more noise of TWSTFT. In other terms two clocks located at the NPL and the NIST at the distance of 8 000 km are compared by TWSTFT without noise of time transfer for averaging times of 5 days. GPS data indicates the noise of the technique. TWSTFT shows clock noise.

14.10 Conclusion

The data seems to support the use of TWSTFT as a high precision clock and frequency comparison technique. While the costs of establishing a TWSTFT capability are initially high, the ease of data reduction also makes it an attractive alternative to other techniques. Because the potential of this technique is just now being expanded to include such experiments as carrier phase tracking, TWSTFT promises to provide improved capabilities in the future.

References

ASHBY N. and ALLAN, D. W. [1979] Practical Implications of Relativity for a Global Coordinate Time Scale. Radio Science, **14**, p. 649-669.

20th BIPM TWSTFT Report, (http://www.bipm.fr/pdf/cctf/wg_twstft.html).

De JONG, G. *et al*. [1995] Results of the Calibration of the Delays of Earth Stations for TWSTFT using the VSL Satellite Simulator Method. Proceedings of the 27th Annual PTTI Meeting, p. 359-372.

De JONG, G. and POLDERMAN, M. C. [1994] Automated Delay Measurement System for an Earth Station for Two-Way Satellite Time and Frequency Transfer. Proceedings of the 26th Annual PTTI Meeting*,* December 6-8, Reston, Virginia, USA, p. 305-317.

De JONG, G. and VAN BEMMELEN, R. [2001] Evaluation and Improvement of the Calibration of a TWSTFT Station Using SATSIM. Proceedings of the 33rd Annaul PTTI Meeting, p. 256-262.

FLOCK, W. L., SLOBIN,S. D. and SMITH, E. K. [1982] Propagation effects on radio range and noise in earth-space telecommunications. Radio Science, **17**, No. 6, 1982, p. 1411.

HARTL, Ph., GIESCHEN, N., MOSSENER, K. M., SCHAFER,W. and WENDE, C. M. [1983] High Accuracy Global Time Transfer via Geosynchronous Telecommunication Satellites with MITREX. Journal of Flight Sciences and Space Research*,* **7**, p. 335-342.

JESPERSEN, J. [May 31-June 2, 1989] Impact of Atmospheric Non-reciprocity on Satellite Two-Way Time Transfers. Proceedings of the 43rd Annual Symposium on Frequency Control*,* Denver, Colorado, USA, p. 186-192.

KIRCHNER, D. [1991] Two-Way Time Transfer via Communication Satellites, Proceedings of the IEEE (Special Issue on Time and Frequency), **79**, p. 186-192.

KIRCHNER, D., RESSLER, H., GRUDLER, P., BAUMONT, F., VEILLET, Ch., LEWANDOWSKI, W., HANSON, W., KLEPCZYNSKI, W. and UHRICH, P. [1993] Comparison of GPS Common-View and Two-Way Satellite Time Transfer over a Baseline of 800 km.

KIRCHNER, D. , RESSLER, H., HETZEL, P., SORING, A. and LEWANDOWSKI, W. [1998] Calibration of Three European TWSTFT Stations using a Portable Station and Comparison of TWSTFT and GPS Common-View Measurement Results. Proceedings of the 30th PTTI Meeting, p. 365-375.

KIRCHNER, D. [1999] Two-Way Satellite Time and Frequency Transfer (TWSTFT): Principle, Implementation and Current Performance. Review of Radio Science 1996-1999, Oxford University Press.

KLEPCZYNSKI, W. [1995] Two Way Satellite Time Transfer", Tutorial at PTTI Meeting.

PETIT, G. and WOLF, P. [1993] Relativistic Theory for Picosecond Time Transfer in the Vicinity of the Earth. Proceedings of the 25th Annual PTTI Meeting, p. 205-214.

VEENSTRA, L. B. [1990] International Two-Way Satellite Time Transfers Using INTELSAT Space Segments and Small Earth Stations. Proceedings of the 22nd Annual PTTI Meeting*,* December 4-6, 1990, Vienna, Virginia, USA, p. 383-398.

CHAPTER 15

SUMMARY TIME AND FREQUENCY DISSEMINATION

Time and frequency can be transferred via a number of techniques depending on the accuracy required. The primary means of accurate time transfer is the global positioning system (GPS). GPS uses a constellation of satellites each containing atomic clocks. These spaceborne atomic clocks, combined with the monitor station caesium standards establish GPS time, the system synchronization time. Using GPS for time and frequency dissemination relies upon the stability and precision of GPS time for positioning. Simultaneous passive reception of multiple GPS satellites requires the satellites to be precisely synchronized to each other with less error than that expected from the individual satellite pseudorange measurement with the user receiver. The stability of the individual satellite clock between updates or re-synchronization with GPS Time, determines the system synchronization error. Signal propagation of the GPS signals, receiver instrumentation, user position uncertainty and UTC(USNO) satellite correction message offset are the other determining factors in passive time transfer accuracy to users. GPS time transfer takes two forms:

1. passive time transfer used predominately by the radio-communication users;
2. common view and carrier phase common view time transfer used for scientific and international timescale operations.

Passive operation is the primary mode of time transfer for the vast majority of user. As a passive service the GPS broadcasts are available over a wide area independent of the user's position for reception. The timing information is determined along with the position and velocity in the user's calculations during flight or other mobile operations. Consequently, estimates of time transfer accuracy are dependent upon the uncertainty of the user's location in the navigation process. For fixed sites with accurate knowledge of position near optimum results less than 10 ns, 1 σ, can be expected. Effective use of this capability in mobile platforms is dependent on the user's instrumentation and ability to use the high precision timing information.

GPS time transfer between the worldwide timing centers and the scientific community utilize another technique known as common view and its variant, carrier phase common view. common view is a point to point technique rather than a general broadcast as in the passive reception case discussed above. Two sites requiring time transfer exchange measurements taken from individual GPS satellites. Differencing these tracking data results in a precise comparison between the local clocks at the two sites. Carrier phase measurements increase the precision of the pseudorange or range measurement between the receiver and the individual satellite. Increased precision results from measuring the ambiguous RF carrier phase rather than the unambiguous PRN code modulation. The ambiguity of the continuous RF signal results in precise frequency measurement rather than time measurements. Development of techniques to utilize GPS carrier phase in operations is being conducted by the International GNSS service (IGS). The participating IGS stations and analysis centers have been able to achieve sub-nanosecond precision frequency comparisons between the participating network of stations. Results to date have indicated that to achieve the full capability of this technique, technology to calibrate the receiving systems at picosecond levels must be developed. Calibration of geodetic receiving systems by using GPS system simulators is the subject of a small effort at NRL. This technique which provides complete control of all the conditions of signal reception, offers the potential of an absolute calibration for determination of time epoch transfer.

The most precise time transfer technique in general use is TWSTFT. This technique takes advantage of the two way capability of communication satellites to transmit timing signals in both directions to virtually eliminate the transmission and common instrumentation delays between the two participating sites. It is a point-to-point technique used primarily between timing centers suitably equipped. The single measurement precision of a single two-way transfer is approximately 10 ps. Overall accuracy is dependent upon non-reciprocal instrumentation and satellite transponder delays, possible satellite motion during the transfer process. Time transfer accuracies of 100 ps are theoretically possible if the non-reciprocal errors can be sufficiently reduced.

The methods discussed above are direct time transfer systems. They are either designed specifically for time transfer, such as TWSTFT, or use time synchronization as a primary means for operation, such as GPS. Other local communications systems which require synchronization for CDMA or TDMA communications protocols and data transfer can potentially be used to distribute timing information over their local area of coverage, derived from GPS or other sources as an alternative time transfer mechanism.

A summary of the performance from the different techniques is provided in Tables 15-1 and 15-2 below as an overall summary of the techniques and technologies discussed in this Handbook.

TABLE 15-1

GNSS Time transfer techniques

Parameter	**Passive GPS (SPS)**	**Passive GPS (PPS)**	**Common view (Short base)**	**Common view (Long base)**	**Advanced Common view**	**Carrier phase**	**WAAS/GPS**
Precision (ns) r.m.s. (Range)	≤ 8 ns(1), (2) wrt UTC(USNO)	≤ 8 ns wrt UTC(USNO)	3-8 ns (point to point)	5-10 ns (point to point)	≤ 5 ns (point to point)	≤ 5-10 ns (point to point)	≤ 20 ns w.r.t. UTC(USNO)
Major error sources	SA, Multi-Path, Clock, Iono, Tropo, UE, RF Enviro, Temp (RX & Ant)	Multi-Path, Clock, UE, RF Enviro, Temp (RX & Ant)	UE, Path reciprocity, Ephemeris, Enviro (Temp)			UE, Multi-Path, Cycle Slips	Clock, ephemeris
Stability (Value @ Ave)	≤ 8 ns @ 13 min ≈ 1 ns @ 1 day	≤ 5 ns @ 13 min ≈ 1 ns@ 1 day	≤ 4 ns @ 1 h ≤ 1 ns @ 48 h	≤ 4 ns @ 1 h ≤ 1 ns @ 48 h	≤ 4 ns @ 1 h ≤ 1 ns @ 48 h	<< 1ns @ 6 min	< Passive SPS
Calibrati-bility	3-5 ns Against Std RX					<< 1 ns With Abs Cal	3-5 ns Against Std RX
Sample rate	1 per 13 min	1 per 5 min 1 per 13 min	1 per 13 min	≥ 1 per 13 min (post processed)	1 per 5 min 1 per 13 min	Similar to passive & common view	TBD
Availa-bility	Real Time		Schedule dependent			Processing dependent	Real-time

(1) Fixed location with 3D position known to > 1 m, 3D.
(2) Depending on user equipment.

TABLE 15-2

Two-way techniques both satellite and terrestrial

Parameter	**TWSTFT**	**Fiber LAN-WAN**	**Fiber long haul**	**Two-way in comms (OTA)**
Accuracy (pt To pt) (Range) (ns r.m.s)	≈ 1 ns (Ku-Band) ≈ 1 ns (X-Band) ≈ 3 ns (C-Band)	≤ 1 ns @ 200 km	≤ 2 ns @ 8 000 km	≤ 5 ns @ 200 km
Major error sources	Path Reciprocity, Sys Cal, Enviro (Temp)	Path reciprocity Enviro (Temp)		Path reciprocity, Sys Cal, Enviro (Temp)
Stability (Value @ Avg'g time)	200 ps @ 1 h 100 ps @ 12 h	100 ps rms	TBD	TBD
Calibratibility (Level in ns)	≈ 1		≈ 2	≈ 3-5
Sample rate	1 per 5 min	Continuous		
Timeliness	Near real time			

Printed in Switzerland
Geneva, 2010
ISBN 92-61-13301-0

Photo credits : www.itu.int